The University Of Sheffield.

Plant-soil interactions: the impact of plant water use efficiency on root architecture and soil structure

By:

Tinashe Mawodza, B.Sc. (Hons.), M.Sc.

A thesis submitted in partial fulfilment of the requirements for the Degree of Doctor of Philosophy

The University of Sheffield

Faculty of Science

Department of Molecular Biology and Biotechnology

September 2019

"Paswera badza hapanyepe"

Mrs A. Mawodza (2015)

"Of all occupations by which gain is secured, there is none better than agriculture, nothing more productive, nothing more worthy of free men!!"

Marcus Tullius Cicero (circa. 44 B.C.E)

Declaration

I, Tinashe Mawodza, declare that this thesis has been composed entirely by myself unless otherwise referenced in the text. I confirm that this thesis has not been submitted for any other degree. All quotations have been distinguished by quotation marks and the sources acknowledged.

Acknowledgements

I would like to firstly thank my very patient and unwavering supervisors, Stuart Casson and Manoj Menon who have guided me through this whole arduous four-year journey culminating in this thesis. This journey would not have been possible without them. I would also like to extend my deepest gratitude to the Geography technical staff, Alan Smalley, Rob Ashurst and Joseph Hufton who have provided technical guidance and support. I would also like to thank Genoveva Burca and Oxana Magdysyuk from the STFC for technical help in the scanning done at the IMAT and Diamond facility respectively.

I would also like to thank my family, Mom, Dad, Nyaradzo 'Nyarie', Tapiwa 'Taps', Ngonidzashe 'Nx', Emannuael 'Mabhun', Lovelace, Christopher and the rest of the Mawodza's who have not only been a family second to none but have provided me with the fuel to continue when the days were dark. I would also like to extend my thanks to my uncle, Sekuru Jonh, who has inspired not only myself, by everyone else in the family by being the trailblazer, setting us new challenges every step of the way. I would also like to extend my gratitude to the Mangudya Family with special mention to Nyasha and Sekai who have been the family I needed away from home.

This whole PhD journey would also not have been possible without the patience, guidance and support of one person very close to my heart, Rukudzo 'Kuku' Charakupa, my girlfriend. I would like to thank you, my love, form the depth of my heart and hope you always remain the same.

I would also like to express my gratitude to my Sheffield 'Zimganda' family Patie, Carol, Nancy, Erick and Rumbie who have made Sheffield home for me. Not forgetting Shanon (Mai Gwala) the Leuvenite who always speared me forward, supporting me from just across the pond in Belgium.

Lastly, I would like to extend my deepest gratitude to the Grantham Centre for Sustainable Futures (GCSF) for funding this research and making it possible for me to dream of a brighter and more sustainable future.

Abstract

Improving the worlds' agricultural productivity is paramount for the eradication of hunger, a key sustainable development goal. As agricultural production across the world currently accounts for more than 70% of global freshwater withdrawals. The increased agricultural production required to feed an ever-expanding global population is set to put serious strain on the worlds' already limited freshwater resources. Development of plants with improved water use efficiency to maximise on the erratic global freshwater supply has largely been suggested as a possible strategy to bring about significantly increased crop production per unit of water available. The effectiveness of the utility of such plants, however, may come at a cost to soil health, which would ultimately lead to reduced sustainability of crop production. In cognisance of this, this study aimed at investigating how genetically altering plant water use efficiency (WUE) may have a bearing on a plant's root system architecture (RSA) and consequently soil structure. This research was focused on the water use efficient mutants of three different plant species, namely Thale Cress (*Arabidopsis Thaliana*), common bread wheat (*Triticum aestivum*) and rice (*Oryza Sativa*). I investigated how genetically altering WUE in these different plants affects their RSA using both invasive (Root washing) and non-invasive (X-Ray and Neutron computed tomography) methods to unravel their RSA in 2 and 3D. Subsequently, changes in soil structure were inferred using aggregate stability testing. I did not find conclusive evidence suggesting that genetically altering WUE in wheat and Arabidopsis had an effect on their RSA and soil structural stabilisation. On the other hand, I found reasonable evidence suggesting that rice plants with genetically enhanced WUE had reductions in their RSA development. There was also evidence suggesting that in wetland grown rice, the aggregate stability of at least one aggregate size fraction (1-2mm) was significantly reduced.

Research highlights and major findings

- Results from my experiments highlight that the fact that X-Ray CT scanning can be used to produce detailed 3D images of Arabidopsis RSA when grown in a mineral soil
- My results also demonstrated that NCT can successfully be used to reveal wheat RSA in a heterogeneous aggregated soil with moderate amounts of soil organic matter
- It was also demonstrated that improving WUE of rice plants by altering the *PHYB* gene could have a negative impact on their RSA of the rice mutant plants used.

List of abbreviations

Δ	Carbon isotope discrimination
2D	Two dimensional
3D	Three dimensional
ANOVA	Analysis of Variance
ARF	Auxin Response Factor
AS	Aggregate Stability
c_a	Atmospheric carbon dioxide partial pressure
CAM	Crassulacean Acid Metabolism
CEC	Cation Exchange Capacity
c_i	Internal carbon dioxide partial pressure
CM	Coarse particle Mass
CPC	CAPRICE gene
CT	Computed Tomography
DAS	Days After Sowing
DNA	DeoxyRibonucleic acid
EC	Electrical Conductivity
EDDL	Electrical Diffuse Double Layer
EIR	Ethylene-Insensitive Root
EPF	EPIDERMAL PATTERNING FACTOR gene
GL	GLABROUS gene
HMP	Sodium Hexametaphosphate
IMAT	Imaging and Materials Science & Engineering
IM	Initial particle Mass
IRGA	Infra-Red Gas Analysis
IW	Intermittently Watered
iWUE	Integrated Water Use Efficiency
MRI	Magnetic Resonance Imaging
MWD	Mean Weight Diameter
NCT	Neutron Computed Tomography

NH_4OAc	Ammonium Acetate
NI	Neutron Imaging
NR	Neutron Radiography
PCR	Polymerase Chain Reaction
PEPCase	Phosphoenolpyruvate carboxylase
PHYA	PHYTOCHROME A gene
PHYB	PHYTOCHROME B gene
PHYC	PHYTOCHROME C gene
RHD	ROOT HAIR DEFECTIVE gene
RSA	Root System Architecture
RUBISCO	Ribulose-1,5-bisphosphate carboxylase/oxygenase
SD	Stomatal Density
SI	Stomatal Index
STFC	Science and Technology Facilities Council
TaEPF	EPIDERMAL PATTERNING FACTOR gene in wheat
TOC	Total Organic Carbon
UN	United Nations
VSA	Visual Soil Assessment
VESS	Visual Evaluation of Soil Structure
w_a	Atmospheric water vapour pressure
WFP	Water Filled Pores
WFPS	Water Filled Pore Space
w_i	Internal Water vapour pressure
WSA	Water Stable Aggregates
WT	Wild Type
WUE	Water Use Efficiency
WUE_B	Biomass determined Water Use Efficiency
WUE_I	Instantaneous Water Use Efficiency
WW	Well-Watered
XRSI	X-Ray Synchrotron Imagery
XRST	X-Ray Synchrotron Tomography

θ	Volumetric moisture content
θ_g	Gravimetric moisture content

Contents

I General Introduction

1.0 Overview of thesis

This thesis is made up of six chapters that address different aspects of my research

Chapter 1 Provides a generalised introductory to my research. This Chapter provides the background to why the research was embarked on as well as explaining some of the important concepts pertaining to this thesis.

Chapter 2 presents a detailed description of most of the different techniques and chemicals used in the course of conducting this research. It also presents an analysis of the results obtained from the physiochemical analysis of the different soils used in this research.

Chapter 3 is the first results chapter presenting results from all the experiments carried out using the model plant Arabidopsis Thaliana. The chapter starts off with a brief introduction and literature review of issues relevant to this particular plant prior to the presentation of results and a plant-specific conclusion

Chapter 4 is the second results chapter which details all the results from the experiments carried out using wheat plants. It similarly also contains a brief introduction and literature review proceeded by the experimental results obtained. *(Parts of this chapter have been accepted for publication in Geoderma. The accepted version of this paper is attached in the appendix)*

Chapter 5 is the third and final results chapter presents all the results from experiments done with rice plants. It also gives a brief introduction and literature review pertaining to my rice experiments and subsequently gives the results obtained.

Chapter 6 is the final thesis chapter which brings together all the important results from each plant species, summarising all the results obtained then highlighting some of the major limitations to my results and highlighting future work that may be needed to address questions still outstanding after my research.

1.1 Background

"The power of population is indefinitely greater than the power in the earth to produce subsistence for man".

(Malthus 1798)

The famous words of Thomas Robert Malthus written over two centuries ago, still resonate even in the 21 century where the challenge of sustainably feeding an ever-increasing global population is seemingly an insurmountable one in a world of limited resources. With the global population estimated to reach at least 9.7 billion by the year 2050, numerous scholars have highlighted the monumental task of meeting the food requirement of this growing population as one of the greatest challenges of the 21st century (Wallace 2000, Alexandratos and Bruinsma 2003, The Royal Society of London 2009, Godfray *et al.* 2010, Berners-Lee *et al.* 2018, Dillard 2019, United Nations 2019). According to current estimations, food production will need to increase by a staggering 70% of current production levels by the middle of the 21st century to catch up with projected demand (FAO 2009). This scenario, although daunting, has been noted by some as not unprecedented as comparable increases in food production have been achieved in recent and historic times (Smith 2015). The 'green revolution' of the mid-20th century is often cited as a comparable example of the world having nearly doubled productivity in a relatively short space of time (Borlaug and Dowswell 2003, Godfray *et al.* 2010, Smith 2015). Under the current food production system, however, meeting future global food demand will require considerable expansion and intensification of our current agricultural production systems, with the latter being considered most likely to be feasible in a world of increasingly meagre natural resources (The Royal Society of London 2009, Rockström *et al.* 2017).

The intensification of global agriculture in the face of the projected increased global food demand will exacerbate the current strain on the world's natural resources that are already under immense pressure from overexploitation, poor management and a changing global climate (Lal 1997a, 2016, Lynch 2007, Morison *et al.* 2008, Ludwig *et al.* 2014, Wang, Zhang, *et al.* 2016, FAO 2017, D'Ambrosio *et al.* 2018). An improvement in agricultural water use efficiency is urgently needed to reduce pressure on the worlds' scarce water resources. Recognising this dire need, the then Secretary-General of the United Nations (UN), the late Kofi Annan in his address to the 'Group of 77 developing countries' in Cuba emphasised the need for a 'Blue Revolution' that seeks to provide the world 'more crop per drop' of water utilised (UNIS 2000, Pennisi 2008). Wallace (2000), Morison et al. (2008) and Ruggiero *et al.* (2017) in their respective comprehensive reviews on the improvement of water use by plants, similarly acknowledged the importance of enhanced agricultural water use and encouraged the development of plants with improved water use

efficiency (WUE) to deal with the water crisis. Definitions of WUE and a detailed discussion are provided in section 1.3.

The development of plants with increased WUE called for is an ongoing process with researchers recording significant progress in the understanding and development of plants with enhanced water use patterns (Karaba *et al.* 2007, Katerji *et al.* 2008, Abogadallah *et al.* 2011, Franks *et al.* 2015, Bertolino *et al.* 2019, Caine *et al.* 2019). Unfortunately, however, most of these developments have by default, focused on the easily accessible above ground plant physiology, often neglecting the role of subterranean roots and their impact on soil properties (Eshel and Beeckman 2013, Atkinson *et al.* 2019). As a consequence, this passive neglect of soil-related issues in ensuring heightened water productivity through increased WUE could have major implications for the sustainability of global agriculture.

Soil degradation, the loss of a soil's inherent ability to perform its socio-economic and environmental function often results from the adoption of new technologies that aim to increase productivity (Lal 1997a, Koch *et al.* 2013, Squire *et al.* 2015). This has been demonstrated historically with interventions such as the adoption of mechanised tillage equipment in the 18th century and the advent of the use of nitrogen-based fertilisers during the 'green revolution' of the 1960's, which although leading to higher yields and a reduction in land exploration, resulted in massive soil loss and degradation where used (Derpsch 1997, Gibbs and Salmon 2015, Lal 2015). About 2 billion ha of agricultural land are estimated to have been degraded by the end of the 20th century with the methods used to achieve increased productivity often being sighted as the main driver of this soil degradation (Oldeman *et al.* 1991). It is even more worrying that currently an estimated 6 billion ha of land equating to about two-thirds of global arable land resources have already been degraded to some degree (Bot *et al.* 2000, Gibbs and Salmon 2015).

The land degradation linked to contemporary technologies that improve productivity make it clear that simplistic interventions such as genetic engineering of plants alone, although potentially useful in conserving water, would in isolation not help the world sustainably attain more crop per drop, unless coupled with other mechanisms to foster good agronomic practice (Passioura 2006). As 99% of global agriculture is reliant on soil resources for production, it is imperative that we should protect our soils from degradation (Bot *et al.* 2000, Gibbs and Salmon 2015). This is important especially for the topsoil that holds the bulk of the edaphic nutrients and carbon required for plant production. As a result of issues outlined, this research will thus focus on the interactions between plants with different WUE and the soil in an attempt to uncover the implications of their relationships to soil structure and ultimately sustainable agriculture.

1.2 Global freshwater crisis

Freshwater is one of the most critical resources for human existence. It is paramount to the maintenance of human health and well-being providing vital hydration and enabling general sanitation. Freshwater is also key for economic development as it is used in many different industries, chief among them, agriculture which consumes at least 70% of the freshwater used by humans (Bonsch *et al.* 2015, FAO 2017). The majority of the worlds' hydroelectric power plants that provide about 17% of total electric energy consumed globally and 85% of global renewable electricity are also largely powered by freshwater bodies (International Energy Agency 2012, Zhao and Liu 2015). Earth's freshwater bodies also provide essential hydration to terrestrial organisms and supports various freshwater ecosystems.

Despite this profound importance, however, the world's freshwater resources are currently under direct and indirect threat from many human activities which include, but are not limited to anthropogenic climate change, pollution, and overexploitation (IPCC 2007, Boutraa 2010, Schwarzenbach *et al.* 2010, IPCC 2013, 2018). The ever increasing pressure on the world's freshwater resources has mainly been brought about by a rapidly growing world population as well as heightened economic growth and an increased standard of living which have fuelled increased freshwater demands for agricultural, municipal (domestic) and industrial purposes (Vörösmarty *et al.* 2010, Hejazi *et al.* 2013, UNESCO 2019). Global water withdrawal has increased by a factor of about 8 from 500km^3/year to 4000km^3/year in the past century (Hoekstra and Wiedmann 2014, Wada *et al.* 2014, 2016). These increased water withdrawals have worsened water scarcity, adversely affecting the sustainability of food production especially in the arid and semi-arid regions of the world (IPCC 2018). An increasing trend of overuse of surface water and non-renewable groundwater resources has resulted in nearly 80% of the global population being exposed to high levels of threat to water security (Vörösmarty *et al.* 2010, Wada *et al.* 2016, UNESCO 2019).

As crop irrigation is the biggest user of the world's freshwater resources (Koech and Langat 2018), it is apparent that a reduction in water used by plants for irrigation alone would greatly reduce the threat level of water security in many parts of the world. Reductions in the volume of water used for irrigation would also make crop production cheaper and allowing for better water access for other uses(WWF 2003, Ruggiero *et al.* 2017). The reduction in water used by crops can be successfully achieved by developing more efficient management of irrigation systems and by developing crops that inherently use less water for crop production i.e. the use of WUE plants, which are the main focus of this research.

1.3 Water use efficiency in plants

1.3.1 Definitions and important concepts

The concept of plant water use efficiency (WUE) has been in existence for at least 300 years with experiments by Woodward (1699) marking some of the earliest work investigating plant productivity per unit of water consumed (Briggs and Shantz 1913, Hatfield and Dold 2019). The WUE concept has significantly evolved since then with the contemporary use of the term WUE in plant biology often being largely obscure when considered without context (Bacon 2004, Ruggiero *et al.* 2017). It, however, most generally refers to the ratio between the total amount of assimilate (carbohydrates) produced by (a) plant(s) and the total amount of water used to produce the assimilate (Bacon 2004, Morison *et al.* 2008, Franks *et al.* 2015, Hatfield and Dold 2019). The major source of ambiguity in the term plant WUE arises from the fact that it can be used at different spatial (e.g. catchment, field, plant or leaf level) and time (e.g. over a season, years or a few minutes) scales and can include or exclude evaporation from the soil (Bacon 2004, Leakey *et al.* 2019).

The earliest and most common measurements of WUE in literature have been done at the whole-plant level probably due to the relative simplicity and directness of deriving the individual components used to calculate WUE (Briggs and Shantz 1913, Stanhill 1986). Plant level WUE (WUE_B) is calculated using the equation:

$$WUE_B = \frac{dry\ plant\ biomass(or\ seed\ mass)(g)}{water\ use\ (g)} \quad [1]$$

Although the plant biomass referred to in the equation is total dry biomass, for convenience, many studies often use only above-ground biomass due to the difficulty of measuring root biomass. Seed mass could also be used for this calculation depending on the main aim of the experiment (Bacon 2004, Morison *et al.* 2008, Leakey *et al.* 2019).

WUE at leaf level is often referred to as transpirational efficiency and can either be measured instantaneously (WUE_I) or over the lifetime of the leaf i.e. integrated WUE (iWUE). WUE_I is measured using Infrared gas analysis (IRGA) on single leaves, thus allowing for the direct quantification of transpiration and carbon assimilation. It is governed by the formula

$$\boldsymbol{WUE_I = \frac{A_{max}(mmol_{CO_2})}{g_s\ (mmol_{H_2O})}\ or\ \frac{A_{max}(mmol_{CO_2})}{E(mmol_{H_2O})}} \quad [2]$$

Where A_{max} is maximum (Assimilation) photosynthetic rate, g_s is stomatal conductance and E is evapotranspiration. These parameters operate closely with the internal and external carbon dioxide (c_i and c_a) and water vapour pressure (w_i and w_a) as illustrated in Figure 1, with any factor lowering c_i

whilst keeping all others constant, resulting in an increased WUE_I. iWUE is often inferred over an entire leaf growing period and can be measured using the carbon isotope discrimination method as described in the next section (1.3.2) (Farquhar *et al.* 1989).

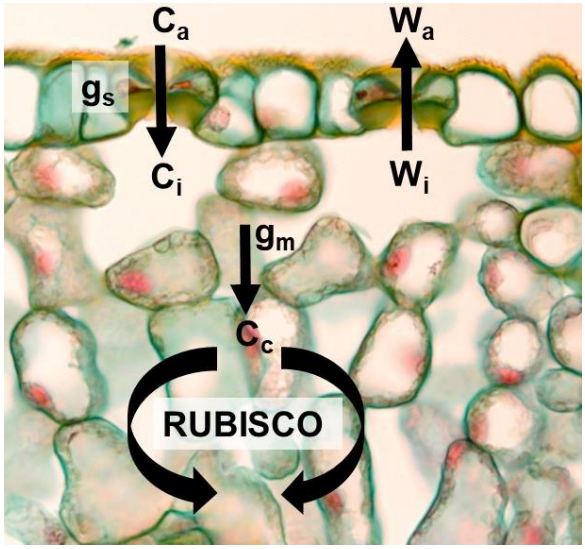

Figure 1: Showing pathway of diffusion of CO_2 facilitating for carbohydrate assimilation via photosynthesis in C_3 plants. [Image adapted from (Impre Media 2019)]

1.3.2 Carbon isotope discrimination (Δ) in measuring WUE

The carbon isotope discrimination method as proposed by Farquhar et al. (1989) is based on the fact that photosynthetic processes normally discriminates against the heavier isotope of carbon (^{13}C) as compared to the more abundant lighter alternative (^{12}C) when using the ambient gas CO_2 to make assimilate. This is primarily due to RUBISCO (Ribulose-1,5-bisphosphate carboxylase/oxygenase), the enzyme responsible for the first step of carbon fixation, having a preference for ^{12}C, as well as diffusion kinetics of $^{13}CO_2$ versus $^{12}CO_2$. Stomatal pore restrictions limit the diffusion of ^{13}C by a factor 4.4‰ in C_4 plants whilst in C_3 plants the isotopic effects of RUBISCO limits uptake of the heavier isotope by a factor 27‰ (Farquhar *et al.* 1989, Cregg and Zhang 2000). This discrimination often results in plant matter containing substantially less ^{13}C as compared to the ambient air, assuming no carbon is lost. The discriminatory effect in C_3 leaves is summarised by the equation;

$$\Delta = a\frac{c_a - c_i}{c_a} + b\frac{c_i}{c_a} \approx a + (b - a)\frac{c_i}{c_a} \qquad [3]$$

Where Δ is the leaf carbon isotope discrimination, 'a' is the fraction occurring due to diffusion in air, 'b' is net fraction caused by carboxylation using RUBISCO and c_a and c_i are ambient and intercellular partial pressures of CO_2 respectively. From [2], it can be noted that when stomatal conductance is low in comparison to photosynthetic capacity, as is the case in plants with reduced

stomata or when plants partially close their stomata under stress. The c_i becomes low and c isotope Δ tends towards lower discrimination (4.4‰) with plants less able to discriminate between the two isotopes of carbon, being forced to use more of the heavier ^{13}C isotope. This has, therefore, identified stomatal function and number as potential targets for improving plant WUE.

1.3.3 Strategies of increasing WUE

Various strategies aimed at attaining increasing WUE in plants have been suggested in literature with Gregory (2004) in: Bacon (2004) noting that many practices that increase yield by reducing physiological plant limitations often inadvertently also lead to increases in the efficiency of water use (Bacon 2004). In optimal conditions, however, physiologically attaining increased WUE requires manipulation of plants to reduce the water cost of acquiring CO_2. In nature, C_4 plants have evolved a comparative advantage in obtaining CO_2 at a lower cost as compared to C_3 plants (Way *et al.* 2014, Leakey *et al.* 2019). This is because they are able to use biochemical and structural modifications that enhance carbon capture and thus productivity. C_4 plants have a unique carbon fixation pathway mediated by phosphoenolpyruvate carboxylase (PEPCase). This is in contrast to C_3 plants that carry out the Calvin cycle directly using the less reactive RUBISCO in the mesophyll. C_4 plants use the PEPCase enzyme that reduces c_i by reacting with the available CO_2 in the mesophyll and shuttling the products (e.g. malate) to the bundle sheath where RUBISCO then uses the CO_2 transported to make assimilate in a carbon concentrating mechanism. This thus results in increased WUE as governed by [1] and [2] by limiting photorespiration.

Plant scientists have in recent years been actively seeking to genetically engineer the C_4 photosynthetic pathway that is native only to 3% of the worlds' plants, into the more common C_3 plants to improve productivity as well as WUE (Schuler *et al.* 2016). Others like Borland et al. (2014) have also suggested the integration of even more water-use efficient photosynthetic pathway Crassulacean Acid Metabolism (CAM) into major crops.

WUE has also recently been shown in the model plant Arabidopsis as a result of manipulation of stomatal characteristics by reducing stomatal density and ultimately conductance (g_s) resulting in improved water use by plants (Masle *et al.* 2005, Franks *et al.* 2015, Bertolino *et al.* 2019). This mechanism has been achieved by altering epidermal peptide signals also known as epidermal patterning factors (EPF's), which in turn regulate key steps in stomatal development and reduce the number of stomata on the leaf surface (Doheny-Adams *et al.* 2012, Tanaka *et al.* 2013). Many other mechanisms have also been used to improve WUE, Table 1 summarises several recent studies that been successful at improving WUE in different plant species transgenically.

Table 1 Showing selected examples of studies where transgenic plants displayed greater water use efficiency [Adapted from (Leakey *et al.* 2019)]

Gene target(s)	Species	Proposed mechanism(s)	Reference
AtHDG11	Peanut	Upregulation of stress-responsive genes and reduced stomatal density	(Banavath *et al.* 2018)
PeCHYR1	Poplar	Increased abscisic acid (ABA) sensitivity	(He *et al.* 2018)
OsGA2	Rice	Gibberellin-mediated plant architecture modifications	(Lo *et al.* 2017)
Hv-miR827	Barley	Maintenance of photosynthesis during drought	(Ferdous *et al.* 2017)
HvEFP1	Barley	Reduced stomatal density	(Hughes, Hepworth, Dutton, Dunn, Hunt, Stephens, Waugh, *et al.* 2017)
ZmXerico1 and ZmXerico2	Maize	Increased ABA sensitivity	(Brugière *et al.* 2017)
MoHrip1 and MoHrip2	Rice	Increased ABA sensitivity	(Wang *et al.* 2017)
SoCyt*Sod* and PsCyt*Apx*	Plum	Improved enzymatic antioxidant capacity	(Diaz-Vivancos *et al.* 2016)
PdEFP1	Poplar	Reduced stomatal density	(Wang, Liu, *et al.* 2016)
PaAQUA1	Poplar	Improved regulation of water homeostasis	(Ariani *et al.* 2016)
ZmNAC111	Maize	Increased ABA sensitivity	(Mao *et al.* 2015)
OsHVA1	Rice	Lateral root initiation promotion and maintenance of cell metabolism under drought	(Chen *et al.* 2015)
ZmSDD1	Maize	Reduced stomatal density	(Liu *et al.* 2015)
AtERECTA	Tomato and rice	Reduced stomatal density	(Shen *et al.* 2015)
AtAREB1	Soybean	Reduced transpiring leaf surface area and reduced stomatal conductance	(Leite *et al.* 2014)
AtEDT1/HDG11	Rice	Reduced stomatal density and more extensive root system	(Yu *et al.* 2013)
AtDREB1A	Wheat	Mechanism not elucidated	(Pierre *et al.* 2012)
vgb, SacB, JERF36, BtCry3A, and OC-I	Poplar	Elevated fructan and proline accumulation and increase maximum quantum yield of photosystem II	(Su *et al.* 2011)
AtDREB1A	Peanut	Improved antioxidative performance	(Bhatnagar-Mathur *et al.* 2009)
OsEPF1	Rice	Reduced stomatal density	(Caine *et al.* 2019)
LeNCED1	Tomato	Increased ABA sensitivity	(Tung *et al.* 2008)

Although all these interventions to improve water use efficiency may be noble, they could potentially come with an as yet unexplored costs to soil properties as they are largely dependent

on root water use by plants with some plants having reduced roots when WUE. This study thus seeks to answer questions related to the possible impacts of increased water use efficiency to plant RSA and consequently soil structure with main focus on the effect of the altered shoot and root characteristics.

1.4 Root system architecture

Roots being the main interface between the soil and the rest of the plant, have the critical role of acquiring nutrients and water essential for plant growth and development. They do this via an intricately linked, branched network within the soil that may extend for tens of meters below the soil surface. The unique arrangement of this root network is often referred to as the root system architecture (RSA) which is defined as the 3-dimensional geometric configuration of plant roots within a growing media (usually soil) (Lynch 1995, Gregory 2006, Kochian 2016, Himmelbauer *et al.* 2017). RSA is an often hidden but key determinant of plant productivity under various environmental conditions. It influences the ability of plants to survive even when exposed to various perturbations that may adversely affect plant growth such as inadequate soil moisture and/or nutrient deficiencies (or toxicities) (Lynch 1995, Hammer *et al.* 2009, Koevoets *et al.* 2016).

Historically researchers have overlooked below-ground factors due to the relative inaccessibility of roots systems however RSA studies have gained popularity over the past two decades. This is mainly due to improved imaging technologies coupled with the growing need for developing plants that are better able to forage for scarce water and nutrient resources (de Dorlodot *et al.* 2007a, Lynch 2007, Eshel and Beeckman 2013, Bodner *et al.* 2015). Lynch (2007) even goes as far as suggesting that a second agricultural 'green revolution' may come from the development of plants with unique RSA's that will enhance the efficiency of water and nutrient uptake, especially in developing countries. In recognition of this importance, numerous studies exploring the Root System Architecture (RSA) of different plants to identify specific characteristics that may be advantageous in different environments have been undertaken with various degrees of success (Manschadi *et al.* 2006, 2008, Sanguineti *et al.* 2007, Gregory 2009, Paez-Garcia *et al.* 2015, Tron *et al.* 2015, Himmelbauer *et al.* 2017)

The great diversity in RSA exists both within and between species, which has mainly been attributed to both genetic and environmental signals that affect the root development (Rogers and Benfey 2015, Ogura *et al.* 2019a). Variation in RSA can lead to plants with variable water resource capture abilities. As a result of this, geneticists and plant breeders alike, especially in water-limited areas, are actively seeking to develop plants that have a superior water acquisition abilities to confer increased water use efficiency and drought resistance (Blum 2005, 2009, de Dorlodot *et al.* 2007b,

Giehl *et al.* 2014, Rogers *et al.* 2016). Plants with inherently deep and extensive root systems have often been thought to be ideal for conferring drought resistance and improved water use efficiency (Lynch 2013, Uga *et al.* 2013, Ramalingam *et al.* 2017). This resulted in the proposal of a 'deep steep and cheap' root ideotype for maize that has been shown to be ideal in certain environments.

The idea of an ideal root ideotype has however recently been critiqued by Tron et al. (2015) who modelled the growth of 48 different root architectures in 16 different drought scenarios. Their results indicated that none of the diverse RSAs they studied had the best water acquisition and use efficiency under all the hydrological scenarios modelled suggesting that there was no unique root ideotype for all existing hydrological conditions (Tron *et al.* 2015). A study by Palta et al. (2011) also concurred with Tron et al. (2015) in their examination of the benefits of vigorous wheat RSA noting that although larger, deeper root systems conferred an advantage under seasonal rainfall they proved inferior when stored soil water is the predominant water source. Regardless of the predominant RSA plants may exhibit, however, it is important to note that in nature, roots show a significant degree of developmental plasticity allowing them to adapt to different moisture and nutrient stresses by altering their RSA to their advantage (Gruber *et al.* 2013). As such RSA should not be viewed as a static plant trait, but rather a dynamic trait that can be altered to some degree by the environment.

1.5 Methods of measuring RSA

As a result of the great importance of RSA to soil resource acquisition, several methods have been developed to measure and quantify plant RSA both in-situ and ex-situ. These methods have varying degrees of success between them. Several reviews e.g. (Smit *et al.* 2000, Mooney *et al.* 2012, Downie *et al.* 2015) have already highlighted the major differences between these methods and how each one is appropriate in each environment. A brief overview of the essential elements in each of these systems is described in this section with focus on techniques that are relevant to my thesis. In future chapters, there will be a discussion of their use for studying the specific plant species investigated in this thesis. The most common RSA parameters that are often investigated in different studies include root length (and length density), vertical distribution, angle and thickness and tortuosity (Smit *et al.* 2000, Morris *et al.* 2017, Alahmad *et al.* 2019). These are defined in table Table 2.

Table 2 Some important definitions of parameters characterising root system architecture[Adapted from (Smit *et al.* 2000)]

Root parameter (units)	Definition	Significance
Total length (cm)	Cumulative length of all roots of a particular plant	Determines a plants potential for nutrient and water extraction. It is also important for the parametrisation of plant growth models
Thickness (µm)	Average diameter of the different roots (usually assumed to be diameter of a cylinder)	Determines potential for mycorrhizal development and is often measured as the result of a roots response to physical conditions
Angle (°)	Angle between the horizontal and the long axis of each root	Determines how deep a root systems grows
Volume (mm^2)	The volume occupied by the whole root system	Is a determinant of root water extraction and transport
Vertical distribution (cm)	Depth of the deepest root of a plants root system	Determines how deep a root system can tap into below groundwater supplies
Tortuosity	Curvature of root paths of a plant	Important for root anchorage and is essential for early establishment

1.5.1 Traditional (historic) imaging techniques (2D imaging)

Root system imaging and analysis has been done for over a century with some of the earliest recorded studies investigating RSA development being done by Charles Darwin as early as 1880 (Darwin 1880, Rich and Watt 2013) who investigated the architecture of a single roots growing in wet sponges and their response to gravity. Since then a multitude of different approaches have been used to investigate RSA of plants ranging in scale from large trees to pots grown seedling plants(Clark *et al.* 2013, Landl *et al.* 2018).

Many of the traditional methods of studying plant RSA involved the excavation of intact root systems from soil and subsequently washing the soil off the roots on using running water before measurements are done (Smit *et al.* 2000). Before the advent of light scanning, washed roots where traced on pieces of paper for quantification of different root properties of interest to each investigation (Darwin 1880, Weaver 1919, Downie *et al.* 2015). This process was labour intensive and was often marred in inaccuracies and were subjective in nature (Downie *et al.* 2015). With the advent of relatively cheap, high-resolution flatbed scanners and cameras, the process of analysis of roots excavated from soil has become more accurate and allowing for higher throughput in the analysis of RSA of different plants (Ortiz-Ribbing and Eastburn 2003, French *et al.* 2009).

The major advantage of studying RSA using traditional methods is that they are relatively simple and inexpensive thus allowing for a large number of experiments to be carried out. The primary drawback with many of the traditional methods of visualisation and quantification of RSA, on the other hand, stems from the fact that even though root systems grow in 3D, these techniques only characterise root properties in two of the three dimensions, thus omitting vital information about root growth and distribution in space. Traditional RSA characterisation methods are also labour intensive and time-consuming thus preventing high throughput when studying RSA. Also, root washing often results in the accidental loss of some root material especially when looking at plants with fine root systems. They are also invasive and thus this prevents the investigation of the development of roots over time.

1.5.2 Contemporary non-invasive imaging

Non-invasive soil radiography and tomography scanning such as X-ray, neutron, Magnetic Resonance Imaging (MRI) and gamma-ray CT scanning methods have recently been gaining popularity in the assessment of RSA as well as different rhizosphere processes (Southon *et al.* 1992, Tumlinson *et al.* 2008, Oswald *et al.* 2015, Pfeifer *et al.* 2015). This is due to their ability to allow the imaging of roots in opaque and obscure mineral soil. This thus allows for the analysis and characterisation of plant-soil interactions and their evolution over time. Information obtained from non-invasive scanning is quantifiable and enables the modelling of root system properties as well as allowing the study of soil properties such as pore size distribution, bulk density and compaction (Helliwell *et al.* 2013, Tracy 2013). The different imaging techniques of interest to this study include:

a) <u>Conventional X-Ray CT systems</u>

Of the various non-invasive imaging techniques available, X-ray CT has proved the most popular in the study of RSA studies. This is due to its suitability for use in wide a variety of types of soil such as those containing paramagnetic soil components (e.g. Ferrasols) that technologies such as Magnetic Resonance Imaging (MRI) and Nuclear Magnetic Resonance (NMR) would not be suitable for use. Pioneered in the 80's using costly (at the time) medical X-ray CT scanners, the use of X-ray CT methods have rapidly evolved and are now widely used to visualise, not only root-soil associations but also the interaction of plant roots and other soil organisms in situ. This can enable the 3D mapping of root structural architectures and their interaction with the soil (Tracy *et al.* 2010, Martin *et al.* 2012, Mairhofer *et al.* 2013, Keyes *et al.* 2016).

$$I = I_0 . e^{-\Sigma . d} \qquad [4]$$

X-ray CT scanners work based on the Beer-Lambert law as described by equation [4] where I_0 is the incident X-ray beam, which produces an attenuation of I when passing through a material of d thickness, governed by a linear attenuation coefficient Σ, dependent on the radiation energy principle of the different attenuation values produced by materials of different densities when exposed to X-rays (Wildenschild *et al.* 2002, Mooney *et al.* 2012). This difference of attenuation of rays produced by an emitter captured by a detector is then used to create a 2D image in the plane of view. These images are then combined together using computer reconstruction software to produce a 3D image of a sample. Three different categories of scanners are available, the medical, industrial and synchrotron X-ray scanners illustrated in Figure 2.

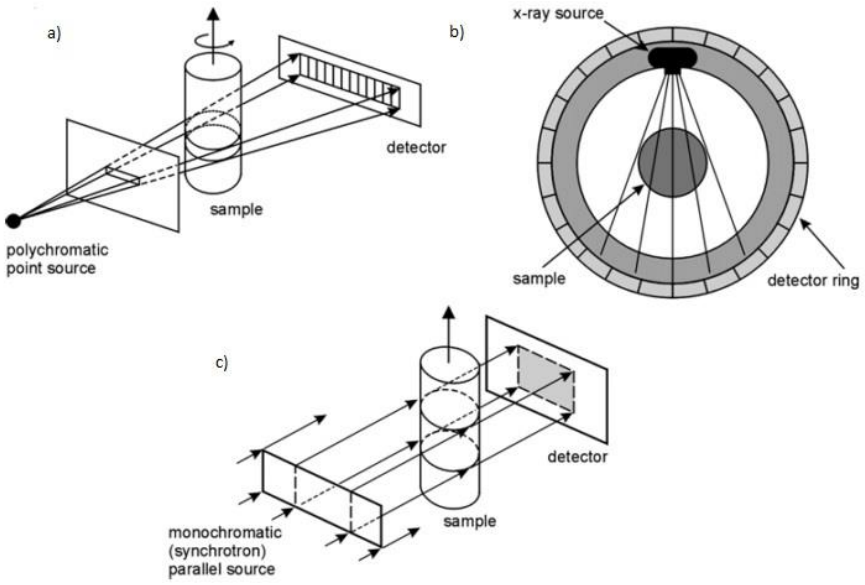

Figure 2: Different categories of available X-Ray CT scanners with a) Industrial system, b) Medical system, c) Synchrotron [Source (Wildenschild *et al.* 2002)]

The medical scanners have been the most extensively used in soil structural studies. These, however, are optimised to produce images of human and animal tissues and thus are restricted in their use in soil studies as they use low dose X-rays that often fail to penetrate soils. Industrial scanners have optimized energy X-rays and are now increasing in popularity as x-ray technology is becoming cheaper. Lastly, the synchrotron X-ray scanners are the least used in soil structural studies due to their relatively prohibitive cost. This is despite the fact that they produce higher intensity beams that limit noise in scanning whilst also reducing the time taken for each scan. The use of X-ray CT scanners in soil observation is associated with various challenges. One of the major challenges involving X-rays CT techniques is the compromise between sample size and image resolution with larger sample sizes often leading to a reduction in image resolution (Pires *et*

al. 2010). Problems also arise from the difficulties in resolving between materials that have similar densities and thus attenuation of X-rays, e.g. between roots, organic matter and air-filled pores. Comparability between different scanning equipment and protocols also limits this technology with human subjectivity in segmentation in image processing software and image quality differences sighted as the source of variances between measurements. Despite these and other challenges however, X-ray CT scanning of soil remains an invaluable resource for root and soil structural analysis and will thus be used in this study to assess soil structure in combination with other invasive methods in this study.

b) <u>X-Ray Synchrotron imaging (XRSI)</u>

XRSI systems are broadly similar to conventional X-Ray imaging systems with the difference that XRSI use a parallel monochromatic X-ray beam (unlike cone or planar fan beam in conventional X-ray systems) generated by a synchrotron light source (Aravena *et al.* 2013). A synchrotron light is a form of electromagnetic radiation produced when fast-moving polarised high energy particles are forced to alter their direction by a strong magnetic field as (Vijayan *et al.* 2015, ESRF 2019). This occurs in an imaging system similar to the one illustrated in Figure 3B. XRSI systems are able to produce images with much higher resolutions as compared to conventional systems (Vijayan *et al.* 2015). This is because they produce a beam with a much higher brilliance (high photon flux) in comparison to conventional systems as illustrated in Figure 3A. This makes XRSI highly suitable for applications requiring high-resolution images as the resolution of images produced ranges from 1-50μm as opposed to 10-100μm in conventional industrial X-Ray systems (Aravena *et al.* 2013). As a result of this very high image resolution features such as root hairs and soil microorganisms can successfully be visualised in detail (Koebernick *et al.* 2017).

The limitations associated with the use of XRSI systems in RSA studies include their poor sensitivity to low-density materials such as roots. XRSI also produces images that contain artefacts (although generally lower than those from conventional systems) e.g. from beam hardening and X-Ray scattering (Aravena *et al.* 2013). Being parallel beam-based, XRSI systems are limited in terms of sample sizes they can scan at a time with several scans often being required to fully image the RSA of a single plant pot. As XRSI facilities are complex, requiring large expensive operational facilities to generate synchrotron light sources, this limits the general availability such imaging systems with only around 50 (operational or under construction) facilities available world (Lightsources.org 2019).

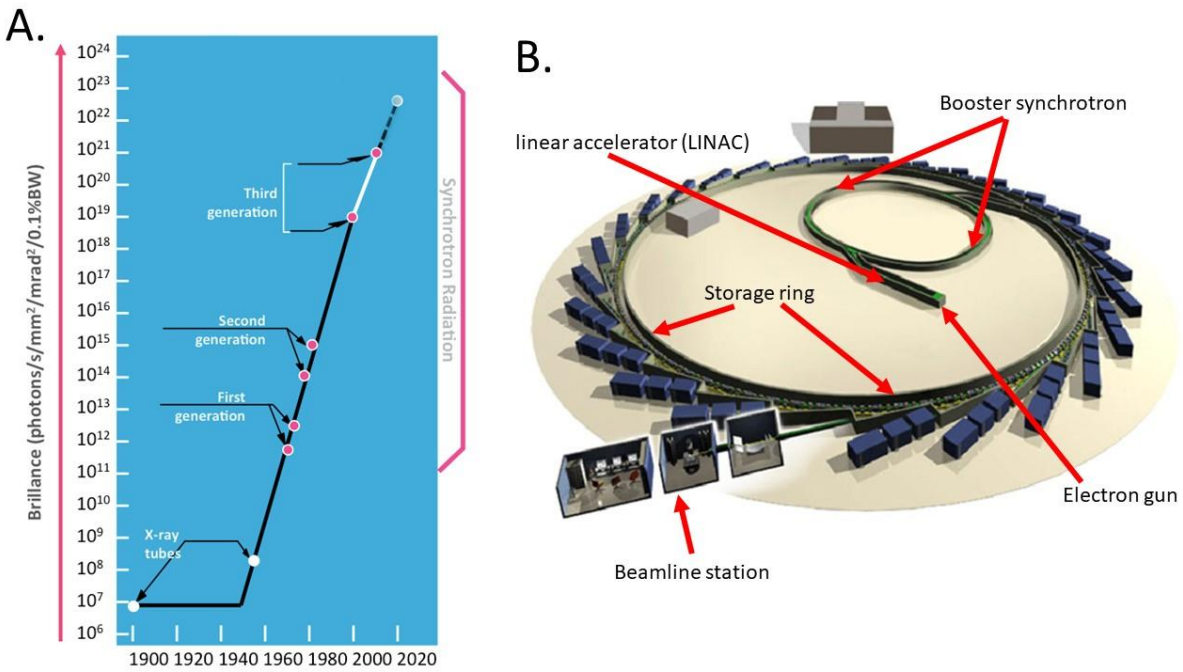

Figure 3 Graph showing the brilliance of different X-Ray systems and how the brilliance of XRSI facilities have improved over the generations. B) A simplified illustration of an XRSI facility showing the important operational components [Adapted from (Diamond Light Source 2019, ESRF 2019)]

c) Neutron Imaging

Neutron imagery is another non-invasive imaging technique that involves the use of subatomic particles (neutrons) which are able to penetrate different substances with varying degree of attenuation (Strobl *et al.* 2009). Similar to X-ray imaging, it is governed by Beer-Lambert law (eq 4). Neutrons, however, unlike X-rays are not charged and thus interact with nuclei instead of electrons (Tumlinson *et al.* 2008, Moradi *et al.* 2013). As a result, neutrons are able to penetrate through some substances that would ordinarily stop X-rays such as electron-dense metals e.g. Lead. On the other hand, neutrons are heavily attenuated by elements with dense nuclei that would normally allow X-Rays to pass such as water (containing normal hydrogen) and glass (often containing boron). The interaction of X-rays and neutrons with matter and different elements with X-Rays is illustrated in Figure 4. As a result of this variable interaction with matter, X-Ray and Neutron imagery are often considered complementary to each other as attenuation differences enable the highlighting of different features this providing a more detailed view of complex features (Oswald *et al.* 2008, Karch *et al.* 2017).

Neutrons used for NI are generated by nuclear fission in large, high energy nuclear reactors or spallation sources were high energy protons hit a massive target (spallation source). This produces fast moving high energy neutrons that are then channelled towards a moderator (usually water or heavy water [D_2O]) that reduces their energy levels (cold [low] or thermal [high]) (Anderson 2009,

Kockelmann *et al.* 2013). This makes them useful for different applications such as imaging and diffraction. After this, a collimator is then used to sort the neutrons by energy level before guiding them towards an imaging station where they can be used for imaging. A simplified schematic view of a neutron facility is shown in Figure 5.

A

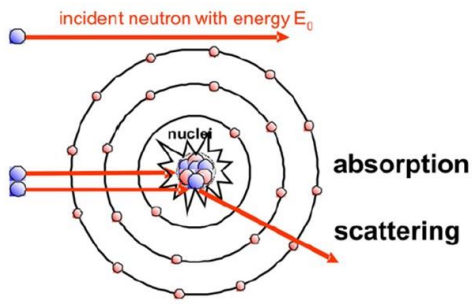

B

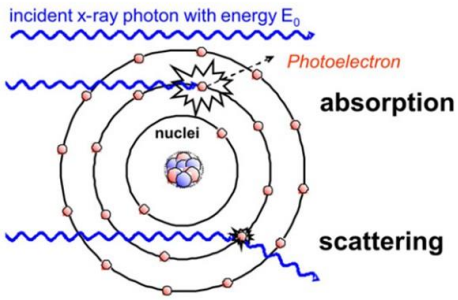

C.

1a	2a	3b	4b	5b	6b	7b	8			1b	2b	3a	4a	5a	6a	7a	0
H 0.02																	He 0.02
Li 0.06	Be 0.22											B 0.28	C 0.27	N 0.11	O 0.16	F 0.14	Ne 0.17
Na 0.13	Mg 0.24											Al 0.38	Si 0.33	P 0.25	S 0.30	Cl 0.23	Ar 0.20
K 0.14	Ca 0.26	Sc 0.48	Ti 0.73	V 1.04	Cr 1.29	Mn 1.32	Fe 1.57	Co 1.78	Ni 1.96	Cu 1.97	Zn 1.64	Ga 1.42	Ge 1.33	As 1.50	Se 1.23	Br 0.90	Kr 0.73
Rb 0.47	Sr 0.86	Y 1.61	Zr 2.47	Nb 3.43	Mo 4.29	Tc 5.06	Ru 5.71	Rh 6.08	Pd 6.13	Ag 5.67	Cd 4.84	In 4.31	Sn 3.98	Sb 4.28	Te 4.06	I 3.45	Xe 2.53
Cs 1.42	Ba 2.73	La 5.04	Hf 19.70	Ta 25.47	W 30.49	Re 34.47	Os 37.92	Ir 39.01	Pt 38.61	Au 35.94	Hg 25.88	Tl 23.23	Pb 22.81	Bi 20.28	Po 20.22	At	Rn 9.77
Fr	Ra 11.80	Ac 24.47	Rf	Ha													

Lanthanides	Ce 5.79	Pr 6.23	Nd 6.46	Pm 7.33	Sm 7.68	Eu 5.66	Gd 8.69	Tb 9.46	Dy 10.17	Ho 10.91	Er 11.70	Tm 12.49	Yb 9.32	Lu 14.07
*Actinides	Th 28.95	Pa 39.65	U 49.08	Np	Pu	Am	Cm	Bk	Vf	Es	Fm	Md	No	Lr x-ray

D.

1a	2a	3b	4b	5b	6b	7b	8			1b	2b	3a	4a	5a	6a	7a	0
H 3.44																	He 0.02
Li 3.30	Be 0.79											B 101.60	C 0.56	N 0.43	O 0.17	F 0.20	Ne 0.10
Na 0.09	Mg 0.15											Al 0.10	Si 0.11	P 0.12	S 0.06	Cl 1.33	Ar 0.03
K 0.06	Ca 0.08	Sc 2.00	Ti 0.60	V 0.72	Cr 0.54	Mn 1.21	Fe 1.19	Co 3.92	Ni 2.05	Cu 1.07	Zn 0.35	Ga 0.49	Ge 0.47	As 0.67	Se 0.73	Br 0.24	Kr 0.61
Rb 0.08	Sr 0.14	Y 0.27	Zr 0.29	Nb 0.40	Mo 0.52	Tc 1.76	Ru 0.58	Rh 10.88	Pd 0.78	Ag 4.04	Cd 115.11	In 7.58	Sn 0.21	Sb 0.30	Te 0.25	I 0.23	Xe 0.43
Cs 0.29	Ba 0.07	La 0.52	Hf 4.99	Ta 1.49	W 1.47	Re 6.85	Os 2.24	Ir 30.46	Pt 1.46	Au 6.23	Hg 16.21	Tl 0.47	Pb 0.38	Bi 0.27	Po	At	Rn
Fr	Ra 0.34	Ac	Rf	Ha													

*Lanthanides	Ce 0.14	Pr 0.41	Nd 1.87	Pm 5.72	Sm 171.47	Eu 94.58	Gd 1479.04	Tb 0.93	Dy 32.42	Ho 2.25	Er 5.48	Tm 3.53	Yb 1.40	Lu 2.75
**Actinides	Th 0.59	Pa 8.46	U 0.82	Np 9.80	Pu 50.20	Am 2.86	Cm	Bk	Cf	Es	Fm	Md	No	Lr neut.

Figure 4 A) Neutron and B) X-Ray interaction with matter illustrating the scattering and absorption relative to different materials. Periodic table of elements highlighting C) X-Ray attenuating coefficient (cm^{-1} at 100keV) and D) Thermal neutron attenuating coefficients (cm^{-1}) for each element. [Source (Strobl *et al.* 2009, Moradi *et al.* 2013)]

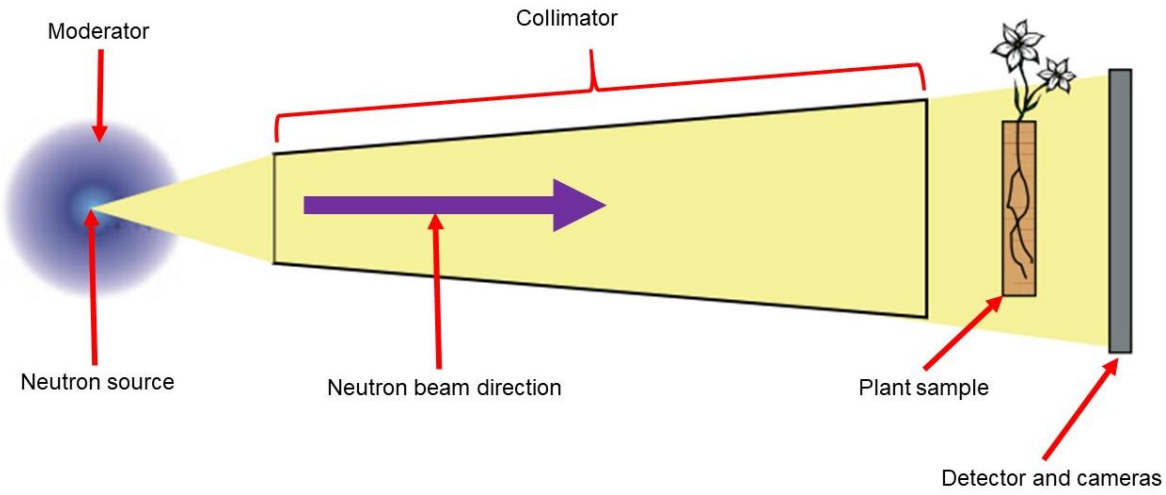

Figure 5 Simplified schematic diagram showing the essential components of a neutron imaging facility. [Adapted from (Robinson *et al.* 2008)]

One of the biggest factors that make NI attractive to plant science is that the imaging technique is sensitive to water (containing nuclei dense hydrogen) whilst easily passing through minerals in soil (Si and Al-containing). This makes NI ideal for the visualisation of plant RSA in situ as contrast between roots (which normally contain >80% water) and mineral soil is high. This sensitivity to water also makes it possible for the visualisation of plant water dynamics within the soil. NI is better for visualisation of water dynamics as compared to other techniques sensitive to water such as MRI as it is not sensitive to magnetic and paramagnetic soil components, which often hinder the use of MRI technology in a wide variety of soils. The ability of NI to discriminate between different isotopes of hydrogen, ^{1}H and ^{2}H (Deuterium) allow for the use of heavy water (D_2O) as a tracer of water movement that has nearly identical properties (Zarebanadkouki *et al.* 2013, 2014, Tötzke *et al.* 2017).

Like many other imaging techniques, NI has its flaws. One of the biggest drawbacks to the use of NI in plant science is the limited penetration capacity of neutrons due to the low energy (cold neutron) of the neutrons used in most facilities (Strobl *et al.* 2009). This limits the sample that can be imaged to only a few cm thickness (2cm in this study). Higher energy beams neutron sources are available which have better penetration but this comes at a cost to image resolution which is already a magnitude lower than in X-Ray imaging. Another major drawback of NI is that due to the size and complexity of neutrons sources, NI similar to X-Ray synchrotron imaging is primarily only done in limited, specialised facilities across the world. (Lehmann 2017) was able to identify only 17 operational 'state of the art' imaging neutron sources worldwide. Finally, since NI is sensitive to hydrogen, this also limits its use to predominantly sandy soils that contain little or no organic matter to optimise root: soil contrast (Menon *et al.* 2007, Wang *et al.* 2019).

1.6 Soil structure and health

Soil structure is an essential soil physical property defined as the three dimensional arrangement of soil mineralogical primary units (clay, silt and sand) in space which includes their biochemically mediated coalescing into secondary structural units, the soil aggregates, giving rise to a defined pore volume (Jastrow and Miller 1991, Lal and Shulka 2004, Bronick and Lal 2005). Unlike soil texture, a generally stable soil property, soil structure is a dynamic soil entity that can be modified by human activities via different land management strategies such as tillage and heavy vehicle traffic (Oades 1993, Munkholm *et al.* 2013, Nyamangara *et al.* 2014). It is also influenced by different natural phenomena such as climate and is dependent on soil texture. Soil structure is one of the most important soil properties considered when establishing soil health. Soil health being defined by Pankhurst et al. (1997) as the sustained capacity of soil to function as a vital living system within ecosystem and land-use boundaries, to sustain plant and animal productivity, maintain or enhance water and air quality, and promote plant, animal and human health.

The aggregation of soil is the fundamental basis for the establishment of soil structure in most soils. Due to the heterogeneous nature of soil, however, the precise mechanisms of aggregate formation and stabilisation are complex and not well understood with various models being suggested in literature e.g. Emmerson's model (1965) and the quasi crystal theory (1971). Generally, however, aggregation is thought to originate from two successive processes that are essential but not sufficient for soil aggregate formation, namely flocculation and cementation (Hillel 2004, Bronick and Lal 2005). The initial process of flocculation of clays is mediated by several forces, namely the inter- and intra- molecular, van der Waals, gravitational and electrostatic forces that allow clay particles to adhere to each other forming clay domains. This adhesion is strongly governed by the charge of the cations dominating a soil solution such that when monovalent cations such as sodium (Na^{+}) (e.g. in Sodic soils) dominate the solution, an expansion of the electrical diffuse double layer (EDDL) around clay particles cause repulsion and dispersion. On the other hand, dominance of di- and tri- valent cations (e.g. Ca^{+2} and Al^{3+}) results in the reduction of the EDDL and enhanced flocculation. After flocculation, cementation of soil takes precedent with flocculated particles being bound together by a variety of cementing agents (usually organic matter, carbonates and various iron and aluminium oxides) that act as a 'glue' stabilising flocculated clay particles and giving rise to micro- and macro-aggregates that are a prerequisite for soil structural differentiation as shown in Figure 6.

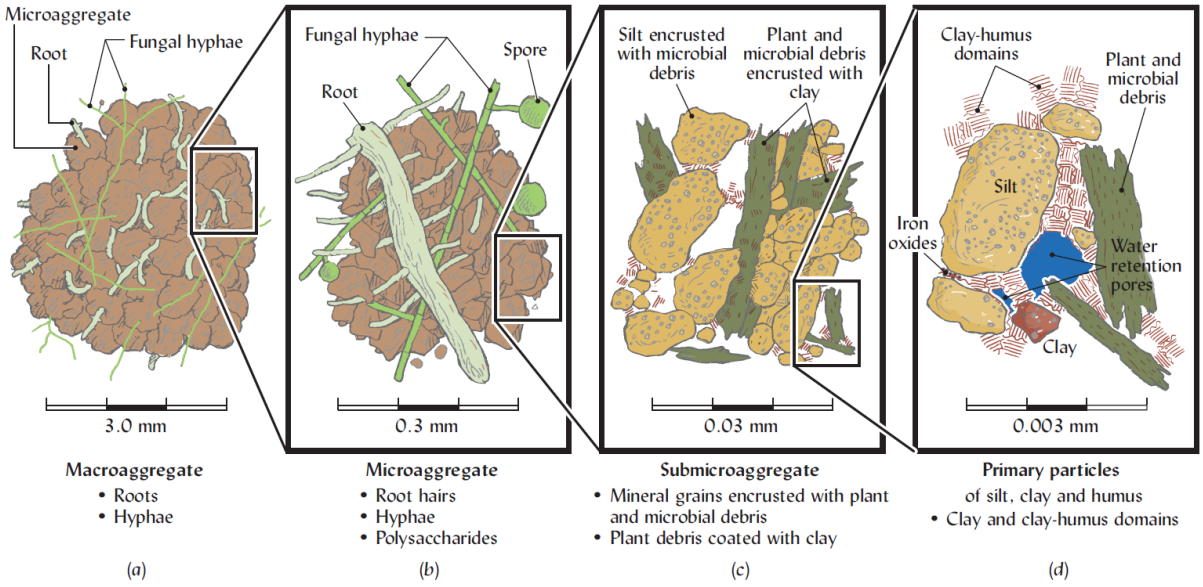

Figure 6: An Illustration of the hierarchical organisation of aggregates showing various soil materials that give rise to soil aggregates [Source: (Brady and Weil 2017)]

The importance of soil structure to life on earth cannot be overemphasised, contributing to several processes enabling plant growth whilst performing vital ecosystem services. Maintenance of good soil structure is paramount for sustainable food production with good soil structures enhancing root penetration thereby fostering better plant establishment through the prevention of surface crusting and sealing (Bronick and Lal 2005). Soil structure also determines the porosity of a particular soil which not only allows for the infiltration of water to plant roots but also enables the aeration for subterranean plant roots which is essential for their respiration during growth (Braunack and Dexter, 1989; Materechera *et al*, 1994). It is also critical for various ecosystem services including the storage and sequestration of carbon as the soil is the greatest sink for atmospheric carbon, encompassing approximately 1500 billion tons of carbon (Scharlemann *et al.* 2014). Soil structure is not only important for the carbon cycle but also facilitates cycling and storage of other nutrients such as nitrogen and phosphorus (Six *et al.* 2004). Good soil structure can also increase the quality and amount of groundwater resources as with improved structure the soil reduces runoff thus increasing groundwater recharge and becomes a more efficient filter of penetrating groundwater (Bronick and Lal 2005). Stable soil structures also have the ability to resist soil erosion, a process that may lead to water body siltation. Maintenance of a good soil structure also improves environmental quality as it creates a habitat for soil fauna and microbes thus enhancing biodiversity which enables efficient nutrient cycling within the soil (Blankinship *et al.* 2016).

1.7 Soil structural assessment

Despite the profound importance of soil structure to global livelihoods, its assessment has for long been a contentious matter in soil science mainly due to the heterogeneous and dynamic nature of soils (Díaz-Zorita *et al.* 2002). Available methods for soil structural assessment are often bespoke and often determined by the application of the intended assessment. Lal & Shulka (2004) identified two broad categories of structural assessment, namely field (pedological) as well as a diverse range of laboratory methods of soil assessment as outlined in Figure 7.

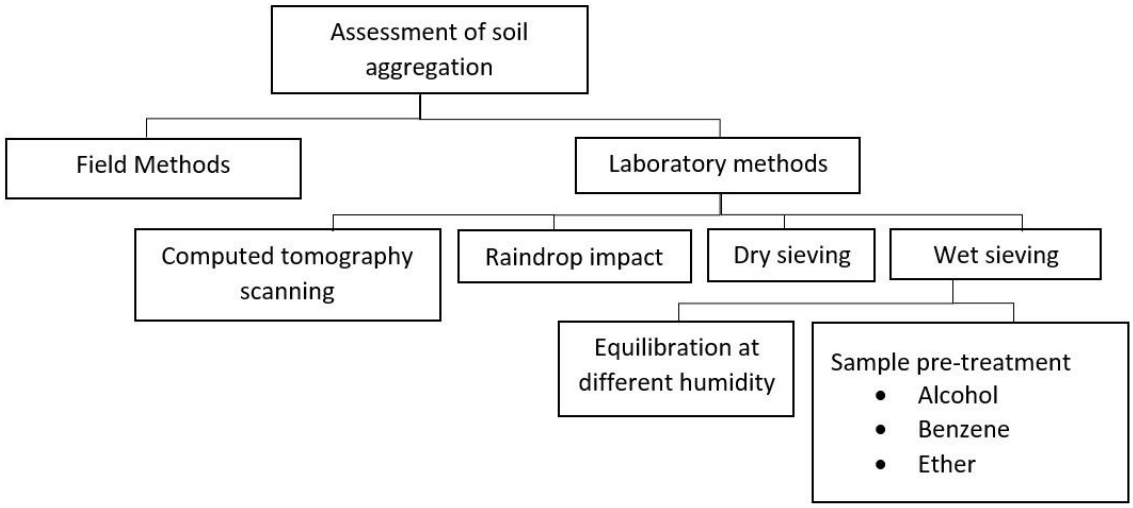

Figure 7: Methods of soil structural assessment [Adapted from Lal and Shulka (2004)]

Field methods of soil structural assessment are qualitative rather than quantitative and due to this are often not reproducible and require a great degree of expertise to carry out. They are, however, used for soil taxonomy alongside other relevant tests. An attempt to quantify qualitative field methods in recent years has led to the introduction of two soil scoring systems, the Visual Soil Assessment (VSA) and the Visual evaluation of soil structure (VESS) as proposed by Shepherd (2000) and Ball *et al.* (2007) respectively.

Laboratory methods of soil structural assessment often use a uniform means of soil disturbance assessing how soil structure resists variable perturbation. Many of the traditional laboratory methods assess aggregate distribution and stability via sampling and subsequent sieving to separate different aggregate size classes (Nimmo and Perkins 2002). The nature and magnitude of the perturbations of soil aggregates vary from wet sieving, usually performed to assess stability of aggregates to erosion by water, whilst simulation of raindrop impact assesses the susceptibility to splash erosion. An important consideration when using water to assess aggregate stability is the initial water content with dry aggregates and being more susceptible to slacking as compared to

moist aggregates. It is thus essential to have aggregates at an equilibrium water content to obtain comparable results. Dry sieving is less frequently used and generally determines soils resistance to wind erosion and also gives the fractional distribution of soil aggregates in the soil.

1.8 Soil structural modification by WUE plants

Despite the great strides that have been made in the genetic development of WUE plants over recent years, relatively limited research has been carried out to investigate their role in influencing soil properties. Many of the published articles seem to focus on the effect increased WUE on crop physiology and yield. It is however also essential to look at the effects of WUE plants on soil properties as the soil influences plant productivity and sustainability of agricultural systems. Sposito (2013) stressed the importance of understanding soil-plant feedbacks noting their role in enhancement of productivity and the fostering of a holistic approach to attaining agricultural sustainability. Although the effects of the soil properties on crop growth as well as the converse effect of plant growth on soil properties are relatively well known, Ehrenfeld et al. (2005) duly note that clear demonstrations of the of plant-soil feedbacks are lacking despite abundant evidence that their independent occurrence is available.

Plants generally play a major role in modifying soil structure. Angers & Caron (1998) identified five major effects of plants on soil structure. These are (i) Root penetration, which can exert pressure up to 2MPa on soil, compressing the soil thus resulting in pore formation and enlargement. Root penetration has also been noted to enhance water flow as well as fragmenting compact soil. (ii) Modification of soil moisture regime, which mainly affects soils with shrinking and swelling clays like smectite and results in the development of macropore cracks caused by differential desiccation of soil. An increase in soil strength is generally expected. (iii) Soil enmeshment, enabling the stabilisation of soil aggregates and enhancement of soil strength-giving rise to better soil resistance. (iv) Rhizosphere effects are associated with the stabilisation of soil aggregates within the vicinity of roots. This can occur via the production of exudates as well as the alteration of the chemical ion composition the around roots, which encourages microbial growth that then enhances rhizosphere soil stability. (v) Carbon input via root and shoot decay which plays a major role in the stabilisation of soil aggregates whilst also encouraging the growth of soil organisms, providing them with a suitable energy source. Root associated organisms have also been noted to change soil structure by stabilising aggregates with arbuscular mycorrhizal fungi playing a major role in this effect (Hallett *et al.* 2009, Daynes *et al.* 2013).

Plants with altered WUE patterns have the potential to affect the soil in a different way as compared to more conventional plants. For instance, as plants with reduced stomata generally

transpire less; this could reduce their water uptake capacity which decreases their impact on the soil moisture regime of associated soil. This may have a negative impact on soil structure as the alteration in soil moisture as induced by roots is known to improve soil aggregate stability (Materechera *et al.* 1994, Angers and Caron 1998). A reduction in differential desiccation would also result in a decrease in macropore cracking, which reduces preferential water and airflow. The increase in root biomass production as shown by Karaba et al. (2007) overexpressor of the gene HARDY, which affects WUE, could also positively affect soil structure as increased root biomass generally affects soil structure positively. Karaba et al. (2007) also showed an increase in the root entanglement of soil in WUE plants which could potentially lead to an increase in their ability to stabilize and strengthen aggregates.

With the seemingly complex relationship between root properties of WUE plants and soil structure, there is need to evaluate experimentally how different changes in root and water use patterns affect soil structure, either confirming or dispelling the possible effects that could be concluded from literature. This research will thus delve into it, assessing the impact of soil-plant relations of identified plant mutants on soil structure.

1.9 Research aims and key questions

The overall aim of this study was to investigate the impact of genetically altering plant WUE on the RSA and soil structural stability in plants of three different species, namely Arabidopsis, wheat and rice. The key research objective and questions that I aimed to answer in fulfilment of this aim for all the species grown were:

a) Identify plant genotypes that show significantly altered WUE as compared to the wild type plants.
b) How do physiological properties of the identified mutants compare to that of the wild type plants?
c) How does the alteration in WUE of the mutant plants affect their RSA?
d) How does the soil structural stability of a sandy loam soil respond to the growth of plants with altered WUE as compared to wild type plants?

These are investigated in the forthcoming chapters with chapter 2 outlining Methods and materials used whilst Chapter 3, 4 and 5 investigate the different species individually then concluded by a general discussion (Chapter 6).

II Methods and materials

2.1 Seed lines

2.1.1 Arabidopsis seed lines

Table 3 List of Arabidopsis seed lines used in this study

Name	Phenotype	Reference
Columbia-0 (Col 0)	Wild type	
phyB-9	Reduced chlorophyll, narrower leaves, early flowering, shorter root	Reed et al. (1993)
werewolf (*wer*)	Excessive root hairs (both hair and non-hair positions)	Lee & Schiefelbein (1999)
ethylene insensitive root (eir1-1)	An auxin efflux carrier. Agravitropic roots and reduced lateral roots.	Luschnig et al. (1998)
caprice (*cpc-1*)	reduced root hairs	Schellmann et al. (2002)
root hair defective (rhd1)	Abnormally shaped roots hairs.	Schiefelbein (1990)
auxin response factors (*arf7-1 arf19-1)*	Auxin response factors. Double mutant has severe reduction in lateral roots.	Okushima et al. (2007)
glabra1 and root hair defective2 (*gl1-1, rhd2-1*)	Defective root hairs, absent trichomes	Aida et al. (2002); Blilou et al. (2005)
epidermal Patterning factor2 (epf2-1)	Increased stomatal density	Hunt & Gray (2009)
EPIDERMAL PATTERNING FACTOR2 Overexpressor *(EPF2OE)*	Reduced stomatal density	Hunt & Gray (2009)

2.1.2 Wheat seed lines

Table 4 List of Wheat seed lines used in this study

Name	Phenotype	Reference
Fielder (WT)	Wild type var. Fielder	
TaEPF1OX1 (line 1)	Reduced stomatal density	(Dunn *et al.* 2019)
TaEPF1OX2 (line 2)	Reduced stomatal density	(Dunn *et al.* 2019)
phyB-null		(Pearce *et al.* 2016)

2.1.3 Rice seed lines

Table 5 List of rice mutant lines used in this study

Name	Reference
Nipponbare (WT)	
phyA-4	(Takano *et al.* 2001)
phyB-1	(Takano *et al.* 2001, Takano, Inagaki, *et al.* 2005)
phyB-2	(Takano *et al.* 2001, Takano, Inagaki, *et al.* 2005)
phyC-1	(Takano *et al.* 2001, Takano, Inagaki, *et al.* 2005)
phyA-4 phyC-1	(Takano *et al.* 2001, Takano, Inagaki, *et al.* 2005)
phyA-4 phyB-1	(Takano *et al.* 2001, Takano, Inagaki, *et al.* 2005)
phyA-4 phyB-1 phyC-1	(Takano *et al.* 2001, Takano, Inagaki, *et al.* 2005)

2.2 Plant growth conditions

2.2.1 Growth environment

All plants used in this research were grown in specially designed plant growth spaces with conditions optimised to suit the plant species in question. Arabidopsis was grown at the Sir David Read Controlled Environment Facility, in a chamber maintained at a temperature of 22°C (day)/18°C (night) (SD ±2°C) and at a relative humidity of 55% with a 9 hour day length. Arabidopsis plants were grown at a distance of 30cm (maximum) from the light source and received light averaging 180 μmol m^{-2} s^{-1} (±15 μmol m^{-2} s^{-1}) in intensity at plant height.

Wheat plants were grown in an air-conditioned room maintained at a temperature of 22°C (day)/18°C (night) (SD ±2°C) with ambient relative humidity. These plants received light at an intensity of 400 μmol m^{-2} s^{-1} (±20 μmol m^{-2} s^{-1}) at top of canopy level with a photoperiod of 12 hours. Rice plants were grown in a growth room maintained at 26°C (day)/22°C (night) with ambient relative humidity. These plants received light with an average intensity of 500 μmol m^{-2} s^{-1} (±30 μmol m^{-2} s^{-1}) and a 16 hour (Long) or a 9 hour (Short) day length.

2.2.2 Growth Media

In terms of growth media, several plant growth substrates were used in this thesis. As the main aim of my thesis was studying the interactions between plants and soil, most of the experiments I carried out, unless otherwise stated, were done a sandy loam soil obtained from Cove farm in Doncaster (53°30'03.7"N 0°53'57.2"W) sieved to <4mm. This soil had the physical and chemical properties as outlined in Table 6 that were determined in experiments described in Section 2.3 and 2.4.

Table 6 Soil chemical and physical properties summary

								Exchangeable base cations (NH4OAc) (mg/100g)					cmol (+)/kg
Soil used	pH	EC (µS/cm)	%SOM	%Sand	%Silt	%Clay	%N	Na	K	Ca	Mg	P (mg/kg soil)	CEC
Bulk soil (4mm sieved)	6.8	205	5.59	70	16	14	0.19	3.02	27.85	349.50	28.35	35.49	20.63
<0.25mm fraction	6.9	262	5.51				0.22					28.00	
0.25-0.5mm fraction	7.0	182	3.58	74	14	12	0.14	2.04	26.20	283.00	22.50	25.64	16.74
0.5-1mm fraction	7.0	119	6.58				0.19					25.59	
1-2mm fraction	7.1	227	5.96				0.21					44.91	
2-4mm fraction	6.6	200	6.49	68	18	14	0.20	2.61	30.70	417.00	32.80	43.14	24.41

Other growth media used for plant growth

a) **Soil aggregates**

Soil aggregate fractions of the size classes: <0.25mm, 0.25-0.5mm, 0.5-1mm, 1-2mm and 2-4mm derived from the dry sieving of the sandy loam soil obtained from Cove farm with the chemical and physical properties as described in Table 6. These aggregates were used for the growth of Arabidopsis and Wheat plants.

b) **Compost**

Levington M3 high nutrient compost (204N 104P 339K) obtained from ICL Specialty Fertilizers (Suffolk, England) was used. This compost had a particle size of 1-10mm and pH of 5.3-6. It was used for most of the preliminary experiments done with Arabidopsis plants.

c) **½ Murashige and Skoog (MS) agar media**

This was made by dissolving 2.2g of MS media (SIGMA-ALDRICH, M5519-50L) (Murasnige and Skoog 1962) in 1L of deionised water and adjusting the pH to 5.7 by dropwise addition of 2-3 drops 1M KOH. This was then added to 6.4g of Plant Agar (Duchefa Biochemie, 1100g/cm2, P1001), mixed using a magnetic flea and then autoclaved at 121°C for 30 minutes (Brown 2018). This MS agar media was used in axenic vertical plate experiments.

2.3. Soil Chemical analysis

2.3.1 Soil pH and Electrical conductivity (EC) determination

The pH of soil samples was determined using a combined electrode (Jenway 3540) calibrated with pH 4 and pH 7 buffers. In this test 5g of air-dried soil was used for this procedure with 25ml (1:5 ratio) of either deionised water(pH_W) or 0.01M CaCl (pH_{CaCl}) being added to the soil. The soil solutions were shaken for either 60 (pH_W) or 30 minutes (pH_{CaCl}) before insertion of the pH meter into the soil suspension (Minasny *et al.* 2011, Hong *et al.* 2018). Measurements were taken only after waiting for 3-5 minutes for stabilisation of the reading from the electrode. Similarly, soil electrical conductivity was also measured using the (Jenway 3510) in the same distilled water solutions used to measure pH_W after similar shaking stabilisation of readings.

2.3.2 Total Soil Organic Carbon via loss on ignition

Total organic carbon was estimated by loss on ignition (Davras 1974, Hoogsteen *et al.* 2015). In this method, 5g of soil to be tested was weighed and dried at 105°C for a minimum of 24 hours then reweighed to determine the oven-dry mass of the soil. Afterwards, the samples were then

further furnaced in a Carbolite AAF 1100 ashing furnace (Carbolite, Hope Valley, UK) at 450°C for 24 hours then reweighed. The amount of carbon in the samples is estimated from the percentage lost weight from the oven-dry soil. The formula for this calculation is:

$$\%\ Organic\ Carbon = \frac{M_{105°C} - M_{450°C}}{M_{105°C}} \times 100 \quad [5]$$

The carbon estimated using this method includes both organic and possible inorganic C.

2.3.3 Total Nitrogen and Carbon (C:N analysis)

Total Nitrogen as well as Carbon (simultaneously), was determined using an Elementar Vario EL cube analyser (Hanau, Germany) set in C, N mode. In this method, soil samples were initially oven-dried at 105°C and then subsequently ball milled into a fine powder before analysis. During the analysis, samples(<1g) are heated at high temperature and the gasses from this furnacing are separated and analysed to determine the carbon and nitrogen in the samples as illustrated in Figure 8.

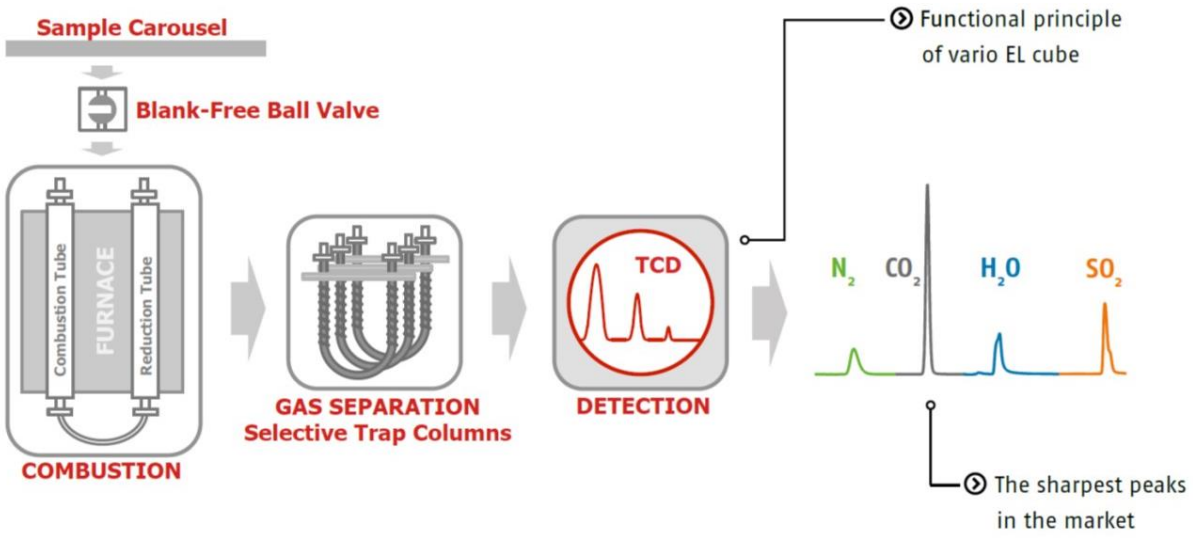

Figure 8 Operational principle of the Elementar Vario EL cube analyser illustrating the several steps used to determine Nitrogen and Carbon content in soils [Source Elementar Vario manual]

2.3.4 Available Phosphorous

Extractable Phosphorus was determined by using the P-Olsen method (Olsen *et al.* 1954, Carter and Gregorich 2006). In this method, approximately 1g of soil was added to 50ml of 0.5 M sodium bicarbonate in a centrifuge tube. This was shaken end-over-end for 30 min in and then centrifuged at 1000 g for 5 minutes to sediment out the soil. The supernatant liquid was then filtered through a 0.45µm syringe before analysis.

Determination of Phosphorus was done by the Vanadomolybdanate phosphoric acid colourimetric method adapted from Kuo, (1996). In this method, a 500µL aliquot of the supernatant liquid were mixed with 250 µL of the molybdanate reagent (2.1mM $[(NH_4)_6Mo_7O_{24}]$, 10.6mM NH_4VO_3, 39.5mM HNO_3 and 34.9mM H_2SO_4) and incubated in the dark at 37°C for 1 hour. This mixture was then transferred to a plate reader where the absorbance between 400 and 700nm of the samples were measured then compared to standard calibrated samples of known concentrations.

2.3.5 Potassium, and Cation Exchange Capacity

Available Potassium and Cation Exchange Capacity (CEC) of soil was determined using a modified version of the ammonium acetate (NH_4OAc) extraction method (Lavkulich 1981, Carter and Gregorich 2006). In this method, 2g of air-dry soil was added to 50ml of 1M NH_4OAc and shaken for 30 minutes on a horizontal shaker then centrifuged at 1000 g for 5 minutes to sediment out the soil. After this, the supernatant liquid was filtered using a 45µm filter and subsequently analysed for cations (including Potassium) using Inductively Coupled Plasma Mass Spectrometry (ICP-MS).

An alternative more classical method for determining soil CEC was also used (Chapman 1965). In this method, 5g of air-dry soil was added to 25ml of 1M NH_4OAc and shaken for 30 minutes on a horizontal shaker. This was then filtered using a 45µm filter, retaining the filtered soil. This process was repeated 3 times then the filtered soil was added to 20ml of 95% Ethanol and shaken for 1 hour in a horizontal shaker, repeating this ethanol washing for 3 times. After this washing 20ml of 1M KCl was used to extract the adsorbed NH_4 by shaking on a horizontal shaker for 1 hour for 5 times, centrifuging each time after shaking. The collected supernatant liquid (100ml) was then used to determine the CEC by measuring the previously adsorbed NH_4. This was measured by a Skalar San plus analyser (Breda, The Netherlands)

2.4 Soil Physical analysis

2.4.1 Soil textural analysis

Soil texture was determined using the standard hydrometer method (Day 1965, Carter and Gregorich 2006). In this method, as the samples had >2% organic matter, it was pre-treated with hydrogen peroxide (H_2O_2) overnight then heated over a bath at 90°C for 30 minutes before drying the soil in an oven at 60°C for 24 hours. After this, a 40g sample of this treated soil was then dispersed in 10% sodium hexametaphosphate (HMP) overnight and then placed in a 1l measuring cylinder and shaken vigorously before the soil was allowed to settle. After 40s a hydrometer measurement (R_{40s}) was made with a second reading being made at 7 hours(R_7). A blank

hydrometer measurement of the HMP is also taken then (R_L). These were then used in the calculation for sand, silt and clay as follows:

$$Sand\% = 100 - (R_{40s} - R_L) \times \frac{100}{\text{oven} - \text{dried soil (weight in grams)}} \quad [6]$$

$$Clay\% = (R_{7h} - R_L) \times \frac{100}{\text{oven} - \text{dried soil (weight in grams)}} \quad [7]$$

$$Silt\% = 100 - (Sand\% - Clay\%) \quad [8]$$

2.4.2 Soil aggregate stability tests

Several methods of assessing soil aggregate stability and distribution were used in this thesis. Initial experiments employed hand sieving of aggregates, which proved inconsistent as compared to more mechanical methods used in literature. As a result, a wet sieve shaking machine was developed in collaboration with engineers from the Mechanical Engineering department at the University of Sheffield. This machine is broadly similar in design to the one described by Kemper and Rosenau, (1986) which itself drew inspiration from the original design by Yoder, (1936). In this machine, 6 different sieves (100mm diameter) could be accommodated with an automated timer and adjustable shaking speed incorporated to enhance the accuracy and consistency of the wet sieving measurements. This designed machine is shown in Figure 9.

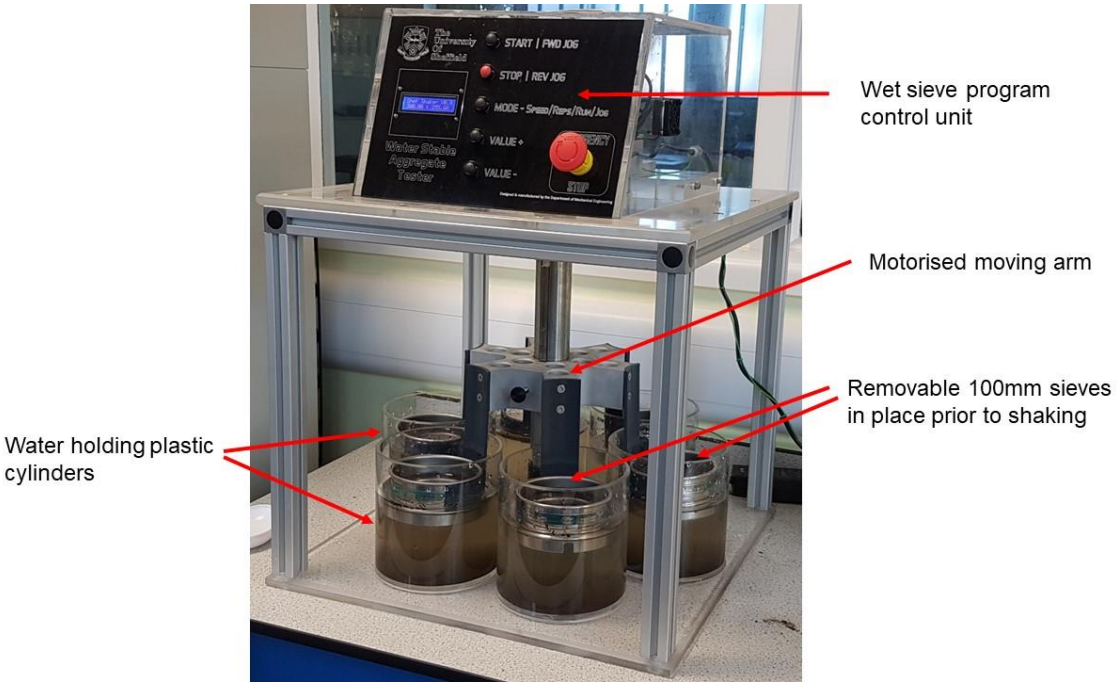

Figure 9 Automated wet sieve shaker used for wet aggregate stability tests.

a) Wet sieving of 1-2mm aggregates (Kemper and Rosenau 1986)

To determine the stability of aggregates of the 1-2mm size fraction, soil samples from different pots were oven-dried at 40°C for 24 hours to standardise the water content of the different samples under investigation. These were then dry sieved into the appropriate aggregate size class for analysis (1-2mm). A 4g (IM) sample of these aggregates was then placed on the top of a 250µm sieve and pre-wet in ethanol (a non-polar solvent) to reduce the slaking during sieving. The aggregates were then either hand stroked 60 times within a minute (manual sieving) or for 3min at a speed 35 cycles per minute (automated sieving) over a distance of 2.5cm. Enough water was used in either method ensuring aggregates were completely coved in water throughout the strokes. After this, the soil was washed into pre-weighed aluminium trays and dried for at 105°C for 24 hours then weighed to determine the dry mass of water-stable aggregates (SA). 10% w/v HMP was then added to the dried soil to chemically disperse it, this was further dispersed by placing in a sonicating bath or probe for 2min before re-sieving using the initial 250µm sieve. The remnants were then washed into the previously weighed aluminium tray and dried for 24 hours in a 105°C oven for 24 hours before weighing again to get the mass of coarse particles (CM). The percentage of water-stable aggregates (%WSA) is then calculated as follows:

$$\%WSA = \left(\frac{SA(g) - CM(g)}{IM(g) - CM(g)}\right) \times 100 \quad [9]$$

b) Multiple aggregate stability sieving

As a further extension of the method by Kemper and Rosenau, (1986) instead of using a single aggregate class, macro-aggregates of multiple sizes were used to determine the effect of different plants on soil aggregate stability. Aggregates of four different size classes encompassing all the macro-aggregates in the <4mm sieved soil were used, these were namely, the 0.25-0.5mm, 0.5-1mm, 1-2mm and 2-4mm aggregate fractions. A similar test to the one described in the previous section was applied with the exception that the aggregates were sieved using a sieve at the limit of their size i.e. the 0.25-0.5mm size class was sieved using the 0.25mm sieve whilst the 0.5-1mm aggregates were sieved using the 0.5mm sieved. The results of these tests were then calculated in a similar way to those from the previous experiment as well.

c) Wet aggregate size distribution

To determine the wet aggregate distribution of the samples under investigation, a method adapted from different studies was used (Kemper and Rosenau 1986, Amezketa *et al.* 1996, Haynes and Beare 1997, Nimmo and Perkins 2002). In this method, 25g of air-dried sample was wet sieved through several different sieves (0.25mm, 0.5mm, 1mm, 2mm,4mm) starting with the largest sieve size and subjecting it to 90 hand strokes in 3 minutes. Taking the remnants from each aggregate sieving process to the next sieve size up until all the sieves have been used. After this, the soil remaining on each sieve after sieving was then washed into pre-weighed aluminium trays and dried for at 105°C for 24 hours then weighed to determine their mass. These were then subsequently sieved in their corresponding sieve after dispersal with HMP as described in 2.4.2a to determine coarse particle fraction. The mean weight diameter (MWD) of each soil under review was then calculated using the formula

$$MWD = \sum_{i=1}^{n} x_i w_i \qquad [10]$$

Where w_i is the proportion of the sample with a mean size of x_i μm.

d) Dry Aggregate size distribution

To determine the distribution of aggregates of different sizes, air dry bulk soil samples were placed at the top of a series of sieves similar to those used in the previous experiments. These were shaken over by a mechanical Retsch AS 200 control vibratory tower sieve shaker (Haan, Germany) at a speed of 3g for 5 minutes and weighing the amount of aggregates retain by each sieve.

2.4.3 Field capacity determination

To determine the field capacity of different samples, packed and weighed soil columns were saturated with deionised water and then allowed to freely drain for 48 hours before being reweighed to determine the gravimetric moisture (θ_g) content at field capacity.

2.5 Plant analysis

2.5.1 Stomatal impressions

Stomatal impressions were done differently for the three plants in this thesis. For Arabidopsis 3 fully expanded leaves per plant for at least 4 plants of each genotype were removed from the plant and a thin layer of dental resin (Coltene, PRESIDENT) was applied onto the abaxial surface of each leaf and left to dry for at least 10 minutes. The resin was then removed from the leaf and a thin coat of nail varnish was applied onto the impressed resin and left to dry for at least 5 minutes. Clear tape was then used to remove the nail vanish from the resin impression then stuck onto a glass slide for viewing under a light microscope. For wheat stomatal properties, impressions of abaxial surface were made of either the 4th or 5th leaf at their widest point using the same method as described for Arabidopsis.

Leaf impressions of rice plants was also done on the 5th and 6th leaf however, clear nail varnish was applied directly to the leaf surface instead of using dental resin as applied for wheat and Arabidopsis. Clear tape was used to remove the nail varnish form the leaf and this was stuck onto a clear glass slide for viewing under a light microscope.

2.5.2 Microscopy

A light Leica DM IRBE Inverted Microscope with Planachromat 20x/ 0.4∞/ 0.17-A lens as well as a Brunel SP 150 microscope with a 6V Halogen lamp using a 20x lens was used for visualisation of abaxial stomata from the different plant impressions taken for stomatal and pediment cell counting with Z-Stack images being taken for each leaf section.

2.5.3 Stomatal counting

The Z-stack files obtained from microscopy were opened using ImageJ software (v.1.52p) which was calibrated using a stage micrometre prior to imaging. In this calibration, images were set to scale using distances obtained from micrometre images at the same magnification. As stomatal properties vary along the leaf surface, to attain a more uniform characterisation of stomatal properties, the different leaves were divided into 3 sections as illustrated in Figure 10. Stomatal properties for each different section were calculated and an average value across the entire leaf was determined.

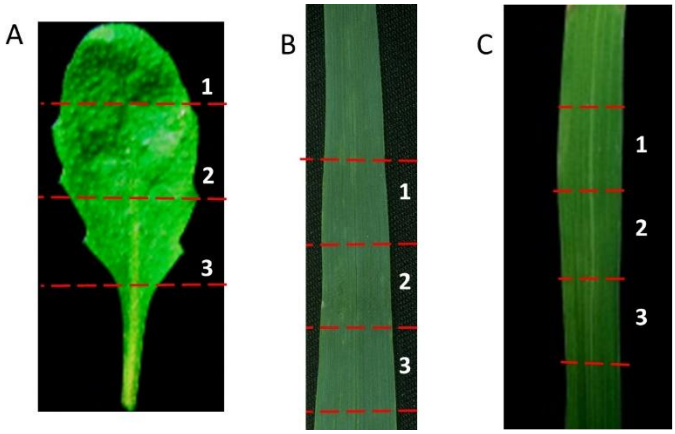

Figure 10 Diagram illustrating the different sections of the leaves where stomatal counts were made in A. Arabidopsis, B. Wheat and C. Rice plants.

For Arabidopsis leaves a 400x400 pixel Region of Interest (ROI) was selected which corresponded to a 0.16mm^2 region. Stomata and epidermal cells with a surface area 50% or more inside the ROI were counted with the data stored in a separate Microsoft Excel sheet. Stomatal and epidermal cell information obtained from counting was then used to calculate stomatal density (SD) per mm^2 of leaf area and Stomatal index (SI) using the following formula:

$$SD = \frac{Total\ number\ of\ stomata}{mm^2} \quad [11]$$

$$SI = \frac{Total\ number\ of\ stomata}{Total\ number\ of\ stomata + total\ epidermal\ cells} \times 100 \quad [12]$$

For rice and wheat leaves, instead of calculating stomatal index, the number of stomatal cell containing file lines as well as the total number of cell lines was counted in the FOV of the microscope (0.27mm^2). Stomatal density was also calculated from the FOV instead of the smaller ROI used for Arabidopsis.

2.5.4 Dry Weight Measurements

The dry weight of shoot and root biomass for all the different plants was determined by oven drying the plant material at 65°C for 48 hours then weighing the dry material to determine the dry biomass.

2.5.5 DNA extraction

This was done using Edwards method as described in Edwards, Johnstone and Thompson, (1991). In this method plant material was excised from relatively young leaf material that was approximately 5mm^2 in size from each plant. This was placed in a 2ml Eppendorf tube containing

a 5mm steel ball bearing and filled with 400 µl Edward's Solution (200mM Tris-HCl (pH7.5), 250mM NaCl, 25mM EDTA, 0.5% SDS). Leaf tissue was disrupted in a ball mill (Qiagen Tissuelyser) for 5minutes. The sample was centrifuged at 13,500rpm for 5-10mins before the supernatant liquid was transferred to another 2ml Eppendorf tube where 400 µl of isopropanol was added and mixed then the sample was again centrifuged at 13,500rpm for 5-10mins to precipitate the DNA. The supernatant liquid was aspirated and discarded then the DNA pellet was air-dried for 10 minutes before 100µl sterile water was added to it and mixed. This was stored at -20°C up until required (Brown 2018).

2.5.6 Polymerase Chain Reaction

Polymerase Chain Reaction (PCR) for the DNA samples used in this thesis was done using the methods described in Sigma Aldrich JumpStart™ RedTaq® ReadyMix™ PCR Reaction technical bulletin. In this method, the components used, including autoclaved H_2O, forward and reverse primers (10µM stocks), DNA template and RedTaq (Sigma-Aldrich JumpStart™ RedTaq® ReadyMix™ PCR Reaction Mix with MgCl2) were melted at room temperature. For use in each specific reaction was 25 µl of the RedTaq ready mix, 0.5 µl of each forward and reverse primer, 2.5 µl of DNA template and 21.5 µl in a 200 µl tube and mixed by vibrating the tubes then centrifuging down the contents to remove any air bubbles. These samples were then put into a thermal cycler (Biorad T1000) and set up to heat up the reagents to the cycles shown in Table 7. The results from this test were then analysed by running on an agarose gel.

Table 7 The thermal profile and incubation for the PCR reactions run using RedTaq (Adapted from the PCR Reaction technical bulletin)

	Step1	Step2	Step3	Step4	Step 5	Step 6	Step7
Temperature(°C)	95	95	55	72	Repeat steps 2-4 (×40)	72	12
Time (s)	300	30	30	60		300	∞

2.5.7 Gel Electrophoresis

PCR products were separated on 1% (w/v) agarose gels made from 1X TAE buffer solution with Alfa Aesar Ethidium Bromide $C_{21}H_{20}BrN_3$ (10mg/ml) added as a fluorescent indicator. This agarose gel prepared by microwaving for 3 minutes at (800W) to dissolve the components and then allowed to set on a transparent plate with a comb that created wells in the gel. The gel was then submerged in 1X TAE buffer and the samples loaded in each individual well alongside a DNA ladder (2.5µl GeneRuler, DNA LadderMix) to determine DNA fragment sizes. This gel was run at 120V for 20-30 minutes using BioRad mini sub-cell and power supply (Hercules, California).

Images of the gel products were visualised using the GelDoc-It™ system (UVP LLC) with the images being taken by the VisionWorks® LS analysis software (UVP LLC).

2.5.8 Thermal imaging

Thermal imaging was done on plants of varying ages in all the genotypes. These images were taken in the same growth chambers that the plants were grown under their normal growing conditions. The images were acquired using a FLIR T650SC (FLIR Systems AB, Taby, Sweden) handheld camera with adjustable colour grading according to a variable scale.

2.5.9 Carbon isotope discrimination

The plant leaves used to determine the carbon isotope discrimination of a particular plants was sampled from each plant at the same developmental stage for each different plant species. Sampled material was dried in an oven at 65°C for 48 hours then ground using a ball bearing in a tissue lyser machine to a fine powder. This powder was then used to determine the $^{13}C/^{12}C$ carbon using an ANCA GSL 20-20 Mass Spectrometer made by Sercon PDZ Europa (Cheshire). The sample $\delta^{13}C$ results reported by the machine were not absolute measurements but indicated the difference between our given samples (R_{sample}) *vis a vis* the standard Vienna Pee Dee Belemnite (PDB) ($R_{standard}$). The sample $\delta^{13}C$ was then calculated using the formula specified in Farquhar et al. (1989) that is as follows:

$$\delta^{13}C_{sample} = \left(\frac{R_{sample}}{R_{standard}} - 1\right) \times 1000 \quad [13]$$

The C isotope discrimination of the plant sample was then calculated using the formula:

$$\Delta^{13}C = \frac{\delta^{13}C_{air} - \delta^{13}C_{sample}}{1 + \delta^{13}C_{sample}} \quad [14]$$

Where $\delta^{13}C_{air}$ was obtained from at least five samples of air taken from the growth chamber or greenhouse where the plants material analysed were grown.

2.5.10 Direct Water use efficiency measurements

Water use efficiency was measured as the ratio between the plant biomass and the amount of water used by the plant in during its growth cycle. To get better estimates of water use by the plant, we needed to reduce evaporation of water from the surface of the soil in which the plants were grown. This was done by growing the plants in a closed system. In the case of Arabidopsis, plants were

grown in 55cm^3 centrifuge tubes filled with sandy loam soil with a bulk density of between 1.2 and 1.25g cm^{-3}. This was watered to saturation and a small hole was bored at the centre of the centrifuge tube where a single seed is germinated and grown till visible signs of water stress. For wheat and rice, plants were plated into PVC pipes filled with sandy loam soil as described and sealed at the top and bottom with flexible PVC sheets of plastic. A hole was made in the centre of the tube to allow for the germination of the plant.

2.6 Invasive and non-invasive root measurements

2.6.1 Root washing and analysis

Roots from the different plants were gently removed from the pots they were grown in and loosely attached soil removed by gentle handshaking of the roots. After this, the roots were then immersed in 500ml of 10% HMP for 1 hour to disperse soil aggregates closely attached to the root matter. The roots were washed using running water over a 0.25μm (Arabidopsis) or 0.5 mm (wheat and rice) sieve to further remove the adhered soil whilst trapping any root material. When the roots were deemed sufficiently clean from soil particles, they were then stored in deionised water at 4°C for further analysis.

For analysis of root properties, roots were spread over a 31×21cm water-filled tray and then light scanned using an Expression 10000XL Pro (Seiko Epson Corporation, Nagano, Japan) at either 400dpi or 600dpi resolution in Greyscale mode. After this scanning WinRhizo® basic software 2016a (Regent Instruments) was used to determine the root properties of the different plants.

2.6.2 X-Ray micro-computed tomography imaging

a) Image acquisition system

The X-Ray Computed Tomography (CT) imaging work done in this thesis was carried out using three different scanning systems. Firstly, the initial preliminary scans of Arabidopsis were done using a Bruker, SkyScan 1172 desktop CT scanner (Kontich, Belgium) at the Skeletal analysis laboratory in the University of Sheffield Medical School. This machine was capable of scanning relatively small samples with a maximum size of 27mm in diameter (50mm in offset scan) producing images with a maximum resolution of 1μm at highest resolution. This instrument used a closed 20-100kV air-cooled X-Ray source with a maximum power of 10W and a spot size of <5μm. This X-Ray source produces radiographs in on a 12-bit, fully distortion corrected 11Mp CCD camera which is fibre optically coupled to its scintillator.

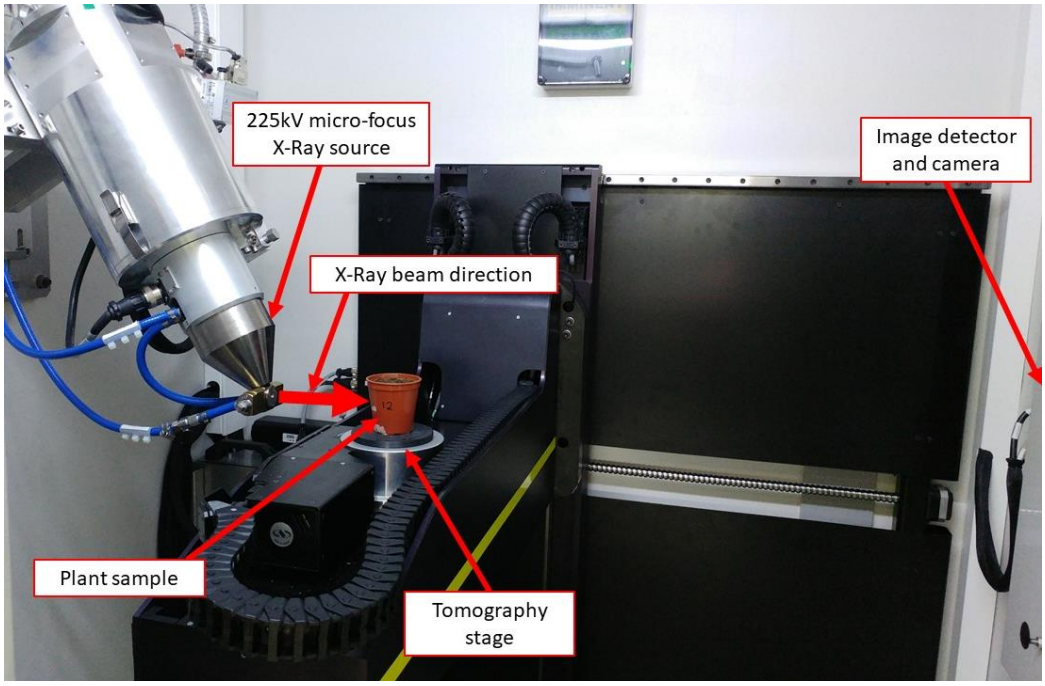

Figure 11 General overview of the Nikon XTH 225 LC scanner at the AMRC showing some important imaging instruments and sample placement

The second scanner which was used for the majority of the X-Ray CT scans in this thesis was an industrial-grade Nikon Metrology X TH 225 LC CT scanner (Nikon Metrology, Derby, UK) at University of Sheffield's Advanced Manufacturing and Research Centre (AMRC) as illustrated in Figure 11. This scanner has an open 225kV X-Ray source with a maximum power rating of 225W and a spot pixel size of 3μm (depending on the size of the sample). The X-rays produced by this machine are picked up on a 16bit Varex detector that has 2000×2000 active pixels.

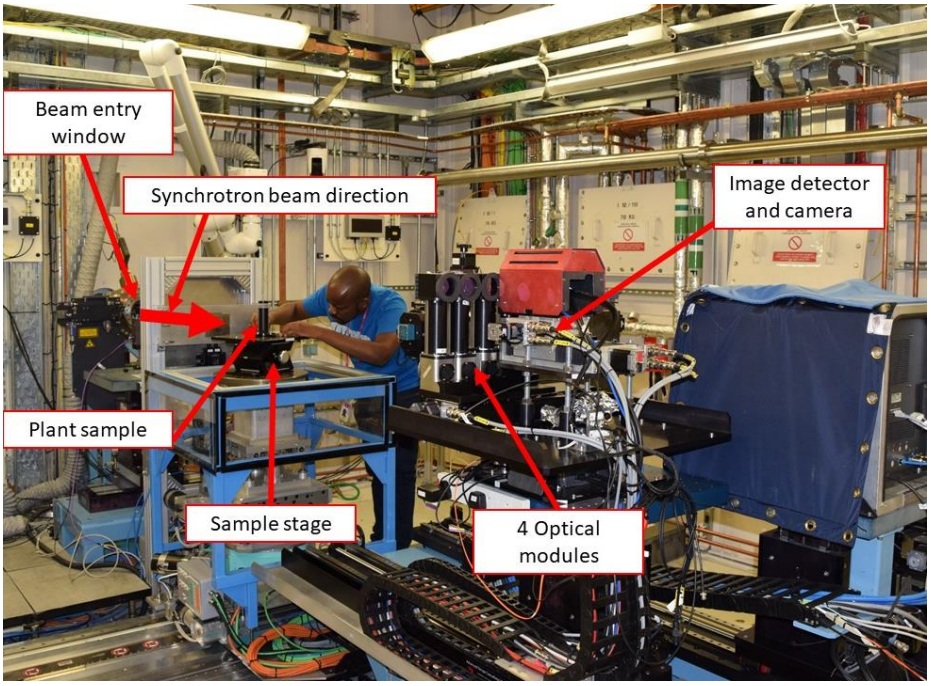

Figure 12 General overview of the Diamond light source JEEP i12 facility showing some important imaging instruments and sample placement

The last scanning system used was the monochromatic X-Ray synchrotron tomography system (XRST) located at the I12: The Joint Engineering, Environment and Processing (JEEP) beamline at Diamond Light Source facility (Rutherford Appleton laboratory) of the Science and Technology Facilities Council (STFC) as illustrated in Figure 12. The profile of this beamline has be described in detail in Drakopoulos *et al.*, (2017) and basically consists of either a polychromatic ('white beam') or monochromatic high-intensity beam with a selectable energy between 53 - 150 keV (1.8×10^{11} photons s^{-1} mm^{-2} flux at 53 keV). This was operated on the operating module 1 in the experimental hatch 1 with a field of view of 46mm × 12mm and an image resolution of 18µm per pixel for each scan.

b) Image reconstruction, processing and segmentation

Image reconstruction of the scans using the different experimental systems was done by proprietary software for both the Skyscan and Nikon scanners. For the XRST however, reconstruction was done using SAVU, a python-based image reconstruction software for large data sets developed at the Diamond light source facility (Wadeson and Basham 2016).

The TIFF images acquired from reconstruction were first cropped in ImageJ to remove unwanted pixels outside the field of view of the different samples. The resultant scans were then downsized from 32-bit to 8-bit images to reduce their size for computational purposes. In the case of XRST images, these were further downsampled to half the resolution from the original scans (37 µm) to further reduce their size as scanned images for one scan was at least 200 Gb in size.

After this initial processing images were then imported into AVIZO 9.0.1 software (FEI, Hillsboro, Oregon) and then filtered using the non-local means filter module. The filtered images were then inputted into two different automated root segmenting software systems. The first image segmenting software system used was the RooTrak 0.3.2 program which has been used in other similar studies as well. After this, the images were further inputted into FiJi enhanced ImageJ software where the Root1 macro root as described by Flavel *et al.*, (2017) was also used to track segment out roots from the different plant scans. The two methods produced variable results with Root1 being able to identify relatively more roots as compared to RooTrak for wheat and Arabidopsis images. Segmentation of rice roots, on the other hand, proved difficult using both automatic segmentation techniques as they were not optimised to deal with complications arising from aerenchyma air cavities in roots characteristic of rice plants. As a result, manual and semi-automated magic wand and paintbrush tools in the Avizo segmentation option were used for rice root segmentation.

After segmentation of the different root systems were complete, analysis of the different root properties was done using various modules in Avizo software. These include the use of the Label analysis, Auto-skeleton, Average object thickness, Tortuosity modules to compute the different segmented root properties. Finally, visualisation of the segmented root and plant parts was computed in the project view of Avizo with the Volume rendering module being used to display the 3D images of different root systems. A summary of the different image processing steps taken is given in Figure 13.

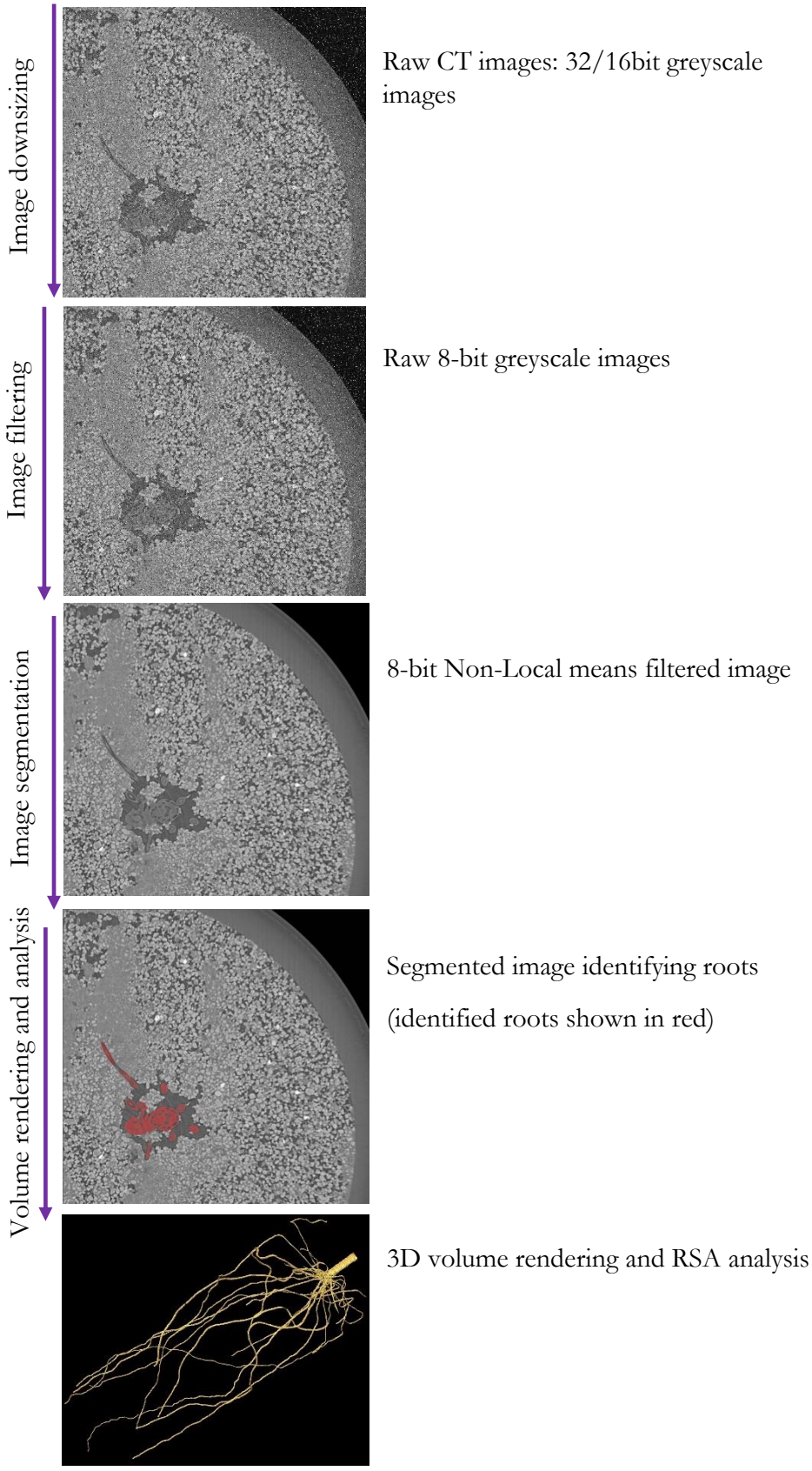

Figure 13 Image processing protocol showing examples of output obtained from in the various steps

2.6.3 Neutron imaging tomography and radiography

a) Imaging system

Neutron radiography and tomography was carried out at the IMAT neutron imaging beamline of the ISIS Neutron and Muon Source at the Rutherford Appleton Laboratory, UK with its design as illustrated in Figure 14. A more detailed description of the IMAT imaging station can be found in Burca et al., (2013); Kockelmann et al., (2013) and Burca et al., (2018). For my experiments, the neutron beam was shaped to the field of view of 112.7 mm × 112.7 mm accompanied by a multiaxial tomography stage allowing for 2 simultaneous scans. The neutron radiographs were acquired with an optical camera box equipped with Andor Zyla 4.2 PLUS sCMOS with 2048×2048 pixels, an 85mm lens and 100 µm 6LiF/ZnS: Ag scintillator. The images produced had a pixel and voxel size of 55µm with 30s being the exposure time for each projection and an L (10000mm)/D (40mm) = 250. The time taken for a single scan of the plants was almost 6 hours with 654 radiographs being recorded using a rotation step of 0.55°. This was the best set up achievable on IMAT, suitable for our experiment (Mawodza *et al.* 2018).

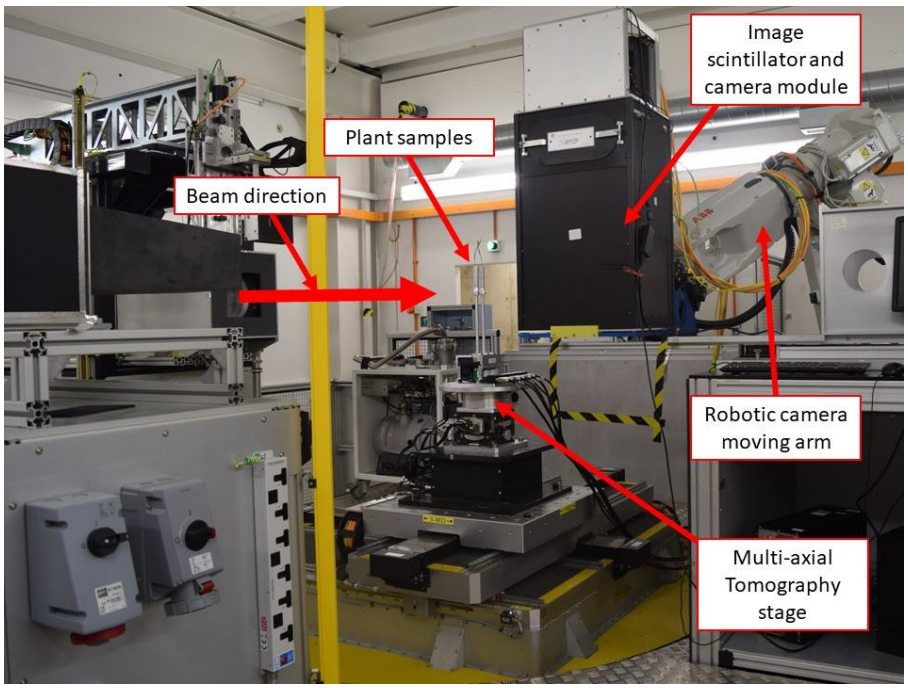

Figure 14 General overview of the ISIS IMAT imaging facility showing some important imaging instruments

b) Image reconstruction, root segmentation and analysis

The images acquired during the imaging sessions were reconstructed using the commercial available Octopus 8.9 software (Octopus 2019). These images were corrected for neutron beam

variation and camera noise using the flat images and dark images taken before and after image acquisition (Dierick *et al.* 2004, Vlassenbroeck *et al.* 2006).

The final reconstructed stack of images were imported into Avizo ® 9.0.1 for root segmentation and analysis (FEI 2015). Where they were filtered using the non-local means filter. I attempted to use automated root segmentation algorithms RooTrack (Mairhofer *et al.* 2012a) and Root1 (Flavel *et al.* 2017) but due to the great heterogeneity in water content both the soil and within roots, these proved unreliable for my samples. To get the best results, roots were manually segmented using the limited range paintbrush editor in the segmentation module in Avizo software. The segmented roots obtained from this process were then used to calculate root properties. Segmentation of the larger seminal roots was primarily done using automated thresholding techniques available in Avizo as there was a clear attenuation contrast between the soil and these roots. This was however not done universally throughout the whole root system as most of the smaller lateral roots as well as some sections of the larger seminal roots had attenuation values that poorly contrasted or were even lower than that of moist soil and aggregates surrounding them as shown in Figure 15. Time-consuming manual segmentation based on a combination of localised differences in attenuation and the connectivity of circularly shaped pixel groups (as roots are usually circular in shape) enabled the segmentation of the outstanding lateral roots and seminal root sections throughout the soil columns.

c) Calibration for water content in neutron images

Calibration for water content was done using the same soil used in my experiments with known volumetric water contents similar to what was done in Moradi et al., (2011). Soil filled aluminium tubes with ascending volumetric moisture content were imaged and then subsequently used for this calibration to relate the relative neutron attenuation to the moisture content for all the images we acquired.

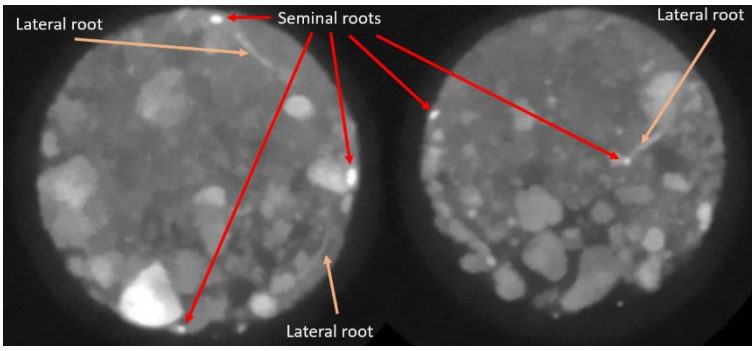

Figure 15 Grayscale images used to segment out roots showing how the different root types contrasted with the soil

2.6.4 Electron microscopy

Electron microscopy was used to view the interactions of soil and root in great detail in the Arabidopsis samples. For this method, three different roots with soil aggregates attached to them were attached to a $1mm^2$ imaging stage and oven-dried at 50°C for 3 days to eliminate moisture from the samples. The samples were then sputtered with gold using particles and then imaged using a Philips CM100, 100 kV electron microscope (Philips, Netherlands) which was equipped with a LaB6 gun and Gatan 1Kx1K digital camera (Schrader *et al.* 2007).

2.7 Data analysis

All statistical analysis in this thesis conducted using Graphpad Prism (Version 8). In this, analysis data was first checked for normality and homoscedasticity before either an ANOVA, t-test or non-parametric Kruskal-Wallis test was used to check for significant differences at an alpha level of $P< 0.05$. All error bars denote standard error of the mean (SEM).

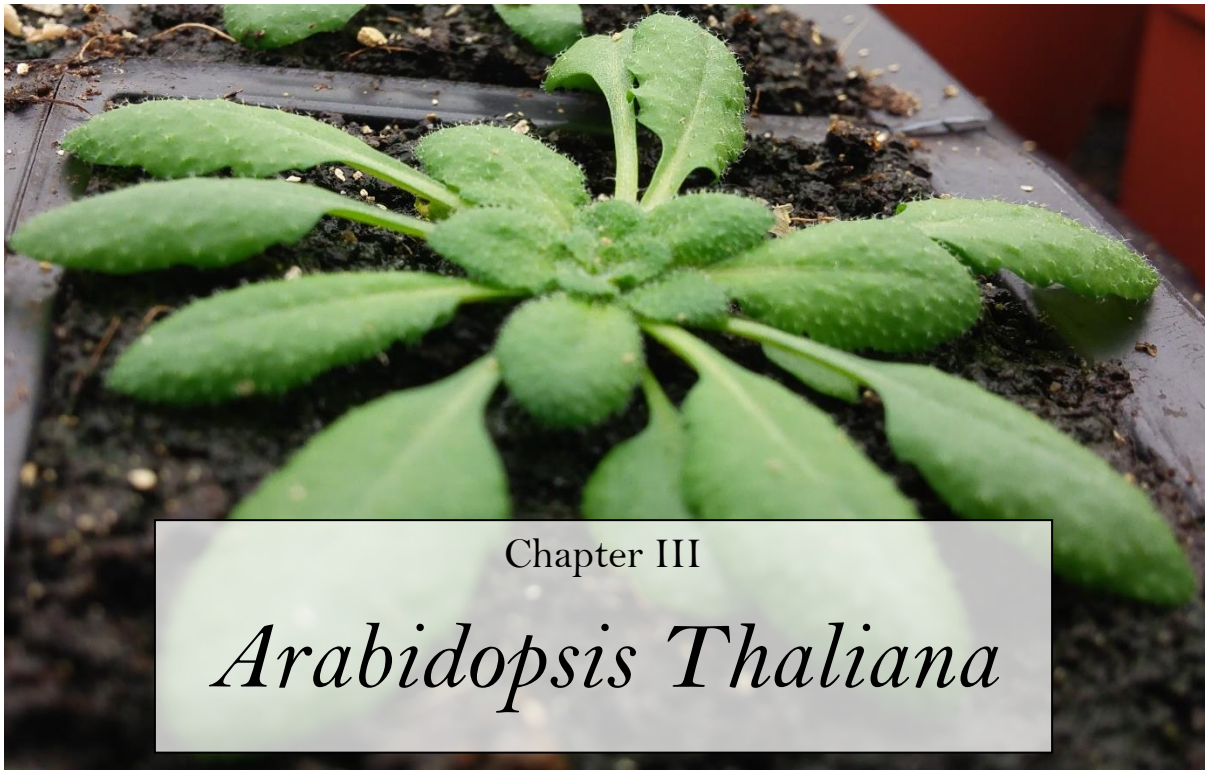

Chapter III

Arabidopsis Thaliana

III Arabidopsis thaliana

3.1 Chapter overview

This chapter will provide results from several experiments carried out using various mutants of the model plant Thale Cress (*Arabidopsis thaliana*. L). A wide variety of root and shoot mutants that were hypothesised to have attributes that could potentially alter their WUE were chosen for this study. The WUE of each line was measured by C isotope discrimination and transpiration experiments for mutants and controls. Having identified mutants that consistently showed alterations in WUE, I then looked at how the mutations affected their biomass production as well as their root architecture and consequently how this would feed into changes in soil structure. The ideal soil aggregate size for the growth of Arabidopsis under my conditions was also determined and subsequently used for some of the experiments that proceeded. Two non-invasive imaging techniques were used to visualise plant root growth in situ with varying degrees of success between them. Results from these experiments generally did not show any significant differences in the root architecture of the different mutants that lead to improved WUE. There were also no significant differences in the soil structure of the soils where the different plant lines were grown with slight weakening being observed in soils where Arabidopsis plants were grown. X-Ray CT imaging was shown to be an appropriate method to use for non-invasive visualisation of Arabidopsis root system architecture with Neutron CT only being able to produce partial visualisation of Arabidopsis roots.

3.2 Introduction

3.2.1 Arabidopsis and its importance to plant science

Arabidopsis thaliana is a small, annual, dicotyledonous weed plant of the Brassicaceae family that is native to Eurasia but has spread to many places around the world (Hoffmann 2002). In spite of it being a small weed plant of little agronomic significance, over the past 50 years, Arabidopsis has grown to arguably become the most scientifically important plant of our time with thousands of scientific studies focusing on it (Page and Grossniklaus 2002). This increase in its scientific use is mainly due to the pioneering work by Friedrich Laibach in the 20th century, who noticed that Arabidopsis had one of the smallest genomes (125Mbp) of all known angiosperm plants and thus would be an ideal candidate for use as a model for plant genetics (Laibach 1943, Meinke *et al.* 1998). This was further reinforced by efforts in the mapping of the Arabidopsis genome in the early 80's which ultimately culminated to the full sequencing of the Arabidopsis genome in the year 2000 (Koornneef *et al.* 1983, The Arabidopsis Genome Initiative. 2000). As a result of it being one of the few plants that has been fully gene sequenced, Arabidopsis has become an invaluable resource in plant genetics and molecular biology, helping to answer many questions about gene structure and function.

Arabidopsis has numerous advantages that made it the ideal model plant species for molecular biology and biotechnology. These include its relatively short life cycle (as short as 6 weeks in optimal conditions), it's relatively small size which makes it ideal for laboratory conditions as well as its high fecundity (with the ability to produce as much as 10000 seeds per plant) (Page and Grossniklaus 2002). It is also easy to maintain or cross using conventional methods and has been shown to be easily transformed by *Agrobacterium tumefaciens* allowing for rapid gene manipulation (Clough and Bent 1998). Arabidopsis being a weed plant is also relatively easy to grow and has the adaptability to thrive in many different environments. It also has a small, relatively simple root system that enables it to grow well in soil or cultured media thus making the plant ideal for a wide range of experiments (Meinke *et al.* 1998).

As a result of these desirable traits, an extensive number of well characterised Arabidopsis mutant lines have been developed and are used to answer vital questions pertaining to plant growth and developmental processes as influenced by specific genes (Alberts *et al.* 2002). Gene knockout or overexpression have been used extensively to determine the role of specific genes and answer fundamental questions of how genes affect plant phenotypes. Following functional analysis in Arabidopsis, orthologues of the gene of interest can then be identified in more agronomically important crop plants and manipulated to improve crop performance.

3.2.2 WUE in Arabidopsis

Improvements of WUE and drought resistance in global agriculture is of paramount importance to the sustainability of the current global crop production systems (Tron *et al.* 2015). As such many genes in Arabidopsis have been manipulated in order to find possible mechanisms to improve plant water use with the ultimate aim of transferring the knowledge acquired from these investigations into field crops of agricultural importance. Several different genes that control WUE of Arabidopsis plants have been identified in the quest to improve plant water productivity. These include *HARDY* (Karaba *et al.* 2007), *PHYB* (Boccalandro *et al.* 2009), *ERECTA* (Masle *et al.* 2005), *EPF1 and EPF2* (Franks *et al.* 2015) among others. Many of the genetic mechanisms employed to improve WUE in these studies involve the reduction in the rate of transpiration of Arabidopsis plants as induced by alterations in their stomatal properties whilst ensuring biomass production is not severely compromised. Some of these genetic mechanisms proffering improvements in WUE first identified in Arabidopsis have been successfully translated into of field crops such a barley (Hughes *et al.* 2017), wheat (Dunn *et al.* 2019) and rice (Karaba *et al.* 2007, Mohammed *et al.* 2019). Despite this success, however, there still remains a need to identify more mechanisms that lead to improvements in WUE to further improve agricultural sustainability. In this study, several different Arabidopsis root and shoot mutants were screened for novel improvements in WUE for use to answer the main aims of this thesis. Details of the selected mutants are given below.

3.2.3 Selection of WUE mutants of Arabidopsis

In order to identify plant genotypes that exhibited significant alterations in WUE (both reduced and increased). Arabidopsis lines that had mutations known to affect their root and/or shoot development in some way were studied (as listed in the methods Chapter). Most of these mutants were selected from locally available seed stocks, and had not previously been tested for alterations in WUE but based on their phenotypes, it was hypothesised that these mutations could affect water dynamics of the plants thus resulting in altered WUE (Blum *et al.* 1996, Ruggiero *et al.* 2017, Dharmappa *et al.* 2019).

For instance, two contrasting mutant lines *werewolf* (*wer-1*), and *caprice* (*cpc-1*) that produce phenotypes with either excessive or reduced root hairs respectively were used. The *wer-1* mutant has a mutation causing loss of function to the *WEREWOLF* gene which encodes an MYB-type protein. This gene is responsible for determining non-root hair differentiation in root epidermal cells and thus its loss of function as in *wer-1* results in excessive root hair production (Lee and Schiefelbein 1999). On the other hand, the *cpc-1* mutant has a mutation causing loss of function of

the *CAPRICE* gene encoding for an MYB-like DNA binding domain that positively controls root hair cell differentiation (Wada 1997, Wada *et al.* 2002). Its loss of function thus results in a phenotype with only a quarter of the root hairs present in wild type plants. These two mutants were selected due to the known role of plant root hairs in water and nutrient uptake (Cailloux 1972, Grierson *et al.* 2014). It was hypothesised that these contrasting mutations would result in differences in WUE between these lines.

phyB-9 mutants have a mutation in the photoreceptor gene, *PHYTOCHROME B* (*PHYB*) that regulates light responses in both young and mature plants (Reed *et al.* 1993, 1998). This mutant was selected for this study primarily due to preliminary work carried out in the Casson lab showing alterations in WUE especially under high light conditions (Brown 2018). The *ethylene insensitive root1* mutant (*eir1-1*) which has mutations in the gene *EIR1* primarily expressed in the root, produces plants with an agravitropic root and also shows reduced root growth sensitivity to ethylene (Luschnig *et al.* 1998). This mutant was selected due to the fact that its agravitropic nature has the potential of compromising its water acquisition capacity, as it would be unable to extract water from deeper in the soil profile when the surface dries.

The *arf7 arf19* double knockout mutant has a phenotype exhibiting reduced lateral root production as the two knocked out genes, *AUXIN RESPONSE FACTORs* (*ARF7* and *ARF19*), control auxin-induced lateral root formation and thus resulting in the above-mentioned phenotype (Okushima *et al.* 2005, 2007, Wilmoth *et al.* 2005). This mutant was selected as its reduced lateral root phenotype had the potential to limit its water uptake capacity thus potentially inducing alterations in its WUE. The rest of the mutants also had traits I hypothesised would alter WUE. The *root hair defective1* (*rhd1*-1) mutant has a mutation in the *RHD1* gene controlling the normal formation of hair cells and thus this results in a phenotype with defective root hairs that have a bulbous appearance at the base. It was hypothesized that this defect in root hairs, similar to those in *cpc1-1* and *wer-1* would affect water relations within the plants. Finally the *gl1 rhd2* double mutant, which had mutations in the *RHD2* gene responsible for regulation of root hair formation as well as the *Glabrous 1* (*GL1*) gene responsible for the formation of hair-like structures found on the surface of Arabidopsis leaf surfaces called trichomes. The mutations in both these genes results in plants with a phenotype exhibiting short root hairs accompanied by the absence of trichomes (Müller and Bartelheimer 2013).

Apart from the different root and shoot mutants with potentially relatively novel associations with WUE, two different stomatal lines *epf2-1* and *EPF2-overexpressing (EPF2OE) transgenic* mutants that have already been shown to exhibit improvements in WUE were also used. These mutants have

alteration in the *EPF2* gene controlling asymmetrical divisions in stomatal cells during their development which affects stomatal density, thus affecting transpiration and WUE (Hara *et al.* 2009, Hunt and Gray 2009, Franks *et al.* 2015). The *epf2-1* line with loss of function in the EPF2 gene specifically exhibits an increase stomatal density thus reducing its WUE whilst the *EPF2OE* line has increased activity of the EPF2 gene with largely restricts the production of stomata thus resulting in reduced transpiration and consequently improving in WUE (Franks *et al.* 2015, Hepworth *et al.* 2015).

In this study, we use the Columbia (Col-0) accession line as the wild type background for all the mutant plants used in this thesis. This line was because it is the most dominant line used for research and has an extensive number of readily available mutants that have been developed and are well characterised (Berardini *et al.* 2015).

3.2.4 RSA of Arabidopsis

Arabidopsis being a dicotyledonous plant has a 'simple' branched tap root system that is often used as a model root system providing insightful views into plant root growth and development (Smith and De Smet 2012). This root system has a tree-like, hierarchical system made up three different types of roots (Kellermeier *et al.* 2014, Zobel 2016). These are namely, the taproot, lateral roots and the adventitious roots. The single tap root in Arabidopsis emerges from the radicle and branches into several different orders of lateral roots resulting in the branch like root system characteristic of most dicotyledonous plants (Ogura *et al.* 2019b). Arabidopsis, contrary to the general assumption from historical research also has a few adventitious roots that emerge from either the hypocotyl or the coleoptile regions of the plant (Falasca and Altamura 2003, Zobel 2016). The adventitious roots are similar to the main taproot and thus are also dominated by lateral roots of different orders. An illustration of this root system is given in Figure 16.

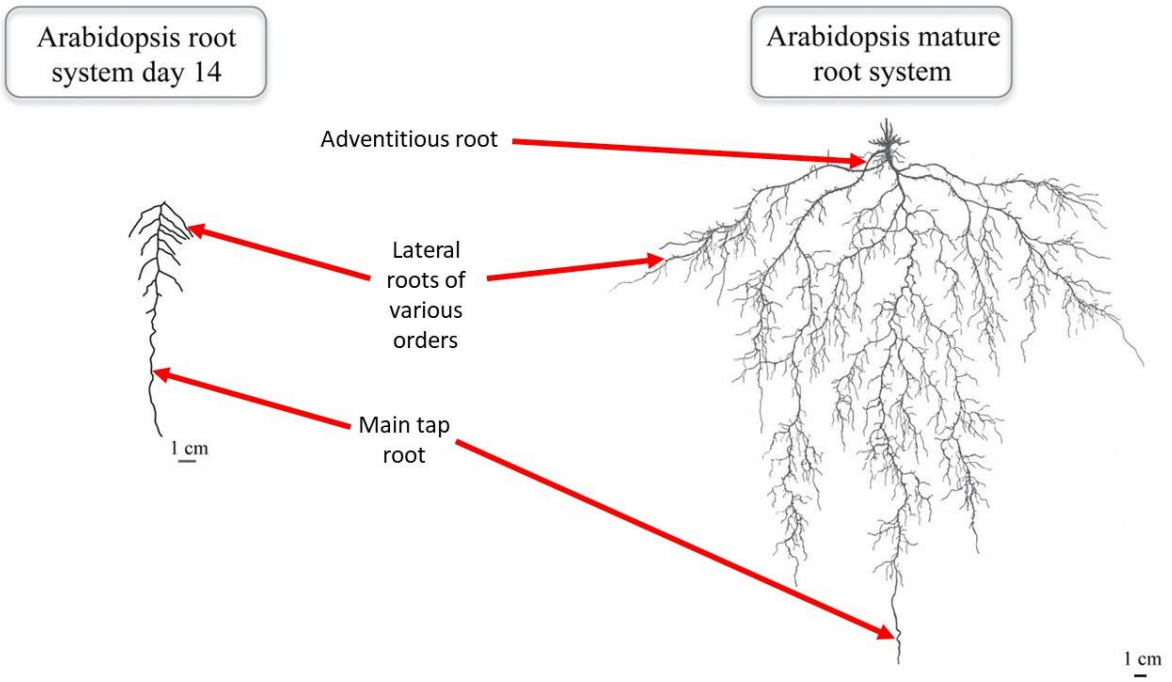

Figure 16 Illustration of the root morphology of 14 day old and mature Arabidopsis [Adapted from (Satbhai *et al.* 2015)**]**

3.2.5 Measurement of Arabidopsis RSA in soil

In spite of the importance of studying RSA traits, there are great complexities associated with unravelling the plants' RSA especially when growing in an opaque medium such as soil in my case. Lynch, (1995) in his review of root architecture lamented the lack of techniques and technologies adequate to reveal in full detail, the great complexities that characterises a plants RSA. Traditional methods of examining RSA involving the excavation of plants roots from soil and measuring different traits ex-situ although useful, are tedious and time-consuming whilst also not being able to give essential spatial information detailing the roots orientation in soil. In the case of Arabidopsis as in this study, excavation of the plant roots could prove even more challenging as compared to many other studies considering the thickness of Arabidopsis roots (often <250µm) that make them delicate and difficult to extract successfully without breaking. Furthermore considering that the estimated loss of root material from washing of bigger and less delicate roots such as that of wheat, estimated to be in the magnitude of around 20-40% (van Noordwijk and Floris 1979), much greater inaccuracies may arise when Arabidopsis roots are analysed using this technique.

Several other techniques to unravel the root architecture of Arabidopsis plants such as the use of transparent agar in vertical plates, growth in hydroponic media and in "transparent soil" (nafion) although providing useful information, lack the physical and chemical attributes characterising a

mineral soil (Downie *et al.* 2012, Dayod *et al.* 2013, Gruber *et al.* 2013, Fulgencio *et al.* 2014). Performance of Arabidopsis in these media may vary considerably to that when growing in soil. Recognising this Hepworth *et al.*, (2015) grew their Arabidopsis plants in specially designed vermiculite (a 2:1 clay material) filled rhizotrons with a glass fibre sheet preventing the Arabidopsis roots from interacting directly with the vermiculite. This method, although also providing detail about Arabidopsis growth as influenced by a 2:1 clay material (Vermiculite), was not a representative of soil conditions in which many plants grow as the glass fibre prevented plant-soil interactions.

None of the methods for analysis of Arabidopsis RSA outlined above would satisfactorily enable the study of Arabidopsis roots grown in soil. Therefore, in this study, the use of non-invasive imaging techniques to unravel the RSA of Arabidopsis plants in soil was employed. Two relatively contemporary methods of non-invasive soil imaging techniques were employed, namely X-Ray and neutron Computed Tomography (CT) imaging. X-Ray CT is a relatively popular soil imaging technique often used to study plant-soil interactions in many different plants. For instance it has been used to reveal the root architecture of wheat (Flavel *et al.* 2012, Tracy *et al.* 2012, Ahmed *et al.* 2016), rice (Rogers *et al.* 2016, Fang *et al.* 2019) and maize (Ni Jiang *et al.* 2018, Gao *et al.* 2019). On the other hand, neutron CT is relatively less common method of visualisation of RSA *in situ* with only a few plants species e.g. lupine (Moradi *et al.* 2011) being frequently studied using this technique.

Analysis of Arabidopsis RSA using X-Ray CT has only been shown in a few studies, for instance, Lucas *et al.*, (2011) revealed how the RSA of *SHORT ROOT* mutants differed to that of the wild type using the technique, albeit, complimented by other measurements. Tracy *et al.*, (2010) were also able to show a single Arabidopsis root growing in a loamy sandy soil demonstrating that the level of resolution achieved by current X-Ray CT (<500nm) machines is good enough to enable the viewing of roots as small as that of Arabidopsis. Even scarcer in the literature is information patenting to the visualisation and measurement of the RSA of Arabidopsis using neutron CT. To the best of my knowledge, this is the first study that has attempted to reveal the root architecture of Arabidopsis using neutron CT.

3.2.6 Soil structural development and Arabidopsis

As Arabidopsis is not grown as a field crop, investigations of how it affects soil structure are very limited if any. Inferences of how it could potentially affect soil structure could be made from other similar dicot plants. Dicot plants are often considered inferior to monocots in terms of improving soil structure as they have a less extensive root system as compared to monocots (Oades 1993, Raj

Ratta 2018). In arabidopsis this is further compounded by its relatively small root system, which is expected to have limited impact on soil structure. It is thus essential to find methods of soil structural assessment that are very sensitive to small changes in soil structure. In this study, a combination of conventional and bespoke methods were used to find out the impact of Arabidopsis plants with variable WUE on soil structure. As soil structure is also known to be affected by variable moisture extraction from soil (Materechera *et al.* 1994), the impact of variable moisture extraction as induced by variable transpiration in Arabidopsis mutants was also investigated.

3.2.7 Research objectives

To fulfil the overall aim of this chapter, the following objectives were pursued;

1) Identify Arabidopsis mutant lines that show significantly improved WUE as compared to wild type plants when grown in soil.
2) Determine whether the improvement in WUE of the selected mutant affects their RSA under different watering regimes.
3) Determine how changes in WUE of the identified mutants affect soil structure as determined by aggregate stability tests.

3.3 Screening for mutations that lead to altered WUE

Preliminary experiments investigating plant properties were initially carried out in Levington M3 high nutrient compost, however, as this study was ultimately aimed at assessing plant performance in mineral soils, similar plant growth properties of the mutants plants were also carried out in a sandy loam soil. Transparent plant growth agar was also used to characterise some of the root properties of the mutants as it was difficult to obtain such measurements from opaque media such as the compost or mineral soil. The main questions under investigation for this section were:

Main questions:

- What are the growth characteristics (root growth properties, biomass production, and stomatal characteristics) of the selected root and shoot mutants in different media?
- Which root or shoot mutation(s) results in alterations in WUE?

3.3.1 Root growth properties on agar

As many of the selected mutants had known alterations in root growth characteristics, my initial experiments focused on characterisation of these differences when the plants are grown on agar. This media was a slight departure from mineral soil of interest in this thesis, however, the growth

properties derived from agar-based experiments would provide a useful insight into how the roots may perform when grown in opaque media.

a) Lateral root growth

In the first experiment, the total lateral roots, as well as lateral root density per cm of root, were determined after 28 days of growth on agar in vertical plates the results are given in Figure 17.

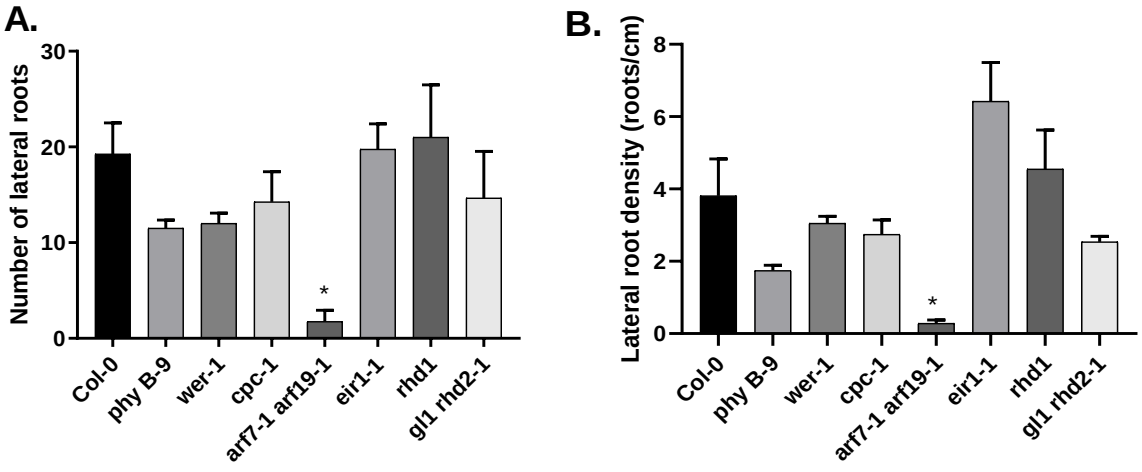

Figure 17: Lateral root number (A) and density (B) of Arabidopsis mutant grown on agar filled vertical plates for 28 days (n≥6). Error bars indicate SEM. Symbols indicate significant difference as compared to Col-0; Kruskal-Wallis test with post-hoc Dunn test, (*=≤0.05)

Both lateral root numbers (Figure 17A) and lateral root density (Figure 17B) varied considerably between the different plant lines with most of the mutants having a lower average number of lateral roots and lateral root density as compared to the wild type. Many of these differences, however, were not significant with only the *arf7-1 arf19-1* mutant having a significantly reduced number of lateral roots and lateral root density as compared to that of the wild type. Two of the mutants, *eir1-1* and *rhd1* had comparatively higher average numbers of lateral roots and lateral root density as compared to the wild type plants.

b) Root hairs density

In the second experiment, root hair density of the different lines was investigated just above the root tips of 7 days old plants grown on agar in vertical plates. The results obtained are shown in Figure 18.

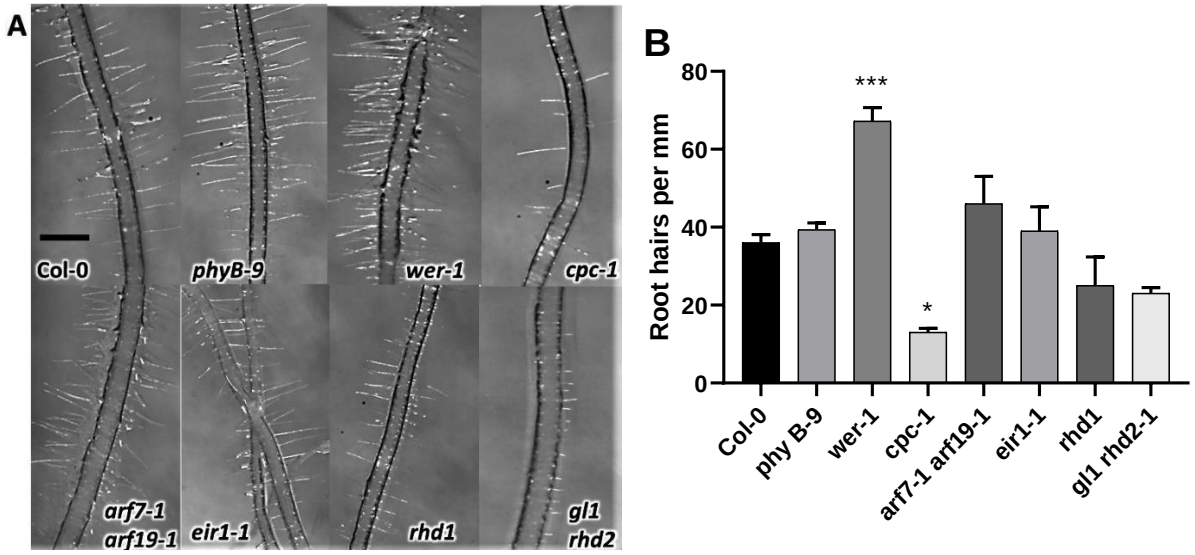

Figure 18 Root hair distribution among the different mutant plants 7 days after germination on agar. A) Representative images showing roots hairs on roots of the different lines, (scale bar: 500μm) **B) Comparison between the different Arabidopsis lines (n≥3).**Error bars indicate SEM. Symbols indicate significant difference as compared to Col-0; Kruskal-Wallis test with post-hoc Dunn test, (*=≤0.05, ***≤0.0001)

The root hair distribution in the different Arabidopsis lines as shown in Figure 18 similar to lateral root growth also showed great variations in root hair density of the different plant lines when grown on agar. The *wer1-1* mutant had the highest lateral root density as compared to the other genotypes. The *cpc-1* mutant, on the other hand, exhibited significantly reduced root hair density throughout the length of the root whilst the *gl1 rhd2* double mutant showed a reduction in root hair density(although not statistically different to WT), accompanied by relatively shorter root hairs as compared to the wild type plants (Figure 18A).

3.3.2 Shoot and root biomass production

Having investigated root phenotypes in tissue culture, I next focused on measuring the biomass of the different genotypes when grown in M3 compost or sandy loam soil. For each of these experiments, the plants were grown for 65 Days After Sowing (DAS) and then harvested to characterise their root (in sandy loam only) and shoot growth properties when grown in the two different media. The results obtained are given in Figure 19.

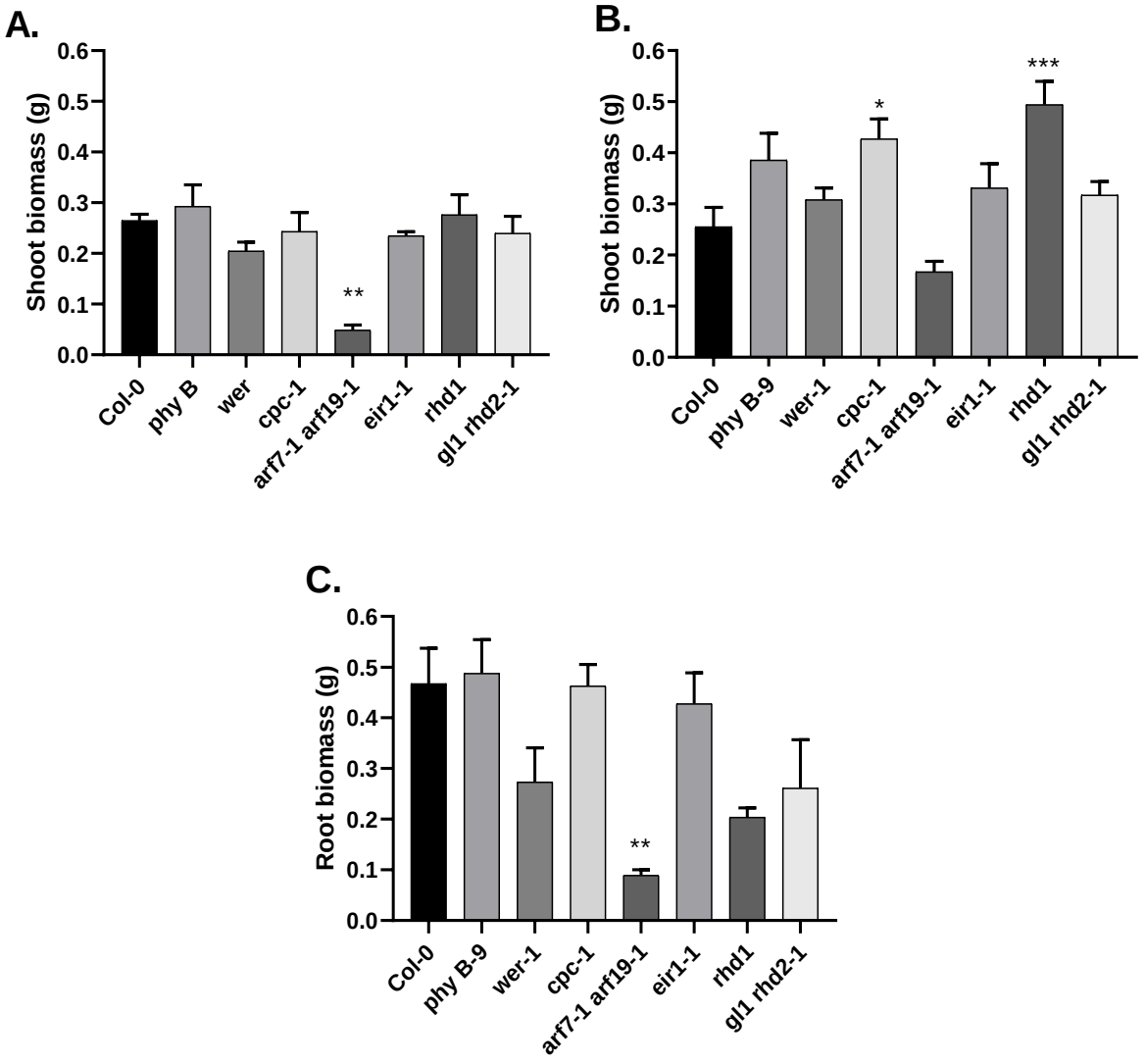

Figure 19 Shoot biomass of selected mutants when grown in A) Levington M3 high nutrient compost and B) A sandy loam soil. C) Root biomass of the same mutants grown in sandy for a 65 day period (n≥5). Error bars indicate standard error of the Mean (SEM). Symbols indicate significant difference as compared to Col-0; One-way ANOVA test with post-hoc Bonferroni test, (*=≤0.05. **= ≤0.01, ***=≤0.001)

The shoot biomass of the selected mutants, when grown in compost (Figure 19A), was relatively consistent amongst all the lines with the exception of the *arf7-1 arf19-1* mutant. This mutant exhibited significantly lower shoot biomass as compared to the wild type plants as well as most of the mutants as well. On the other hand, shoot biomass of soil-grown plants (Figure 19B) showed considerable variation with the *cpc1-1* and *rhd1* mutants exhibiting significantly increased shoot biomass production as compared to the wild type plants. The *arf7-1 arf19-1* double mutant similar to the compost experiment also had the lowest average shoot biomass however this was not statistically different to that of the wild type plants.

The root biomass of compost grown plants was not measured primarily due to the fact that it was very difficult to wash off compost from Arabidopsis root material as the two have a similar texture and properties. As a consequence root biomass of the mutants was only measured in plants grown in the sandy loam soil (Figure 19C). There was a significant difference in root biomass between the wild type and the *arf7-1 arf19-1* double mutant similar to the results seen with shoot biomass. The rest of the mutants did not show any statistically significant difference as compared to the wild type, however, the *wer*, *rhd1* and *gl1 rhd2* mutants had root biomasses lower than that of the wild type despite their respective shoot biomass being the same or significantly higher (*rhd1*) than that of the wild type.

3.3.3 Stomatal properties

Leaf stomatal properties are one of the most important factors affecting plant WUE as stomata are the primary gateway for water loss via transpiration (Bertolino *et al.* 2019, Leakey *et al.* 2019). Several metrics are used to characterise stomatal properties such as stomatal density, size, index and aperture. For these screening experiments, I focused on Stomatal Index(SI) and stomatal density (SD) as they have been shown to significantly affect plant water use in Arabidopsis (Franks *et al.* 2015, Hepworth *et al.* 2015). These experiments, similar to those done in the previous section were also done in both compost and soil with the results being shown in Figure 20.

SI of most of the mutant plants growing in compost (Figure 20A) was generally higher than that of the wild type plants with four mutants, wer-1, cpc-1, rhd1 and gl1 rhd2-1 having a stomatal index that is significantly higher than that of the wild type. On the other SD in compost (Figure 20C) among the same group of mutants was relatively similar to that of the wild type plants with only the *cpc-1* mutant exhibiting a significantly increased SD as compared to the wild type plants.

In the soil-grown plants(Figure 20B), only the SI of *phyB-9* (reduced) and *rhd1*(increased) mutants were significantly altered as compared to the wild type with many of the other plants having a SI similar to that of wild type plants. In terms of SD (Figure 20D) however, only the double mutant *arf7-1 arf19-1*, had a significantly increased density as compared to the wild type. The *cpc-1* mutant similar to the results from compost grown plants also had a relatively higher (although not significantly different) SD as compared to the wild type.

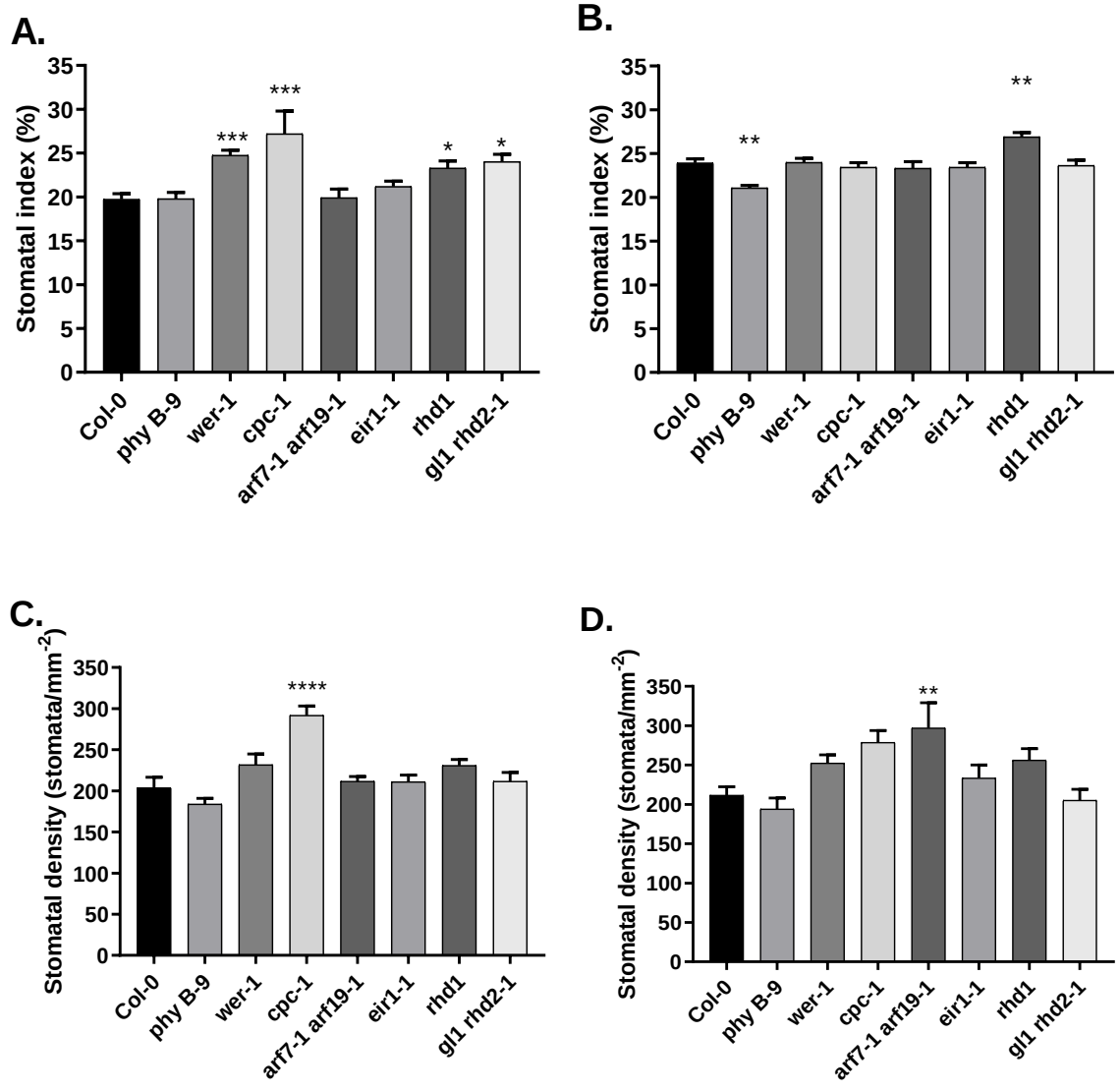

Figure 20 Stomatal density and index of the selected root and shoot mutants when grown in A and C compost, and B and D when grown in a mineral soil (n=6). Error bars indicate standard error of the Mean (SEM). Symbols indicate significant difference as compared to Col 0; One-way ANOVA test with post-hoc Bonferroni test, (*=≤0.05. **= ≤0.01, ***=≤0.001)

3.3.4 WUE of mutant lines

WUE of the mutant plant lines was determined by two different methods. Firstly, by directly measuring evapotranspiration as reflected by the weight of water loss from plants growing in a modified centrifuge tubes. This was used together with the total biomass obtained at the end of the growth period to estimate the WUE in terms of biomass production per unit of water (g/L). The second method I employed was an indirect one, which involved the use of the Δ (given in equation 3) to estimate the WUE as proposed by Farquhar et al, (1989). The results from these experiments are given in Figure 21.

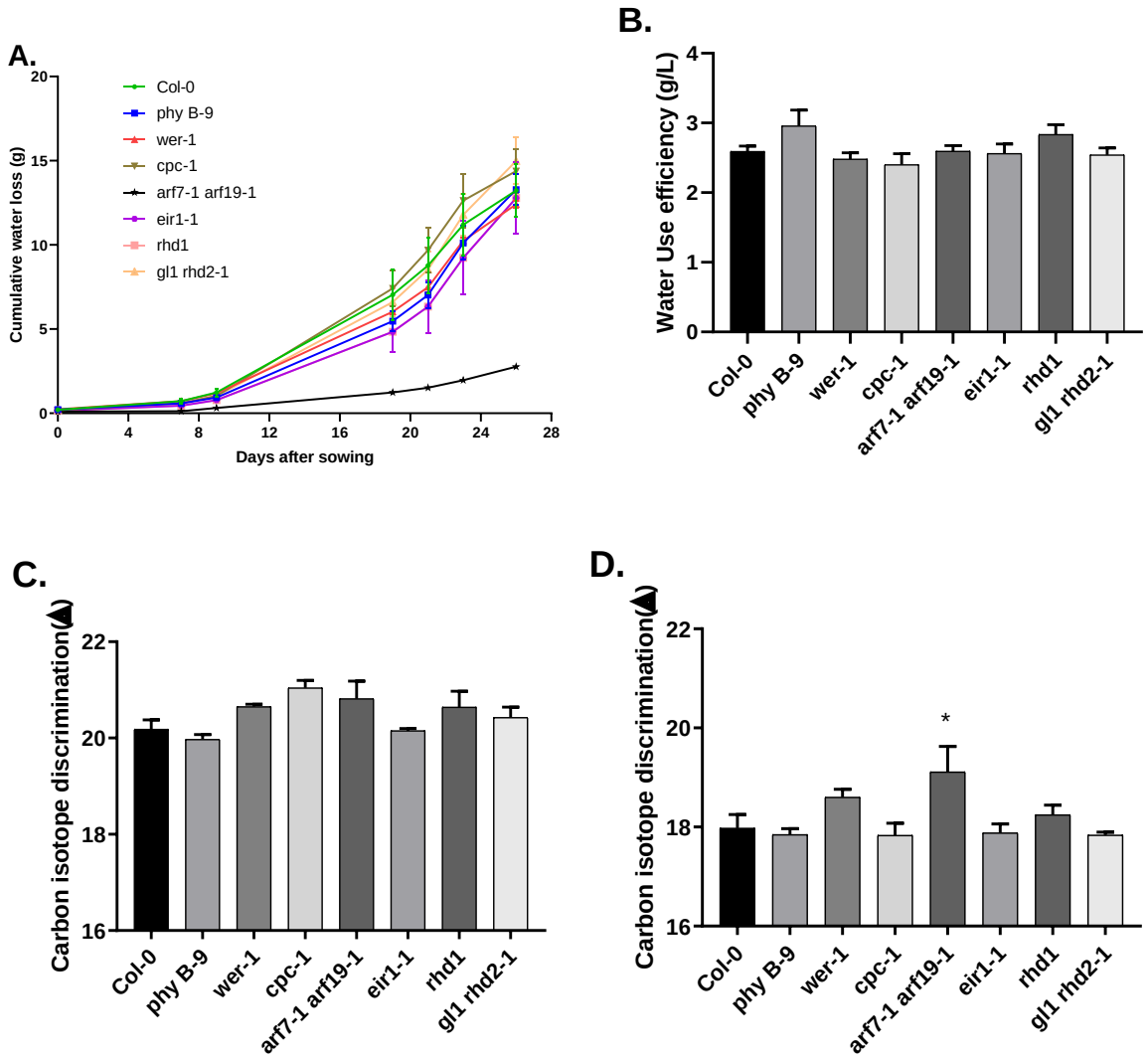

Figure 21 A) Evapotranspirational water use of the different plant lines over a 26 day growth period in modified centrifuge tubes, B) WUE estimated from total biomass and evapotranspiration of plant lines grown in modified centrifuge tubes for between 26 and 41 days. C) Carbon isotope discrimination (^{12}C: ^{13}C) of mature plant leaves of the different mutants grown in compost and b) mineral soil (n=4). Error bars indicate standard error of the Mean (SEM). Symbols indicate significant difference as compared to Col 0; One-way ANOVA test with post-hoc Bonferroni test, (*indicates ≤0.05.)

Evapotranspiration (ET) of the mutant lines as shown in Figure 21A indicates that ET of the different plants was low for the first 9 days after germination and gradually increased from then. Most of the mutants transpired more or less at the same rate as compared to the wild type with only the double mutant *arf7-1 arf19-1*, showing significantly reduced ET over the entire growth period. Towards the end of the experiment however, the ET from this double mutant began to increase, probably indicating delayed growth in its initial stage of establishment. Further experimentation with this particular mutant (not shown in the graph) indicated that the ET of this mutant eventually reached the same level to that of the wild type plants, albeit after nearly double

the growth time. The *rhd-1* mutant showed the highest transpiration among all the mutants after 21 days of growth, however, this was not significantly different to that of the wild type plants.

WUE as estimated from ET and total biomass (Figure 21B) was relatively similar for most of the mutants with no significant differences in the estimated biomass produced per unit of water transpired. The *phyB-9* mutant showed the highest average WUE among the different plant lines and with the *rhd1* mutant being the second-highest in terms of productivity per unit of water. The *cpc-1* mutant showed the lowest WUE among all the plants grown which may probably be due to the fact that it has an increased SD and SI in comparison to the rest of the mutants and the wild type.

Long-term water use efficiency as estimated by the Δ method revealed similar WUE patterns to those observed from the ET and biomass measurements. In the compost grown plants (Figure 21C), there was no significant difference between the wild type and the mutants, however, similar to biomass/ET estimations, the *phyB-9* mutant had the lowest average Δ and thus had comparatively increased WUE among the all the lines grown in compost. The *eir1-1* mutant had a similar average Δ to that of *phyB-9,* however, this did not follow the trend from the biomass/ET WUE estimations. On the other hand, the *cpc-1* mutant had the highest Δ, suggesting that the mutant was comparatively the least WUE among all the lines grown in compost. This is also supported by the results from biomass/ET estimations of WUE, where *cpc-1* showed the lowest biomass production per unit of water used in the experiment.

In the sandy loam soil (Figure 21D), WUE of the different lines seemed to vary considerably as compared to the estimates made when the same mutants were grown in compost. Δ across the lines was considerably lower suggesting plants are forced to conserve water i.e. become more WUE when they are grown in the sandy loam soil, even when a similar watering regime was implemented. In this experiment, similar to all the other estimations of WUE for these mutants, the *phyB-9* mutant had the lowest average Δ and thus suggesting the highest WUE. On the other hand, the *arf7-1 arf19* double mutant had the lowest WUE, which was significantly lower than that of the wild type. This is contrary to what was found in the compost experiment (Figure 21C). The *wer-1* mutant also had relatively lower WUE as compared to the wild type plants, this concurred with the reduction in WUE as shown in compost grown *wer-1* plants. The rest of the mutants showed WUE largely similar to that of the wild type.

From these initial screening experiments, it was clear that I could not proceed with the selected mutants as they did not have the desired differences in WUE as required to answer the primary

research question in this study. As a result, I then decided to use mutants that have already been shown to have alterations in WUE in literature that were at my disposal. Specifically, I chose to trial the *epf2-1* mutant and the *EPF2-overexpresser* (EPF2OE) transgenic line (Doheny-Adams *et al.* 2012, Franks *et al.* 2015, Hepworth *et al.* 2015).

3.4 Characterisation of stomatal mutants

In order to confirm the phenotype of the newly selected mutants, initial experiments were performed with the aim of finding out if they met the selection criteria of having altered WUE in the available growth conditions. To achieve this, the following questions were investigated:

Main questions:

- What are the growth characteristics (biomass production, stomatal characteristics) of the *EPF2* mutants?
- Do the mutations in the *EPF2* gene result in alterations of WUE as predicted in literature?

3.4.1 Biomass and stomatal characteristics of stomatal mutants

In this experiment, the different plant lines were grown in 120ml pots filled with a sandy loam soil and were watered to field capacity every 2-3 days via surface irrigation. These were harvested after 90 days of growth with the results of their characterisation being shown in Figure 22.

There were no significant differences in both shoot and root biomass production (Figure 22A and B) between the different plant lines which suggests that plant productivity was not affected by the different mutations. Shoot biomass among all the plant lines was broadly similar however in terms of root biomass production the EPF2OE lines showed marginally increased root biomass as compared to the wild type plants whilst on the other hand the *epf2* mutant had marginally reduced root biomass.

As expected the SD (Figure 22C) of the different mutants was significantly different as compared to that of the wild type plants with *epf2-1* mutants showing a 44% increase in SD whilst the EPF2OE had a 73% reduction. There was also a significant reduction in the SI (Figure 22D) of both the mutants as compared to the wild type with the *EPF2OE* line plants showing the greatest reduction in SI as compared to the *epf2-1* line.

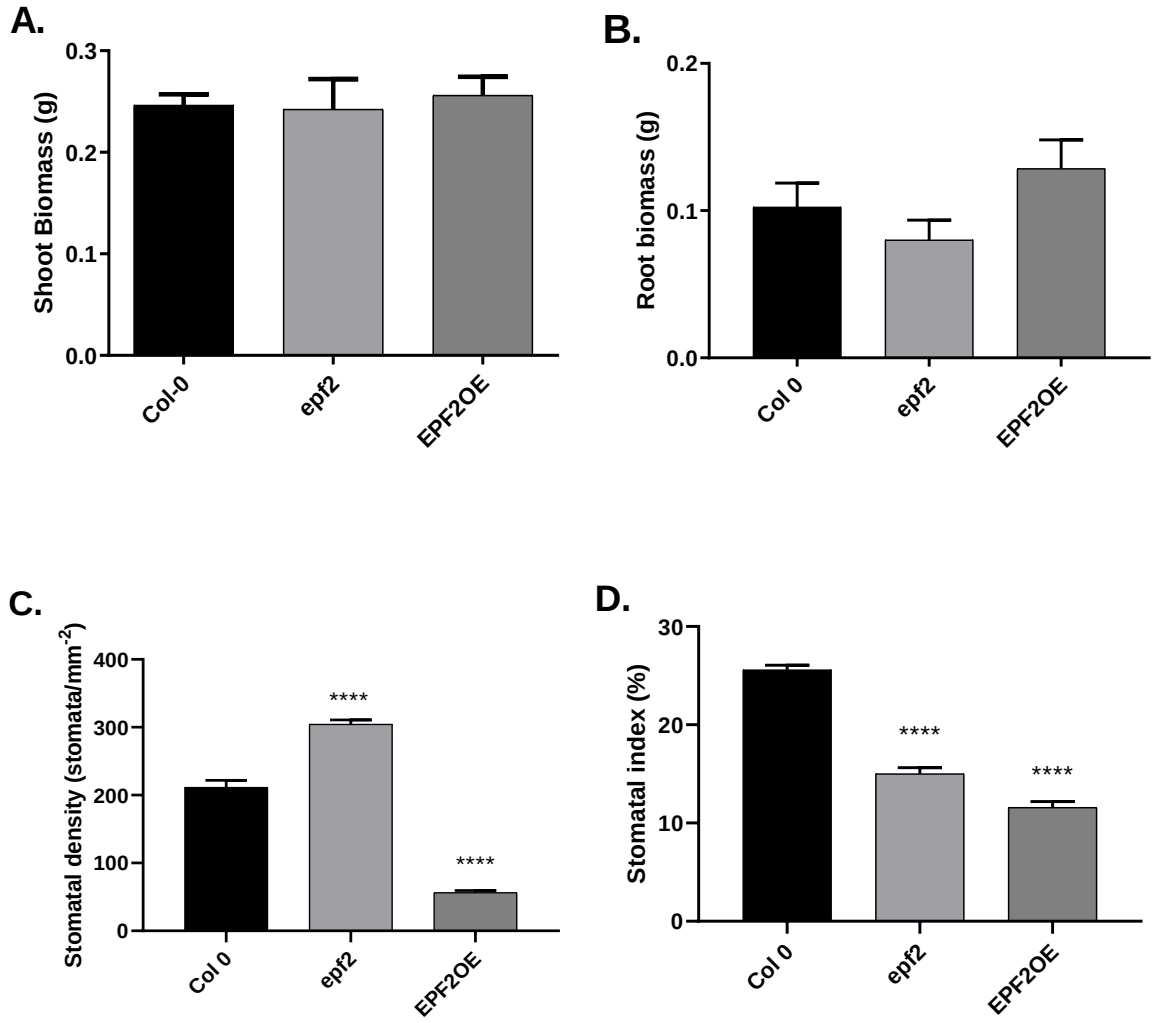

Figure 22 Biomass production and stomata properties of the wild type and EPF2 mutants grown in a sandy loam soil for 60 days (n≥8). Error bars indicate standard error of the Mean (SEM). Symbols indicate significant difference as compared to Col 0; One-way ANOVA test with post-hoc Bonferroni test, (*=≤0.05. **= ≤0.01, ***=≤0.001, ****=≤0.0005)

3.4.2 Water use efficiency of stomatal mutant lines

Further to the biomass and stomatal property characterisation in the previous section, the WUE of the different plant lines was also investigated. Two different methods of estimating WUE were employed, namely the Δ method as well as the use of experimentally determined plant transpiration and biomass productivity. The results obtained are given in Figure 23.

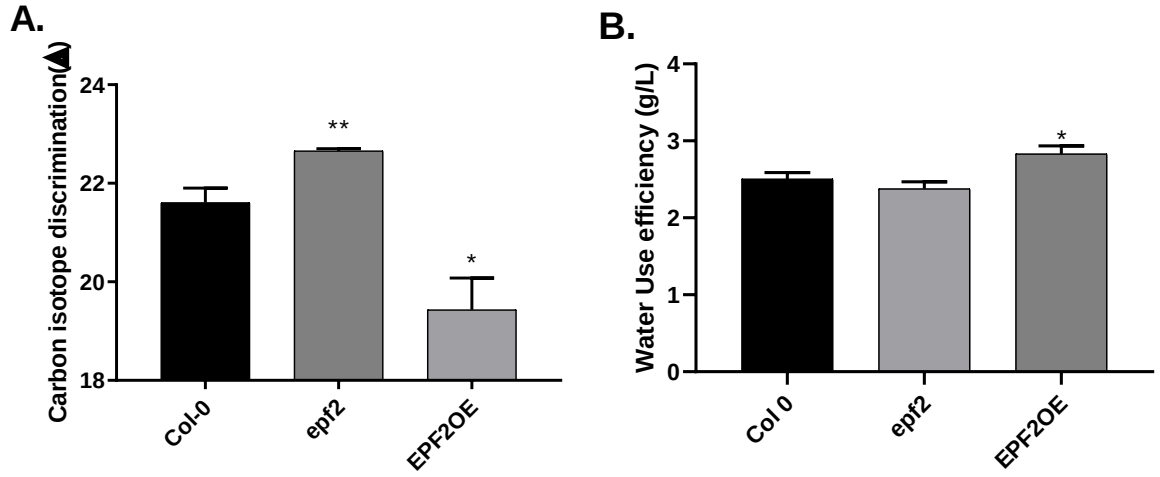

Figure 23 WUE of stomatal mutants as compared to that of the wild type as inferred by Δ C as well as directly measured form transpiration and biomass productivity (n≥3). *Error bars indicate standard error of the Mean (SEM).* Symbols indicate significant difference as compared to Col-0; One-way ANOVA test with post-hoc Bonferroni test, (*=≤0.05. **= ≤0.01)

Significant differences in Δ (Figure 23A) were found between both the mutants as compared to the wild type plants with the *epf2* mutant showing significantly increased Δ, indicating lower WUE whilst the *EPF2OE* lines showed significantly reduced Δ indicating improved WUE. Complimentary to this, WUE measurements in terms of biomass production per unit water loss (Figure 23B) also showed a significant increase in WUE for the EPF2OE line plants over a 50 day growth period in comparison to the wild type plants. Unexpectedly, however, there was no significant decrease in WUE of the *epf2* mutant as estimated using this method despite the significant increase in Δ. The WUE of this mutant was only marginally lower than that of the wild type plants.

3.5 In situ 3D imaging to unravel root architecture of Arabidopsis plants

After having narrowed down to the mutants of interest in previous experiments, the next experiments aimed at revealing the root architecture these mutants in comparison to wild type plants under different moisture conditions. In pursuit of this, the following questions were investigated:

Main questions:

- How does the root architecture of the mutants identified to have alterations in WUE differ to that of the wild type when grown in soil under contrasting moisture regimes?

- Which of the available non-invasive imaging techniques is ideal for unravelling Arabidopsis root architecture?

3.5.1 X-Ray CT imaging

a) Preliminary scanning

Skyscan 1172 experiments

Preliminary attempts at imaging and visualisation of Arabidopsis RSA in soil were carried using the Bruker Skyscan 1172 Micro CT X-Ray desktop scanner as described in the methods section. As the scanner had a maximum field of view (FOV) of 25mm in standard mode, it was necessary to use plant growth containers that could fit into the scanner for imaging whilst also allowing for significant root growth. I designed miniature growth containers specially adapted from 5 ml plastic syringes excised at the 4ml mark (45mm height) with a diameter of 13mm as shown in Figure 24. These were plugged with cotton wool at the base and filled with either a sandy loam soil or sand the 3ml level. Arabidopsis wild type seeds were then sown at the surface and the soil was surface and capillary watered for the entirety of the experiment. After 6 weeks of growth, the 3 randomly selected plants were then taken for imaging using the Skyscan 1172.

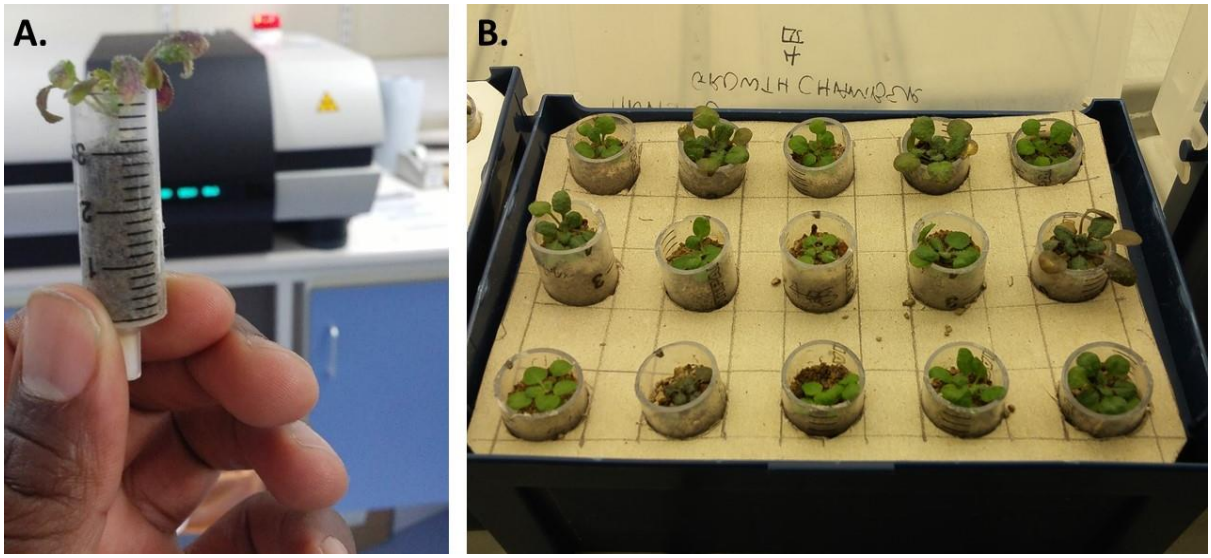

Figure 24, A. One of the plants removed from the growth chamber, just before scanning, B. Arabidopsis wild type plants as grown in specially adapted syringes

Images obtained from the scanning of the different tubes revealed the above-ground parts of the plants scanned clearly, however, as plant roots from the scans entered the soil, plant material became increasingly obscure and very difficult to identify, making both automated and manual segmentation of RSA nearly impossible. The images obtained also had considerable noise, which

was minimised by the application of a non-local means filter. Root recovery was better in the aggregated sandy loam soil as compared to the sandy soil. The noise and inability of the scanner to produce clear images of roots was thought to have arisen from the density that my samples had as the 4-watt power of the scanner might not have been able to produce X-rays with adequate flux to produce the contrast to differentiate between root and soil within my samples. This is as evidenced by the sand sample in particular where due to the high X-ray attenuation of quartz material that dominates sand soils (Figure 25 C and D). Root material could not be segmented from the point it entered the sandy soil.

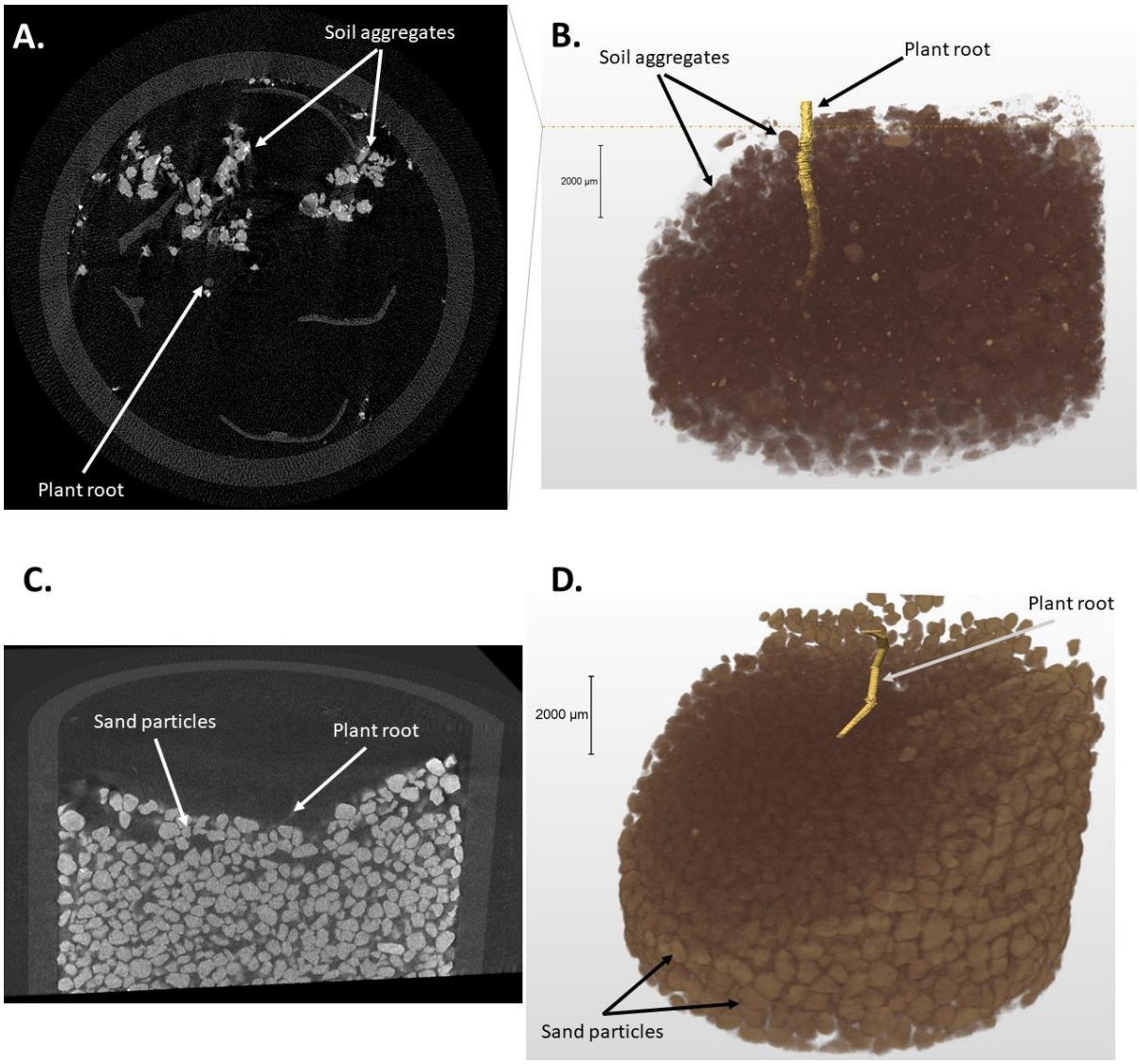

Figure 25 A) Greyscale image and B) 3D volume rendering of Arabidopsis seedling grow in a sandy loam soil. C) Greyscale image and D) 3D Volume rendering of Arabidopsis plants seedling grown in coarse sand.

Nikon Metrology XTH 225 experiments

Because of the relatively small sample size and poor capacity for differentiation between roots and soil in the first preliminary experiments. I decided to trial the use of a more powerful industrial grade scanner that could image my fully-grown Arabidopsis plants in their native pots. The Nikon Metrology XTH 225 as described in the Methods section was used for the second phase of trials. For these experiments, Arabidopsis plants were grown in 50ml centrifuge tubes identical to those used in the transpiration experiment in Section 3.3.3 with only the wild type plants being scanned. The wild type plants germinated in these tubes were grown for 62 days before imaging. At imaging, the centrifuge tubes had a volumetric moisture content (θ) of <10% which was ideal to enhance the contrast between air spaces and roots. To speed up the scanning process, only the top 3cm of the tubes were scanned instead of the entire tube.

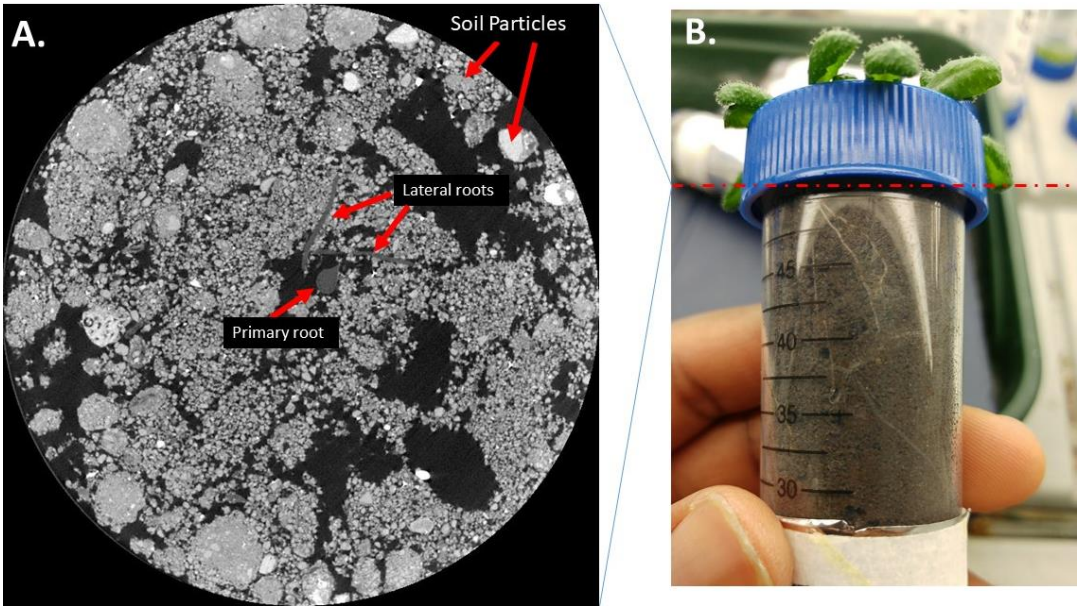

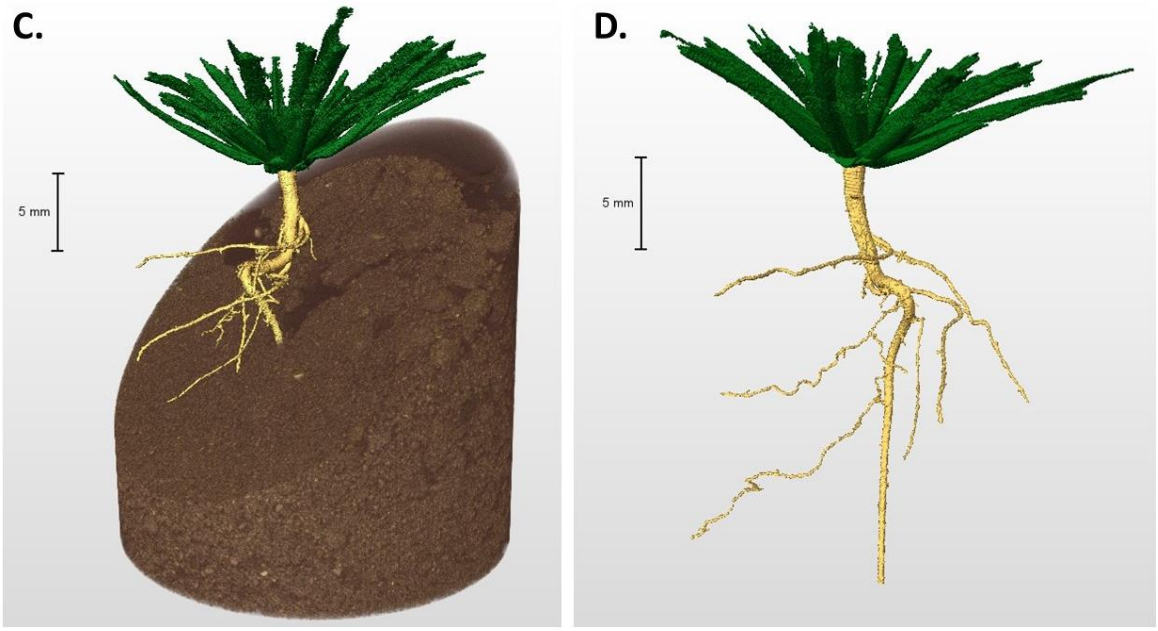

Figure 26 A) Cross-sectional greyscale image of Arabidopsis obtained by X-Ray CT scanning using the Nikon XTH 225 with B) showing the tube that was imaged. The 3D volume rendering of the segmented image of Arabidopsis plant with and without volume rendering of the soil is shown in C and D respectively.

Results from the scanning with the more powerful scanner yielded visibly improved image quality, producing images with significantly minimised image noise. This thus enabled the clear visualisation of plant root material throughout the imaged section of the column (e.g. in Figure 26A). I was able to segment out the primary plant root as well as several lateral roots from these initial scans as shown in Figure 26C and D. It was clear that using the more powerful scanner, I could successfully image the RSA of my Arabidopsis mutants under investigation. The preliminary scans revealed not only details of the primary root, but also the smaller lateral roots stemming from the lateral root.

b) RSA of Arabidopsis mutants under two different moisture regimes

Having established the possibility of visualisation of Arabidopsis RSA in initial trials, the next experiment investigated how the RSA of the different plant lines varied under contrasting moisture regimes. In this experiment, two different moisture regimes were implemented to assess the impact of periodic droughting on the RSA of the Arabidopsis plant lines grown in soil. This investigation was complementary to experiments detailed in the forthcoming section (Section 3.6) assessing the impact of variable plant soil moisture extraction on soil structure as assessed by soil aggregate stability tests. The two moisture regimes implemented in this study were namely the Well-Watered (WW) treatment, where soil was either kept at field capacity for the entirety of the experiment and the intermittently watered (IW) treatment where the soil allowed to dry to 25% of field capacity

before re-watering. This experiment was set up as shown in Figure 27A with plants being grown in 120ml pots as shown in Figure 27B. The results from the different scans done are shown in Figure 28.

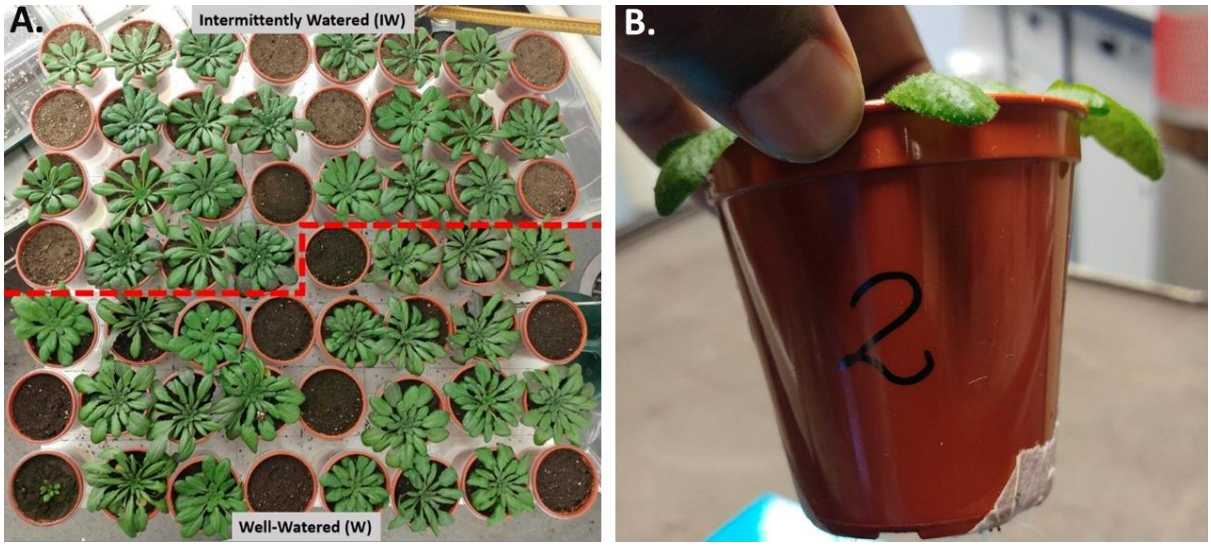

Figure 27 A) Pots with the different Arabidopsis lines subjected to two treatments namely IW(top of image) and WW(bottom of image). B) One of the plants growing in the 120cm^3 pots soon after watering and weighing.

Figure 28 RSA of Arabidopsis thaliana plant lines when grown in soil under the two different moisture regimes with A: Col-0 WW, B: Col-0 IW, C: epf2 WW, D: epf2 IW, E: EPF2OE WW, and EPF2OE IW.

Table 8: Showing some of the root properties of the different mutant lines obtained from segmented CT scans and biomass measurement

Genotype	Water treatment	Root length(mm)	Root Volume(mm^3)	Root surface area(mm^2)	Root diameter (mm)	Number of laterals	Root biomass (g)
Col 0	WW	322.71	46.23	185.10	0.246	14	0.105
epf2	WW	186.70	21.60	91.11	0.098	15	0.065
EPF2OE	WW	289.67	36.74	157.64	0.098	14	0.106
Col 0	IW	295.89	34.20	137.02	0.091	18	0.077
epf2	IW	141.38	14.54	61.15	0.108	12	0.038
EPF2OE	IW	239.18	19.91	70.53	0.080	18	0.053

The results from X-Ray CT scanning as shown in Figure 28 and detailed in Table 8 show that the RSA of mature Arabidopsis can successfully be visualised in when grown in soil using this technology. The scans were not only able to reveal details of the primary and larger lateral roots alone but were also able to reveal some smaller 2nd order lateral roots branching away from the different laterals. An average of about 15 lateral roots were visible in all the pots imaged.

Comparatively, under both moisture treatments, the wild type plants showed the greatest RSA as compared to the two mutants with root length, volume and surface area being higher as compared to both mutants. On the other hand, the EPF2OE mutant plants under both water treatments had a greater root length, volume and surface area as compared to the *epf2-1* mutant which generally had the smallest RSA. In terms of the individual moisture treatments however, all the plant lines had a larger RSA under WW conditions as compared to IW treatments.

3.5.2 Neutron CT imaging

In addition to the RSA properties revealed using X-ray CT imaging, I attempted to use Neutron CT to further provide details of the root architectural properties of my different Arabidopsis plants whilst also comparing the two technologies. I hypothesised that neutron CT technology would enable better segmentation and visualisation of the Arabidopsis RSA as the high amount of water in Arabidopsis roots would provide better contrast between roots and surrounding soil unlike in X-Ray images.

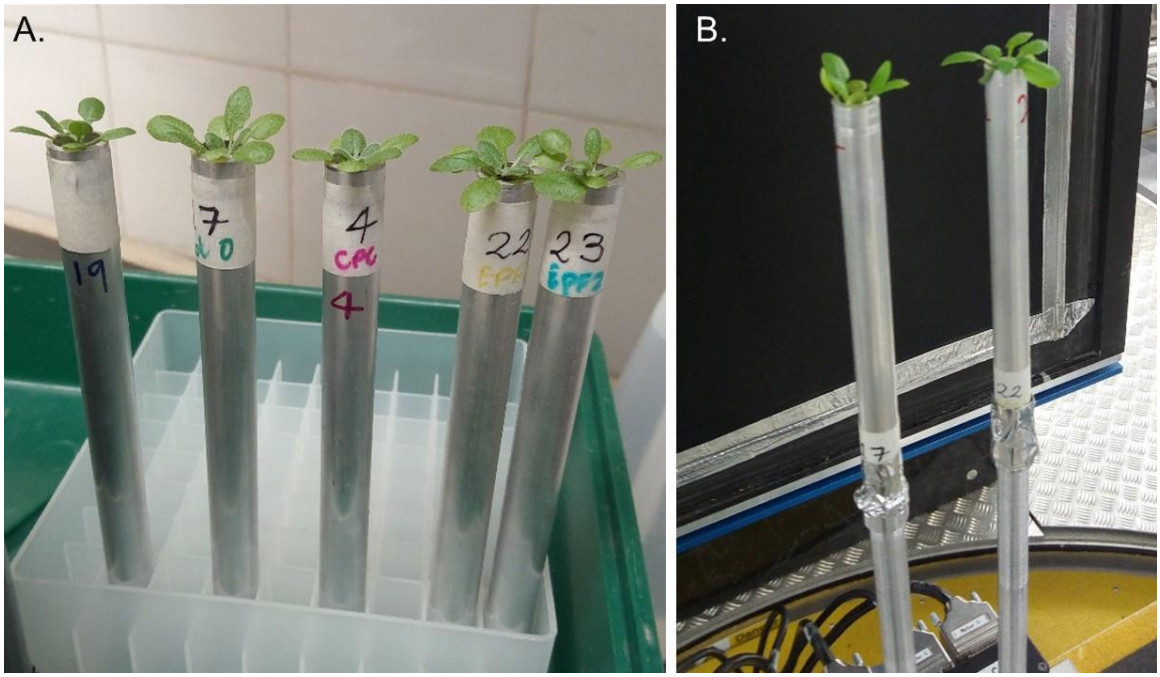

Figure 29 (A) Showing 5 Arabidopsis plants just before neutron scanning as well as (B) 2 plants on a multi-axle stage in front of the neutron scintillator soon after scanning.

For this specific experiment, Arabidopsis plants were grown in specially designed cylindrical aluminium tubes with a diameter of 10mm and a length of 140mm as shown in Figure 29. These were bottom sealed with Aluminium tape then filled with a sandy loam soil leaving a 10mm gap from the top of the tube to allow for surface irrigation. Three Arabidopsis seeds were then planted in each tube and subsequently thinned to a single seedling after a week of growth. The single plant was allowed to grow for 5 weeks before imaging at the IMAT facility. The same plants were also scanned using the Nikon X-ray CT scanner and a side by side comparison of some of the images acquired is shown in Figure 30.

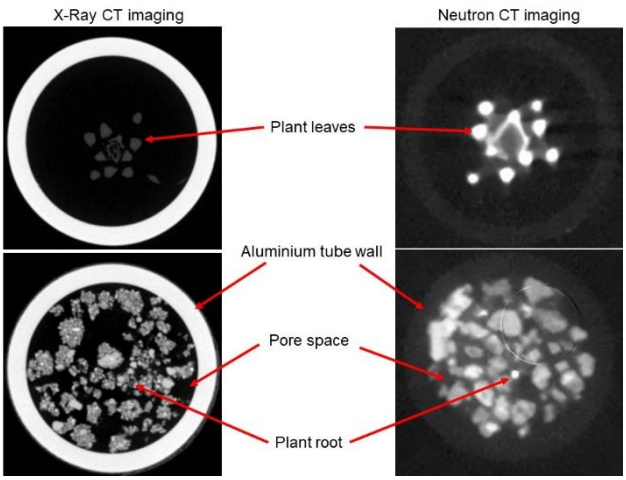

Figure 30 Comparison of the complementary greyscale images from X-Ray and Neutron CT imagery of an Arabidopsis growing in the Aluminium tubes

The results from the NCT imaging as shown in Figure 31 indicate that RSA of Arabidopsis can successfully be visualised this technique. However, only part of the Arabidopsis RSA was visualised in the plants that I imaged with only the top and bottom few cm of the Arabidopsis roots were visible under in all my scanned plants with the wild type plants showing the greatest length of root that was distinguishable from the soil. The mid-section of the tubes had similar attenuation to the roots possibly due to having a relatively high moisture content. This prevented accurate root segmentation.

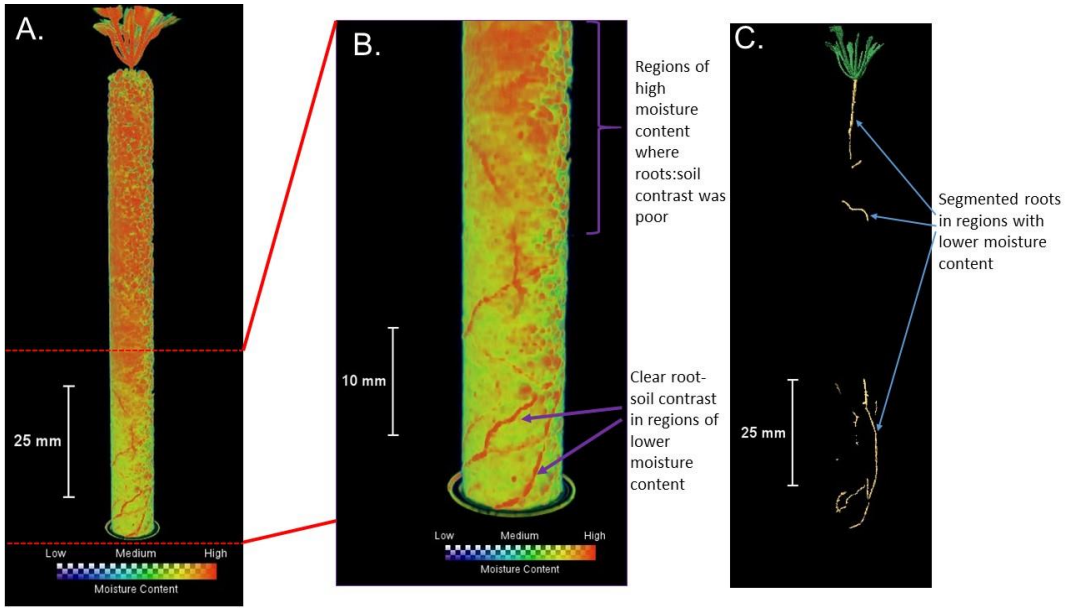

Figure 31 Illustrating raw volume rendering images (A and B) of Wild type taken from Neutron CT scans and according to neutron CT scans. Regions in red represent increased neutron attenuation whilst regions in green represent reduced attenuation. C) 3D volume rendering of segmented roots and shoots with omissions in the regions with increased moisture where contrast between roots and soil was low.

3.6 Effects of improved WUE in plants on soil structure

Further to determining the impact of improving WUE on RSA in the different Arabidopsis lines, this section further examines how improving WUE affects soil structural stability in the same plant lines. To achieve this objective, the following research questions were investigated in this section.

Main research questions:

- How does altered plant WUE affect soil structure as indicated by soil aggregate stability tests?
- How do the different mutants perform in the selected aggregate size?
- How do Arabidopsis roots interact with aggregates of different sizes?

3.6.1 Aggregate stability in <4mm sieved soil

In order to answer the question patterning to soil structural modification by the different plant lines, In this experiment, the three Arabidopsis plant lines were grown in sandy loam(<4mm) filled pots similar to those used in section 3.6.3a for 12 weeks with a single moisture regime being applied. Plants were watered to gravimetrically determined field capacity 3 times a week for the entirety of the experiment. At the end of the growth period, a bulk soil sample was extracted from each pot and subsequently used for aggregate stability tests as described in the Methods section. The results I obtained from this experiment are shown in Figure 32.

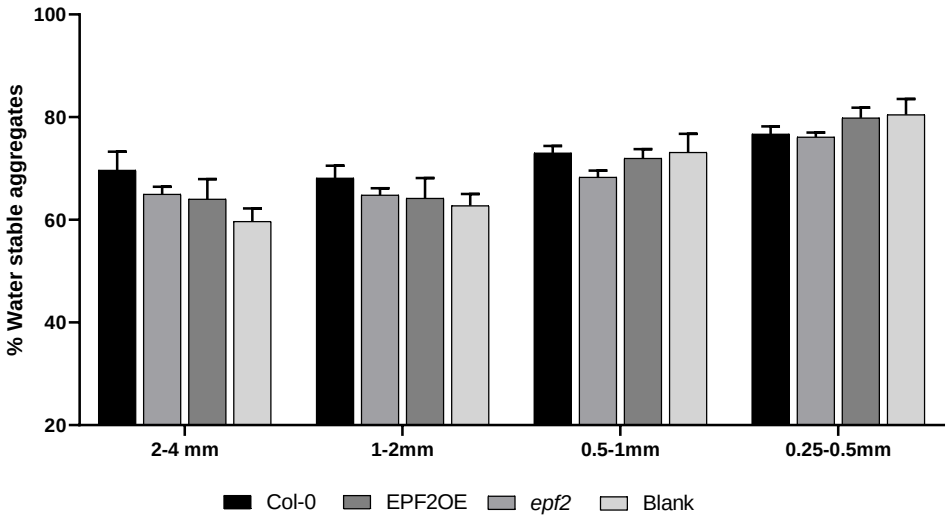

Figure 32 Stability of aggregates of different size classes after growth the of the 3 plant lines as well as the control bank (treatment) (n≥10). Error bars indicate standard error of the Mean (SEM).; One-way ANOVA tests.

As shown in Figure 32, aggregate stability of the different plants did not significantly differ between each other in all the aggregates size classes we tested. Generally, however, in the two largest aggregate fractions (2-4mm and 1-2mm), the blank treatment had the lowest average aggregate stability as compared to the plant treatments suggesting an increase in aggregate stability as a result of the Arabidopsis plants. On the other hand, for the smaller aggregate sizes (0.25-0.5mm and 0.5-1mm), the aggregate stability in the control soil was higher than that of all the plant treatments suggesting a reduction in aggregate stability of the smaller aggregates.

3.6.2 Selection of growth media ideal for aggregate stability tests

As no significant differences in AS were observed using bulk soil, to further investigate the slight differences observed, I decided to focus on one particular aggregate size fraction as this would make the comparison of aggregate stability between the different plant lines relatively less complex (as only one value for stability is computed). This was essential for Arabidopsis which has relatively smaller roots as compared to most field crops for which most of the aggregate stability methods have often applied (Materechera *et al.* 1994, Haynes and Beare 1997). To determine the ideal growth media that would be used for aggregate stability tests, three different aggregate fractions derived from dry sieving the sandy loam soil were obtained. These were namely soil aggregates of size classes; 0.25-0.5mm, 0.5-1.0mm and 1-2mm. Seeds of the wild type plants were grown in each of these different sized aggregates as well as in bulk soil sieved to below 4mm to eliminate large aggregates. The plants were grown in the specially designed centrifuge tubes as described in previous sections (section 3.3.3) to monitor plant transpiration for calculation of WUE under the different media. A similar moisture regime was applied to each media ensuring plants did not experience moisture stress through the course of the experiment. The results from this experiment are given in Figure 33.

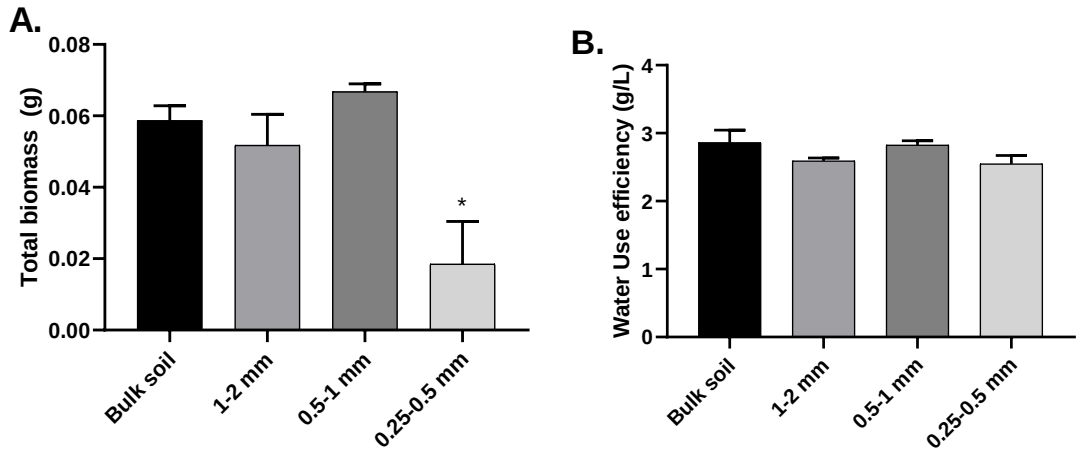

Figure 33 Comparison between the different growth media with A) total biomass of plants in the different growth media compared to bulk soil and B) WUE of the wild type Col-0plants grown in the contrasting soil media (n≥4). Error bars indicate standard error of the Mean (SEM). Symbols indicate significant difference as compared to Col 0; One-way ANOVA test with post-hoc Bonferroni test, (*=≤0.05.)

Results from these experiments as shown in Figure 33A show that biomass production was significantly lower in the 0.25-0.5mm aggregates as compared to bulk soil. The 0.5-1mm and 0.5-1mm aggregates did not show any significant difference in biomass productivity compared to the bulk soil however the 0.5-1mm sized fraction showed marginally increased biomass production as compared to both the bulk soil and the 1-2mm fraction.

WUE estimated from the biomass produced relative to transpiration as shown in Figure 33B was shown to generally not be affected by different growth media with no significant differences being shown between different plant growth substrates. Plants grown in the bulk soil showed marginally higher WUE however as compared to the other media. As a result of these experiments, I decided to use the 0.5-1mm aggregates for further soil structural experimentation as they comparatively had the greatest average biomass production and WUE among the different sized aggregates used.

3.6.3 Plant growth characteristics in selected aggregate size (0.5-1mm)

As I had altered the growth substrate I was using (from soil sieved to <4mm soil to 0.5-1mm soil aggregates), it was essential to re-examine the performance of my plant lines to ensure that the change in substrate did not impact on the plant growth characteristics I had already established in the 4mm sieved soil, I analysed all the essential plant characteristics previously measured in prior sections, namely shoot and root biomass, SD and SI as well as WUE as determined by Δ as well as inferred from biomass and ET. This was done for both the treatments I was using, namely the WW and IW treatments as described in section 3.5.1b on. The results I obtained are given in Figure 34

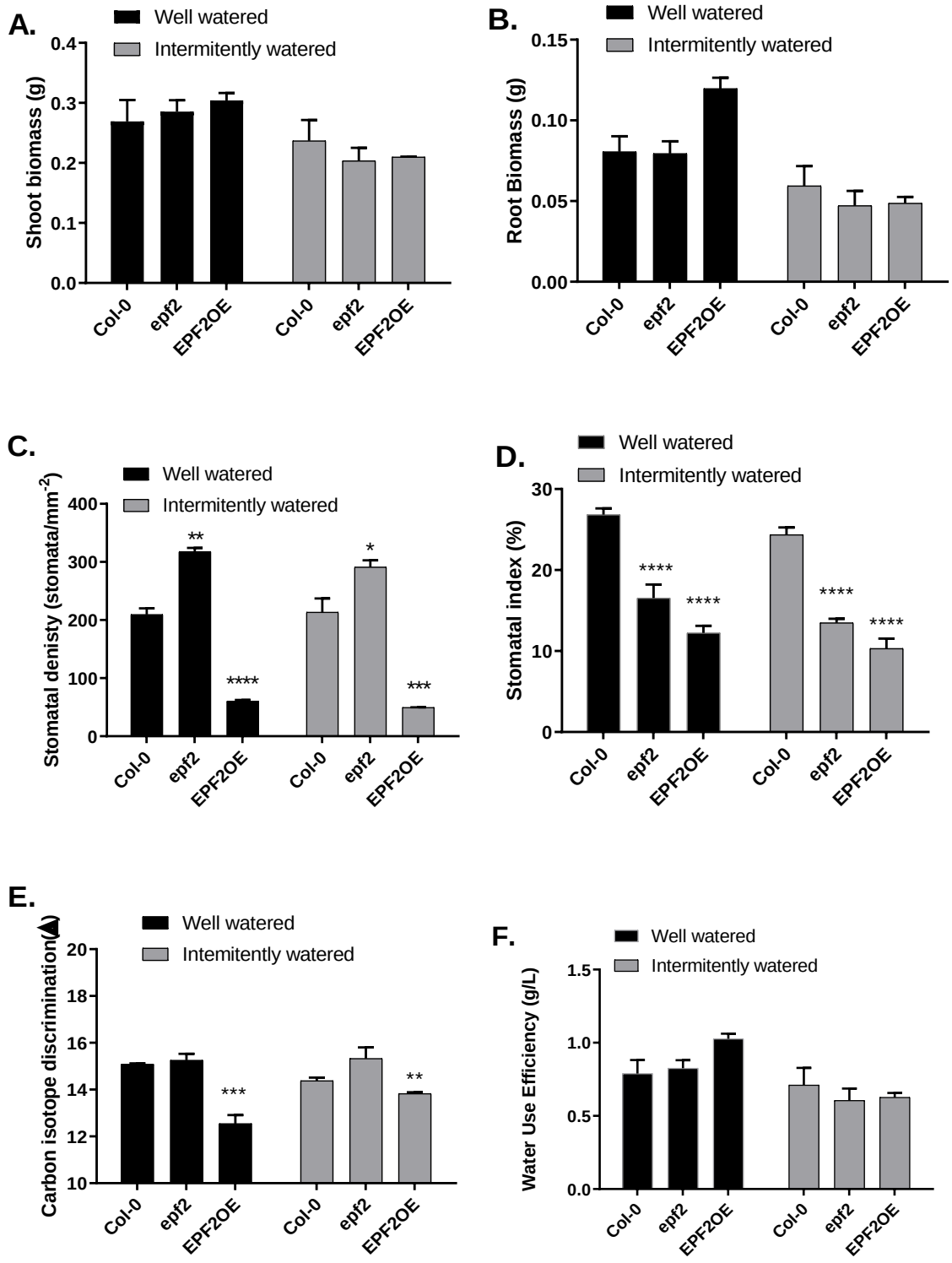

Figure 34 Growth characterisation of Arabidopsis mutants grown in 0.5-1mm soil aggregates under two moisture regimes(Well-watered and Intermittently-watered) with A) Shoot biomass, B) Root biomass, C) Stomatal density, D) Stomatal Index, E) Carbon Isotope discrimination and F) WUE derived from biomass measurements (n≥6). Symbols indicate significant difference as compared to Col 0; One-way ANOVA test with post-hoc Bonferroni test, (*=≤0.05. **= ≤0.01, ***=≤0.001)

Results obtained from these tests were broadly similar to those obtained when the same plants when grown in bulk soil. In terms of root and shoot biomass productivity (Figure 34A and B), the mutants did not differ significantly to that of the wild type under each moisture regime. Both root and shoot biomass productivity were however adversely affected by the intermittent watering regime and thus root and shoot biomass production were notably reduced under this treatment. Root biomass of the EPF2OE line was comparatively higher than those from the wild type and *epf2* mutant in well-watered conditions.

In terms of SD and SI(Figure 34C and D), again similar trends as observed when plants were grown in bulk soil prevailed under both my treatments. SD remained highest in the *efp2* mutant whilst being lowest in the EPF2OE line. SI was also significantly reduced in both the stomatal mutants with the EPF2OE lines showing the lowest SI as expected.

In terms of WUE as determined by the Δ and via direct biomass measurements (Figure 34E and F), there were some unexpected differences as compared to the results obtained when the plants were grown in bulk soil (Figure 34E compared to Figure 23A). In terms of Δ although the EPF2OE line had significantly increased WUE under both treatments as compared to the wild type, the *epf2* mutant did not show the significant reduction in WUE as compared to the wild type as had been demonstrated earlier. Under the well-watered treatment, the differences in Δ C was much less evident in comparison to the wild type indicating very little differences in WUE. Under the IW treatment, however, although the differences between the wild type and *epf2-1* were not significant, a noticeable reduction in WUE was seen in the *epf2-1* mutant.

In terms of directly measured WUE (shown in Figure 34F), no significant differences were observed between the different lines under both the WW and the IW treatments as had been observed when plants were grown in bulk soil. The *EPF2OE* line showed marginally increased WUE under the WW treatment. Under the IW treatment, however, this trend seemed to have been different from the wild type showing the greatest WUE.

3.6.3 Aggregate stability measurements in 0.5-1mm aggregates

In order to better detect differences that may arise from the growth of the different plant lines this experiment made use of the fact that alteration of the *EPF2* gene as is the case with the mutants used in this study, has been shown in literature to produce plants with altered transpiration rates (Doheny-Adams *et al.* 2012, Franks *et al.* 2015, Hepworth *et al.* 2015). This has also been demonstrated in my experiments, with the *epf2-1* and *EPF2OE* lines having increased and reduced transpiration as compared to wild type plants respectively. The changes in transpiration of the

different plant lines may lead to a variation in soil drying rates which may result in exposure of soil around the roots to different soil moisture regimes in the different plants.

As variable soil moisture regimes as imposed by different roots has previously been shown to affect both aggregate stability and strength (Materechera *et al.* 1994). To investigate the possible impacts of the variable soil drying on soil structure, in this study different soil moisture regimes were imposed to soils in order to enhance (by allowing soil to dry) or reduce (by maintenance at a high soil moisture content) the impact of transpiration on soil structure. It was hypothesised that the different Arabidopsis mutant plants would be able to produce differences in the soil moisture regime due to their contrasting transpirational rates. This would enable me to contextualise how changes in the transpirational pull as exerted by the different plants with varying stomatal characteristics affects soil structure whilst also investigating the different ways that plants affect soil structure (alteration in soil moisture regime) alluded to by Angers and Caron (1998). Similar studies have been carried out by Materechera et al. (1994) however, they focused on differences between plant species whilst this study looks at intraspecies differences.

To determine changes in aggregate stability as brought about by growth of the different genotypes and the respective moisture treatments was assessed. The method as suggested by Kemper and Rosenau, (1986) with slight modifications as described in the methods chapter was used. The different plant lines were grown for 12 weeks in 120cm^3 pots and watered as described in section 3.5.1b for the entirety of their growth period. After this growth period, the plants were then harvested to determine their shoot and root biomass with the results of this being presented in Section 3.6.2. Two different soil samples were also extracted from pots where the plants were grown, namely bulk soil and rhizosphere soil. The bulk soil was the soil that was freely released from the growth pot unbound by the roots whilst rhizosphere soil was the soil that was tightly adhered to the roots and requiring vigorous root shaking to release from the roots. The soil removed from the pots was then packed in plastic bags and stored at 4°C up until aggregate size distribution and stability measurements were to be made. The aggregate stability and total carbon was determined for both rhizosphere and bulk soil samples and the results from these tests are shown in Figure 35.

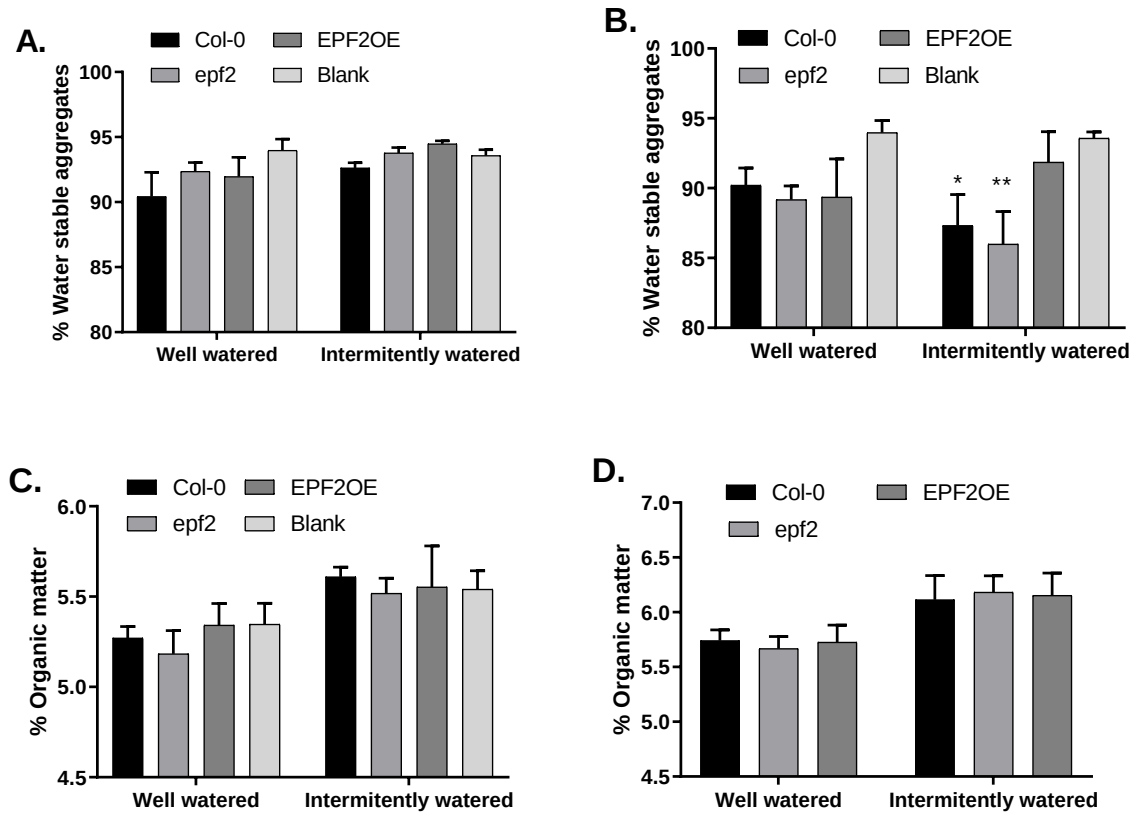

Figure 35: Water stable aggregate stability of results from A. bulk soil and B. rhizosphere soil and Total organic matter content in C. bulk soil and D. Rhizosphere soil (n≥5). Symbols indicate significant difference as compared to Col 0; One-way ANOVA test with post-hoc Bonferroni test, (*=≤0.05. **= ≤0.01,)

In terms of bulk soil measurements (Figure 35A), there were no significant differences in the aggregate stability (AS) between the different plant lines as compared to the control (blank) in both the WW and IW treatments. Under the WW treatment, however, the AS of the blank samples was marginally higher than all the plant samples, which suggests that the plants reduced AS of the soil. Under the IW treatment, there was also a noticeable marginal increase in AS for all the plant lines as compared to WW plants. For the rhizosphere soil (Figure 35B), there was no significant difference between the different plant lines as compared to the control treatment under WW conditions. However, under IW treatments, AS of the wild type and the *epf2* mutant were significantly lower than that of the control treatments. The EPF2OE line's AS although not statistically different from that of the wild type, was lower than that of the control, which also suggests that in general, root action reduced the stability of the aggregates.

In terms of total organic carbon (TOC) in the rhizosphere soil (Figure 35C and D), there were no significant differences in TOC in the rhizosphere of all the plant lines under every treatment,

however, under IW conditions, there was a general increase in TOC around the root for all the plants.

3.6.4 Electron microscope scanning

Having shown very few significant differences in aggregate stability between the different plant lines in my study, my last experiments focused on the visualisation of the interaction between Arabidopsis roots and the 0.5-1mm sized aggregates using electron microscopy. This qualitative visualisation of the microscale interaction between plant roots and soil aggregates could help explain some of the observations made during aggregate stability testing. This visualisation was complementary to X-ray and Neutron CT scanning of plant RSA with a higher resolution being used in this technique (up to 500nm vs up to 50pm) (Erni *et al.* 2009).

For this experiment as the amount of sample that I could visualise was limited, I randomly selected a 5mm section of aggregate adhering roots from the wild type and the EPF2OE lines plants for visualisation. These were extracted from the same plants used in the aggregate stability test detailed in section 3.6.1. The roots were placed side by side on a small electron microscope mounting stage and preparations were done to optimise my sample for imaging. The results I obtained from this experiment are shown in Figure 36.

I was able to visualise various sections of my Arabidopsis roots showing detailed interactions between them and the adhered soil aggregates as shown in Figure 36B and C. Different magnification levels were used attaining a spot magnification of between 100x and 800x. At the lower magnification levels, root enmeshment into the aggregates could clearly be visualised in both the wild type and the EPF2OE lines with numerous fibrous looking root material (possibly root hairs) penetrating the parts of the soil aggregate in interaction with it. The fibres were estimated to be about 2 and 15μm in thickness and looked to be the binding force attaching roots to the different aggregates. Root fibres were also seen to be penetrating the aggregates as is shown in Figure 36 D and E, which could potentially lead to their weakening in some cases whilst allowing water transport from the interior of the aggregate to the plant. This weakening could partially explain the marginally reduced aggregate stability after Arabidopsis root growth. I was also able to visualise what appeared to be silt/clay particles adhering to the root even which could have been excised from a larger aggregate.

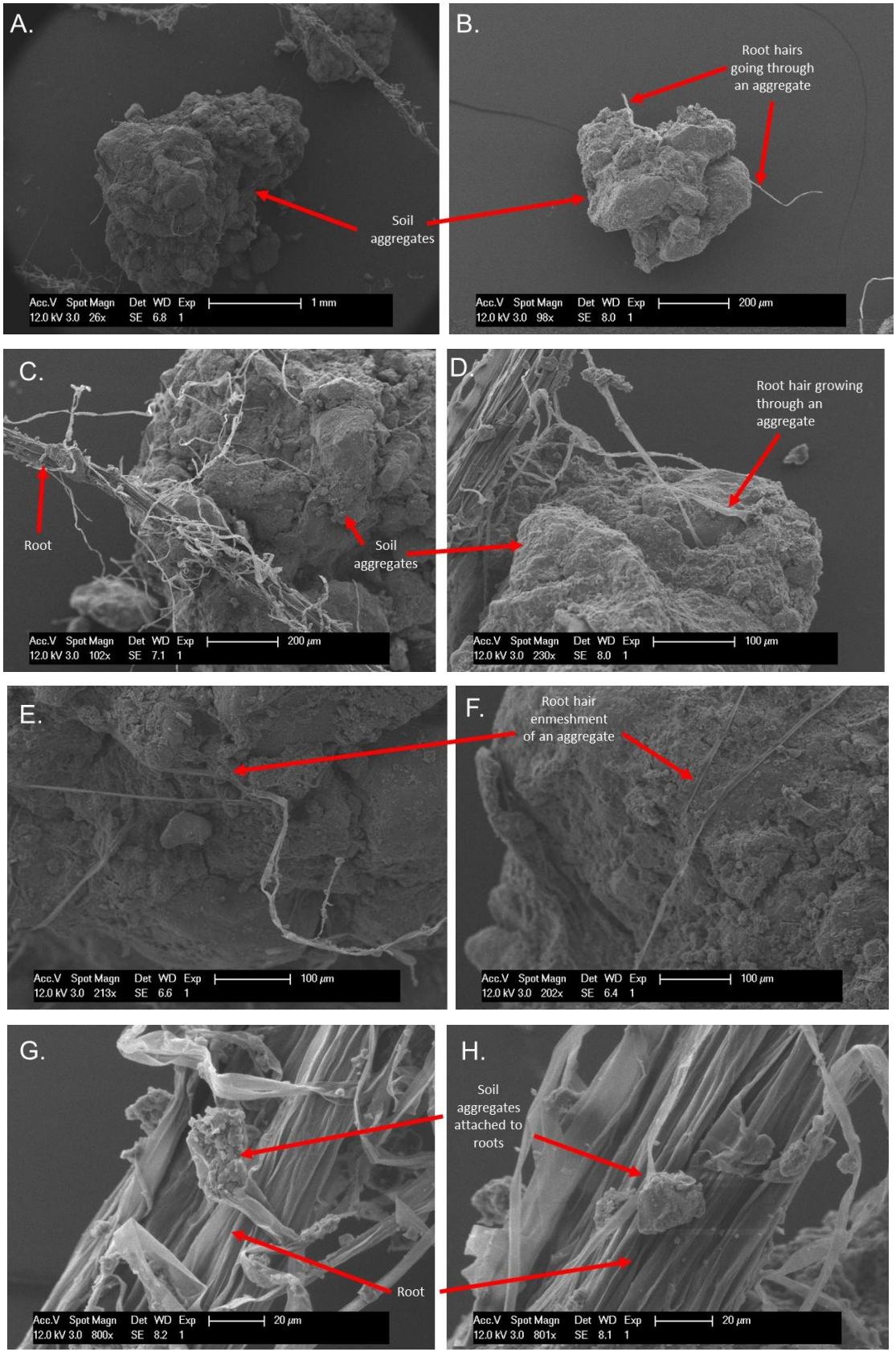

Figure 36 Electron microscopy of soil adhered to an Arabidopsis roots of the Col 0(A, C, D) and the EPF2OE lines (B, D, E)

3.7 Discussion

3.7.1 Screening for WUE in root and shoot mutants

My random screens for novel altered WUE in the wide range of different root and shoot mutant did not yield my expected outcomes as I was unable to identify a mutant that showed a robust alteration in WUE. Although the literature suggests that altering root properties such as root hair density plants improves their water and nutrient uptake from the soil (Blum 2009, Tanaka *et al.* 2014, Ruggiero *et al.* 2017, Leakey *et al.* 2019). My results showed on the contrary altering root hair density does not result in significant changes in the WUE of my contrasting root hair mutants (*cpc-1*, *rhd1* and *wer-1*) as compared to the wild type. This may have been the case due to the fact that the plants were not subjected to drought conditions as was the case in Tanaka *et al.*, (2014). The *phyB-9* and the *eir1-1* mutants were the most promising mutants in terms of WUE with their average Δ C being marginally (but not significantly) more WUE than that of the wild type, however, these differences were insufficient for their further experimentation. The relatively unchanged WUE in the *phyB* mutants is different to what was found by Boccalandro *et al.*, (2009) who found a greater magnitude of difference using *phyB* mutant of a different background (Landsberg Erecta) to the one used in this study(Columbia).

As I used two different growth media for my experiments, I discovered that WUE tended to increase when plants are grown in a more mineral soil as compared to a high nutrient organic compost mix. These differences may have possibly been attributed to, among other things, the different nutritional status of the soil as well as the lower moisture retention by mineral soils which may have induced plants to use water more conservatively resulting in improved WUE across the board (Cao *et al.* 2007). The *arf7-1 arf19-1* double mutant was the least WUE line showing significant reductions in WUE as compared to the wild type plants when grown in a sandy loam soil but not in the nutrient-rich compost. This may have been as a result of its delayed growth in comparison to the other plant lines including the wild type. I noticed the *arf7-1 arf19-1* double mutant plant exhibited sluggish growth in the initial stages of its development but recovered to reach nearly similar biomass levels long after all the other mutant lines have senesced has not previously been reported.

3.7.2 Physiological measurements of EPF mutants

As a result of not being able to identify plants with the required WUE, I, therefore, focused on mutants with altered EPF2 as they had previously been shown to have altered WUE, which was confirmed by my experiments. The SD of the selected mutant plants were largely consistent with what has been observed in literature with alterations in the EPF2 gene resulting in a 44% increase

and 73% reduction in SD for *epf2-1* and *EPF2OE* mutants respectively. This is in comparison to results by Hunt and Gray, (2009) who showed a 70% increase and an approximately 5 fold reduction in *epf2-1* and *EPF2OE* lines respectively. In term of SI, as expected the EPF2OE showed largely reduced SI due to a reduction in stomatal cells. On the other hand, the *epf2* mutant, which also showed a reduced SI had increased stomata and would have been expected to have an increased stomatal index. However, this mutant has numerous stomatal precursor cells and this increased cell division in the leaf epidermis explains the reduced stomatal index (Hara *et al.* 2007, Hunt and Gray 2009, Zoulias *et al.* 2018).

The results I obtained showed that alterations in WUE as induced by changes in the *EPF*2 gene did not significantly affect their shoot and root biomass production when grown in a sandy loam soil. This is contrary to what was observed by Hepworth *et al.*, (2016) who reported a general reduction in root size of the EPF2OE lines line when grown in a vermiculite filled rhizotrons behind a glass microfibre paper. The differences I observed from this study could have been as a result of the use of a different growth media which may have resulted in the EPF2OE lines responding differently to the sandy loam soil used in this study. The WUE of the different mutant largely conformed to what has been reported in literature, with the EPF2OE plants having improved WUE whilst the epf2-1 mutant plants had reduced WUE according to Δ measurements (Hepworth et al. 2015, Hughes et al. 2017, Caine et al. 2019). This was however variable in biomass determined WUE with the epf2-1 mutant showing similar WUE as compared to wild type plants. This may be due to the fact that WUE is not only determined by SD with other factors such as stomatal size and function may also dictate their transpiration efficiency.

3.7.3 Impact of altered WUE on RSA

It was clear that X-Ray CT could be used to study RSA of Arabidopsis as was proposed by Tracy *et al.*, (2010). Differences in RSA of the different plant lines was evident in the X-Ray CT scans with the wild type plants showing a comparatively more extensive root system as compared to both stomatal mutants albeit with only two replicates (1 under each different soil moisture regime). The *epf2* mutant surprisingly had the least expansive RSA with consistently lower root numbers, volume and surface area under the different moisture regimes. This is also contrary to findings by Hepworth *et al.*, (2016) who studied a mutant with closely related properties (increased stomatal density and index) i.e. the *epf1epf2* (double mutant) that showed broadly increased root length when grown in vermiculite behind a glass microfibre paper. Although my findings are from a different genotype, they put some of their models suggesting explaining increased root density in *epf1 epf2*

double mutants to question as in my case, high transpirational rates did not increase root length and density but rather it decreased.

From my X-Ray CT data, however, it should be noted that the RSAs recovered from the use of this scanning technology were not complete as some of the smaller lateral roots were smaller than the image resolution and thus these small roots could not be picked up in these images. As with an image pixel resolution of about 33μm, only roots greater than 66μm could be visualised (Nyquist–Shannon theorem), and even then, segmentation of such small root would prove difficult as the roots appear similar to the edge of the soil aggregate boundaries due to partial volume effects. Another factor that limited root segmentation and ultimately may have led to the reduction in segmented roots was the presence of organic matter, which had a similar X-Ray attenuation as compared to the root and thus may prevent accurate root identification.

In terms of NCT, I speculate that the RSA were not clearly visible in totality due to a number of factors, which include the small thickness of my plants' roots, which ranges from 50 to 250μm in diameter (average 130μm) (Sotta and Fujiwara 2017). This root thickness meant that some of the roots on the lower boundaries of thickness would clearly not be visible as our detector, which had a pixel size of 55 microns would only mean that only roots with a diameter of higher than 110μm (double the pixel size according to the Shannon-Nyquist theorem) would be visible (Minniti *et al.* 2018). Another factor that could have interfered in my root visualisation was the heterogeneous distribution of water and organic matter in my soil samples as these reduce the contrast between the root and soil media the roots are growing. For example, the soil moisture gradient increased towards the bottom of the tube due to drying from the surface and residual water from irrigation. I also used a soil with ≈ 6% OM which meant the high organic matter content had higher potential for obscuring roots as compared to other experiments in literature that predominantly use sand (Menon 2006, Esser *et al.* 2010).

3.7.4 Impact of altered WUE on soil structure

In terms of soil structure, in <4mm sieved soil, there was no significant difference in the aggregate stability between all the plant lines used in this experiment suggesting that the mutants largely did not significantly affect the structure of soil. This was as expected as variations in aggregate stability between plants of similar genotypes, which is not often measured, may be negligible or may take a considerable amount of time to observe. Furthermore, the small size of the Arabidopsis roots (50-250μm in diameter) also points to them having limited ability to coalesce soil aggregates together forming stable aggregates.

Further investigations with soil having a single aggregate size class as well as altered soil moisture regimes revealed interesting findings. Plants seemed to reduce the AS of the 0.5-1mm aggregates used especially under well-watered treatments. This is contrary to what is dictated by many in literature (Materechera *et al.* 1992, 1994, Haynes and Beare 1997). However, this has previously been shown by Reid and Goss, (1981) as well as Nakamoto and Suzuki, (2001). There was also an increase in AS under IW treatment. This is similar to what was observed by (Materechera *et al.* 1994) who showed that WSA increased when variable moisture regimes are implemented as compared to continuous wetting similar to my experiment. Apart from variable moisture affecting the aggregates, my results can partially be explained by the results from the measurement of TOC in the respective samples, with IW samples exhibiting higher carbon contents as compared to the WW treatments. This suggests that reduced carbon under the WW may be affecting aggregate stability under the different treatments. This increase in carbon in the rhizosphere was thought to be due to increased root exudation under the IW conditions. This speculation is not unprecedented as several authors have previously demonstrated that the quantity of root exudates may vary depending on magnitude of drying with slight to moderate drying (as in this study) being shown to increase root exudation (Czarnes *et al.* 2000, Ahmed *et al.* 2014, Preece and Peñuelas 2016, Preece *et al.* 2018).

On the contrary, my findings pointed to an increase in aggregate weakening as indicated by a reduction in the aggregate stability of aggregates from the rhizosphere of the Arabidopsis plants.

Further investigations into this using electron microscopy showed that indeed that the small Arabidopsis roots (or root hairs) were able to penetrate the cavities between different aggregates, possibly accessing water and nutrients from them. I speculate that this may result in the weakening of aggregates in two ways. Firstly, as the root grows and expands in the cavity, it may produce stress cracks within the aggregate that make it easier to break down (Oades 1993, Six *et al.* 2004) and secondly, after senescence of the plant roots disintegrate leaving a larger cavity that may become a point of weakness in the aggregate (Papadopoulos 2011).

3.7.5 Conclusions and future work

In conclusion, my research did not find conclusive evidence suggesting that altering WUE as a result of modulating stomatal density could result lead to significant alterations in RSA and soil structural stability of sandy loam soils. More research, however, is necessary to possibly explain some of the interesting results I obtained such as the weakening of aggregates in the rhizosphere. I was also able to show that non-invasive imagery both X-ray and Neutron CT can be successfully used to study the root architecture of Arabidopsis plants when grown in soil under optimal

conditions. Further research with more replicates is required to show how significant the differences in root architectures I observed was thus answering more questions on how Arabidopsis plant mutants' roots respond to growth in soil.

Chapter IV

Wheat

(*Triticum Aestivum*)

IV Wheat[1]

4.1 Chapter overview

In this chapter, in line with my overarching aim of investigating how plant WUE affects RSA and soil structure, I investigated the impact of improved WUE in wheat (*Triticum aestivum*. L cv. Fielder) on the RSA of selected wheat mutants and how it affects the structure of a sandy loam soil. Initial experiments focused on photoreceptor mutants of durum wheat (*Triticum turgidum*); however, due to complications with the genotyping of these mutants, alternative stomatal mutants lines of common bread wheat that had already been proven to show improvements in WUE had to be used. I then proceeded to characterise the growth characteristics of these stomatal mutant lines, particularly looking at WUE and biomass production. Having established that at least one of the mutants was indeed WUE under my conditions, I then performed a series of experiments looking at the RSA of this mutant line in comparison to wild type plants. For this, I used both invasive and non-invasive techniques to uncover changes in RSA of the different plants under investigations. My final experiments looked at the interaction between soil structure and the different wheat lines. In these experiments, I first analysed whether these lines affected the aggregate stability of a sandy loam soil then alternately I also looked at how aggregate size affect root growth of these wheat plants as well. The results I obtained showed that the RSA of WUE plants did not differ significantly from that of the wild type plants and the soil structure did not vary considerably when grown with different plant lines. I was also able to apply a novel imaging technique (Neutron Computed Tomography) to study wheat RSA while revealing details of moisture distributions around wheat roots. Lastly, I was also able to demonstrate differences in wheat root growth in response to different aggregates sizes; i.e. wheat plants produced longer lateral roots in the presence of larger aggregates as compared to those in finely aggregated soils.

[1] Parts of his chapter have recently been accepted for publication in Geoderma and will be part of the special issue: "Recent advances in pore-scale imaging of soil systems". Reference: Mawodza, T., Burca , G., Casson, S., & Menon, J. (2019) Wheat Root System Architecture and Soil Moisture Distribution in an Aggregated Soil using Neutron Computed Tomography. The Accepted version of this paper has been attached to the Appendix

4.2 Introduction

4.2.1 Wheat and its importance

Wheat is one of the most important crops cultivated around the world, accounting for more than 15% (220 million ha) of all arable land use around the world. Global production of this essential crop often surpasses 700 million metric tonnes per annum making it one of the worlds' most important human food crop (FAOSTAT 2019). It is the staple food for millions of people across the world and is the cereal of choice produced mostly in the temperate regions due to its ability to withstand the cooler temperatures characteristic of these latitudes (Porter and Gawith 1999, Sylvester-Bradley *et al.* 2015). This is in contrast to the other major cereals of the world, namely maize, (*Zea mays* .L) and rice (*Oryza sativa* .L) that are typically more adapted to warmer tropical climates (Sys and van Ranst 1993). Wheat is also one of the leading cereal sources of carbohydrate, protein and dietary fibre and thus contributes immensely to human nutrition in regions where it is consumed (Kumar *et al.* 2011, Shewry and Hey 2015)

Wheat is of major global significance due to its status as a staple food. However, it is one of the crops with high estimated water footprint (or consumptive use), requiring an average of 1480L of water to produce a single kg of grain (Malin and Rockström 2004). This huge demand for water by the crop results in straining of already overstretched water resources in wheat-producing regions of the world. It is estimated that approximately 20% of global wheat production is done under irrigation, this is particularly high in China and India where 75-80% of their wheat is produced via irrigation (Pask and Reynolds 2013). In most parts of the world, wheat production needs to increase in order to meet demands from an increasingly affluent population, however this has a negative feedback on water availability in many wheat producing regions with water scarcity set to be an inherent part of the wheat production system in the foreseeable future, all things being equal (Mancosu *et al.* 2015).

4.2.2 WUE mutant selection

As a result of the above-mentioned challenges, optimising water use in wheat production is key to meeting the ever-increasing global wheat requirements especially in nations that are reliant on irrigation for their wheat production. Breeding and genetic engineering of wheat to improve water use efficiency are possible strategies to explore in order to solve the conundrum of poor water availability (Chaerle *et al.* 2005). This has however proved relatively more difficult to achieve in wheat as compared to Arabidopsis (from the previous chapter studied) as wheat has a highly complex genome that has been challenging to sequence and manipulate (*Zimin et al.* 2017,

International Wheat Genome Sequencing Consortium (IWGSC) 2018). Bread wheat, for example, is an allohexaploid (2n= 6x= 42) plant with 3 copies of each of its 7 chromosomes each from a different homeologous ancestor. The size (Figure 37) and complexity of the genome has proven a significant barrier to genome sequencing and only recently, Zimin *et al.*, (2017) has been able to provide a nearly complete genome assembly. Even with this useful sequencing data available, manipulation of this complex genome is often marred with its own challenges such as wheat not being amenable to Agrobacterium-mediated transformation and tissue culture-based regeneration methods. However, with the development of efficient transformation methods, it is now becoming easier to transgenically manipulate wheat, enabling translation of basic research from model species such as Arabidopsis (Shrawat and Lörz 2006).

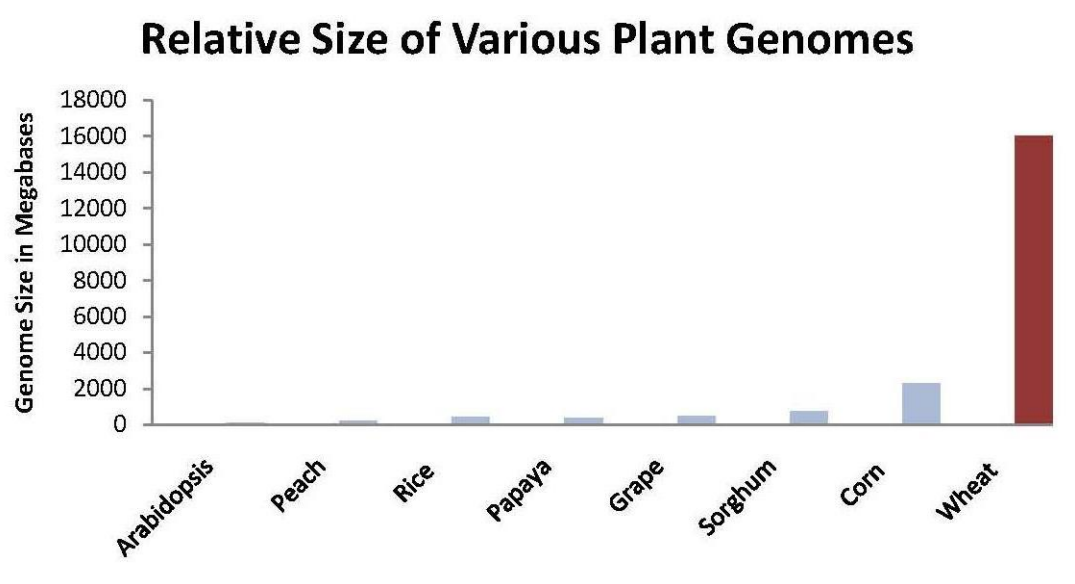

Figure 37 The relative genome size of wheat in comparison to other plants [Source (Colorado Wheat 2013)]

In this study, I use some of the mutants developed by various contemporary gene manipulation techniques in order to answer my overarching questions on the impact of improved water use on RSA and soil structure. Wheat lines with mutations in two different genes, namely PHYB and EPF1 were trialled. Firstly the phyB mutants were selected as plants with potentially novel improvements in WUE as the PHYB gene has been shown to improve photosynthesis at the expense of WUE of some other plants (e.g Arabidopsis) and I hypothesised that this would be the case with wheat (Boccalandro et al. 2009, Pearce et al. 2016). Secondly EPF1 mutant lines of bread wheat (Triticum aestivum) were selected because similar to other stomatal mutants, they had been

shown to exhibit altered WUE due to changes in stomatal density (Hughes et al. 2017, Dunn et al. 2019, Mohammed et al. 2019).

4.2.3 RSA of wheat

Wheat has a fibrous root system which is made up of 2 different types of roots, namely the seminal and nodal (adventitious) roots. Seminal roots in wheat are plagiotropic and emanate from the seed embryo. They are the first and only type of roots present in wheat plants up until the 4th to 5th leaf stage (Nakamoto and Oyanagi 1994). Wheat usually grows 5-6 seminal roots, with the first appearing soon after germination (primary root) (Kirby 2002). This is usually followed by a pair of symmetrical seminal roots that are succeeded by another similar pair of symmetrical roots which grow from a different nodal region as compared to the first symmetrical pair (Nakamoto and Oyanagi 1994, Sanguineti *et al.* 2007). A further 6th seminal root may or may not appear depending on the plant variety and growth conditions. The wheat seminal root system not only sustains early plant development and anchorage but also remain active up till maturity even after the emergence of nodal roots. The seminal root system is also essential for determining the general shape of the wheat RSA. An illustration of the different type of seminal roots present in wheat is given in the in Figure 38.

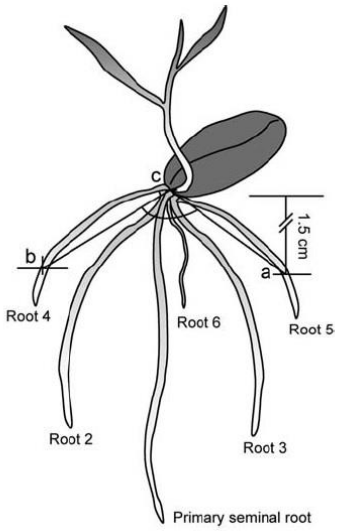

Figure 38 Schematic illustration of early wheat root system architecture showing the different seminal roots as well as root spread angle between the 4th and 5th root. [Source Sanguinetit et al. (2009)]

After the establishment of the seminal root system and subsequent onset of tillering, nodal roots emanating from the base of the stem start to grow. These secondary roots are complementary to the already existing seminal root network and grow almost horizontally into the soil (Kirby 2002).

Nodal roots are often shallow and mainly spread into the top 30cm of the soil surface where they greatly increase nutrient uptake. These roots are also normally thicker than seminal roots and usually look shiny white (white root stage) when they first appear. Most wheat cultivars have a total of 10-15 nodal roots that emanate from the third to seventh node at the base of the plant (Gregory *et al.* 1979, Slack *et al.* 2018). Root growth in wheat is a continuous process that usually proceeds up until the flowering stage, allowing roots to reach as deep as 2m beneath the soil surface depending on the growth conditions (Kirby 2002, Gregory 2009).

4.2.4 Methods of measurement of Wheat RSA

Different methods have been used to measure wheat RSA with more historic studies predominantly employing invasive root recovery methods. On the other hand, with the development of efficient non-invasive soil imagery techniques, more contemporary studies have used a combination of both invasive and non-invasive root measurement methods. Invasive wheat root measurements have been used ever since the onset of investigation in wheat roots with studies dating back as far as the 19th century being recorded in literature (Eyck and Albert 1899). These destructive methods often use equipment relatively widely available thus providing a cheap and relatively simple way of measuring wheat RSA (Mancuso 2012, Mooney *et al.* 2012). Due to this, it is no surprise that the bulk of the wheat studies in literature are based on this method (Wang and Zhang 2009b, Zuo *et al.* 2013, Subira *et al.* 2016). Destructive wheat root measurements are, however, very labour intensive and involve tedious washing of roots over a sieve (Wang and Zhang 2009b). They are also unable to give information on the spatial distribution of roots in the soil which has led to the use of more contemporary non-invasive techniques to study wheat RSA.

Unlike Arabidopsis described in the previous chapter, non-invasive investigations of wheat RSA growing in soil is more routinely performed with numerous studies having investigated wheat RSA in different soils (Jenneson *et al.* 1999, Flavel *et al.* 2012, Mairhofer *et al.* 2012a, Tracy *et al.* 2012, Flavel *et al.* 2014, Mairhofer *et al.* 2015, Ahmed *et al.* 2016). As wheat roots are generally much thicker in comparison to Arabidopsis roots (350μm vs 130μm) they are relatively easier to visualise and segment from non-invasive imagery with even low resolution (>200μm) scanners being able to comfortably visualise wheat roots in situ (Mooney *et al.* 2006). Non-invasive wheat root studies been carried out at different scales, ranging from investigations at the whole plant level (Tracy *et al.* 2012) down to investigations of fine root structures that characterise only a small part of wheat RSA such as root hairs (Keyes *et al.* 2013). Most of the studies looking at wheat RSA have largely employed the use of X-Ray CT scanning systems as opposed to other non-invasive techniques

such as Magnetic resonance imaging (MRI) and Neutron imaging techniques probably due to the relatively better accessibility of high-resolution X-Ray CT scanners in recent years.

Non-invasive 3D imagery of wheat benefits from the fact that many contemporary automated root segmenting algorithms have commonly been tested and calibrated for use with wheat plants and are thus are well suited for high throughput experiments (Mairhofer *et al.* 2012b, Flavel *et al.* 2017). There are, however, a few challenges associated with the use of this technology with wheat plants. One of the most important is the pre-requisite use of small pots (columns) which may limit root growth and shape. This also limits the age of plants that can be scanned with wheat RSA studies usually only being employed on relatively young wheat seedlings (usually <30 days old (Jenneson *et al.* 1999, Tracy, Black, Roberts, Sturrock, *et al.* 2012).

This often means that many of the studies of wheat RSA in situ primarily focus on early development of the seminal root system, ignoring the nodal roots that ordinarily appear at a later stage (Nakamoto and Oyanagi 1994). Increasing pot size to allow a larger root system to be visualised may be desirable to study larger plants, however, this has its own challenges. One of the major drawbacks to the increase in pot size is the loss of image resolution associated with imaging large samples. This is as a result of the increase in the distance between the detector and the sample when imaging relatively large sample objects (Minniti *et al.* 2018). A large cross sectional diameter would also tend to increase scanning time as the number of image projections required for adequate image reconstructions increases with the cross-sectional area of the sample to be scanned. As a result of these limitations, the majority of wheat CT experiments are usually carried out in pots no larger than 10 cm in diameter.

4.2.5 Measurement of change in soil structure after wheat growth

Plant root growth is known to improve soil structure in many ways as outlined by Angers and Caron, (1998) in their review of the mechanisms of plant induced changes to soil structure. This is however not universal for all plants as some studies have indicated no changes or even deterioration of soil structural stability in monocultural systems under cereals such as maize and wheat (Page and Willard 1947, Low 1972, Latif *et al.* 1992, Lal 1997b). The specific effect of wheat root growth on soil aggregate stability is not well understood. Information on the precise effects of wheat roots on soil structure are inconsistent and thought to be dependent on soil type, tillage practice and biological activity among many other factors. Reid and Goss, (1981) for instance, found a reduction in soil aggregate stability after 25 days of wheat grown in a sandy loam soil but did not observe significant differences in another soil (silty loam soil) in the same experiment.

Haynes and Beare, (1997) on the other hand found increased aggregates stability in wheat plants after a 12 week growth period albeit using air-dried instead of field moist aggregates as suggested by Reid and Goss, (1981). Materechera *et al.*, (1994) as well as (Materechera *et al.* 1992) also found an increase in soil aggregation as a result of wheat growth when compared to fallow treatments.

Wheat has been shown in different studies to induce reduced soil structural stability as compared to soils where ryegrass, Lucerne and maize are grown (Tisdall and Oades 1979, Reid and Goss 1981, Materechera *et al.* 1992, Haynes and Beare 1997). On the other hand, wheat has shown to increase stability more as compared to other plants such as peas, lupine and soya beans as monocots are often considered superior to dicots in terms of their effect on soil structure (Monroe and Kladivko 1987, Materechera *et al.* 1992, Francis *et al.* 1994). This has however been contradicted in some studies, for instance, Haynes and Beare, (1997) showed better aggregate stability under lupine as compared to wheat.

Investigations of intra-species differences in aggregate stability as induced by plants of different cultivar or mutants such as in this study have been few if any. This may be due to already existing inconsistencies in investigations involving the comparison of soil structural stability as induced by different plants (interspecies) in different soils such as those found by Reid and Goss, (1981). The complication of further reducing plant differences by using a single plant species may require soil structural stability tests with higher sensitivity (similar to arabidopsis) with minor changes in aggregation, which may not be available.

4.2.6 Wheat roots interactions with aggregates of different sizes

Soil aggregate size is an important factor determining seed germination and root growth (Braunack and Dexter 1989). Several scholars have investigated how aggregates of different sizes affect root growth in many plants including wheat, maize and rice (Agrawal, RP and Jhorar 1987, Donald *et al.* 1987, Alexander and Miller 1991, Thao *et al.* 2008). In general, most studies have revealed that root growth is enhanced by smaller aggregate sizes as compared to larger ones (Anderson and Kemper 1964, Cornforth 1968, Logsdon *et al.* 1987, Glinski and Lipiec 1990). This has been attributed to many factors such as the reduced root-soil contact in larger aggregates which limits moisture extraction from these aggregates (Murungu *et al.* 2003). The difficulty of root penetration into large aggregates has also been sighted as a factor affecting root growth (Voorhess *et al.* 1971, Donald *et al.* 1987). This is because when roots encounter large aggregates they often attempt to grow through them, however because large aggregates often have increased strength as compared to smaller aggregates, buckling usually occurs which limits root axial growth resulting in increased

root thickness (Whiteley *et al.* 1982a, Hewitt and Dexter 1984, Logsdon *et al.* 1987). Increased root impedance by larger aggregates also often results in the use of greater energy to deflect roots around them thereby reducing root growth (Anderson and Kemper 1964, Logsdon *et al.* 1987, Glinski and Lipiec 1990). Reduced nutrient availability in plants growing in larger aggregates has also been highlighted in some studies (Cornforth 1968, Glinski and Lipiec 1990). This is thought to be as a result of the reduced root access to nutrient reserves within larger aggregates due to their reduced surface area (Misra *et al.* 1988, Thao *et al.* 2008). Studies using large aggregates have shown that both phosphorus and nitrogen may become limited with phosphorus deficiencies being most pronounced as the nutrient is relatively immobile as compared to other nutrients like nitrogen (Agrawal *et al.* 1984). Root hair length and root penetration of aggregates has also been shown to be significantly increased in soils with larger aggregates (Misra *et al.* 1988) however root length in larger aggregates was significantly reduced in cotton and sunflower seedlings.

Despite the plethora of studies highlighting increased root growth under smaller aggregates, this notion has been contradicted in other studies as several experiments have also shown reduced root growth with decreasing aggregate size. Most notably Agrawal, RP and Jhorar, (1987), as well as Agrawal et al. (1984), reported increased wheat root growth in larger aggregates as compared to smaller aggregates in a sandy loam soil. Wang et al. (2001) also found reduced growth in smaller aggregates when lettuce and soya bean were grown. These studies attributed the reduced root growth to the better nitrogen holding capacity in larger aggregates which is contrary to what was found by Cornforth, (1968) and Misra et al. 1988). Goss, (1976) on the other hand did not find any significant change in root growth when barley roots were grown in glass beads of different sizes possibly suggesting that soil chemical factors may play more important roles in root growth in different sized aggregates as compared to growth patterns being due to purely physical limitations of aggregates.

As a result of some of the inconsistencies in knowledge surrounding root growth in soils of variable aggregate sizes, especially with wheat. In this study, I aim to reveal for the first time in 3D, how roots interact with soils made up of different aggregate sizes to produce different RSAs. I also use non-invasive NCT to map moisture content within roots and attempt to explore, the apparent loss in moisture that occurs when roots move through large pores as shown in previous experiments.

4.2.7 Research aims and objectives

In this chapter, I focused on understanding how altered WUE in wheat plants impacts on their root architecture and soil structural development.

To achieve this, I had the following objectives:

1) Identify wheat mutants that showed alterations in WUE as compared to wild type plants of the same background.

2) Determine how the change in WUE of the identified wheat plants affects their RSA using both invasive and non-invasive techniques of root characterisation.

3) Assess how changes in WUE of the identified wheat plants impacts on soil structure whilst also looking at how soils of different architectures affect wheat root growth.

4.3: Screening of wheat mutants for improved water use efficiency

Before answering my overarching research questions using wheat, initial investigations to identify wheat mutant lines with the required alterations in WUE as compared to wild type plants was necessary. To achieve this the following research questions were answered in this section were:

Main questions:

- Which of the selected mutants show altered WUE under controlled conditions?
- How do the growth characteristics of the selected mutants perform as compared to wild type plants?

Based on work in Arabidopsis where certain *phyB* mutants exhibit improved WUE (Boccalandro et al. 2009), for my initial trials, I used *phyB* mutants of the tetraploid durum wheat species (*Triticum turgidum* L. subsp. Durum var Kronos) as described in Pearce *et al.*, (2016). I sought to confirm if the *PHYB* gene also plays the same role in wheat thus making it an ideal candidate for my forthcoming experiments.

As complete *phyB* knockouts (*phyB*-null- with no functional *PHYB* genes) mutants in wheat flower relatively late and do not produce seed (sterile), the mutant seed stock has to be maintained as heterozygous for the mutations in the two copies of the *PHYB* gene that tetraploid durum wheat possesses. Therefore, within a population, there would be a mix of wild-type, heterozygous and homozygous mutant seed. As the phenotype of *phyB* double mutants was not clearly distinct from other genotypes in the population during vegetative growth, molecular genotyping was necessary to screen for the required *phyB* mutants for each experiment. I attempted to use standard genotyping Polymerase Chain Reactions (PCR) with primers as described in Pearce *et al.*, (2016) but this proved unreliable in distinguishing the different genotypes. As a consequence, gene

sequencing for each individual plant was required to identify the null mutant plants for further experiments. This proved to be an unsustainable and expensive exercise and thus I opted to find alternative wheat mutants to trial.

I consequently selected transgenic lines of bread spring wheat (*Triticum aestivum. L var* Fielder) as described by Dunn *et al.*, (2019) that had already been shown to exhibit improved WUE. These plants were engineered to overexpress the *TaEPF1* gene, which is a putative orthologue of the *EPF1* gene in Arabidopsis that is responsible for enforcing the one-cell spacing rule and subsequently controls stomatal density (Sachs 2005, Hara *et al.* 2007). Overexpression of *TaEPF1* in wheat results in a reduction in stomatal density, which is broadly similar to the phenotype observed when EPF1 is overexpressed in Arabidopsis. Reducing stomatal density as a result of overexpression of EPF1 like genes has previously been shown to improve WUE and drought resistance in Arabidopsis, barley and rice (Hughes, *et al.* 2017, Caine *et al.* 2019). This is because stomata are the main site of water loss in plants and thus by reducing the number of stomata per unit area of leaf, transpiration is also reduced if everything else remains constant. I selected two of the three TaEPF1 mutant lines described in Dunn *et al.*, (2019) namely the TaEPF1OX1 and TaEPF1OX2 mutant lines. These were of the Fielder wild type variety background.

4.3.1 Stomatal characteristics

To characterise the SD phenotype of the different transgenic lines as compared to the wild type, all the wheat lines were grown in a sandy loam soil. This was necessary to establish that the stomatal density phenotype was not specific to the growth conditions in the original work (Dunn et al. 2019). These plants were grown until the 5th leaf stage (about 3 weeks after germination) where the stomatal impression of the fully expanded 4th and 5th leaf for each plant was taken and characterised. I investigated SD as well as the mechanism through which the reduction (or increase) in SD is achieved in the mutant plants via counting of the number of stomata in each stomatal file line as well as the number of stomata per stomatal file lines observable in a 0.7mm^2 region of the leaf (Illustrated in Figure 39). The results from these characterisations are shown in Figure 40 and Figure 41

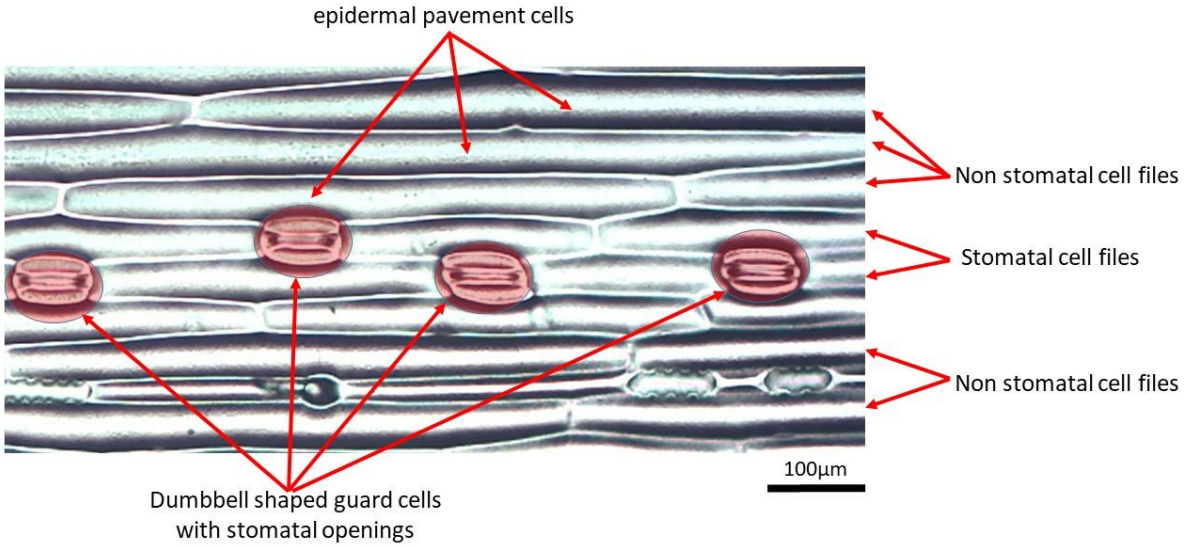

Figure 39 Microscopic image of the abaxial leaf surface of a wheat plant showing the arrangement of different cells. Guard cells with stomatal openings are highlighted in red

My results (Figure 40 and Figure 41) show a significant reduction of SD in both the sampled 4th and 5th leaves of the different transgenic plants as compared to wild type plants with an average reduction of 34 and 45% in TaEPF1OX1 and TaEPF1OX2 respectively (Figure 41A). The stomatal patterning of in wild type plants was also visibly different to that of the two mutants as shown in Figure 40. Investigations into the mechanism through which the SD reduction was achieved (Figure 41B and C) showed that the differences in SD were as a result of decreased stomata per row for both the mutant plants as opposed to a reduction in the number of stomatal cell files.

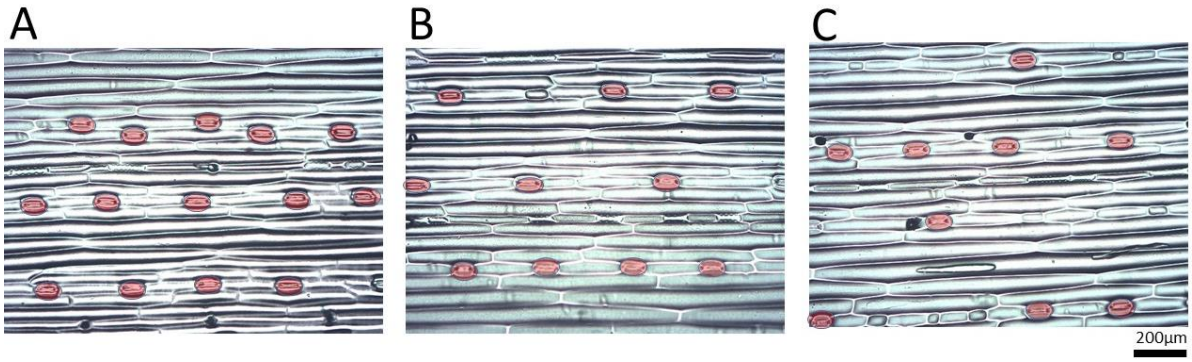

Figure 40 Stomatal distribution on the abaxial surface of the different wheat lines with A) Wild type, B) TaEPF1OX1, C) TaEPF1OX2. Guard cells with stomatal openings are highlighted in red

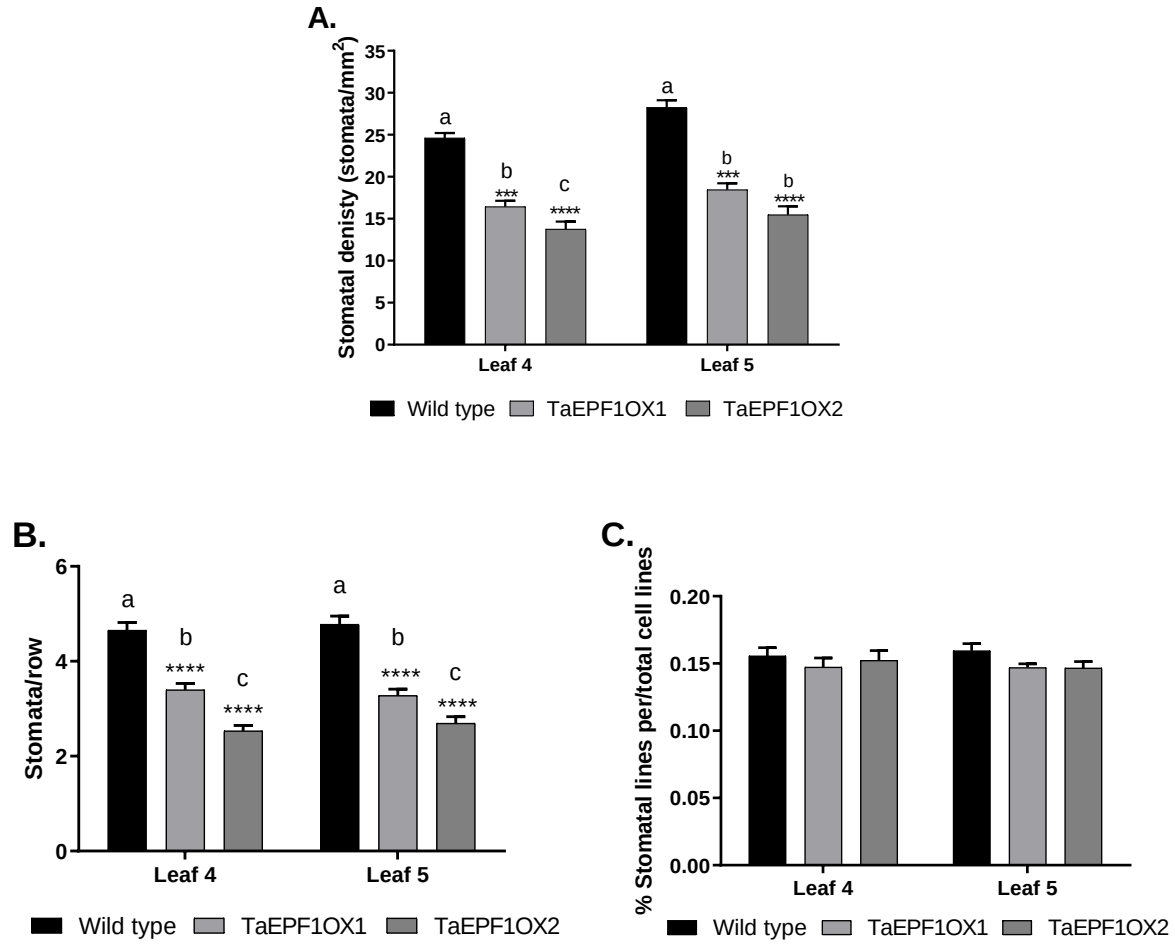

Figure 41 Stomatal density(A.) and distribution(B and C) of 4th and 5th leaf in the different wheat lines. n≥18). Error bars indicate SEM. Symbols indicate significant difference as compared to the wild type; One-Way ANOVA test with post-hoc Bonferroni test, (*=≤0.05. **= ≤0.01, ***=≤0.001, ****=≤0.0001)

4.3.2 Water use efficiency and transpiration

The WUE of the different lines was estimated using two different methods; the Δ method as well as by direct estimation from plant biomass or grain yield in relation to the amount of water transpired during the plants' entire growth cycle(Farquhar *et al.* 1989). Of the two methods, Δ is generally the least direct but relatively easiest to measure. In this study, measurements were done on plants just after the emergence of the wheat inflorescence. On the other hand, direct estimation of the water transpired required measuring the water loss from each pot every other day until plant senescence. This was then compared to either biomass or grain yield of the particular plants measured. Specially adapted plant growth tubes were used for this experiment. These were made from cylindrical Polyvinyl chloride (PVC) pipes with a diameter of 68mm and a height of 12 cm sealed with black PE plastic at the base and soil surface to prevent water loss during experimentation. An example of these tubes is shown in Figure 42A. Watering was done once

every 2-3 days to maintain the tubes at a pre-determined gravimetric (θ_g) water content that corresponded to their field capacity. Results from the various tests I performed are shown in Figure 43.

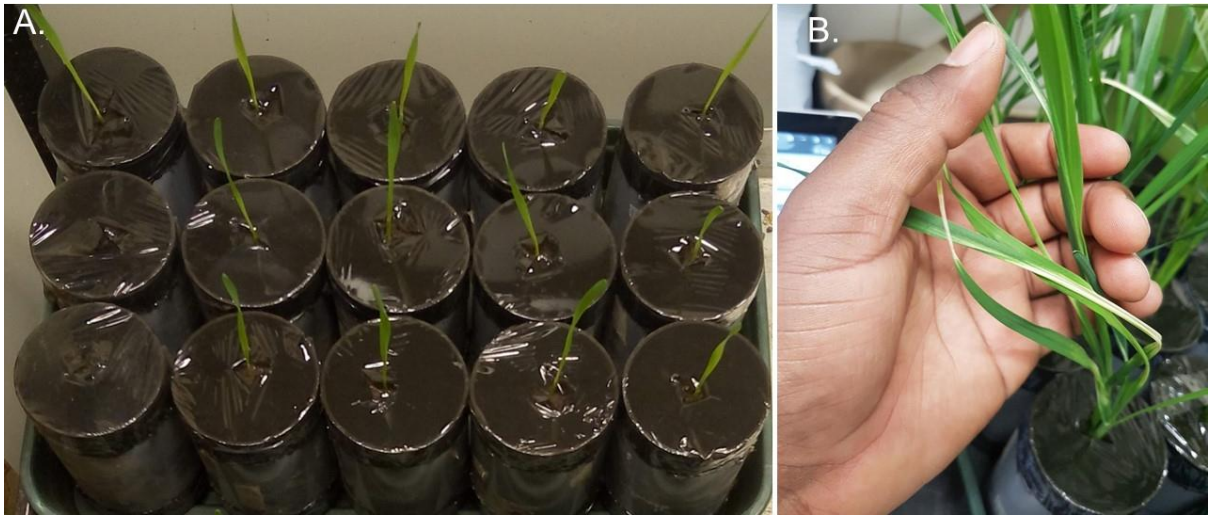

Figure 42: A) An example of the PVC tube used to monitor transpiration during the growth cycle of my wheat lines and B) bleaching/variegation in EPF1OX2 line plants observed 50 days after sowing.

Cumulative evapotranspirative (ET) water loss (Figure 43A) showed significantly reduced transpiration in both the mutant lines from very early stages of growth (around day 20) right up till the end of the observation period. Initially, TaEPF1OX2 line plants showed the lowest ET up till about 50 days after sowing (DAS). Thereafter, the transpiration rate in these plants increased to higher than those of the TaEPF1OX1 plants which was a trend that continued up till the end of the experiment. Unexpectedly, however, despite having lower SD, TaEPF1OX2 mutant lines transpired more than the TaEPF1OX1 mutant lines. TaEPF1OX2 plants were observed to have extensive abnormal variegation/bleaching of leaves and this variegation may have led to disruption of the plants' normal transpiration patterns.

At the completion of the experiment, ET of TaEPF1OX1 and TaEPF1OX2 was significantly reduced by 15% and 8% respectively (Figure 43D). This reduction in ET consequently gave rise to a significant increase in WUE of TaEPF1OX1 plants as calculated as from total biomass (Figure 43B) production and ET shown in (Figure 43E). However, despite having reduced ET, TaEPF1OX2 did not show any significant increases in WUE as inferred from total biomass to water loss ratio due to a reduction in biomass(Figure 43B). In fact, TaEPF1OX2 plants actually exhibited significantly reduced WUE in terms of grain productivity to water use ratio (Figure 43F) probably due to their low grain yield as compared to the wild type (Figure 43C). There was,

however, no difference between the WUE per grain of seed produced by wild type and the TaEPF1OX1 transgenic line. As determined by the Δ (Figure 43G), the WUE of the two transgenic lines used did not significantly differ as compared to that of the wild type plants, however, the two mutants had marginally lower Δ indicating marginally improved WUE.

As the WUE of at least one mutant (TaEPF1OX1) was significantly improved as compared to the WT plants (Figure 43E), I then proceeded to use it in further investigations.

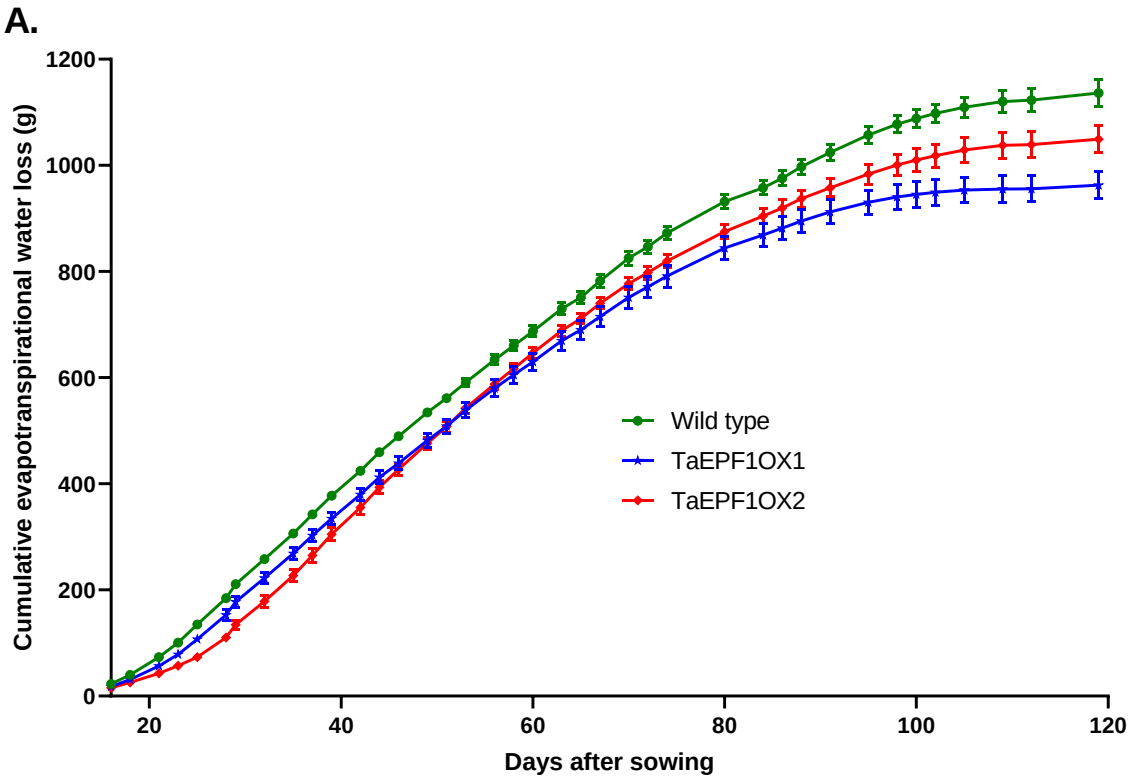

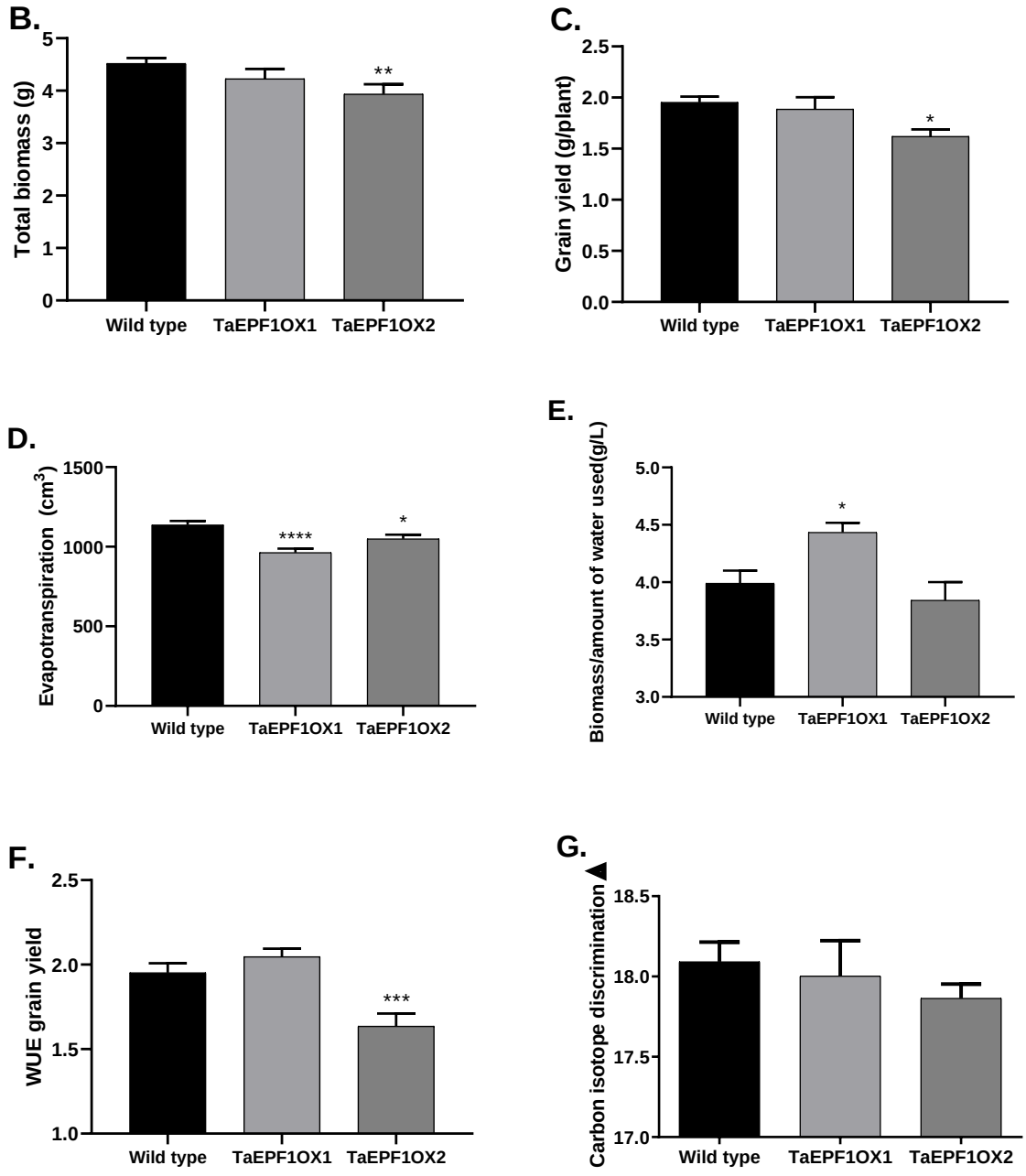

Figure 43: A) Cumulative water loss in the different mutant lines over a 103 day period. B) Total biomass, C) Average grain yield per plant, D) Total transpiration of the plant lines until senescence. E) WUE, as estimated from total biomass, F,) grain yield and G) Carbon isotope discrimination (n≥4). Error bars indicate SEM; One-Way ANOVA test with post-hoc Bonferroni test or Kruskal Walis with post hoc Dunn test, Symbols indicate significant difference as compared to the wild type (*=≤0.05. **= ≤0.01, ***=≤0.001, ****=≤0.0001)

4.4: Effects of WUE in mutant lines on RSA

In line with the overall objectives of this thesis, in this section, I evaluated how the improvement in WUE of the different mutants identified in the previous section affects their RSA. A combination of invasive and non-invasive methods of measurement of RSA is used to answer the following question in relation to my aims;

Main question

- How does the root architecture of the stomatal mutants of wheat compare to that of the wild type plants?

4.4.1 Destructive (invasive) measurements of RSA

In this experiment, an invasive method was used to investigate the RSA development of the three wheat lines that are of importance to this research. In this investigation, the three different wheat lines were grown in a sandy loam soil that was watered to field capacity every 2-3 days until harvesting and analysis. The plants were grown for either 30 or 60 DAS before root washing and subsequent analysis using WinRhizo® software. Several different measurements of RSA properties of my different plants were obtained during this analysis. The results obtained are summarised in Figure 44.

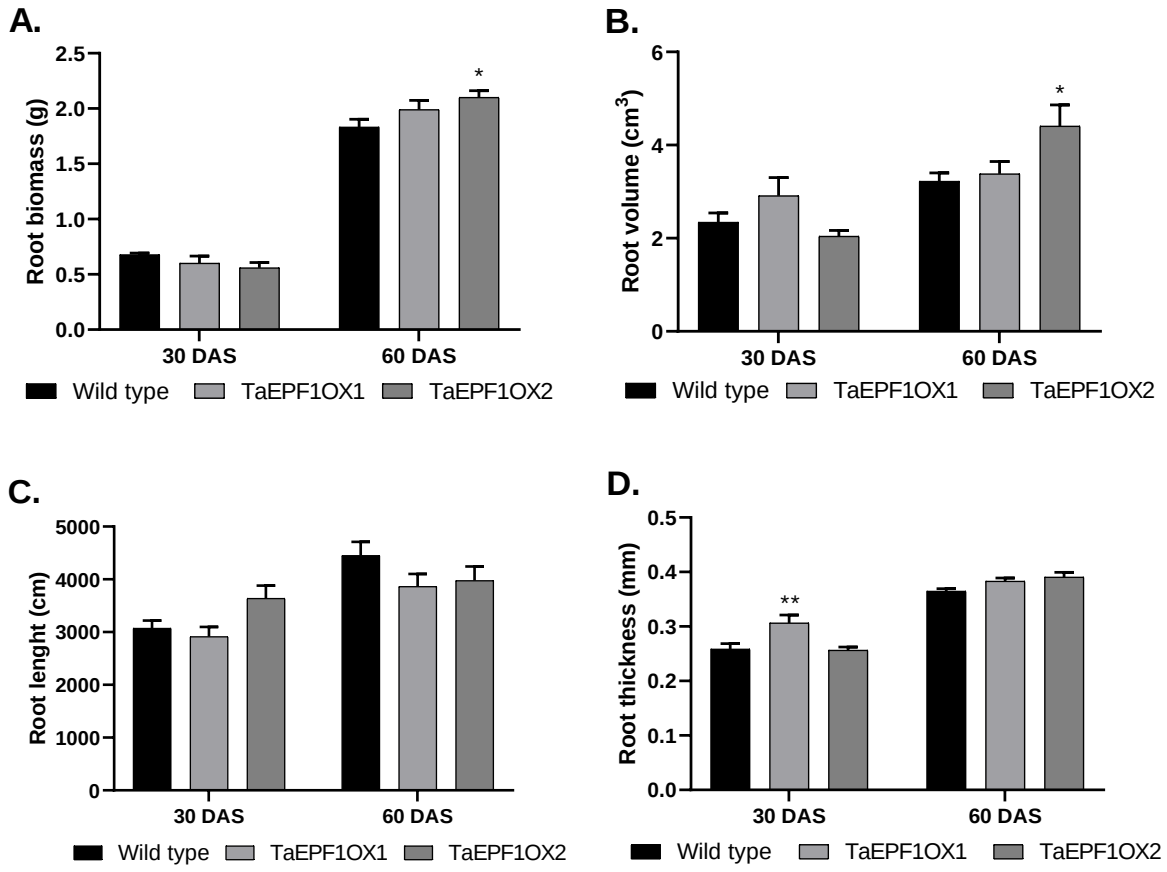

Figure 44 Root growth properties as measured by destructive methods. A) Root biomass, B) Root Volume, C) Root Length, D) Average root thickness (n≥6). Error bars indicate SEM. Symbols indicate significant difference as compared to the wild type; One-Way ANOVA test with post-hoc Bonferroni test, (*=≤0.05. **= ≤0.01)

As shown in Figure 44A, there was no significant difference between the root biomass of the TaEPF1 transgenic plants as compared to the wild type 30 DAS, however, after 60 days of growth, the root biomass of the TaEPF1OX2 mutant was significantly greater than that of the wild type plants. On the other hand, at the same time point, the TaEPF1OX1 mutant had root biomass that was largely comparable to that of the wild type plant. The root volume (Figure 44B) of the TaEPF1OX2 mutant plants, similar to root biomass was also significantly higher 60DAS as compared to the wild type plants with no significant differences between TaEPF1OX1 and the wild type in all at the different time points.

In terms of root length (Figure 44C), there were no significant differences in root length of the different lines at either time point. The average root length of the TaEPF1OX2 mutant, however, was unexpectedly higher than that of the wild type plants 30DAS despite showing marginally reduced biomass at the same time point. Similarly, the average root length of the wild type plants

was higher than that of the TaEPF1OX2 despite having both a lower root biomass and volume. In terms of root thickness, the TaEPF1OX1 mutant had a significantly higher average root thickness as compared to that of the wild type plants 30DAS. This was however not the case when the lines got to 60DAS where there were no significant differences in root thickness amongst the three plant lines.

In general, root growth in all the different mutant lines resulted in a significant increase in all the root parameters measured after between the two time points (30 and 60 DAS). This indicated that root were actively growing between the two time points. Root biomass of all the lines more than doubled over the 30 day time period of the study thus suggesting that root growth rate was higher in the second 60 day period as compared to the first 30 day period (44A).

4.4.2 Non-invasive measurements of wheat RSA

Given the advantages and limitations of different non-invasive imaging techniques, in the forthcoming sections, I analysed wheat plants using two different non-invasive imaging techniques similar to those employed in the previous chapter. I compared the root architecture of my different wheat lines in both 2D and 3D techniques.

a) X-ray CT imaging

For this experiment, I investigated the 3D architecture of the previously discussed wheat plants without prior preliminary testing as similar experiments have already been recorded in literature. I used the same PVC cylinders used in the previous experiments, which had a diameter of 68mm and a height of 120mm. These were filled with the sandy loam soil to a bulk density of 1.25g cm^{-3}. Single wheat seeds were planted at the centre of each of these cylinders and watered every 2-3 days up until 5 days before imaging when the cylinders were allowed to dry to increase contrast in CT images. Imaging was done 35 DAS before the majority of the roots had reached the base of the growth cylinder. Plants were scanned at a pixel resolution of 66.25µm per pixel using the Nikon XTH 225 LC scanner with 3143 projections and an exposure of 280ms. The results from these scans are shown in Figure 45:

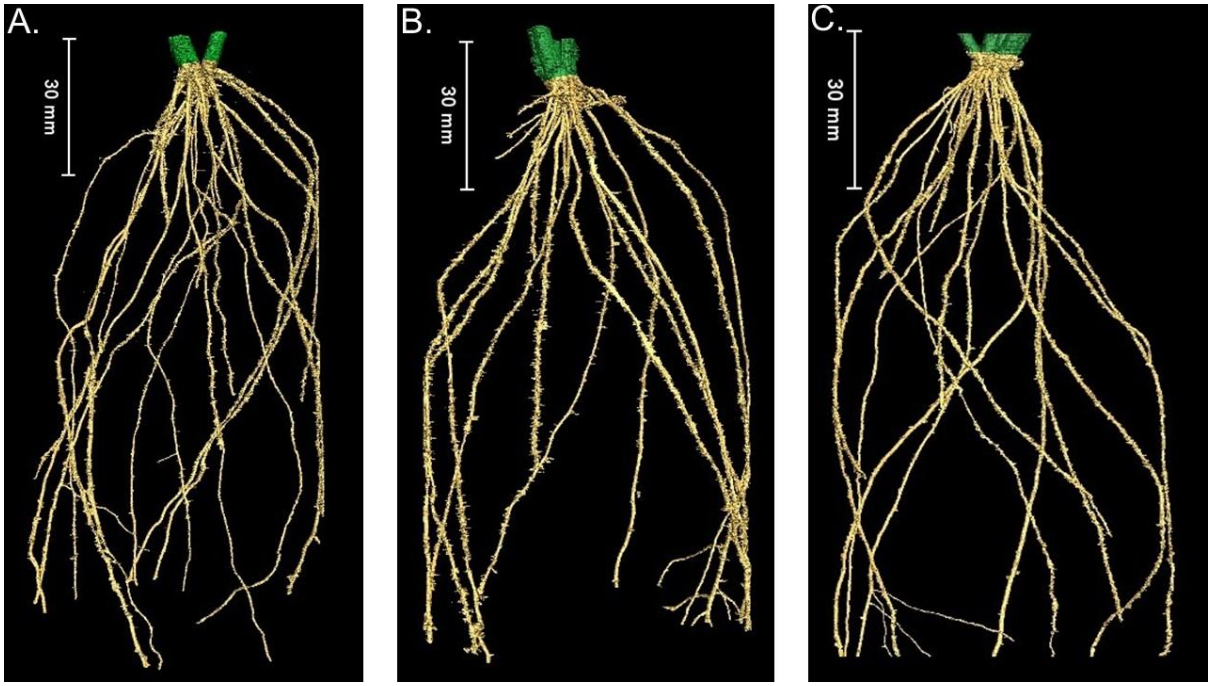

Figure 45 3D rendering of wheat plant roots scanned using the Nikon XTH 225 scanner with A) Wild type, B) EPF1OX1 and C) EPF1OX2 line plants 36 DAS

Table 9 Showing some of the root properties of the different wheat lines obtained from segmented CT scans and biomass measurement

Genotype	Root length(mm)	Root Volume(mm^3)	Root surface area(mm^2)	Root diameter (mm)	Root angle (°)
Wild type	4662.66	494.96127	4035.49	538.558	56.6
TaEPF1OX1	4086.06	393.83279	3884.84	553.605	38.9
TaEPF1OX2	2635.97	358.03387	3586.24	587.606	45.3

As summarised in Table 9, the root length, volume and surface area of the wild type plant was higher than that of the two mutants 36 DAS when imaging was carried out. The TaEPF1OX1 mutant line had the second-largest RSA with root length about 12% lower than that of the wild type whilst the TaEPF1OX2 mutant had a root length 46% lower than that of the wild type. Root volume of the different plants followed a similar trend with the exception that the TaEPF1OX2 mutant had a root volume similar to that of the TaEPF1OX1 mutant. Root surface area also followed a similar trend with the wild type plant having a greater surface area in comparison to the two different mutants. In terms of root diameter, however, the TaEPF1OX2 mutant had the highest root diameter. In terms of root angle, the wild type plants had the highest root angle as compared to the two mutant with the TaEPF1OX1 mutant having the lowest root angle.

The results I obtained using X-Ray CT scanning were broadly coherent to what I observed in the root biomass measurements obtained using the destructive root analysis. There were big differences, however, between the root properties measured using X-Ray CT as compared to root scanning done using WinRhizo® 30DAS. In WinRhizo® analysis, root lengths obtained were up to 9 times greater than the root properties obtained from my scans at 6 days earlier than that of the CT scans. Similarly, the calculated root volumes from CT scans were more than 5 times lower than that from WinRhizo® analysis whilst the average root thickness was significantly higher in CT scans as compared to WinRhizo® analysis. As is seen in Figure 45, very few lateral roots branching from seminal/nodal roots could be seen in the 3D rendered images thus many of the computed properties from out CT scans were crucially missing information on smaller lateral roots.

b) Neutron imaging for RSA visualisation.

The imaging of wheat plants using Neutron radiography and tomography is relatively novel, with very few, if any, publications involving the use of neutron imagery to visualise wheat roots. As this is a relatively new area of research, preliminary testing of the ideal mechanism of visualisation of wheat roots in situ was trialled using the STFC IMAT imaging facilities.

Preliminary neutron imaging

Initial testing of the feasibility of using neutron imagery (NI) to visualise the RSA of my wheat lines involved determining whether the sandy loam soil used in the bulk of my wheat experiments was appropriate to use with this technique. This was done because in literature, the vast majority of the experiments using NI to study roots have primarily utilised sandy soils with >90% sand content, devoid of the organic matter and soil aggregates that my soil had in abundance (Carminati *et al.* 2010, Esser *et al.* 2010, Ahmed *et al.* 2018). This feasibility testing involved growing my wheat plants in specially designed growth containers of different sizes. These were namely; 2D radiography imaging pods (200mm × 200mm ×10mm), cylindrical aluminium tubes (100mm in length, 18mm inner diameter) and square-shaped cylinders (20mm × 20mm ×100mm). I used 4 different soil fractions sieved from the sandy loam soil used in this thesis. These were namely, <4mm sieved (bulk soil), 2-4mm, 1-2mm and 0.25-0.5mm dry sieved soil aggregates. For the smaller square and cylindrical tubes, single wheat seeds were planted whilst for the larger soil pods, 2 seeds were planted 10cm apart. These were grown for either 13 days (for the square and cylindrical tubes) as well as 28 days for the larger 2D neutron radiography imaging pods. Single

radiograph images of the wheat seedlings growing in the different media and growth containers were then taken to establish if roots could be visualised. The images obtained are shown in

Figure 46.

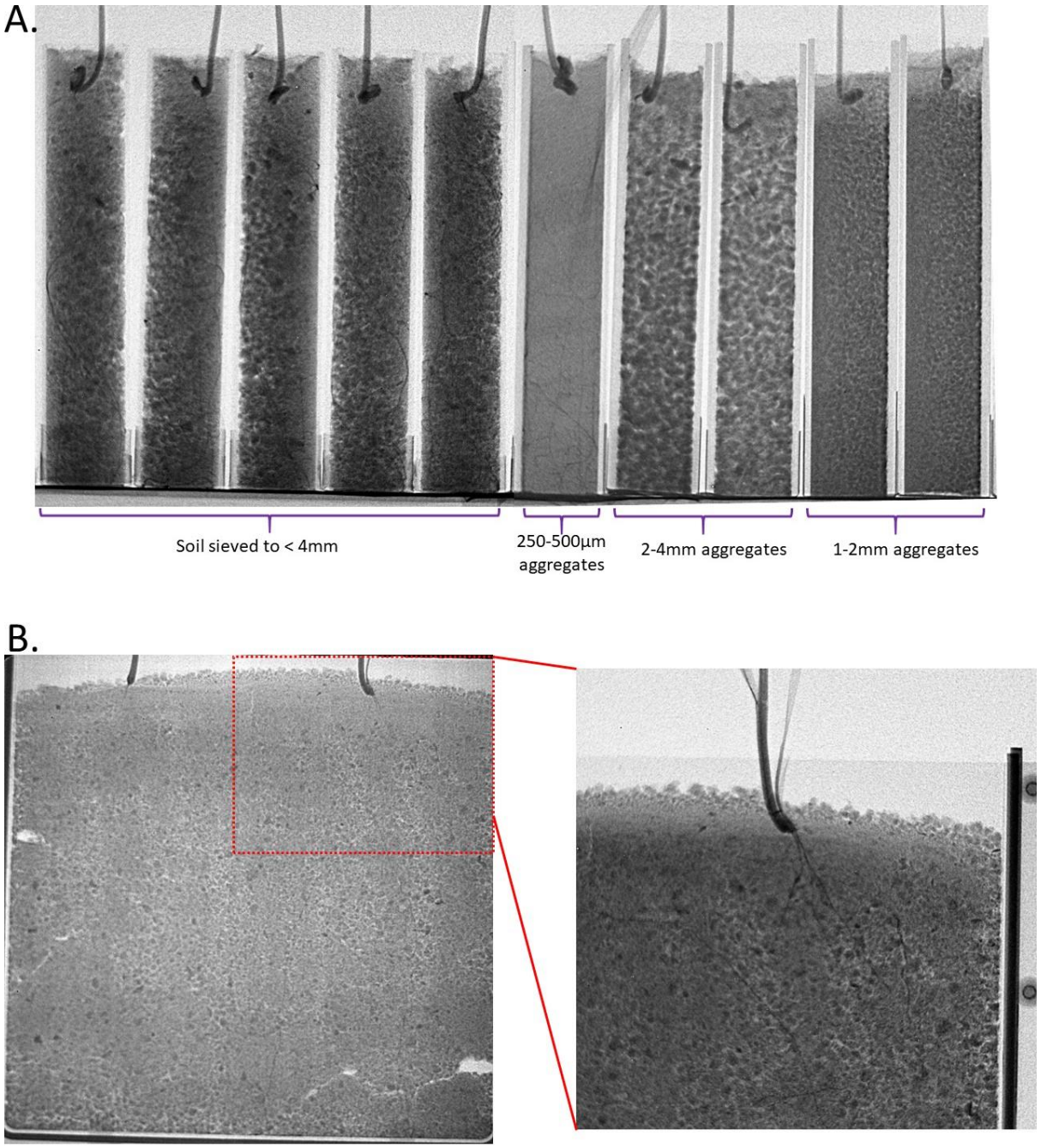

Figure 46 Neutron radiography images of wheat plants growing in different media. A) Shows the radiography image showing 13-day old plants grown in small tubes with filled different media whilst B) Illustrates a representative soil rhizopod showing roots obscured by the soil.

Results from the initial radiographs of tubes where the 13-day old wheat seedlings were grown in different growth media (Figure 46A) showed limited root visibility in nearly all the growth tubes. Roots growing in the 2-4mm and 1-2mm aggregates were completely obscure whilst only a few roots were seen in the were lower half of the tubes with soil <4mm. Soil aggregates 0.25-0.5mm aggregates provided the clearest contrast between soil and roots with numerous roots being visible throughout the column.

Similarly, the 2D rhizopod filled with soil <4mm (Figure 46B), also showed root obscurity with only a few of the roots being faintly visualised in the immediate vicinity of the seed. As a result of these preliminary experiments, I decided to use the 0.25-0.5mm aggregate soil which gave better root-soil contrast for more 2D investigating of root architecture whilst I opted to use the <4mm soil for 3D NCT as it would potentially allow mapping water distribution around the roots and aggregates in the soil used for the majority of my experiments.

NCT imaging

Having established that roots could successfully be visualised in some of my soils, I thus aimed to determine the 3D root architecture of my wheat lines using NCT. Additionally, since NCT could also give valuable information on soil moisture distribution, I also investigated water distribution in my growth tubes to accompany my measurements of RSA. My final objectives were namely to use NCT to:

a) Map in 3D wheat RSA of selected wheat lines within an aggregated sandy loam soil
b) Visualise in 3D, soil water distribution after a brief drying period and
c) Understand how the root system architecture interacts with soil moisture distribution as brought about by soil structural heterogeneity within an aggregated soil.

As I faced problems (as described in section 4.3.2) with one of the two mutants (TaEPF1OX2), I only elected to focus the TaEPF1OX1 in this experiment. To set up this experiment, the sandy loam soil was packed into specially designed, closed bottom, cylindrical aluminium tubes as described previously to ensure a bulk density of 1.2g cm^{-3} within the tubes. A single wheat seed was sown about 1cm underneath the surface of the soil and the tubes were watered to a volumetric moisture content (θ) of 16.0±3.0% which was experimentally determined (using gravimetric methods) to be the field capacity of my growth tubes. This water content was maintained during the course of this experiment by daily surface irrigation to the predetermined weight corresponding to the above-mentioned θ for each tube. The wheat seedlings were grown for 13 DAS in a growth

chamber. Watering was stopped 4 days before neutron imaging was carried out to enhance the contrast between the root and soil. The time taken for a single scan of the plants was almost 6 hours with 654 radiographs being recorded using a rotation step of 0.55°.

The 3D root architectural properties of the 13-day old wheat seedlings rendered from neutron scanning were successfully mapped and are illustrated in Figure 47A. The RSA of the wheat lines was broadly similar with both plant lines having 3-5 seminal roots at the time of imaging. At least one of the roots (mainly the primary root) in each plant line had grown to reach to the base of the growth tubes. There was little difference between the plant lines root properties with no significant differences in the root length, surface area, volume and thickness of each line. This was coherent to the results I obtained from root washing experiments (Section 4.3.2) with little differences being seen between the wild type plants as compared to the TaEPF1OX1 mutant 30DAS. At that time point, root thickness on the TaEPF1OX1 mutant was the only attribute that was higher than at this time point.

Lateral root growth was broadly similar in both mutant plant lines as well. However, I noticed an unexpected pattern of lateral root growth pattern in both plant lines. The lateral roots of the different plants extended throughout the soil column with visible differences in lateral root growth around regions where the seminal roots were in close proximity to larger aggregates (1-4mm) that had large pores in-between them. Lateral roots growing in these regions tended to be fewer and longer whilst those growing in finer soil particles were more numerous but visibly shorter. This can be seen in Figure 48 where due to the random segregation of particles when packing, larger aggregates settled on one side of the column. Roots in some of the columns (mainly in the mutant line) coalesced together and grew side by side in their downwards trajectory, only disentangling lower down the soil column as seen in Figure 47.

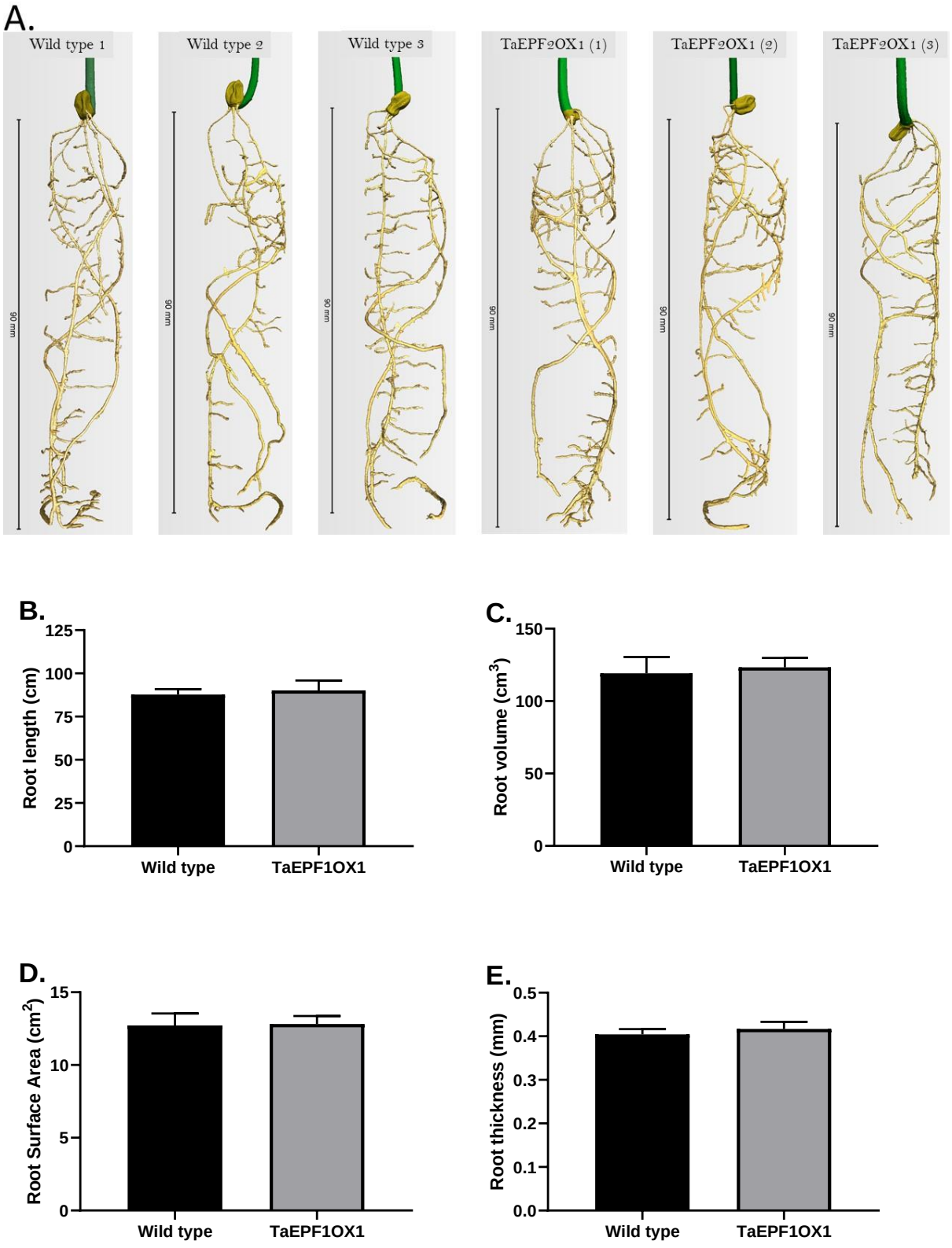

Figure 47 A) 3D volume rendering of the 6 wheat seedlings imaged using NCT. B) Root length, C) Volume, D) Surface area and E) thickness of the wheat lines determined from NCT imaging (n≥3). Error bars indicate SEM. Symbols indicate significant difference as compared to the wild type; One-Way ANOVA test with post-hoc Bonferroni test

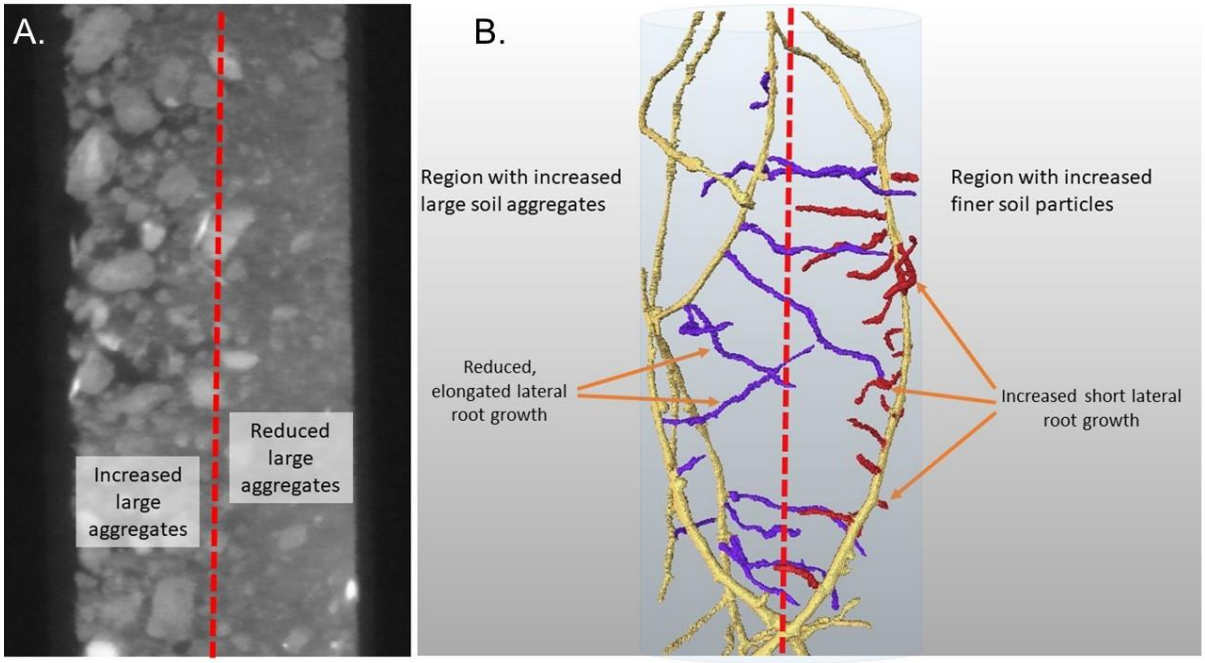

Figure 48 A) Greyscale image of a growth tube showing segregation of large aggregates towards the left side of growth tube. B) increased shorter lateral root growth in regions with finer soil particles whilst lateral roots growing in regions with increased larger aggregates are reduced and longer. The red line demarcates an arbitrary boundary between regions dominated by large aggregates or finer particles. Longer lateral roots are shown in purple whilst short lateral roots are shown in red.

Comparison between 3D and 2D root properties

In addition to the NCT RSA measurements, I also intended to compare the root properties obtained from my NCT analysis with those obtained from flatbed scanning results analysed using WinRhizo® (Regents Instruments, Inc.). Therefore, after CT scanning, the soils columns were destructively sampled and the soil was washed off from the roots over a 250µm sieve. The washed roots were then placed in a specially designed water tray and scanned using an Epson Expression 10000XL Pro at 400dpi (63.5µm/pixel) resolution. This scan obtained 2D images of the plant roots which were then analysed using WinRHIZO® 2016a software to determine the root properties (Wang and Zhang 2009a, Tracy *et al.* 2012). These roots alongside their shoots were then dried at 65°C for 48 hours to obtain their dry biomass. The results obtained are given in **Figure 49**.

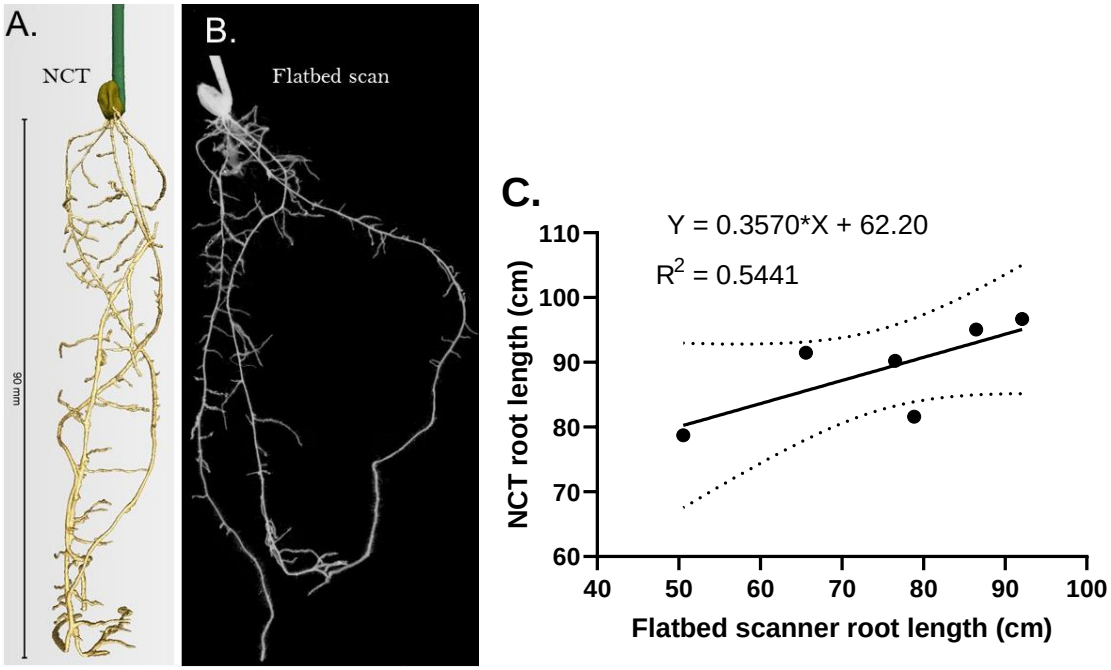

Figure 49: Side by side comparison of the same plant imaged using A) NCT and B) flatbed scanning. C) Linear regression of root lengths derived from NCT and Flatbed scanning respectively (n=6).

Root properties calculated using WinRhizo ® from the flatbed scanning and 3D NCT enabled the correlation of the two methods thus ensuring the validity of the method I used to segment out the roots. Visual comparison between images obtained using the two methods as shown in Figure 49A and B showed great similarities between them. There was also a moderately strong linear relationship (R^2= 0.5441) between the root length estimated by the two methods as given in Figure 49C. As shown in Figure 4950C, estimates of root length from NCT were significantly ($P<0.05$) higher than those from flatbed scanning whilst root volume and thickness did not vary between the two methods. The thinnest roots I could detect were around 110µm in diameter which corresponds to double my image pixel size according to Nyquist–Shannon theorem.

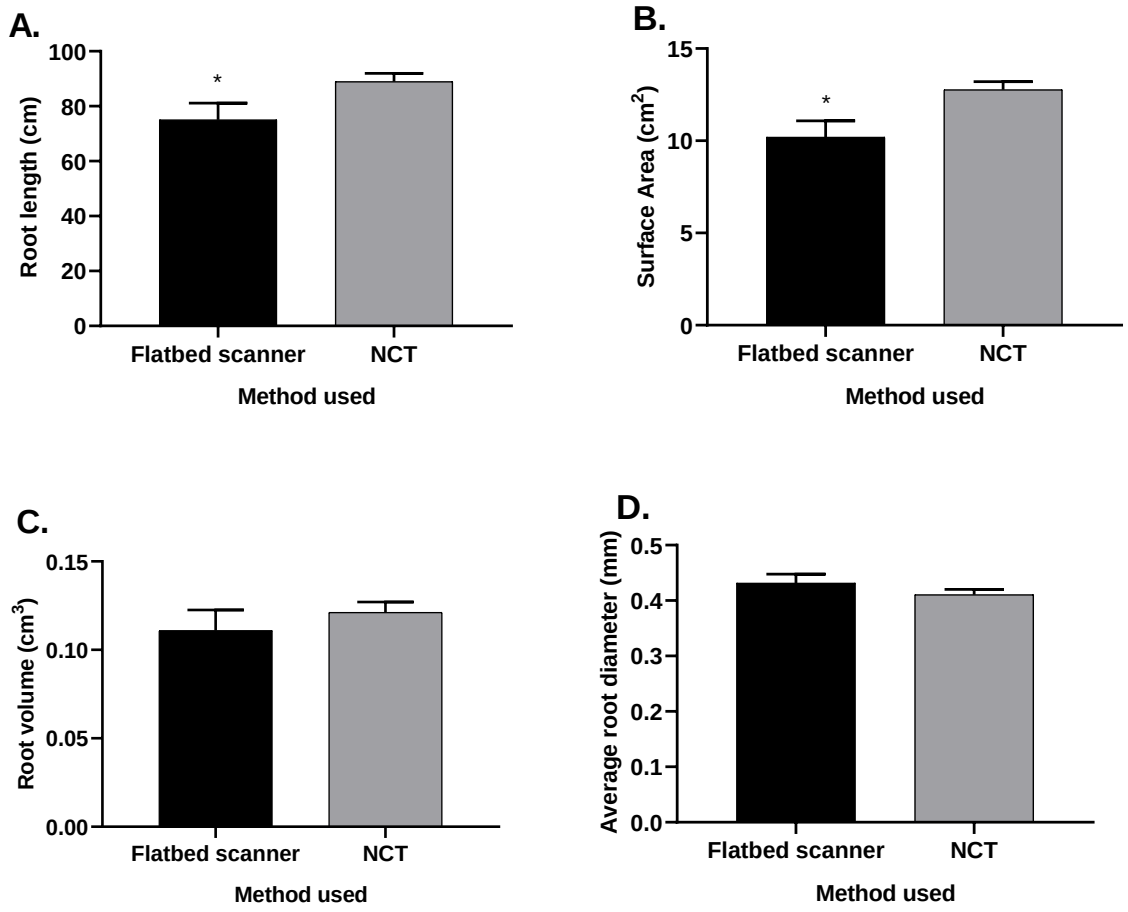

Figure 50: Comparison of root architectural properties as estimated by flatbed scanning and NCT. a) Root length (b) Root surface area, c) Root volume and d) Average root diameter(n=3). The error bars indicate Standard Error of the mean and * indicates significant differences ($P < 0.05$)

Soil moisture distribution

Similar to root architecture, the visualisation of soil moisture distribution was possible in 3D NCT as illustrated in Figure 51A with neutron attenuation being used as a proxy for volumetric moisture content (θ) using calibrated estimates of water content. These were calibrated by a series of scans of dry soil samples similar (but not identical) to those used for plant growth. It is worth noting however that my estimation of moisture content may encompass an add on effect with the high organic matter which increases neutron attenuation.

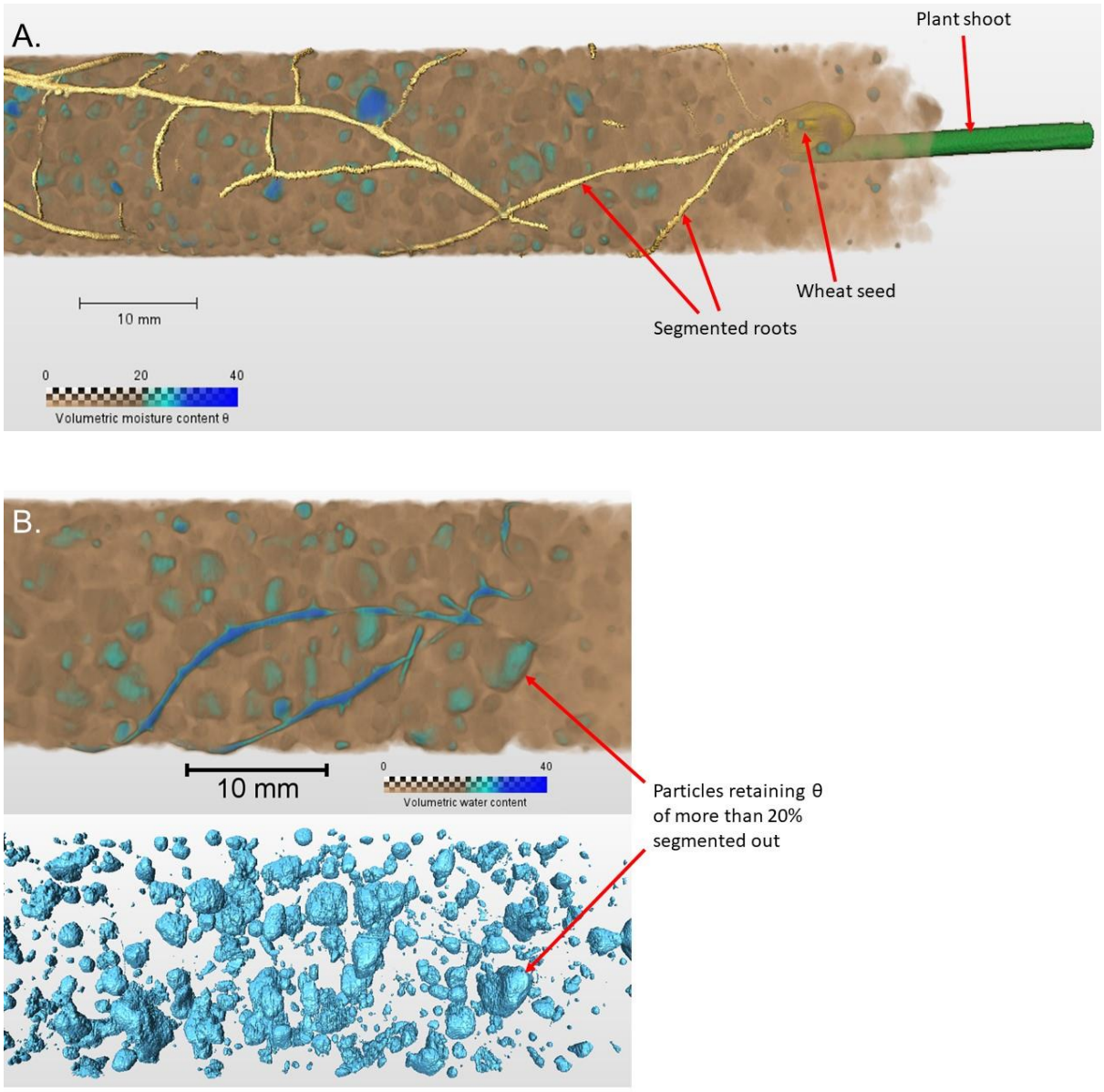

Figure 51: A) 3D NCT rendering of water distribution in aggregated soil where wheat is growing. B) Showing segmenting out of particles retaining greater θ >20%

Water distribution within the columns was sporadic with regions of increased moisture localisation and depletion throughout the different tubes. Water depletion was greatest in the top 20mm of the soil with soil moisture gradually increasing between 20-60mm from the top of the column until it reached its greatest extent at the base of the tube. Water was largely localised in nearly spherically shape regions within the soil as shown in Figure 51B. Upon further analysis, it was discovered that this moisture accumulation was mainly associated with the heterogeneously distributed soil aggregates within the soil.

Root interactions with soil moisture

Wheat roots did not preferentially grow in regions of increased θ (blue regions with θ >20). Many of the roots that were observed did not penetrate into water-rich aggregates but rather grew around them. Roots that were in direct contact with aggregates with a higher θ exhibited an increase in their internal θ. In large pores in-between soil aggregates, roots had reduced θ, which was especially true in smaller lateral roots as opposed to the much larger seminal root network. Some seminal roots however also showed this unexpected internal θ decrease when growing through larger inter-aggregate pores. The rhizosphere around the roots as shown in Figure 52, did not show great differences in θ as compared to the rest of the soil with delineation of the extent of the rhizosphere being difficult to decipher.

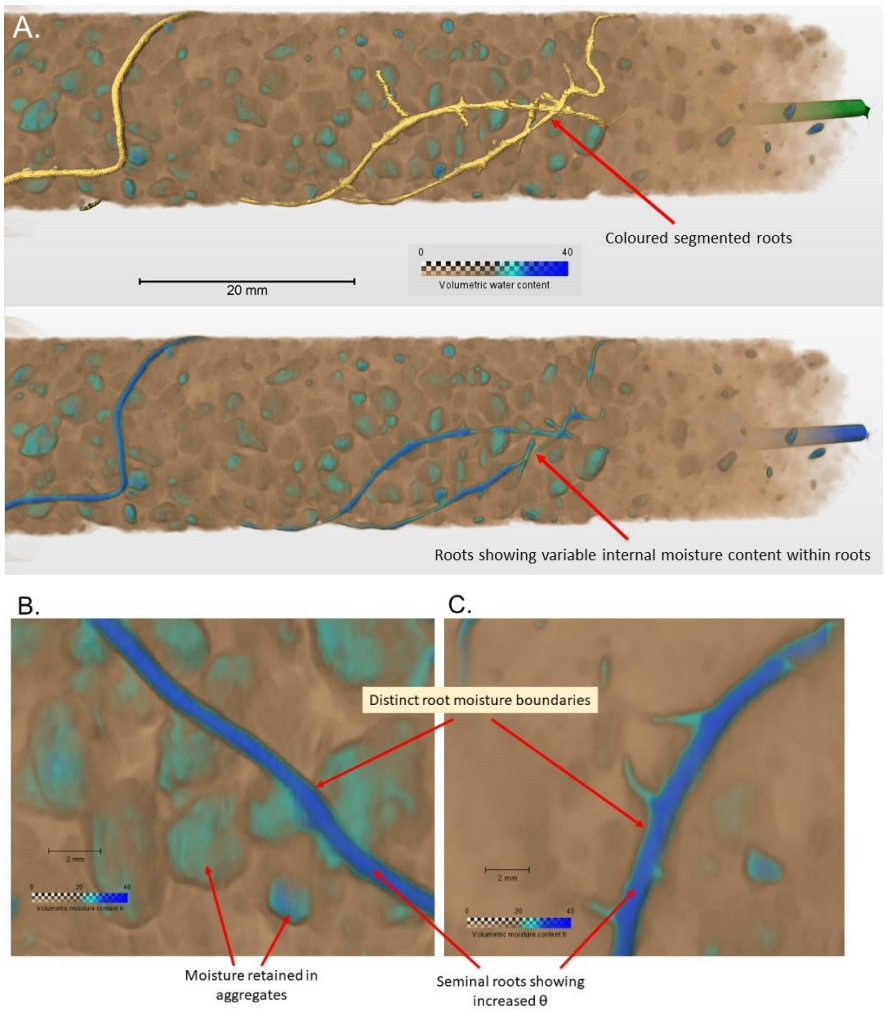

Figure 52: A) Variations in internal water content within roots growing through soil. The top image shows segmented root indicated in yellow whilst in the bottom image, only root moisture content can be visualised. B) Close up view of the water-map in around seminal roots at 3cm and C) 5 cm below the soil surface showing distinct boundaries around the roots.

4.5: The effects of improved WUE on soil structure in wheat plants.

To fulfil the final objective of this chapter, in this section, I look at the interaction between wheat roots and soil. I investigated how roots of the different wheat lines affect soil structure and consequently how soils with different structures affect the growth of wheat roots. The specific research questions for this section are as follows:

Main question in this section:

- How does improved WUE in wheat plants affect soil structure?
- How are wheat roots affected by soil structure?

4.5.1 Soil structural stability tests

To determine differences in soil structure as induced by the different wheat lines, soil aggregate stability of macro-aggregates of a selected size were assessed at 2 different time points following the growth of wheat plants. For this experiment, single wheat seeds were planted in PVC cylinders which were filled with a sandy loam soil to attain a bulk density of 1.25g cm^{-3} in each cylinder. These cylindrical pots were watered to a predetermined field capacity once every 2-3 days up until a week before the harvesting when the soil was allowed to dry. This drying was done to reduce the compression of wet soil aggregates during soil extraction as well as to allow for the shaking off of soil from the roots with minimal effort. The soils extracted from each tube were packed into airtight dark plastic bags and stored at 4°C up until analysis. The root length of the different plant lines was also measured as root length has been shown in the literature to correspond well to soil structural stability (Graf and Frei 2013). Results from the characterisation of root length is given in a previous section (Section 4.4.2) whilst the results from the aggregate stability tests performed at the two different time points (30DAS and 60DAS) is given in Figure 53.

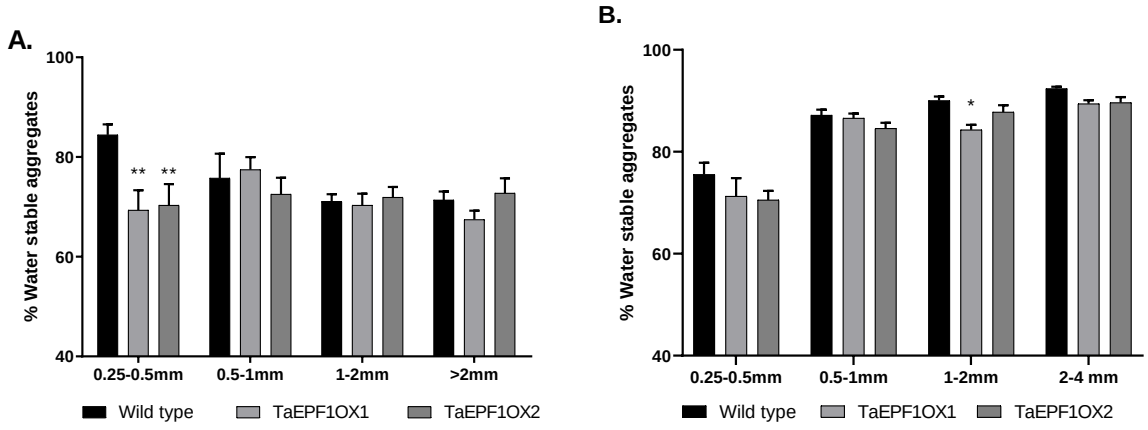

Figure 53 Stability of soil aggregates of different size classes at A) 30DAS and B) 60 DAS (n≥9). Error bars indicate SEM. Symbols indicate significant difference as compared to the wild type; One-Way ANOVA test with post-hoc Bonferroni test, (**= ≤0.01)

Soil aggregate stability 30DAS (Figure 53A) was significantly higher in the wild type soils as compared to both mutants for the 0.25-0.5mm aggregate size with an average increase of about 10% in the stability of this size class of aggregates in the wild type plants. There were no significant differences between the plant lines in the rest of the aggregate size classes.

At 60DAS the aggregate stability of nearly all the aggregate size classes (with the exception of the 0.25-0.5mm aggregates) had significantly (P= 0.04) increased as compared to the results obtained at 30DAS. There was however no difference in the soil stability at the two time points of the smallest aggregate size class (0.25-0.5mm) with only the stability soils under wild type plants being reduced to become comparable to that of the two mutants. Aggregate stability under the different mutants was also relatively comparable with only a single significant reduction in aggregate stability being seen recorded in the 1-2mm aggregate size class for the TaEPF1OX1 mutant.

4.5.2 Investigating the response of roots to aggregates of different sizes using NCT

Having looked at the effect of my mutant plants on soil structural stability, my final experiments was aimed at investigating the alternate influence of soil structure on wheat root growth. This would give an even better understanding of the plant soil-interactions occurring in soils of different structures that may potentially have given rise to the differences in aggregate strength as observed in the previous section. I also aimed to investigate the variation in moisture content in the RSA when growing in soils with contrasting aggregate sizes. This is a follow up to my NCT experiment, which suggested that soil moisture content of roots is not constant and changes when roots enter large pores associated with the increased aggregate sizes.

a) Screening for differences in root properties of wheat plants when grown in aggregates of variable sizes

To achieve this, I set up three different experiments using plants of the wild type genotype. In the first experiment, soils were sieved to 3 different aggregate size fractions (2-4mm, 0.5-1mm and 0.25-0.5mm), along with bulk soil (<4mm sieved) from the sandy loam. These growth media were filled into 435cm^3 cylindrical pots (68mm diameter × 120mm height). A single seed was planted about 1cm underneath the surface of the soil and the pots were watered to a volumetric moisture content (θ) of 16%. This water content was maintained during the course of this experiment by surface irrigation to the predetermined weight corresponding to the above-mentioned θ. The plants were grown for four weeks in a growth chamber maintained at a temperature of 22°C (day)/18°C (night) and a relative humidity of 55% with light intensity averaging 400μmol m^2 s^{-1}. After this growth period, the plants were harvested and their shoots were excised and dried in an oven at 60°C for 48 hours to obtain dry shoot biomass. Their roots were washed off to remove adhered soil on top of a 0.5mm sieve then placed in a water tray were light scanned using an Epson Expression 10000XL Pro at a resolution of 400 dpi. This scan obtained 2D images of the plant roots, which were then analysed using WinRHIZO® 2016a software to determine the root properties. These roots were then subsequently dried under the same conditions as the shoots to obtain their dry biomass. The results I obtained are shown in Figure 54.

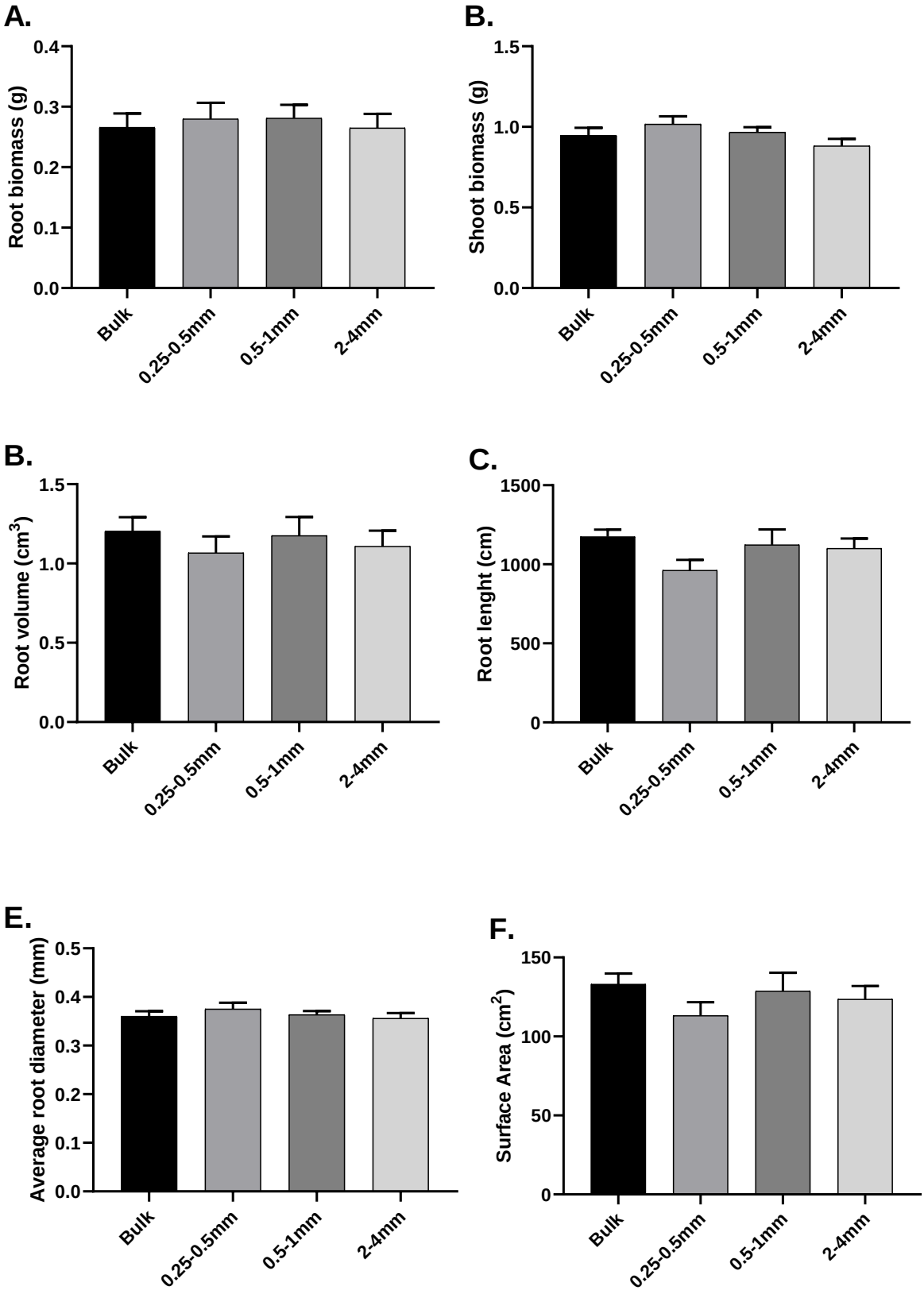

Figure 54 Root and shoot properties of wheat plants grown bulk soil as well as aggregates of different sizes, A)Root biomass, B) shoot biomass, C) Root volume, D) Root length, E) Average root diameter and F) Root surface area

The results I obtained in this preliminary screening experiment did not show any significant differences between root and shoot growth in the different aggregates. Only marginal differences in root and shoot biomass of the plants grown in 0.25-0,5mm aggregates could be identified in the biomass measurements where the plants had a higher average root and shoot biomass as compared to the other treatments. This was different from the results obtained from the WinRhizo® (54B-F)scans where plants from the same aggregate (0.25-0.5mm) size showed slightly reduced root architectural properties.

The great similarities in the plant properties indicated that the plants have the ability to adapt and grow in all of the aggregate sizes I trialled, attaining similar characteristics to the bulk soil used in previous experiments. However, these results may reflect that the length of time the roots were grown in the cylinders as root growth may have been restricted to a particular level as evidenced by numerous roots reaching the base of the pot at harvesting. On the basis of this experiment however, I then selected two of the most contrasting aggregate sizes for further experimentation, namely the 2-4mm and the 0.25- 0.5mm sized aggregates.

b) NCT of plants growing in aggregates of selected size classes

In the second experiment, the two different sized aggregates (2-4mm and 0.25-0.5mm) were packed into bottom sealed cylindrical aluminium tubes (20mm sides × 100mm height) to attain similar bulk densities as used in the 1st experiment. A single wheat seed was then sown 10mm underneath the surface of the aggregates and irrigation was applied to a gravimetrically determined θ of 16% similar to the screening experiment (a). The wheat in the aggregate filled tubes was grown in a growth chamber maintained at 21°C (day)/18°C (night) and a relative humidity of 50%. The moisture content was maintained by watering the tubes every day until 5 days before neutron imaging when the tubes were allowed to dry in order to increase root/soil contrast during imaging. The imaging of these plants was done 12 DAS after planting and the results of this NCT is shown in Figure 55 and Table 10. The plants in this experiment were also scanned using the light-bed scanner as described in 2.5.2(a) and the results of these scans are given in Figure 56 and Table 11.

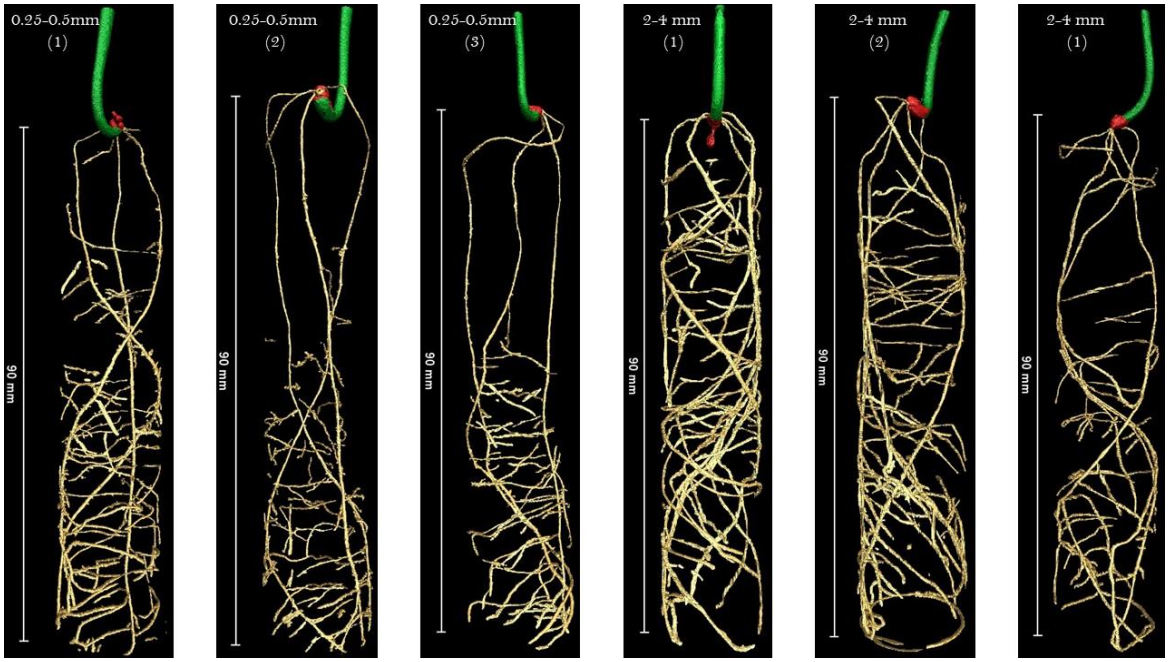

Figure 55 RSA of wheat plants growing in aggregates of different sizes

Table 10 Root properties of individual wheat plants grown in aggregates of different size classes computed from NCT measurements

Aggregate size	Length (mm)	Volume(mm^3)	Seminals Tortuosity	Seminals diameter (mm)	Number of seminals	Laterals diameter (mm)	Laterals average length (mm)
0.25-0.5 (1)	1376.55	0.155	5.549	0.460	3	0.318	4.81
0.25-0.5 (2)	1490.51	0.102	6.570	0.354	4	0.267	4.73
0.25-0.5 (3)	952.21	0.084	5.154	0.359	3	0.258	3.90
2-4mm (1)	1757.33	0.232	9.551	0.403	5	0.279	11.38
2-4mm (2)	1732.48	0.187	7.319	0.343	5	0.263	9.23
2-4mm (3)	1152.32	0.105	10.191	0.324	5	0.260	8.26

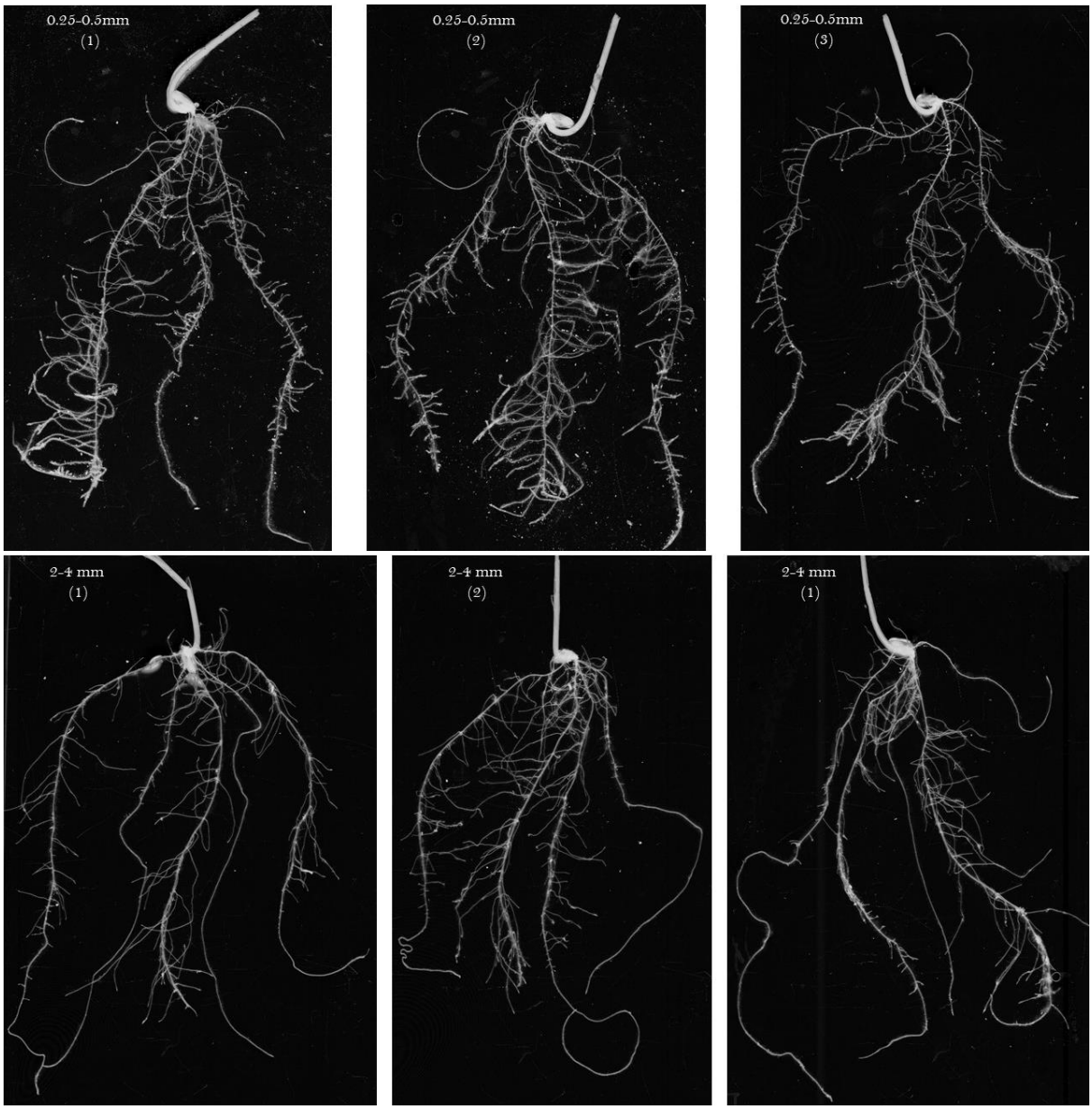

Figure 56 Flatbed scanning images of wheat roots growing in different sized aggregates

Table 11 Root properties of wheat plants grown in aggregates of different size classes computed from flatbed scanning

Aggregate size	Root Length (mm)	Root Volume (mm^3)	Surface area (cm^2)	Average root diameter (mm)
0.25-0.5 (1)	198.67	0.250	25.004	0.4006
0.25-0.5 (2)	228.09	0.342	31.295	0.4367
0.25-0.5 (3)	178.05	0.188	20.516	0.3668
2-4mm (1)	188.56	0.228	23.231	0.3921
2-4mm (2)	184.51	0.246	23.904	0.4124
2-4mm (3)	166.13	0.221	21.458	0.4111

The results I obtained indicate that plants grown in the 0.25-0.5mm aggregates showed increased seminal root length, but relatively shorter lateral root growth as compared to those grown in larger aggregates. This was broadly similar to what I observed in my previous experiment (Section 4.4.2) where segregation of aggregates occurred inadvertently and lateral roots preferentially grew longer in larger size aggregates. The NCT scans showed limited lateral root growth in the top half of the growth cylinder filled with the smaller aggregates whilst on the other hand, the plants grown in the larger aggregates showed a more even distribution of lateral roots throughout the column. Laterals grown in these large aggregate were longer but were fewer as compared to lateral roots growing in the small aggregate size.

In terms of seminal root growth, plants growing in the larger sized aggregates had relatively more seminal roots as compared to those growing in the smaller size despite having been planted and germinated on similar dates. This increase in seminal root growth could indicate that roots growing in the larger sized aggregates could have altered their development to increase seminal root growth at the expense of lateral roots. Seminal root tortuosity of the plants growing in the smaller aggregates were smaller, indicating shorter paths on a downward trajectory as the seminal roots entered into the soil.

Comparing NCT and WinRhizo® measurements, unlike in previous experiments, that the root properties estimated using NCT were lower than those from flatbed light scanning. The visualisation of relative moisture content using NCT revealed that there was a higher moisture content in the larger soil aggregates, which retained a significant amount of water even after the 5 day drying period was imposed. The moisture content of the smaller aggregate only increased lower down the growth tube, possibly as a result of evaporation from the surface of the aggregates as well as the top irrigation, which result in a water gradient increasing towards the base of the growth tubes.

c) Partitioned tube aggregate experiment

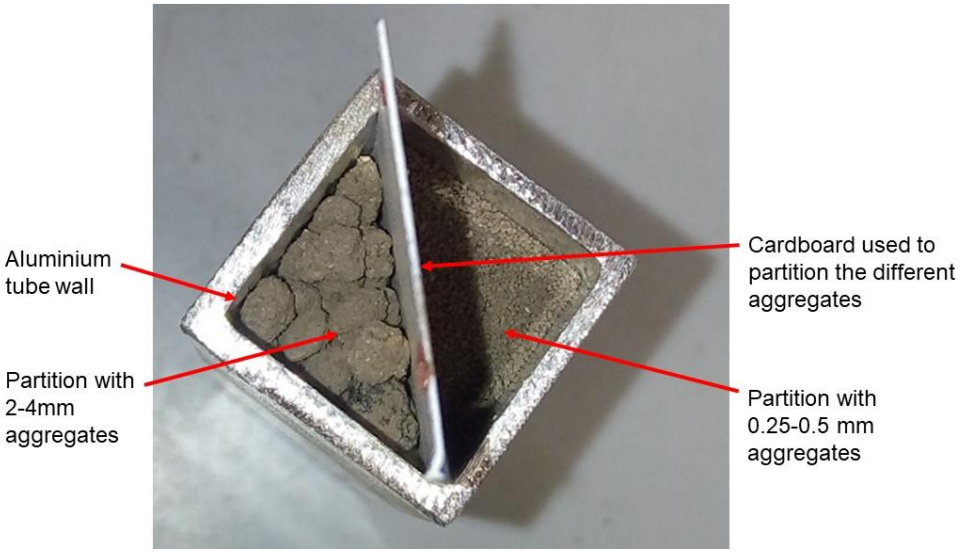

Figure 57 Aluminium tube showing the set-up of the partitioned aggregates before the removal of the separating cardboard

The final experiment with the given aggregates was designed to determine the preference of root growth between the different sized aggregates. This was done to assess the variable interactions of wheat roots with soils of different structures. In this experiment the same two aggregate sizes as used in the second experiment (4.5.2b) were used, however, these were alternatively poured into different sides of the square aluminium tubes separated by cardboard. After careful filling of the tube to within 1cm of the brim as shown in Figure 57, the partition was gently removed, preserving the separation of the different sized aggregates. A single wheat seed was planted at the centre of the tubes, ensuring that the seed was in contact with both aggregates. The seeds were grown for 14 days before imaging was done. A similar 5 day drying period was applied to enhance root-soil contrast in the images produced. The results from these experiments is given in Figure 58 and Table 12.

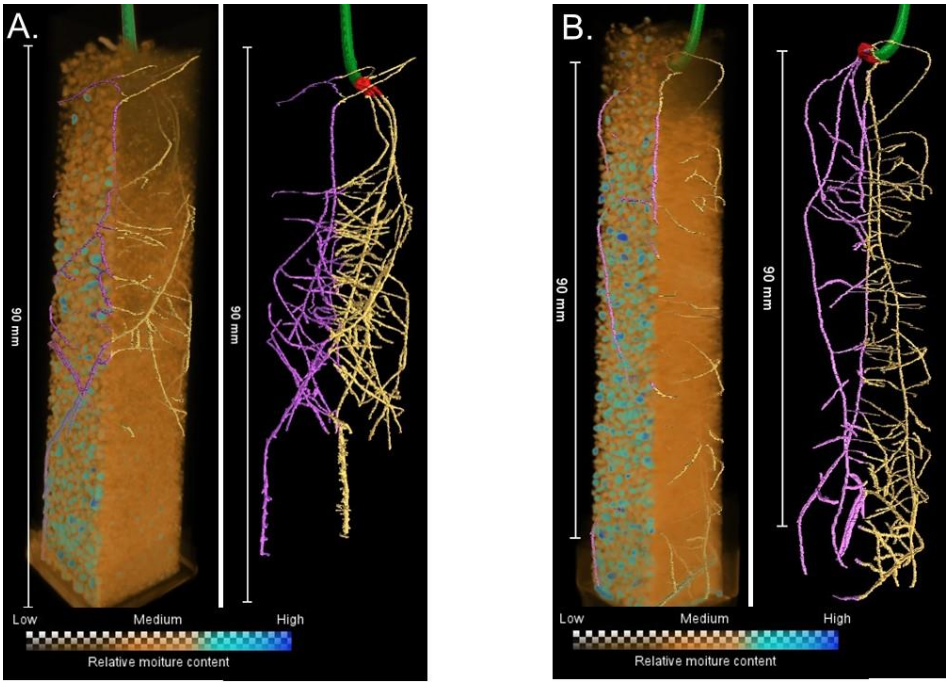

Figure 58: Wheat root growth in aggregates of two different sizes (0.25-0.5mm and 2-4mm) with the roots growing in the side filled with 0.25-0.5mm aggregates being shown in yellow whilst roots growing in the 2-4mm aggregates shown in purple.

Table 12 Root properties of the two wheat plants grown in aggregates of two different size classes computed from NCT measurements

	Root Length (mm)		Root Volume (cm^3)		Surface area (cm^2)		Average root diameter(mm)	
Aggregate size	0.25-0.5	2-4	0.25-0.5	2-4	0.25-0.5	2-4	0.25-0.5	2-4
Plant 1	93.67	57.66	0.0998	0.0520	12.89	7.84	0.337	0.290
Plant 2	114.60	57.52	0.1036	0.0747	13.95	8.63	0.326	0.398

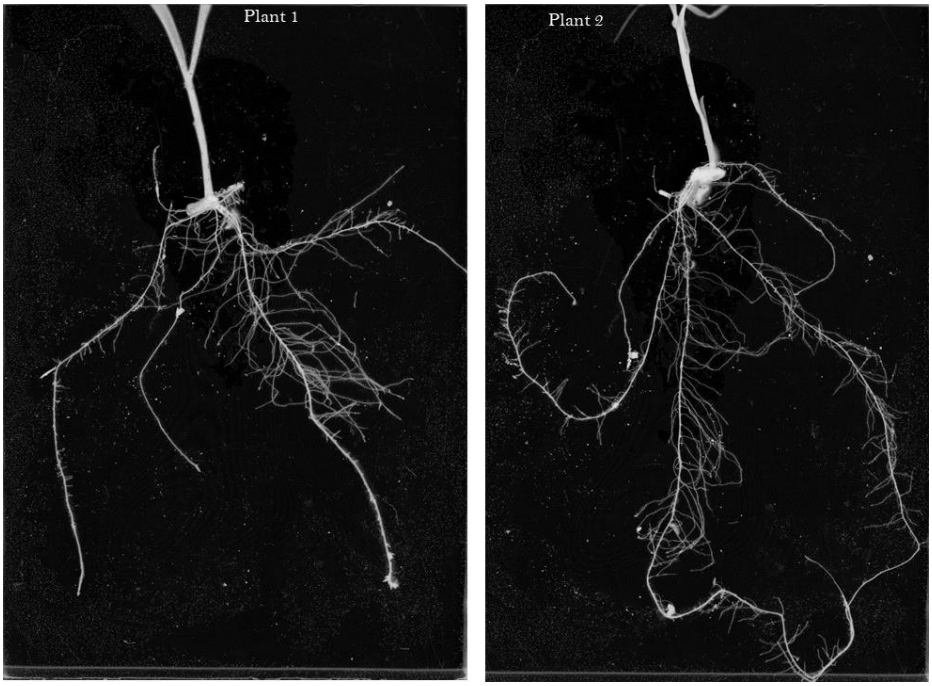

Figure 59: Flatbed scanning images of wheat seedling roots growing in tubes with two different aggregate size classes

Table 13 Root properties of the two wheat plants grown in aggregates of two different size classes computed from flatbed measurements

	Root Length (mm)	Root Volume (mm^3)	Surface area (cm^2)	Average root diameter (mm)
Plant 1	156.119	0.201	19.8571	0.4049
Plant 2	206.181	0.229	24.3703	0.3762

The results from the partitioned tube similarly showed increased root growth in the smaller size aggregates as compared to the larger ones. This is similar to the pattern observed in the previous experiments with root growth being improved in the smaller aggregates. In contrast to the previous experiment, however, roots growing in the smaller drier aggregates could be clearly visible at the centre of the tube even when growing in the relatively drier aggregates. The wheat seedlings also had 5 seminal roots similar to the previous experiment using 2-4mm aggregates.

The water content of the partitioned tubes was also broadly similar to that in the single aggregate experiment with the side that had the 2-4mm aggregates having substantially higher soil moisture available to the root as compared to the partition containing 0.25-0.5mm aggregates. The water content of the roots in the 0.25-0.5mm aggregate was higher than that observed when the plants were grown in the same aggregates individually probably due to the repartitioning of water from the 2-4mm aggregates. The watering schedule for this particular experiment was however

challenging as the precise amount of water required to attain the 16% θ was difficult to estimate as the larger aggregates retained more water and were in contact with the smaller aggregates.

4.6 Discussion

4.6.1 Physiological characteristics and WUE in TaEPF1 stomatal mutants

The stomatal characteristics of the mutant lines used in this study were broadly similar to what was found by Dunn *et al.*, (2019) in their study, however, in this case, the reduction in SD was lower in both TaEPF1OX1 (34% as compared to 46%) and TaEPF1OX2 (45% as compared to 80%) as compared to wild type plants. These variations may have been due to the differences lighting conditions of my experiments as well as the variances in the leaf number selected for these measurements (flag leaf vs 4^{th} and 5^{th} leaves). Differences could also have been as a result of the use of a different soil media (high nutrient compost as compared to a sandy loam soil in my case). In terms of mechanisms responsible for the reduction of the SD in these plants, reduced stomata per cell file instead of a reduction in stomatal cell files was observed. This concurs with the phenotype observed by Dunn *et al.*, (2019) who showed arrested stomatal development in stomatal lineage cells similar to observations made in EPF1 mutant of Arabidopsis (Hara *et al.* 2007).

In terms of WUE findings from this research indicate that alteration of SD via changes in a wheat EPF1 homologue gene can result in improved WUE under my specified conditions. This was true for one of my mutants, namely the TaEPF1OX1 mutant which, had an average reduction in stomatal density of about 34% as compared to wild type plants. This improvement in WUE was shown to have been as a result of a reduction in transpiration by about 15% as compared to the wild type plants. My conclusion for this mutant are similar to the findings of Dunn *et al.*, (2019) who observed improved WUE in the same mutant line using gaseous exchange measurements. On the contrary, however, my second mutant line, TaEPF1OX2 which had an even greater reduction in stomatal density (about 45% more than the wild type) did not show significantly improved WUE in all of my experiments. This is despite the fact that this mutant, similar to the TaEPF1OX1 mutant showed a significant reduction in transpiration as compared to the wild type plants. Further analysis of my data revealed that this mutant had reduced grain and biomass production which resulted in the reduction in WUE. This was contrary to the WUE reported in Dunn *et al.*, (2019) who showed improved WUE in this line as well. These differences in the TaEPF1OX2 line are thought to have been as a result of the abnormal bleaching of the leaves as was visualised 50DAS (42B) which resulted in a moderate increase in transpiration of these plants despite a significant reduction in stomatal density.

In my experiments, the Δ as proposed by Farquhar et al, (1989) surprisingly proved not to be a reliable proxy of WUE in terms of biomass and grain production as has been shown in some studies such as Condon, Richards and Farquhar, (1987), Shaheen and Hood-Nowotny, (2005) and Munjonji, (2017). My Δ results did not show any statistically significant differences in WUE between my mutants and the wild type whilst on the other hand manual measurements of WUE from plant water use and both grain and biomass yields showed an increase in WUE of the TaEPF1OX1 mutant. This was somewhat unexpected as previous studies using EP1 ortholog overexpressing lines in rice have shown a general increase in WUE (Caine *et al.*, 2019), whilst these lines had previously been shown to have increased WUE, albeit by gas exchange methods (iWUE) instead of carbon isotope discrimination (Dunn et al., 2019). This lack of correlation between Δ and reduced stomatal density is similar to that found by Hughes *et al.*, (2017) using similar EPF1 homologue mutants in barley under well-watered conditions. I, however, hypothesize that the disparity in the WUE of the methods could have been be as a result of the limited sets of replicates in my experiment(n=6). Differences could also have been attributed to the quantity of tissue taken from each of my plant for Δ testing, as only 2 leaves (4^{th} and 5^{th} leaf) were sampled which may not be fully representative of the entire plant. However similar lack of correlation between Δ and WUE measured from biomass and transpiration have also been reported by Condon *et al.*, (2004) in wheat and barley whilst this has also been seen on other plants such as sugar beet by Rajabi (2006).

4.6.2 Effect of RSA on WUE

The reduction in stomatal density which gave rise to improved WUE in one of my lines as seen in my one of my stomatal mutants did not seem to affect essential root system properties such as root length and root biomass of this mutant in comparison to that of the wild type plants 30DAS. This was similar to what happened 60DAS with the TaEPF1OX1 line also showing similar biomass productivity. This concurs with earlier results that compared root growth of different wheat varieties and also found more vigorous root growth at similar time points as compared to my study (Figueroa-Bustos *et al.*, 2018). On the other hand roots from the other TaEPF1OX2 mutant showed an increase in their biomass and volume as compared to the wild type plants as well as the other stomatal mutant. This could have been as a result of the abnormalities observed in the leaves of these plants which could possibly have led to increased transpiration and thus increasing root growth (Hepworth *et al.* 2015).

In contradiction to these invasive measurements, however, single non-invasive X-Ray CT scans of the wheat RSA 36 DAS indicated a disparity in wheat RSA of the mutants as compared to the wild

type plants. The wild type plants had an increased root length of between 12 and 46% as compared to the TaEPF1OX1 and TaEPF1OX2 mutants respectively. This disparity may have been due to the fact that the samples chosen could have been a poor representation of the general population of the wheat plants as only one sample was scanned per genotype. More replicates could have given a better indication of how the general trend would be, however, this was not possible in this research due to budgetary constraints. Root property measurements using X-ray scanning could also have been compromised due to the poor ability to segment lateral roots from the different cores due to partial volume effects and poor contrast between wheat roots and the soil (Tracy 2013, Flavel *et al.* 2014). An increase in image resolution could be suggested to reduce such errors however this was not possible in this study.

My results also revealed for the first time, that RSA of wheat plants can be studied in 3D using NCT. NCT of my wheat lines after 14DAS indicated that there was no difference in RSA between wild type plants as compared to TaEPF1OX1 mutant line plants growing under similar conditions. This concurs to the results I found using flatbed scanning of the same wheat lines immediately after NCT scanning. NCT scans, however, were found to underestimate plant root properties similar to X-Ray CT scanning due to resolution and segmentation limitations. As the contrast between roots and soil is better with NCT, I speculate that root recovery from NCT would be better than X-Ray CT imaging at similar resolutions which has also been pointed out by Robinson et al., (2008). Recovery of RSA using NCT may, however, be compromised by variations in root moisture content as evidenced in some of my scans.

4.6.3 Effects of WUE on soil structure

In terms of soil structural stability, many of the aggregate stability test I trialled did not show any significant differences in aggregate stability between my different plants. This was probably due to the fact that most of the test used in literature have primarily been used to compare differences between tillage methods as well as plants of different species (Kemper and Rosenau 1986, Amezketa *et al.* 1996, Le Bissonnais 1996, Nimmo and Perkins 2002). As a result of this, I modified one of the tests proposed in literature to test for the stability of a wider range of aggregates as opposed to the limited range it suggested. My results showed that the growth of my stomatal mutants resulted in significantly reduced aggregate stability of macro-aggregates of between 0.25-0.5mm in diameter as compared to wild type plants 30DAS. This was different 60DAS where similar aggregate stability was seen in this aggregate size. At 60DAS only the TaEPF1OX1 mutant showed reduced aggregate stability as compared to the wild type under in macro-aggregates 1-

2mm in diameter whilst in general all planted pots showed increased aggregate stability. This was thought to have been due to the increased root biomass which could potentially have increased aggregate stabilizing root exudates (Naveed *et al.* 2017). The differences observed in the mutants 30DAS and 60DAS could be explained by the fact that the transgenic lines transpired less, which had could result in reduced alteration in soil moisture regime that has been shown to increase aggregate stability (Materechera *et al.* 1994). This, however, does not explain why differences were only revealed exclusively for one aggregate size. Further investigations may be necessary to establish why this was the case.

My investigations into the interactions between plant roots and different soil structures as derived from growth in different soil aggregates revealed seminal root tortuosity of the plants growing in the smaller aggregates were smaller, indicating shorter paths on a downward trajectory as the seminal roots entered into the soil. This could be explained by the fact that in the smaller aggregates, roots could more easily deflect them and continue their downward trajectory (Misra *et al.* 1988). There was no difference in root thickness in both aggregates indicating that roots in the larger aggregates did not buckle when attempting to enter the large aggregates as has been demonstrated in other experiments such as the increased radial root growth shown by (Logsdon *et al.* 1987) who were also working with wheat plants. This may be due to the increased porosity, which allowed the roots to grow freely around the large aggregates instead of penetrating them.

My investigations also revealed that wheat root growth was comparatively better in smaller macroaggregates as compared to larger macro-aggregates. My results were similar to what has been reported in literature, as many reported increased root growth in smaller aggregates (Misra *et al.* 1986, 1988, Logsdon *et al.* 1987, Alexander and Miller 1991). This is however contrary to the findings by Agrawal et al. (1984) and Agrawal et al. (1987) who showed better root growth in wheat plants in large aggregates. The improved root growth in smaller aggregates was thought to be as a result of a variety of factors such as improved root-soil contact, improved nutrition as well as a general ease of root penetration as roots required smaller amounts of energy to deflect smaller aggregates as opposed to the larger aggregates (Dexter 1978). Surprisingly however roots grown in large aggregates produced reduced longer lateral roots as opposed to more numerous shorter roots in the smaller aggregate size roots. This was thought to be due to the large voids in the structure of the larger aggregates which may possibly hamper lateral root initiation.

4.6.4 Conclusion and future work

Based on my results, improving WUE as was seen in my TaEPF1OX1 mutant did not significantly affect the RSA of mutant plants and thus may not compromise resource acquisition capacity from the soil under my conditions. Further experiments, however, are required to investigate how the reduction in transpiration in this mutant may affect nutrient acquisition as many plant nutrients are acquired via transpiration and reducing it may have an effect on the plant's nutritional capacity, especially in nutrient-limited environments. As my investigations were mainly pot based, root growth and thus root architecture were affected by growth space 'bonsai effect'. This is especially true for plants grown for more than 25 DAS as roots visibly became limited by the pot. Other plant physiological properties may also have been affected by the pot size as studies have shown reductions in net photosynthesis and cell division as a result of limited growth space (Herold and McNeil 1979, Korner *et al.* 1989, Ray and Sinclair 1998, Ronchi *et al.* 2006, Hess and De Kroon 2007, Poorter *et al.* 2012). Some of my plants also grew beyond the recommended 2g of root biomass per L of pot as suggested by Poorter *et al.*, (2012) thus increasing the likelihood that my experiments were affected by the bonsai effect. In order to improve on similar experiments, it may be necessary to trial these mutants in the field to get a better understanding of root growth in nature. Improvements in WUE also seemed to have an effect on aggregate stability of a few selected fractions which may compromise soil structural quality when my WUE mutants are grown on a large scale. Further research may be necessary to find out if this would be the case in other soil types are used in similar tests. It may also be worthwhile investigating the long-term impact of using stomatal mutant plants as changes in soil structure are usually better assessed in long term experiments as opposed to the more ephemeral measurements done in this study.

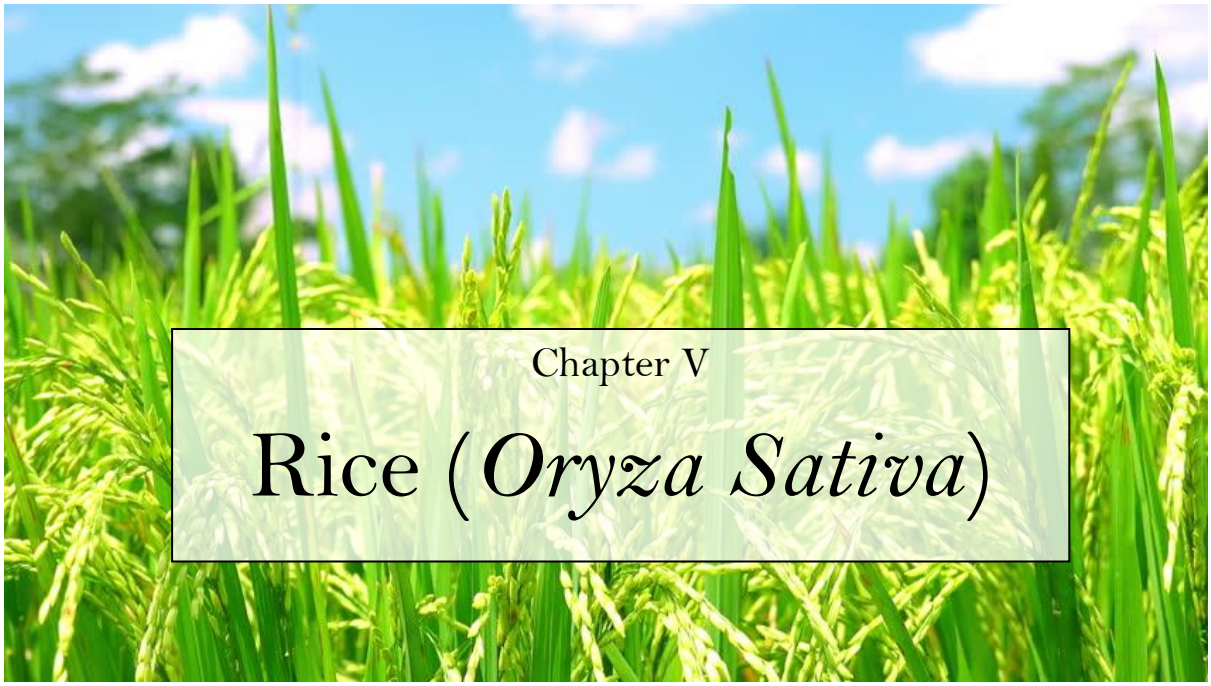

Chapter V

Rice (*Oryza Sativa*)

V Rice

5.1 Chapter summary

In this chapter, in line with the overarching aims of investigating the impact of plant WUE on root architecture and soil structure, I extended my study onto a popular field crop, Rice (*Oryza sativa).* I specifically focused on the commercially grown wetland japonica Rice variety Nipponbare. To achieve the thesis objectives, I firstly screened phytochrome (*phyB*) deficient mutants for improvements in WUE, assessing how these plants performed in a growth chamber. Having identified two allelic *phyB* mutants that showed significantly improved WUE, I then investigated whether the root architectural properties of these mutants varied from those of the wild type plants using both invasive and non-invasive methods. I also investigated the effect of growing the different plant lines on soil structure, as inferred by soil aggregate stability tests similar to those applied in the results given in previous chapters. Furthermore, to determine how the wetland rice variety (Nipponbare) used in this study performed in water-limited upland conditions, I grew the plants under different watering regimes and analysed how root and shoot development were affected by the different moisture treatments. Results from the different experiments showed that RSA of the WUE phytochrome mutants of rice did not significantly different to that of the wild type under controlled growth environment although the trends suggested a slight reduction in RSA of WUE mutant lines. The aggregate stability of soils where WUE mutants were grown was similar to that of the wild type under water-limited conditions however in saturated soils, aggregate stability of 1-2mm aggregates was significantly reduced as compared to wild type plants. This suggested improving WUE may affect soil properties in wetland conditions. Comparing the different methods of studying wheat roots, X-Ray CT scanning was superior as compared to Neutron Radiography (NR) and Computed Tomography (NCT) possibly as a result of rice aerenchyma. Finally, comparison of rice root growth under different soil moisture regimes suggested that the growth of Nipponbare rice variety is negatively affected by cultivation in water-limited conditions.

5.2 Introduction

5.2.1 Importance of Rice

Rice is a semi-aquatic cereal crop which is grown in a wide variety of climates (from temperate to humid tropical) and elevations (from sea level to highlands), producing edible grains that form the basis of human nutrition in many regions of the world (Sys and van Ranst 1993). It accounts for 35-75% of all the calories consumed in East and South East Asia and is the staple food for nearly half of the world's population (Fairhurst and Dobermann 2002, Khush 2005). The majority of the rice produced across the world is grown in Asia with over 90% of all the worlds' rice being grown and consumed within this region (Papademetriou *et al.* 2000). Rice production plays a key role in fighting food insecurity, malnutrition and poverty and as such, its importance was highlighted by the 57th session of the United Nations general assembly who declared the year 2004 as the year of rice. Apart from the importance of its grain, rice plants also produce a considerable amounts of fodder (nearly the same amount as the grain depending on variety) that is often used as a soil amendment and also provides nutrition for livestock after grain harvest (Sarkar and Aikat 2012, Maarastawi *et al.* 2019).

Rice also serves as an important model crop plant, having been the first monocot crop plant to be first draft sequenced in the year 2002 (Yu *et al.*, 2002; Goff *et al.*, 2005) and then fully sequenced to a high quality (Matsumoto *et al.* 2016). It was selected as one of the first crop target for gene sequencing not only because it is one of the most important crops of the world but also because it has one of the smallest genomes amongst most of the worlds' major cereal crops (approximately 400 to 430 Megabase pairs) (Izawa and Shimamoto 1996, Eckardt 2000). These rice genomic resources have been used to unravel the structure and function of different plant genes in cereal plants. This has provided a useful insight into how plant productivity may be enhanced in forthcoming decades.

5.2.2 Water use in rice

Rice is a 'thirsty' crop, which often utilises more than double the amount of water used to grow other major food crops such as maize and wheat per unit area. It is also one of the plants that has a peak water requirement that is more than 20% higher than that of a grass standard as determined by numerous experiments (Brouwer and Heibloem 1986). Globally, rice cultivation accounts for more than half of the total amount of fresh water used for irrigation despite being produced on only 29% of the total land area under irrigation (Barker *et al.* 1999, Tuong and Bhuiyan 1999, AQUASTAT 2014, Hoogeveen *et al.* 2015). It is the crop with one of the largest scarcity footprint

(the potential impact of the quantity of water consumed regardless of water quality) as illustrated in Figure 60 (Hess *et al.* 2015, Lee *et al.* 2018). Much of the vast amount of water utilised in rice production is used to establish and maintain standing water paddy fields where the bulk of the world's rice is grown. It is noteworthy, however, that although often used, standing water is not an absolute essential for rice production as the plant can successfully be grown in dryland, rain-fed systems (Kumar *et al.* 2017, Saito *et al.* 2018). Upland rice varieties, for instance, are specially adapted for cultivation in dryland systems whilst lowland Rice varieties can grow in rain-fed systems, albeit with lower yields. The paddy system of Rice irrigation although useful in allowing the plants to transpire freely is often employed to suppress weed growth. This is because many weed species struggle to grow in anoxic conditions (Roder 2001, Rao *et al.* 2008).

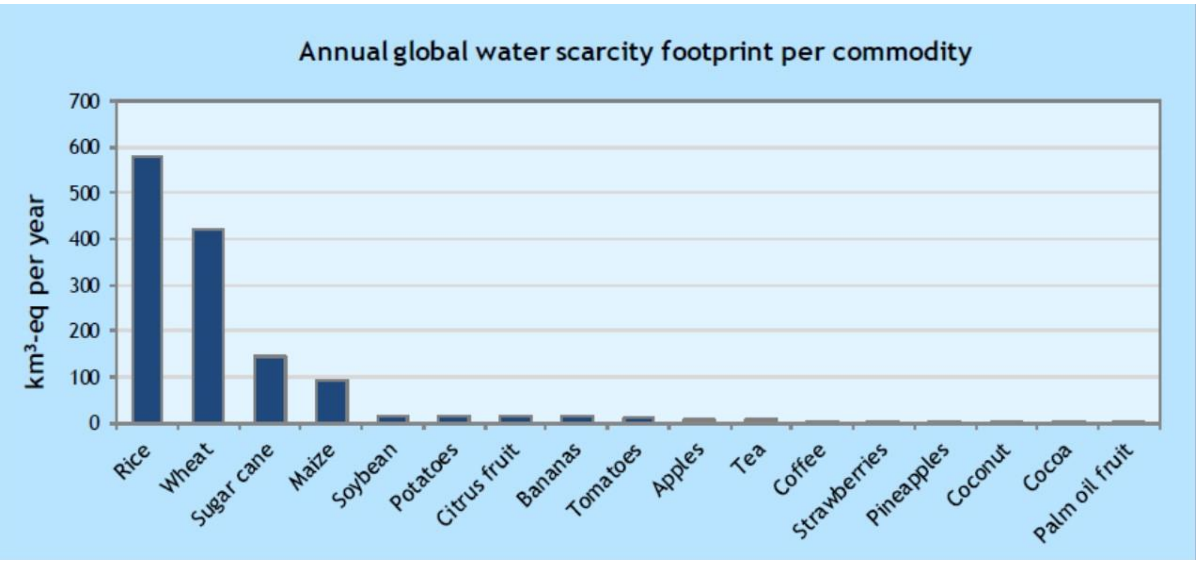

Figure 60 Average global water scarcity footprint for selected agricultural commodities [Source (Odegard et al. 2015)]

As Rice production is a relatively water-intensive process, improvement of WUE especially in Rice cultivation could help prevent or mitigate against both current and projected global water scarcity. This has already been highlighted in numerous several studies (Tuong and Bhuiyan 1999, Sarkar 2006, Karaba *et al.* 2007, Kima *et al.* 2014) that have investigated different strategies that could be employed to minimise the freshwater footprint of Rice production systems. Some of the strategies suggested to improve Rice WUE include intermittent watering, growing Rice in aerobic soils, plant breeding and genetic engineering. In this study, we focused on the latter with WUE mutant Rice plants being used to answer questions of their potential sustainability in terms of plant performance as well as soil structural changes brought about by their growth.

5.2.3 Selection of WUE mutants

Improvement in WUE of Rice is essential in the fight to reduce global freshwater scarcity. As such several rice mutants showing improved WUE have been developed in recent years with the aim of providing a genetic basis to tackle water scarcity (Karaba *et al.* 2007, Dhakarey *et al.* 2017, Moin *et al.* 2017, Caine *et al.* 2019). These mutants are often developed by targeting genes that have been shown to improve WUE for the model plant Arabidopsis e.g. *HARDY* and *EPF1* (Karaba *et al.* 2007, Caine *et al.* 2019). Despite the genetic differences between *Arabidopsis* and rice, several of the Rice mutants show growth characteristics similar to those observed in *Arabidopsis*. A number of mechanisms have been shown to be responsible for the differences in WUE between the developed mutants and wild type plants. These include reductions in stomatal density (Caine *et al.* 2019), increased leaf biomass and bundle sheath cells (Karaba *et al.* 2007), which often limit transpiration in these mutants thus not only improving WUE but also having an impact on drought tolerance often with consequences to overall plant productivity and root growth (Mohammed *et al.* 2019).

In this study, I focus on rice mutants with alterations in all three of the phytochrome genes *PHYTOCHROME A (PHYA)*, *PHY B*, and *PHY C* in rice that were at my disposal. I selected these as research in arabidopsis has shown that functional phyB reduces drought resistance and WUE (Boccalandro *et al.* 2009) and thus I hypothesised this would also be the case in rice plants as well. Many of these mutants have not yet been shown to exhibit improvements in WUE however two allelic mutants, *phyB-1* and *phyB-2*, have been shown to exhibit improved drought resistance as a result of reduced transpiration (Liu *et al.* 2012).

5.2.4 Root System Architecture (RSA) of Rice

Rice similar to most cereals, has a fibrous root system that is characterised by seminal, nodal and lateral roots. This root system is shallow and compact mainly due to its adaptation for growth in sub-aquatic conditions (Morita and Nemoto 1995). Rice has five types of roots, namely a single radicle (seminal) root, embryonic crown (nodal) roots, post-embryonic crown roots, small and large lateral roots as shown in Figure 61 (Rebouillat *et al.* 2009, Eshel and Beeckman 2013). Most Rice plants have a single short-lived seminal root that emerges from the radicle and often extends vertically into the soil. This is proceeded by embryonic nodal roots which usually appear at the 1st and 2nd leaf stage. After embryonic roots have established, post-embryonic nodal roots then grow from different nodes at the base of the tillers. These, as well as the other embryonic roots, are often punctuated by numerous lateral roots, which are divided into two groups, namely the large and small lateral roots (Rebouillat *et al.* 2009, Eshel and Beeckman 2013). Large lateral roots differ

as compared to the small lateral roots in that they are indeterminate. Root branching usually extends in synchrony to shoot growth with lateral roots being able to grow up to the 5th order (Kawata and Soejima 1974, Eshel and Beeckman 2013).

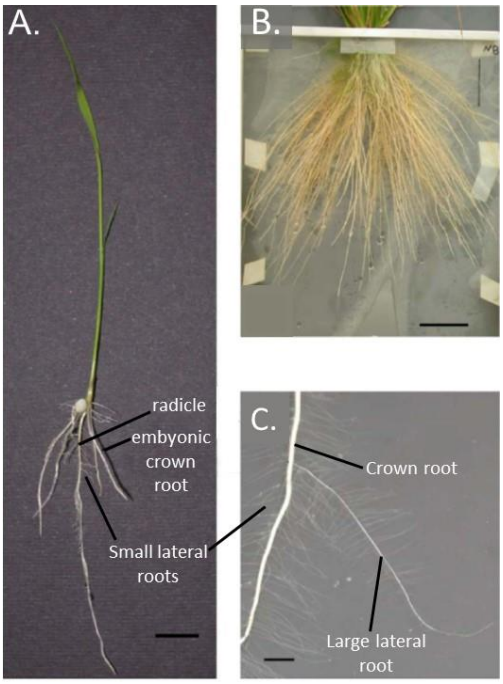

Figure 61 Root morphology of hydroponically grown rice plants cv Nipponbare, A. 7 days after germination, B. 40 days after germination and C. Finer detail of crown roots 40 days after germination. Horizontal scale bars represent (A) 1 cm, (B) 5 cm, (C) 1 cm [Adapted from (Rebouillat et al. 2009)]

5.2.5 Methods of measuring Rice root architecture

Investigation of rice root growth has been of interest to many researchers over the years with several invasive and non-invasive methods of measurement being used to this end. As rice roots often grow obscured by opaque soil, some methods of studying roots involve the use of transparent media such as water (in hydroponic systems) (Panigrahy *et al.* 2014, Negi *et al.* 2016) or agar (Kreuzer *et al.* 2006), to simplify the visualisation and characterisation of RSA in these systems. However, these methods lack crucial detail on the interaction of rice roots with soil. Roots also often grow much faster especially in hydroponic systems where there is limited resistance from the water and thus this makes information on the growth and elongation rate unrepresentative of soil conditions.

In light of this RSA of rice is most often studied by excavating roots from soil and washing the soil off so as to obtain a clear image of the rice plants (Kawata and Soejima 1974, Liu *et al.* 2012, Péret *et al.* 2014, Dhakarey *et al.* 2017, Gu *et al.* 2017, Fang *et al.* 2019). These are usually then scanned using high-resolution flatbed scanners to recover the essential information on root growth and development. This method gives reliable information on the performance of rice roots in soil

but is marred by its own problems, such as the loss of root material during washing as well as crucially lacking spatial 3D information on the RSA (van Noordwijk and Floris 1979).

In light of the shortcomings of root excavation and washing, non-invasive techniques of rice root imaging have been used in order to recover the missing 3D information. The most commonly used non-invasive method of studying RSA of rice involves the use of X-Ray tomography. This has been used effectively to recover RSA of rice plants growing in both saturated and unsaturated conditions (Keyes 2013, Zappala *et al.* 2013, Rogers *et al.* 2016, Fang *et al.* 2019). Neutron Radiography (NR) (Bois and Couchat 1983) and Magnetic Resonance Imaging (MRI) (Liu *et al.* 2014) have also been used however, these are less popular for studying rice plants.

These non-invasive imaging techniques have their own limitations in terms of root recovery, with the biggest limitation being the poor contrast between rice roots and soil edges (Sander *et al.* 2008, Zappala *et al.* 2013). This is especially true when soils are wet or saturated as this further reduces the contrast between roots and other components in the soil (Zappala, Mairhofer, *et al.* 2013). Regardless of moisture content, small lateral roots are often difficult to recover mainly due to resolution limits when imaging thus non-invasive image scans of rice, as well as other plants, almost always underestimate the extent of the RSA.

In light of the above-mentioned strength and advantages of the different methods of studying RSA, for this study, I chose several methods to measure RSA properties of the plants under review, these are namely, X-Ray CT, NI, NCT and root washing.

5.2.6 Soil structure and Rice growth

The literature on the impact of Rice roots on soil structure is scarce. There is evidence to suggest that rice root may cement soil aggregates (Zhou and Pan 2007, Chen *et al.* 2017). However, most studies investigating the soil structural development associated with Rice plants mainly focus on the benefits of zero tillage or incorporating its straw into the soil as opposed to the specific effects of rice roots on soil structure (Cass *et al.* 1994, Yadvinder-Singh *et al.* 2005, Tang *et al.* 2012, Xue *et al.* 2019). Rice is often cultivated in anoxic paddy fields that have different soil structural requirements as compared to oxic dryland fields used for the cultivation of the majority of other crops. Paddy fields, unlike oxic dryland fields, are wet cultivated (puddled) to reduce water and nutrient loss via deep percolation (Kirchhof and So 2005). This puddling reduces transmission pores by the destruction of aggregates which limits the amount of large pores in soil and creating a 'jelly-like' clay soil structure that may harden after drying (Greenland 1981). The Rice production system is thus often at odds with the production of other crop plants as soil management for non-aquatic plants aims to increase transmission pores via improved aggregation (Bhagat 2003). A

hypothetical comparison of pore size distribution between ideal paddy fields and a well-aggregated soil is given in Figure 62.

As a result of the pudding, crops grown subsequent to rice often yield less due to the decrease in porosity and aggregate stability after rice harvesting (Bhagat 2003). Water saturation in paddy fields has also been shown to have a generally negative impact on aggregate stability as the soil organic carbon content decreases due to reduced soil organic carbon inputs (Greenland 1981, Roychoudhury *et al.* 1983).

Due to relatively limited information regarding whether rice root growth affects soil structure, in this study, I investigate the impact of rice roots on soil structure in both saturated and unsaturated conditions.

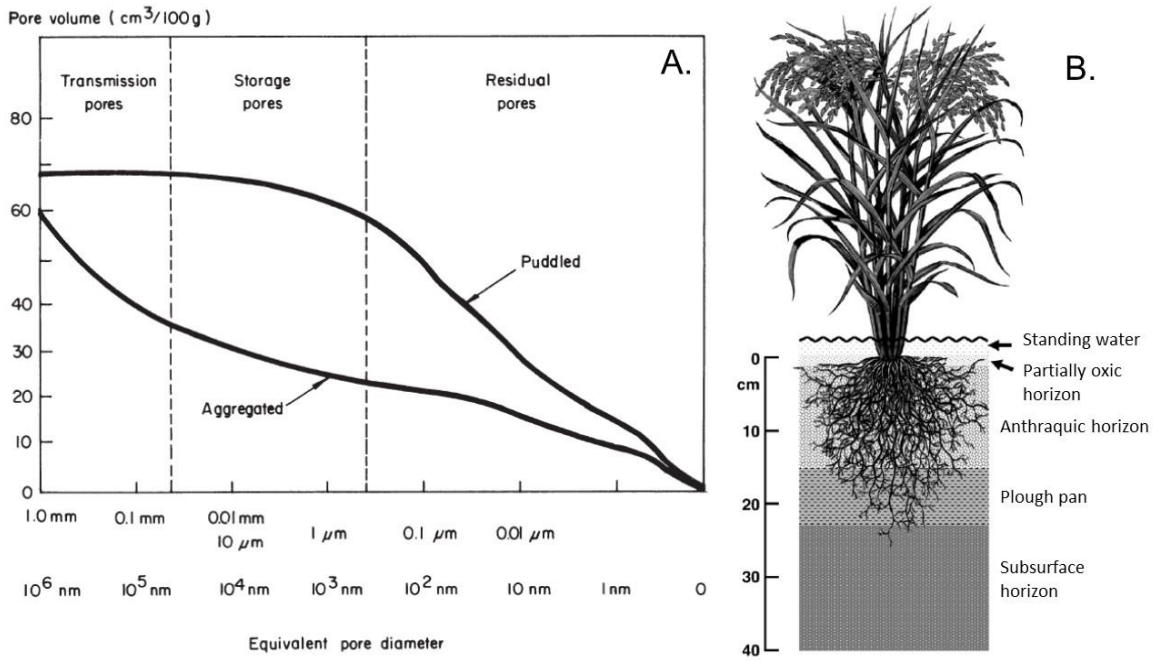

Figure 62 A. Hypothetical ideal pore size distribution in well aggregated and puddled soil. B. a typical paddy rice horizon structure shown showing typical root distribution throughout the horizons [Source (Greenland 1981, Kögel-Knabner et al. 2010)]

5.2.7 Research aims and objectives

In this chapter, I focused on understanding how altered WUE in Rice plants impacts on their root architecture and soil structural stability

To achieve this, I had the following objectives:

1) Identify rice mutants that show alterations in WUE as compared to wild type plants of the same background in sandy loam soil.

2) Determine how the change in WUE of the identified Rice plants affects their RSA using both invasive and non-invasive techniques.

3)Assess how changes in WUE of the identified wheat plants impact on the structure of a sandy loam soil.

5.3 Screening for mutations in Rice plants that lead to altered WUE

In this section, I screened a variety of different *PHYB* mutants for improvement in WUE using the carbon isotope discrimination method. Following the identification of mutants showing improvements in WUE, I then proceeded to carry out physiological measurements of these plants. My specific research questions for this section are as follows;

Main questions:

- Do any *phytochrome* mutants of Rice show significantly altered WUE as compared to the wild type plants?
- How do the physiological properties of the selected Rice mutants differ to that of the wild type plants?

5.3.1 Preliminary screening of phytochrome mutants for improvements in WUE

The initial phase of my research with Rice was to screen the several mutants at my disposal for significant alterations in WUE as compared to wild type plants. I screened seven different *phytochrome* mutants from the study by Takano *et al.*, (2005) namely the *phyA-4*, *phyB-1*, *phyB-2*, *phyC-1*, *phyA-4 phyB-1*(double mutant), *phyA-4 phyC-1*(double mutant) and lastly the *phyA-4 phyB-1 phyC-1* (triple mutant). I hypothesized that some of them could have mutations that may lead to improvements in WUE. This was because the known role of some phytochromes (mainly phyB) in enhancing plant photosynthetic capacity at the expense of WUE as has been shown in arabidopsis (Boccalandro *et al.* 2009). In Rice, *phyB* mutants have also been shown to exhibit drought resistance (Liu *et al.* 2012).

To determine whether Rice plants deficient in phytochromes have changes in their long term WUE. The selected plant lines were grown in cylindrical PVC tubes with a diameter of 68mm and a height of 120mm filled to a bulk density of 1.25g cm^{-3} with the sandy loam soil. Seeds of the different genotypes were sown at the centre of the tubes, 10mm below the surface of the soil and were watered to a predetermined field capacity until germination. After germination, the seedlings were then switched to watering by periodic flood irrigation three times a week for the duration of the experiment. These plants were grown for six weeks in a growth chamber maintained at a

temperature of 26°C/21°C (night/day) with ambient relative humidity and a 12-hour photoperiod. Thereafter WUE using the C isotope discrimination method as well as total shoot biomass measurements were done. The results I obtained are shown in Figure 63.

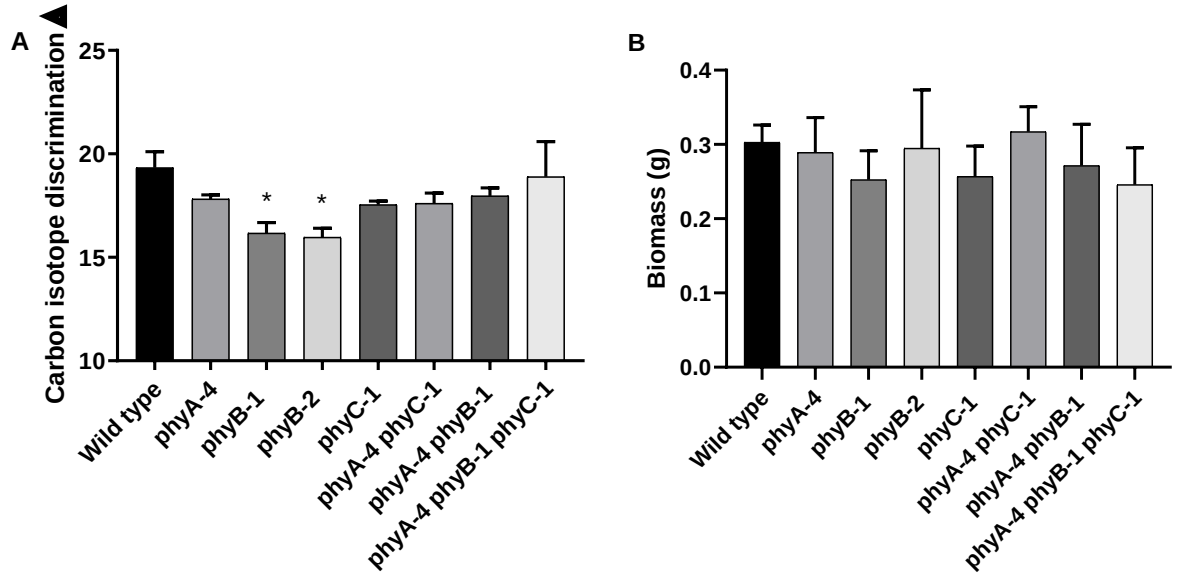

Figure 63 A) Carbon isotope discrimination and B) shoot biomass production in the different phytochrome mutants of Rice (n≥3). Error bars indicate SEM. Symbols indicate significant difference as compared to the wild type; One-Way ANOVA test with post-hoc Bonferroni test, (*=≤0.05)

The average Δ and was reduced thus WUE of all the light-sensing mutants was generally improved as compared to that of the wild type (Figure 63A). Two of the mutants, namely the *phyB-1* and *phyB-2*, showed statistically significantly improved WUE as compared to the wild type plants. The remainder of the mutants also showed a reduction in Δ indicating improved WUE however this was not significantly different to that of the wild type. The triple mutant *phyA-2 phyB1 phyC*-1 showed the highest Δ among the mutants indicating it was the least of WUE mutant plant which had a similar average Δ as compared to the wild type plants. These results were interesting from a genetic perspective in that although *phyB* mutation generally showed improvements in WUE, this effect was not additive as double (*phyA-4 phyB-1*) and triple (*phyA-4 phyB-1 phyC-1*) mutants with similar lack of functionality of the gene as well as other phytochrome genes not showing significant improvements in WUE.

In terms of shoot biomass production, as shown in Figure 63B, there was no significant difference between the different mutant plants as compared to the wild type plants. In general, however, most of the mutants' shoot production was lower than that of the wild type with the triple mutant, phyA-2 phyB1 phyC-1 showing the lowest average shoot biomass production whilst the double

mutant, phyA-4 phyC-1 comparatively exhibited the highest average shoot biomass production amongst all the plant lines grown including the wild type.

As a direct consequence of these results, I narrowed down my research to the two mutants, *phyB-1* and *phyB-2* that were shown to have significantly higher WUE as compared to wild type plants under my conditions. The fact that both these mutant alleles of phyB had very similar phenotypes provides good evidence that phyB has a significant impact on WUE in this variety.

5.3.2 Transpiration and plant productivity

To further investigate the difference in water use characteristics of the selected mutant plants as compared to that of the wild type, an experiment was set up to look at the transpiration rates of the different plant lines over the course of their entire growth lifecycle. This was similar to the experiment done using wheat plants (Section 4.3.2) where plants were grown in specially designed growth tubes, sealed at the base and covered with plastic at the surface to reduce soil evaporation. In this experiment however the watering regime for the Rice plants was altered to ensure that the soil moisture was maintained at around 80% of Water-filled Pore Space (WFPS) (gravimetrically estimated) for the entirety of the experiment by surface irrigation to replace the water lost as estimate by weighing the pots once every 2-3 days. At the end of the 150-day experimental period, the plants were harvested and their total dry biomass was determined and used to calculate WUE of the different plant lines. The results obtained in this experiment are given in Figure 64 and Figure 65.

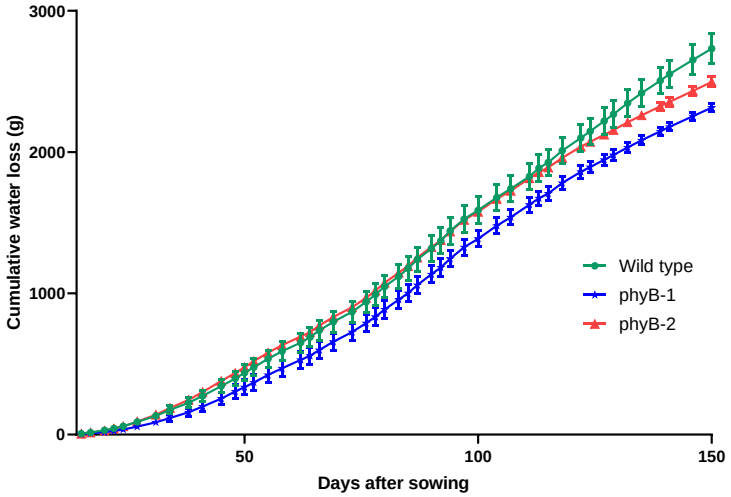

Figure 64 Cumulative ET water loss from the different Rice lines over a 150 day period. Error bars represent standard error of the mean. (n≥5)

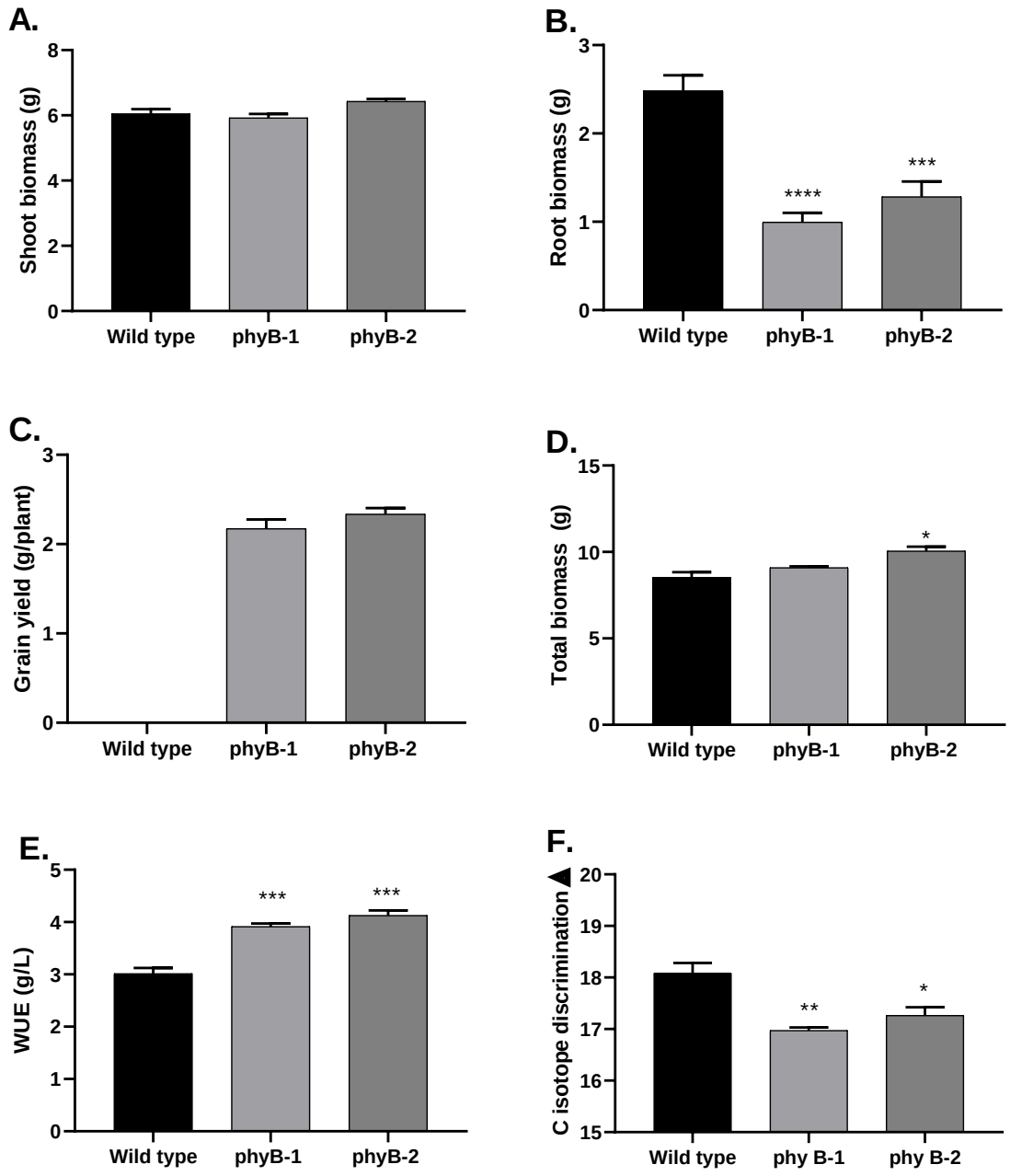

Figure 65 Plant growth characteristics of Rice lines grown for 150 days. A) Shoot biomass, B) Root Biomass, C) Grain yield, D) Total biomass, E) WUE as estimated from total biomass and F) Carbon isotope discrimination measurements (n≥5). Error bars indicate SEM. Symbols indicate significant difference as compared to the wild type; One-Way ANOVA test with post-hoc Bonferroni test, (*=≤0.05, **= ≤0.01, ***=≤0.001, ****=≤0.0001)

Cumulative ET water loss in the Rice lines over the 150 day period (Figure 64) showed a significant difference in the amount of water transpired by the different plants at different time points in their growth. Differences in transpiration between the wild type plants and the *phyB-1* mutant became significant about 30DAS up until the end of the experiment. The *phyB-1* mutant showed the lowest cumulative water loss at the end of the experiment, having transpired 15.27% less water over the

growth period as compared to the wild type plants. Cumulative water loss differences in the *phyB-2* mutant as compared to the wild type plants were less pronounced as compared to that of the *phyB-1* with transpiration rate in these plants even exceeding that of wild type plants between 40 and 80 DAS. A comparatively reduced transpiration rate in the *phyB-2* mutants only became apparent after 120 days of growth up until the end of the experiment. After 150day growth period, the *phyB-2* mutants had used 8.65% less water as compared to the wild type plants.

In terms of shoot Figure 65A biomass from the plants at harvesting, there was no significant difference between the different in the mutants as compared to the wild type plants. The *phyB-2* mutants comparatively had the highest average shoot biomass production whilst the *phyB-1* had the lowest shoot biomass production over the growth period. The results were different in terms of root biomass (Figure 65B) where the wild type plants had significantly higher root biomass as compared to both the mutants with the *phyB-1* mutant showing the lowest root biomass production of the three lines grown. The root biomass of the *phyB-1* mutants was reduced by about 60% as compared to wild type plants was whilst *phyB-2* plants roots were reduced by about 50% in comparison to the wild type plants.

In terms of grain production, only the two mutants were able to produce grain under my growth conditions within the specified time. The wild type plants did not set any seed over this growth period and there was no sign of inflorescence set in all the wild plants despite seed set occurring in the two mutants around 70-80 DAS. Out of interest sake, the wild type plants were grown for a further 30days under the same conditions and only after 170 DAS did a few of the wild type plants start to set seed. The results from the grain production (Figure 65C) show that there was no significant difference in grain production between the two mutants with the phyB-2 mutant showing comparatively higher average grain production as compared to the phyB-1 mutant. In terms of biomass production (Figure 65D), there was a significant difference between the phyB-2 mutant and the wild type plants with the phyB-2 mutant plants showing the highest total biomass production among the plant lines. The total biomass production was also marginally higher in phyB-1 mutant plants although not statistically different to that of the wild type.

In terms of water use efficiency as estimated using the Δ and as computed from biomass and transpiration measurements (Figure 65E and Figure 65F), WUE was significantly increased in both mutants as compared to the wild type plants, similar to the results from the Δ in the section 5.3.1. WUE measurements as calculated from total biomass measurements (Figure 65E) indicated that the phyB-2 mutant had the highest biomass productivity per unit amount of water transpired as compared to the other plant lines whilst the wild type plants had the lowest productivity per unit

of water used during the experiment. WUE as determined from Δ indicated a slight variation from this as it indicated that WUE was highest in the phyB-1 mutant as opposed to the phyB-2 mutant in the biomass experiment (Figure 65F). The wild type plants, however, were estimated to have the lowest WUE using Δ similar to what was found using the alternate method of WUE determination.

5.3.3 Stomatal characteristics

To further investigate, the possible causes of the improvement in WUE in *phyB* mutant plants, a determination of the stomatal properties of these plants was done. These were investigated because stomatal properties are known to affect plant gaseous exchange and therefore water use. In this experiment, the different plant lines were grown in conditions similar to those used in the preliminary screening experiment (section 5.3.1) with stomatal properties of the selected plant lines being determined at the 6th leaf stage with a single 5th leaf single leaf being taken from each plant for characterisation. This was chosen as Δ measurements were determined at this stage. The results of this characterisation are shown in Figure 66.

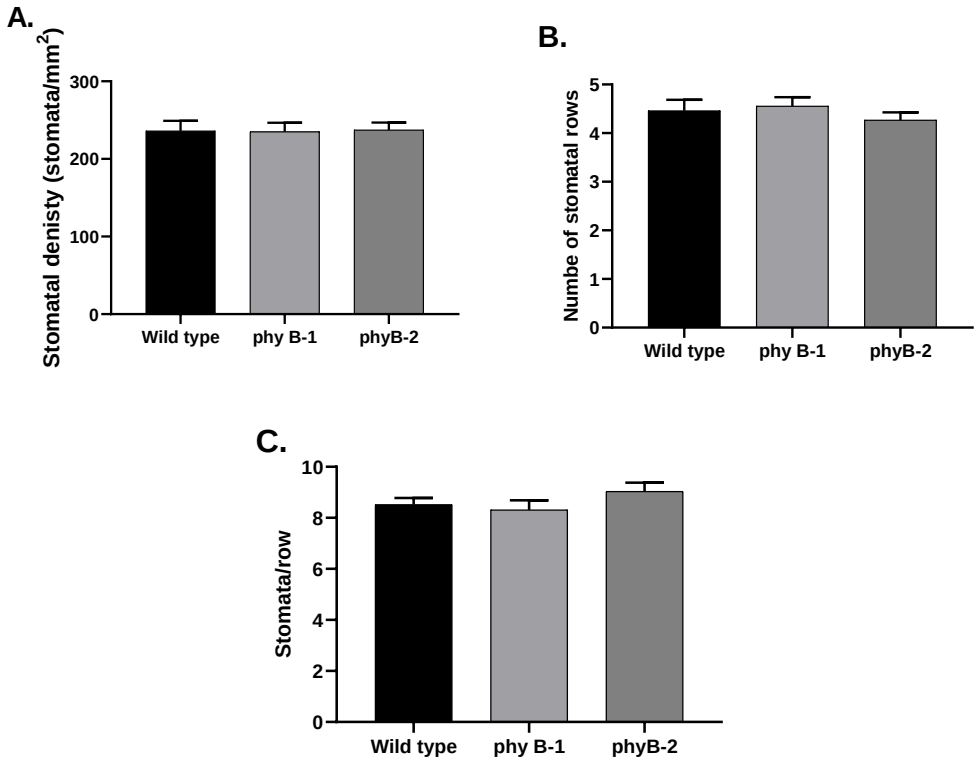

Figure 66 Abaxial stomatal properties of Rice lines with A, stomatal density, B. Number of stomatal cell files per FOV and C. Number of stomata per cell file per FOV. Error bars represent SEM. One-Way ANOVA test with post-hoc Bonferroni test was performed.

There were no significant differences in the abaxial stomatal density of the two mutants as compared to the wild type plants as shown in Figure 66A. An invariable average stomatal density

of about 236 stomates/mm^2 was uniform in all the plant lines grown under my conditions. In terms of stomatal distribution patterns, as shown in Figure 66B and C, there were similarly no significant differences in the number of stomatal cell lines per FOV(0.7mm^2) and the number of stomata per row between the mutants and the wild type plants thus indicating similar stomatal patterning in all the lines we imaged for this specific leaf.

5.4 Effects of improved WUE on RSA in Rice

In this section, I use both destructive and non-invasive methods of root system analysis to investigate the differences in RSA between the selected WUE Rice mutants and wild type plants. The specific research questions for investigation are as follows;

Main questions:

- How does the RSA of the WUE mutants of Rice plants compare to that of the wild type plants?
- How do the different methods of measuring Rice RSA measurement compare in terms of estimating belowground root growth?

5.4.1 Destructive measurements of Rice RSA

a) Preliminary experiment

Experiments to determine the RSA of the Rice lines was carried out in 2 different phases. A preliminary experiment was carried out to determine the most 'appropriate' time to sample Rice roots when grown in sandy loam soil. The appropriate time, in this case, was defined as a time point when root growth has proceeded enough to establish possible differences in RSA whilst not as far as to cause root growth inhibition by being pot bound (bonsai effect). This upper limit of root growth was also estimated because determination of root properties using WinRhizo® becomes increasingly difficult due to problems in separation of overgrown roots as was seen when studying wheat RSA. For this experiment, the Rice plants were grown in aluminium growth pods filled with a sandy loam soil. The Rice seeds were planted at the centre of each pod and maintained at a moisture content at 80% of WFPS by surface irrigation for the entirety of this experiment. The plants were grown for between 21 and 35 DAS in a growth chamber. The results I obtained are given in Figure 67.

Results from the preliminary experiment indicated that root properties of Rice plants could successfully be imaged with minimal problems associated with root tracking right up until 42DAS. After this growth period, roots became too dense and sub-sampling became essential in order to more accurately determined root properties from scanning. At this stage, roots also started to become pot bound, recoiling back into the soil having reached the base of the growth pods. On

the other hand, before the 28 day period, root growth had not proceeded enough for the roots to have occupied the bulk of the growth pods and thus this time would not be appropriate to image the plants before this period of growth. From this experiment, it was clear that under my set up, the greatest rate of growth was between 35 and 42DAS with comparatively exponential plant growth occurring.

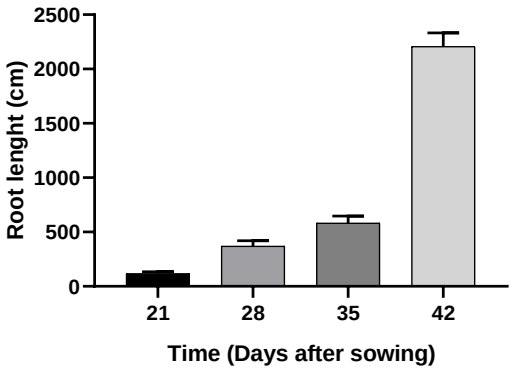

Figure 67 Root length measurements of Rice lines between 21 and 42 DAS(n=3)

b) Comparison of Rice lines RSA in a sandy loam soil.

Following the preliminary experiment in which I determined the best time to be imaging Rice root plants with minimal imaging problems, I then proceeded to compare RSA in the different Rice WUE lines with the wild type plants. In this experiment, Rice plants were grown in rhizopods similar to the ones used in the preliminary experiment. These were filled with the sandy loam soil and a single Rice seed was planted at the centre of each pod then grown for 31DAS. At the end of the growth period, the different plants were harvested and their root were scanned using a flatbed scanner. The root properties from each scan was analysed using WinRhizo® software and after that, shoot and root dry biomass was determined. The results obtained from this experiment are given in Figure 68.

The results from the invasive root washing and subsequent WinRhizo® root property measurements did not show any significant differences between the two mutants as compared to the wild type (Figure 68A-F). Wild type, however, showed the greatest average root length, surface area, volume and biomass as compared to the different mutants (Figure 68A, B, D, E). On the other hand, the *phyB-1* mutant had the lowest average among these parameters which follows a trend broadly similar to the result we obtained in Section 5.3.2. Shoot biomass (Figure 68F) also showed a similar trend as compared to the one obtained in the preliminary screening experiment Section 5.3.2 with average shoot biomass of wild type plants being generally the highest amongst the different mutants, although not statistically significant. There was also no significant difference

in the root thickness (Figure 68C) of the different lines with an average root thickness of about 490μm being uniform among for all the plant lines grown in this experiment.

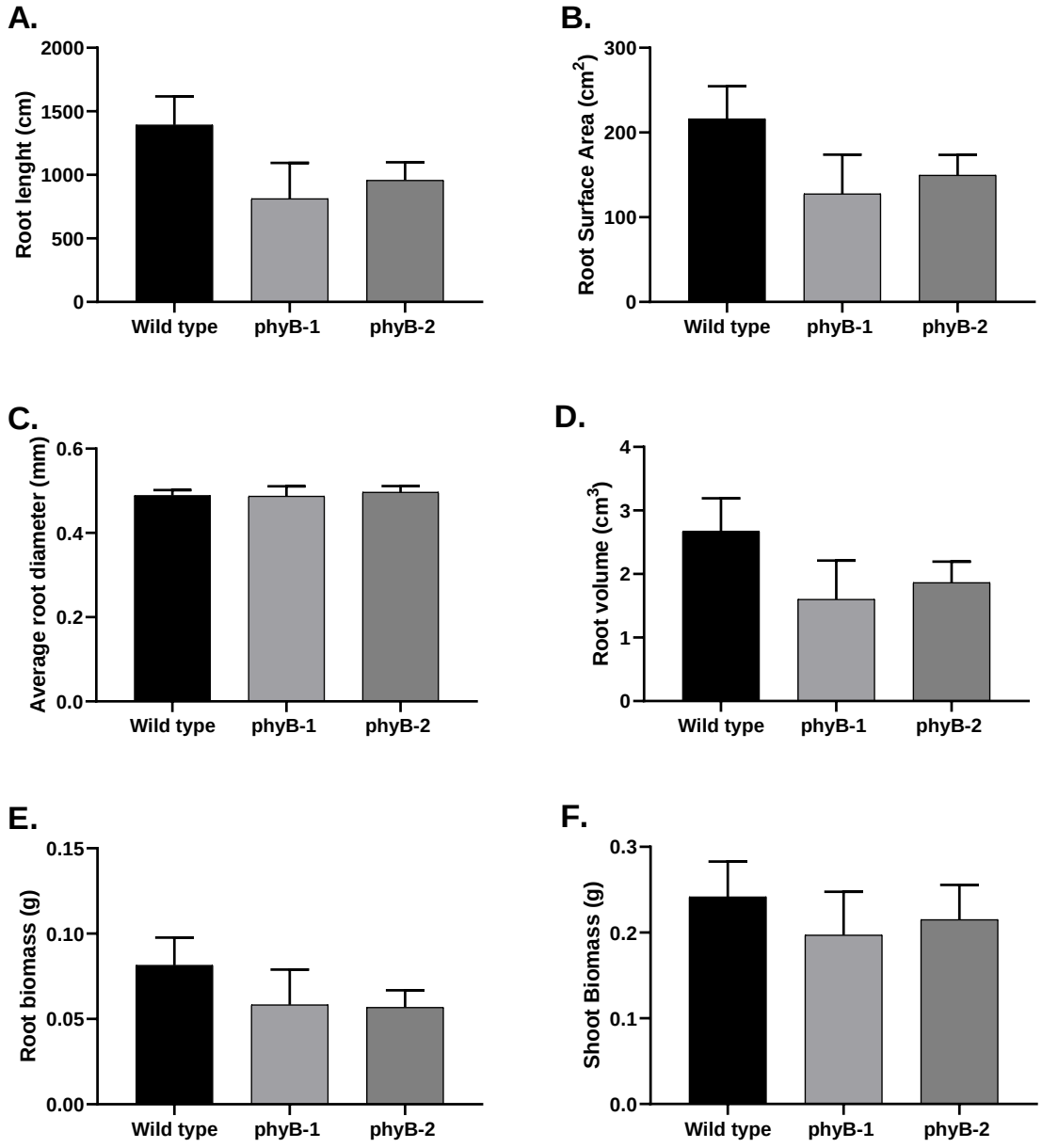

Figure 68 Root properties of the Rice lines grown in a sandy loam soil for 31 days. A. Root length, B. Root Surface area, C. Average root diameter, D. Root volume, E Root Biomass and F. Shoot Biomass (n≥4). One-Way ANOVA test was run with post-hoc Bonferroni test.

5.4.2 Non-invasive measurements of RSA

Non-invasive experiments carried out using Rice plants were broadly similar to the experiments done with wheat plants, where RSA was investigated using two different non-invasive methods of estimating root properties, namely, X-Ray and Neutron CT scanning. These methods would allow

for the investigation of Rice RSA without disturbance of their growth conditions allowing for the visualisation of the 3D RSA of Rice plants in situ.

a) X-Ray CT measurements

In this experiment, the Rice plant lines were grown in PVC tubes similar to those used in Section 5.3.1. These were filled with a sandy loam soil to a bulk density of 1.2g cm^{-3}. A single Rice seed was planted at the centre of each tube and these were watered to field capacity and maintained at this moisture content by surface irrigation. Irrigation was stopped 5 days before imaging to enhance contrast between the soil and the roots. For imaging, three of the most vigorously growing plants of each genotype was scanned using the Nikon Metrology XTH 225 LC scanner as described in the methods chapter with 3143 projections being taken with an exposure time of 286ms per projection and a scan resolution of 69.89µm. The results obtained from the scans are given in Figure 69 and Table 14.

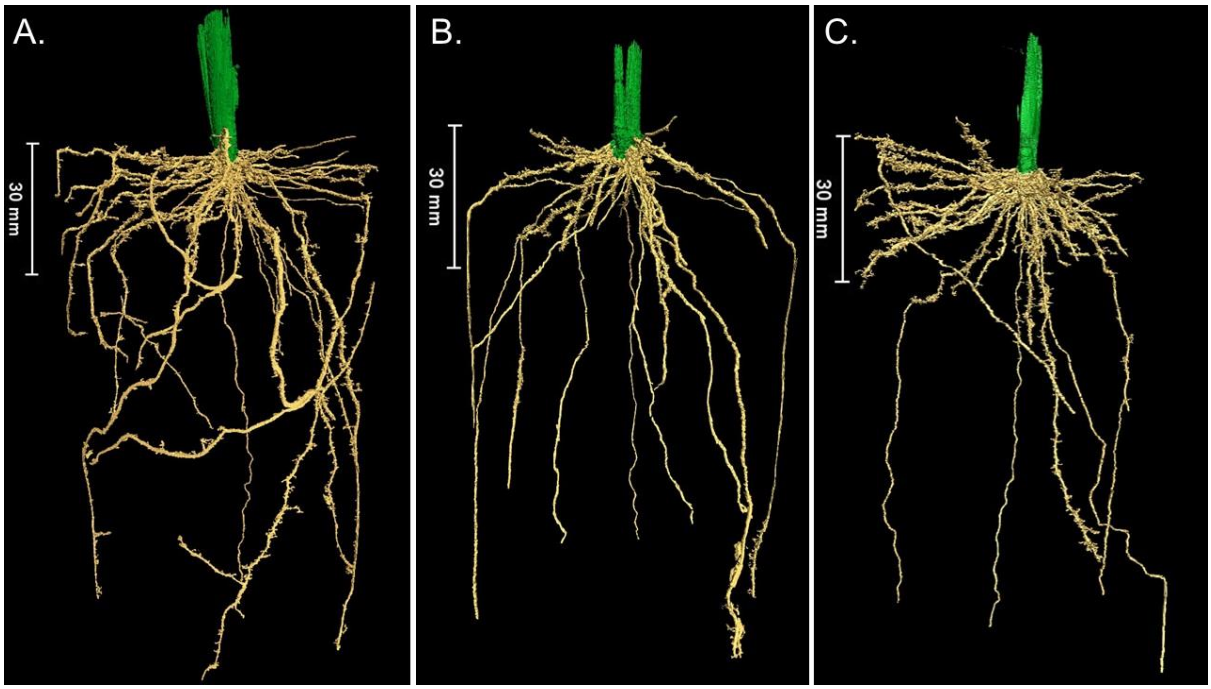

Figure 69 3D rendering of A) Wild type, B) phyB-1 and C) phyB-2 line plants 39 DAS

Table 14 Showing some of the root properties of the different Rice lines obtained from segmented CT scans and biomass measurement

Genotype	Root length(mm)	Root Volume(mm^3)	Root surface area(mm^2)	Root diameter (µm)
Wild type	394.15154	454.63	0.420	394.15154
phyB-1	245.49918	296.375	0.394	245.49918
phyB-2	358.81379	402.518	0.393	358.81379

As seen in Figure 69 and Table 14, root system architectural properties of wild type plants were higher in terms of root length, volume and surface area as compared to the two mutants. The *phyB-1* mutant, on the other hand, showed the lowest RSA parameters whilst the *phyB-2* mutant had properties similar to that of the wild type although lower. These results are similar to what was obtained using destructive RSA characterisation with the same trend being observed among the different Rice lines. The *phyB-1* mutant to had the lowest root length as compared to the other plant lines mainly due to a visible reduction in nodal root growth within the first 30mm from the soil surface in preference to expansion of already existing nodal roots (Figure 69). The *phyB-2* mutant, on the other hand, exhibited a similar root growth pattern in the top 30mm of the soil as compared to the wild type plants, however, the number of elongated roots extending beyond 30mm were much fewer as compared to the wild type plants and thus the mutant had a smaller RSA as compared to the wild type. In terms of average root diameter, the wild type plant also had the thickest roots with the two mutants having a similar but lower root thickness. Root thickness 500 μm vs 400 μm as obtained using this method were however around 100μm lower than those obtained using destructive sampling. Whilst differences were observed between the genotypes in this experiment, the lack of replication prevents statistical analysis to determine if the differences were repeatable and significant.

b) Neutron Imagery (NI)

As NI is relatively novel in the study of Rice plants. The first experiment I carried out using this technique was initially to investigate whether the technique could be used to study RSA of Rice plants grown in situ. In this experiment, Rice plants were grown in the aluminium rhizopods as described in the wheat Chapter Section 4.4.2 filled with 250-500μm sieved soil aggregates. These were used as they had been previously shown to produce enhanced contrast between roots and soil with wheat plants. A single Rice plant was planted in the centre of each pod and watered to field capacity. The pods were maintained at field capacity for the duration of the experiment until 7 days before imaging when the pods were allowed to dry to enhance the contrast between roots and soil. Single radiography images were taken for each pod and the results are given in Figure 70.

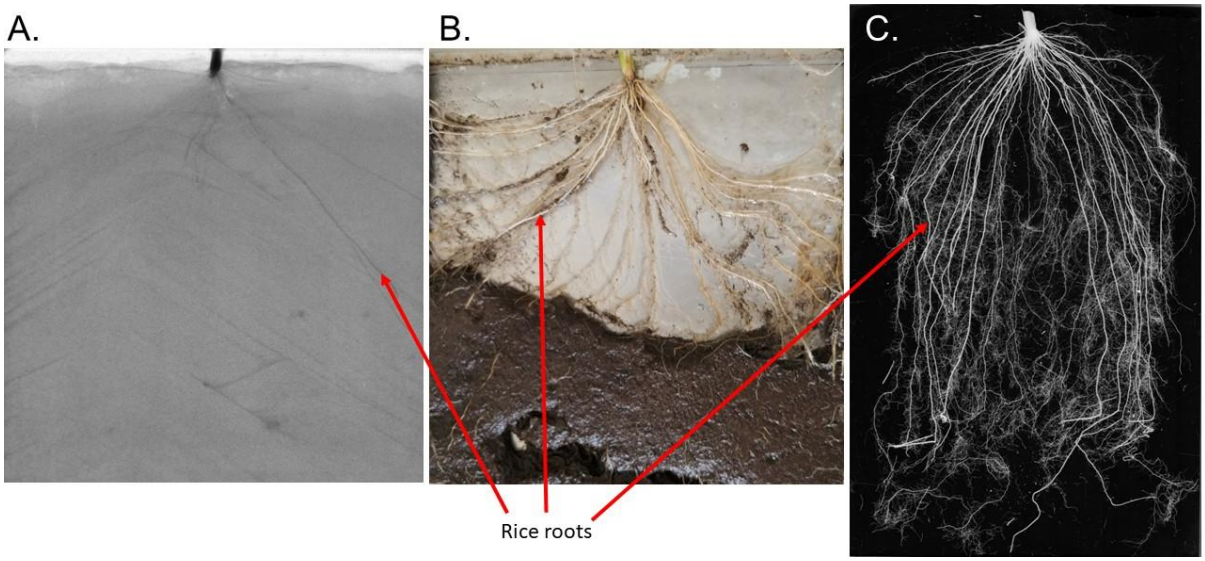

Figure 70 2D Imaging of the RSA of a wild type plant grown in aggregate filled rhizopods. A) Neutron radiography image, B) Camera photograph image C) WinRhizo® flatbed image scan.

As a consequence of the poor contrast between roots and soil in NR images, my next experiment alternatively focused on NCT instead of NR. This technique was chosen as mainly based on the results I obtained in the wheat chapter where the contrast between roots and the soil was comparatively higher relative to NR thus enabling detailed 3D visualisation of wheat RSA. In this experiment, single Rice plants were planted in cylindrical aluminium tubes as described in the wheat chapter (Section 4.4.2b). These were filled with the sandy loam soil as to a bulk density of 1.2g cm-3. Single seeds were planted at the centre of the tubes, 0.5cm below the surface and watered to 50% WFPS. This was maintained by surface irrigation up until 5 days before imaging when watering was stopped to allow soil drying, which enhances root-soil contrast in NCT. The plants were imaged 10 DAS. The results I obtained are given in Figure 71 and Figure 72.

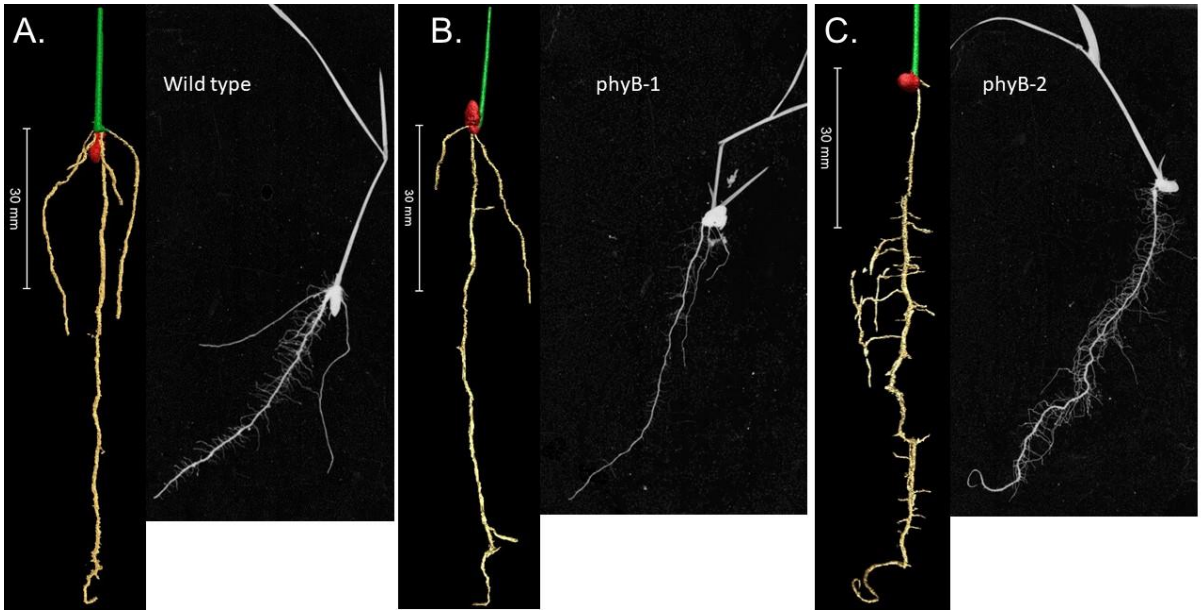

Figure 71 3D rendering of NCT images from selected Rice plants alongside a flatbed scanned image of the same root. A. Wild type, B. phyB-1, C. phyB-2 plants

The results shown in Figure 72 indicate that there were no significant differences between the wild type plants as compared to the two mutants imaged. The wild type, however, had the highest average root length, volume and surface area with the *phyB-1* mutant showing the lowest averages in the same parameters. The root thickness of the mutants was also similar with an average thickness of about 350μm. The *phyB-2* mutant had the lowest root thickness probably associated with it having more numerous lateral roots as indicated in Figure 72C. The results we obtained in this experiment are similar to the results from both X-Ray CT as well as destructive root sampling with the wild type often showing a marginal improvement in RSA although often not significantly different to those from the wild type.

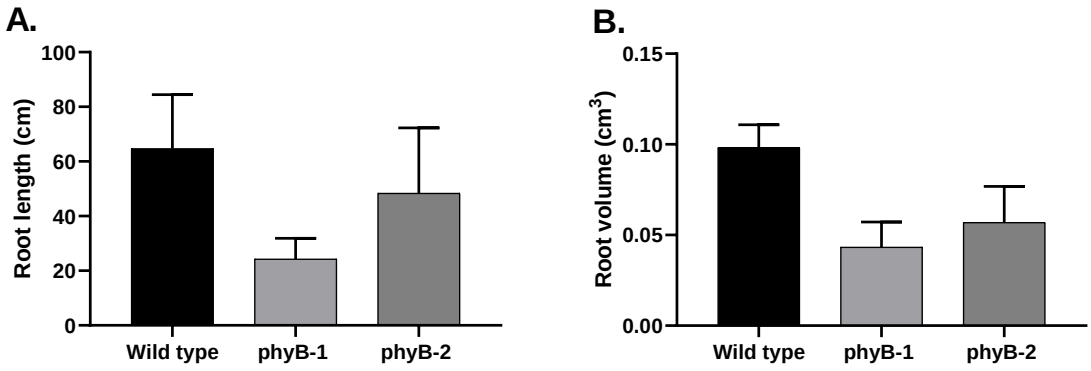

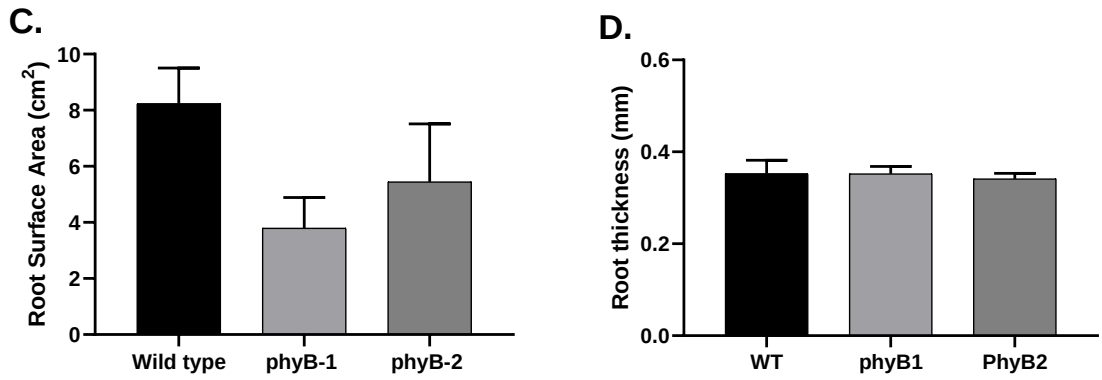

Figure 72 RSA properties of Rice plant lines scanned using NCT. A. Root length, B. Root volume, C. Root surface area, D. Root thickness(n=3). Error bars indicate SEM. One-Way ANOVA test was run with post-hoc Bonferroni test

5.4.3 Performance of Rice RSA under variable moisture conditions

As the practice of growing Rice standing water (puddling) is one of the reasons why Rice uses a large amount of water for its cultivation. Growing Rice plants in dryland conditions could result in a significant saving of valuable water resources. In this section I explore the possibility of growing my different mutant lines in dryland conditions, comparing them to plants grown in fully saturated conditions.

In this experiment, due to limitations of space, I used only the *phyB-2* mutant which often exhibited marginally improved root growth as compared to the *phyB-1* mutant which were grown alongside wild type plants. The Rice seeds for this experiment were germinated in distilled water and transplanted to growth pots 5 days after this when shoots and roots had germinated. These were grown in cylindrical PVC tubes with an internal diameter of 40mm and a height of 150mm filled with sandy loam soil to a bulk density of $1.2gcm^{-3}$. The plants were grown under 3 different moisture regimes, namely, saturated (submerged), 50% of WFP and 25% WFP. Saturated plants were grown in standing water 5cm deep and surface irrigated once every 2-3 days. The 25 and 50% WFP treatments were maintained by surface irrigation to the predetermined gravimetric moisture content corresponding to each watering regime. This was maintained for the entirety of this experiment. The plants were grown for 40DAS and subsequently harvested. Root properties from this growth were determined by flatbed scanning and subsequent WinRhizo® analysis. The results obtained from this experiment are given in Figure 73.

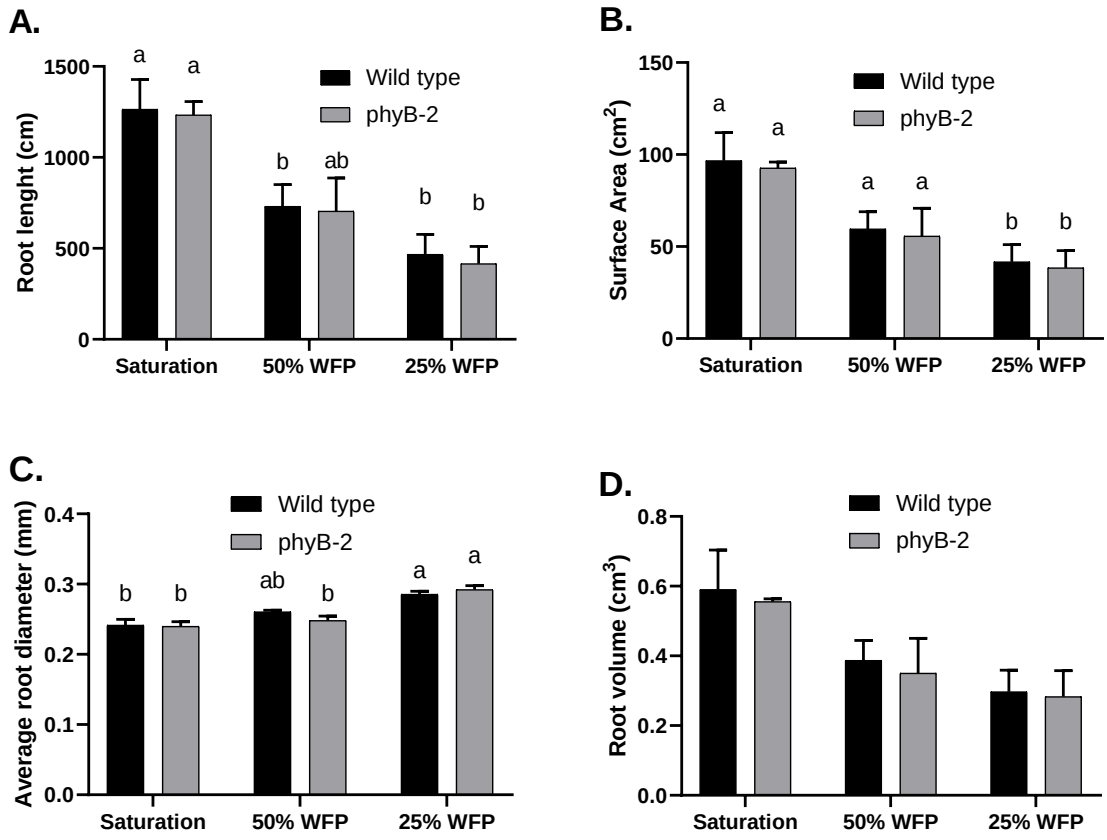

Figure 73 Root properties of Rice plants grown under different moisture regimes. A. Root length, B. Root Surface area, C. Root average diameter and D) Root Volume (n≥3). Error bars indicate SEM. One-Way ANOVA test was run with post-hoc Bonferroni test

As shown in Figure 73A, the different moisture regimes had a significant effect on root properties. There was a significant difference in root length between plants grown in saturated conditions as compared to those grown at 25% WFP in both genotypes with plants grown at 25% WFP having significantly lower root length in comparison. Wild type genotype grown at 50% WFPS also had a significantly lower root length as compared to the wild type plants grown at saturation. On the contrast *phyB-2* mutants grown at 50%WFPS did not show any significant difference as compared to *phyB-2* plants grown at saturation. There was no significant difference between plants grown at 50% and 25% WFP in both mutants although a generally a there was a general reduction in root length in the drier treatment.

In terms of root surface area, as shown in Figure 73B, there was a significant difference between the plants grown at saturation as compared to those grown at 25% WFP similar to what was observed with root length in both genotypes. There was however no difference between the root surface area of plants grown at 50% of WFP as compared to the saturated treatment although a general reduction in root surface area was observed. There was also no significant difference between the plants grown under the 25% and 50% WFP treatments. Similar to root length

however there was also a general reduction in root surface area with reduced soil moisture despite the differences not being significant.

Average root thickness (Figure 73C) did not follow a similar trend to root length and surface area with plants grown at 25% WFP showing the highest root thickness. There was a significant difference in root thickness between plants grown under saturated conditions and those grown at 25% WFP in both genotypes. There was also a significant difference between plants grown at 50% WFP as compared to those grown at 25% WFP of the *phyB-2* genotype whilst, no statistically significant difference was observed in the wild type plants. There was no significant difference as well between plants grown at saturation as compared to plants grown at 50%WFP.

Lastly in terms of root volume (Figure 73D) although a similar trend to root length and surface area was evident, my results did not show any statistically significant difference between all the 3 water treatments in both genotypes. The root volume of the saturated plants of both genotypes was however higher as compared to the other treatments with plants grown under the 25% WFP having the lowest average root volume. In terms of differences between the two genotypes, there was no significant difference between them under all the treatments although similar to many of my experiments, the wild type plants had marginally higher RSA properties.

5.5 The effects of improved WUE in Rice plants on soil structure

In this section, I look at how the growth of Rice plants of the different genotypes with variable WUE may affect soil structure as inferred by soil aggregate stability tests. The specific research question I investigated in these experiments is as follows;

Main question:

- How does the growth of plants with altered WUE affect soil structure of a sandy loam soil under either dryland or wetland irrigation?

To answer the research question under investigation, rice plants were grown in PVC tubes similar to those described in Section 5.3.1 filled with a sandy loam soil packed to a bulk density of 1.2 g cm^{-3}. Single seeds were sown directly into the soil and for the different treatments, the plants were initially kept in soils at gravimetrically determined field capacity for an initial establishment period of 10 days by watering every 2-3 days. After this, the two different soil moisture regimes being implemented up until the end of the experiment. In the dryland irrigation treatment, the rice plants were kept at 50% of WFP by surface irrigating every 2-3 days during the growth of rice plants. On the other hand, the wetland treatment was achieved by growing the rice plants in standing water and ensuring saturation by surface irrigation every 2-3 days for the duration of the experiment.

Soil was sampled at 150 DAS for each of the different treatments then stored at 4°C up until aggregate stability tests were done. The results I obtained are given in Figure 74.

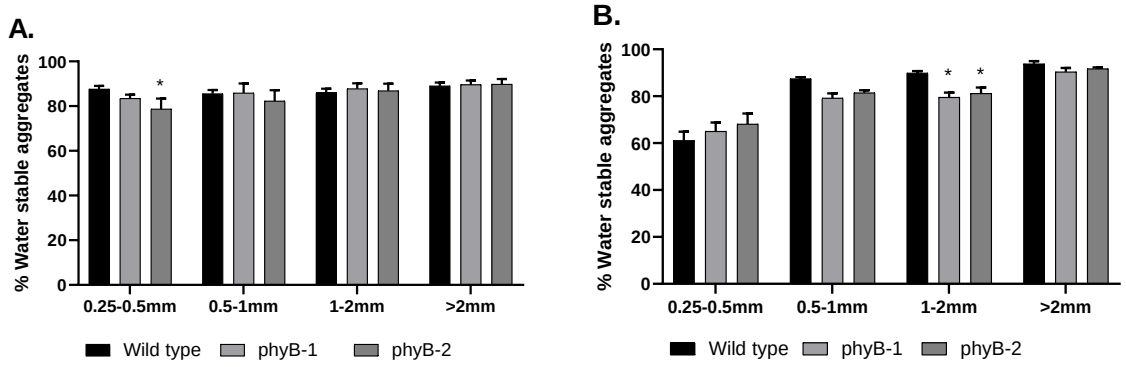

Figure 74 Aggregate stability tests after the growth of Rice plants A. Dryland irrigated Rice and B. Wetland irrigated Rice. Error bars indicate SEM. Symbols indicate significant difference as compared to the wild type; Two-Way ANOVA test with post-hoc Bonferroni test, (*=≤0.05)

The results from the aggregate stability tests in dryland irrigated Rice (Figure 74A) show that the *phyB-2* mutant had significantly reduced aggregate stability in the 0.25-0.5mm aggregates as compared to the wild type plants. There was no significant difference between the aggregate stability of all the other aggregates under dryland watering for each of the different plant lines that were grown. The stability of aggregates of all sizes under investigation was also relatively similar under dryland irrigation, averaging around 80% water-stable aggregates per sample.

Under wetland irrigation, on the other hand, there was a significant reduction in the stability of 1-2mm aggregates of both mutant plants as compared to the wild type plants. There was also a notable reduction in the stability of aggregates of the 0.5-1 mm and >2mm grown under the two mutants as compared to the wild type plants however, these differences were not statistically significant. A notable reduction in aggregate stability of the 0.25-0.5mm aggregate class was also seen under wetland maintained soils as compared dryland irrigated soils in all the plant lines grown in this experiment.

5.6 Discussion

5.6.1 WUE in Phytochrome mutants

This study investigated possible improvements in WUE among seven different phytochrome mutant plants with the aim of identifying WUE mutant plants for use in answering my overarching research questions. The findings from my screening experiments indicated that alterations in the light-sensing phytochrome genes (*phyA, phyB* and *phyC*) may have an effect on WUE in Rice plants as there was a general trend suggesting improvement in WUE in all the phytochrome mutants grown as compared to wild type plants as determined by the Δ measurements. Of major interest

to my overall experiments, however, were the two phyB mutants (*phyB-1* and *phyB-2*) which showed a significant improvement in WUE as compared to wild type plants. My results support the hypothesis that phyB improves plant productivity at the expense of WUE as suggested by Boccalandro *et al.*, (2009) who showed a reduction in WUE when phyB was overexpressed in arabidopsis plants. This was however contrary to the findings of Liu *et al.*, (2012) who, using similar Rice mutants observed a reduction in WUE as estimated by gaseous exchange measurements in the fourth leaf of *phyB-1* plants.

Further investigations into the growth characteristics of the *phyB* mutants also showed a significant reduction in transpiration of *phyB* mutants as compared to wild type plants over a 150 day growth period with the *phyB-1* showing the lowest transpiration as compared to the *phyB-2* mutant. Interestingly, however, the *phyB-2* mutant only showed reduced transpiration as compared to wild type plants 20 days after the onset of flowering which may have suggested this was the beginning of senescence as mutant plants flowered much earlier than wild type plants. My findings are similar to the findings of Liu *et al.* (2012) who also reported a reduction in rice transpiration of phyB mutant plants as compared to wild type plants.

In terms of biomass production, there was a significant reduction in phyB root biomass of both mutants 150 DAS with phyB mutants having as low as 50% of the root biomass recorded for wild type plants. This is contrary to what was seen by Liu *et al.*, (2012) who concluded that there were no significant differences between the root biomass of wild type and phyB mutants at the 6 leaf stage of growth. The differences I observed could have been due to the late flowering of the wild type plants in my experiment which may have resulted in increased assimilate allocation to root growth as reproductive growth affects plant allocation of resources, often sacrificing biomass production for reproductive growth (flowering). Another explanation for this may also be that some of the roots in phyB mutants could have initiated senescence and died off due to plant maturity thus hampering the washing of roots from soil. In terms of overall biomass production however, there was a significant difference in biomass production of the *phyB-2* mutant plant as compared to wild type plants. This was despite the nearly 50% reduction in root biomass production in this mutant. This seems to have been made up by biomass from the grain production in the *phyB-2* mutant. The severely delayed flowering in wild type plants was surprising in this experiment as the critical flowering day for rice is 13.5 hrs of day length (Itoh *et al.* 2010, Osugi *et al.* 2011). In further trials (results not shown in this thesis) even after reducing the day length to 8 hours, the wild type plants still showed severely delayed flower initiation under my conditions. This suggested other factors affecting flowering other than day length alone.

To investigate what characteristic gives rise to the improvement in WUE of the two phyB mutant plants, I looked at the stomatal characteristics of the different mutant lines in comparison to wild type plants. My results did not reveal any significant changes in stomatal density or stomatal distribution patterns between the mutants and the wild type plants. This suggested that differences in WUE may be due to other factors affecting plant growth. My findings were contrary to those found in other studies that report significant reductions in stomatal density in rice *phyB* mutants (Liu *et al.* 2012). This was also different from findings in arabidopsis where *phyB* mutants have also been shown to exhibit reduced stomatal density (Boccalandro *et al.* 2009, Casson *et al.* 2009). Liu *et al.* (2012) suggest that *phyB* mutants in rice may have reduced stomatal length, leaf size and chlorophyll however this was not determined in this study. Regardless, if this were the case, then this would result in a reduction in total pore area in the *phyB* mutants, which could then account for the improved WUE.

5.6.2 Effect of improved WUE on root architecture

In terms of the effect on the mutation on RSA, my results did not show any significant changes in RSA in the mutant plants as compared to the wild type. However, there was a distinct trend in the reduction in RSA in both mutants which was nearly universal in all my experiments. This suggests that RSA in *phyB* mutants may be affected to some degree. This is contrary to the findings by (Liu *et al.* 2012) who did not find any significant differences in root growth in the same mutants that I studied albeit in younger plants. The non-invasive methods of imaging rice plants had varying degrees of success with NR not producing satisfactory results as the full rice RSA could not be visualised. Rice roots were even fainter than wheat (Chapter 4) roots despite having a similar thickness. I hypothesized that the faint nature of rice roots in NR experiments was partially due to the aerenchyma characteristic of rice plants that resulted in a reduced total amount of water in rice roots as compared to wheat thus preventing effective imaging of rice roots. My results are contrary to what was observed by Bois and Couchat (1983) who observed a significant fraction of roots grown in soil using NR. NCT produced better results in comparison to NR imagery. This was as expected because NCT combines several different radiographic projections into a single 3D image thus improving root-soil contrast. In terms of non-invasive imaging, a similar trend in the RSA patterns was this also compared well with the invasive measurements being shown even when plants of the different plant lines are still in the earlier stages of growth. Results from X-Ray CT scanning showed in 3D, a reduction in the nodal root growth of *phyB-1* plants which may be because of reduced RSA in this mutant. The *phyB-2* mutant and wild type plants had similar RSA however WT plants had increased root elongation in a downward trajectory as compared to phyB plants.

5.6.3 Impact of soil moisture regime

The experiments in which Nipponbare rice was grown under upland conditions showed that this variety does not perform as well in upland and conditions in comparison to their more adapted lowland wetland conditions. Under water-limited conditions, both wild type and *phyB-2* mutant showed a reducing trend in terms of RSA with a significant difference between plants grown at 25% of WFP and saturation. The differences were less pronounced at 50% WFP however the reduction in root growth was still evident. My results are broadly similar to those found by Matsuo and Mochizuki, (2009) also using the Nipponbare variety. Matsuo and Mochizuki, (2009) who showed a more than 50% reduction in grain and biomass yield in their experiments, which they hypothesised could be attributed to changes in root activity and morphology. Kato, Kamoshita and Yamagishi, (2006) also found similar but less severe reductions in Nipponbare rice variety yields in dryland conditions. This was, however, reduced in high rainfall seasons. An unexpected reduction in root thickness under saturated conditions was found in my results. This may possibly have been as a result of reduced resistance by the roots when penetrating soil it has been shown that roots increase their radial expansion when encountering soil aggregates of high resistance (Whiteley *et al.* 1982b, Hewitt and Dexter 1984).

5.6.4 Effects of WUE on soil structure

Results from the aggregate stability tests revealed that the rice mutants to some degree reduced soil structural stability as compared to wild type plants with *phyB-2* plants showing a reduction in aggregate stability in unsaturated conditions. This tending towards reduction in aggregate stability among the mutants may be as a result of the reduced biomass and smaller RSA of mutant plants which may affect the aggregate stability of soil. These differences were pronounced especially in plants grown in wetland conditions as these showed a significant reduction in aggregate stability as compared to wild type plants in two different aggregate size classes. A possible explanation of the reduced aggregate stability is the reduced root thickness under wetland conditions which may result in better penetration into soil aggregates thus weaken the aggregates.

5.6.5 Conclusion and future work

In conclusion, there is reasonable evidence suggesting that these mutations could have an effect on RSA. The trends I observed consistently show similar patterns of RSA in the different plants, though this may indicate a reduction in RSA of mutant plants that I could not pick up in my test. Further experiments with even more replicates may be needed to find out if indeed there is no change to RSA after mutations of the *PHYB* gene in rice. Improved WUE, in this case, led to a reduction in soil structural stability of several aggregates suggesting that improving WUE in this

way may compromise soil structure to some degree. This may, however, be of little significance as rice plants are often grown in paddy fields with inherently low soil hydraulic conductivity characteristic of soils of poor aggregate stability. Further research may be required to investigate the precise mechanism that causes the changes in aggregate stability when rice plants are grown in saturated conditions

VI General discussion and conclusions

The overall aim of this study was to investigate the impact of genetically altering plant WUE on the RSA and soil structural stability. To address this aim, plants of three different species were studied, namely Arabidopsis, wheat and rice. The key research objective and questions that I aimed to answer in fulfilment of this overarching aim for all the species grown were:

a) Identify plant genotypes that show significantly altered WUE as compared to the wild type plants.
b) How do physiological properties of the identified mutants compare to that of the wild type plants?
c) How does the alteration in WUE of the mutant plants affect their RSA?
d) How does the soil structural stability of a sandy loam soil respond to the growth of plants with altered WUE as compared to wild type plants?

6.1 Screening of mutants for improvement of WUE

I was able to identify several different mutants that showed significantly altered WUE in all the different species studied. These mutants had previously been shown to exhibit altered WUE and my experiments confirmed that this was the case in my conditions (Liu *et al.* 2012, Franks *et al.* 2015, Dunn *et al.* 2019). In the selected wheat mutant line (TaEPF1OX1) however, there was no significant difference in iWUE despite an increase in WUE_B. For Arabidopsis (Chapter 3) and wheat (Chapter 4), mutants of the EPF family (*EPF1* and *EPF2*) of genes that control stomatal development were selected as they exhibited the significant improvements in WUE required to address the overall aim of this study. On the other hand, rice (Chapter 5) mutants with alterations in the light-sensing gene *PHYB* were found to exhibit altered WUE and were carried forward for further experimentation. This process is summarised in the schematic diagram in figure 75.

Some of the mutants that were hypothesised to exhibit WUE in initial trials were found not to be WUE under the conditions employed. An example of this was in Arabidopsis where the *phyB-9* mutant which has been shown to have improved WUE in some studies but only showed marginal improvements in WUE in this study (Boccalandro *et al.* 2009, Casson *et al.* 2009, Brown 2018). This may have been due to the lower irradiances used in my experiments as well as shorter photoperiods employed as compared to the studies showing improved WUE in *phyB* mutants. The role of stomata in improving WUE as has been shown in many previous studies was highlighted in my results and as most mutants with reduced SD are valuable tools that can be used to improve

WUE. This was, however, not the case with PHYB mutants as they did not have altered SD. I speculate WUE measurements could have been due to reduced conductance as proposed by González *et al.* (2012) however further investigations are required to clarify this.

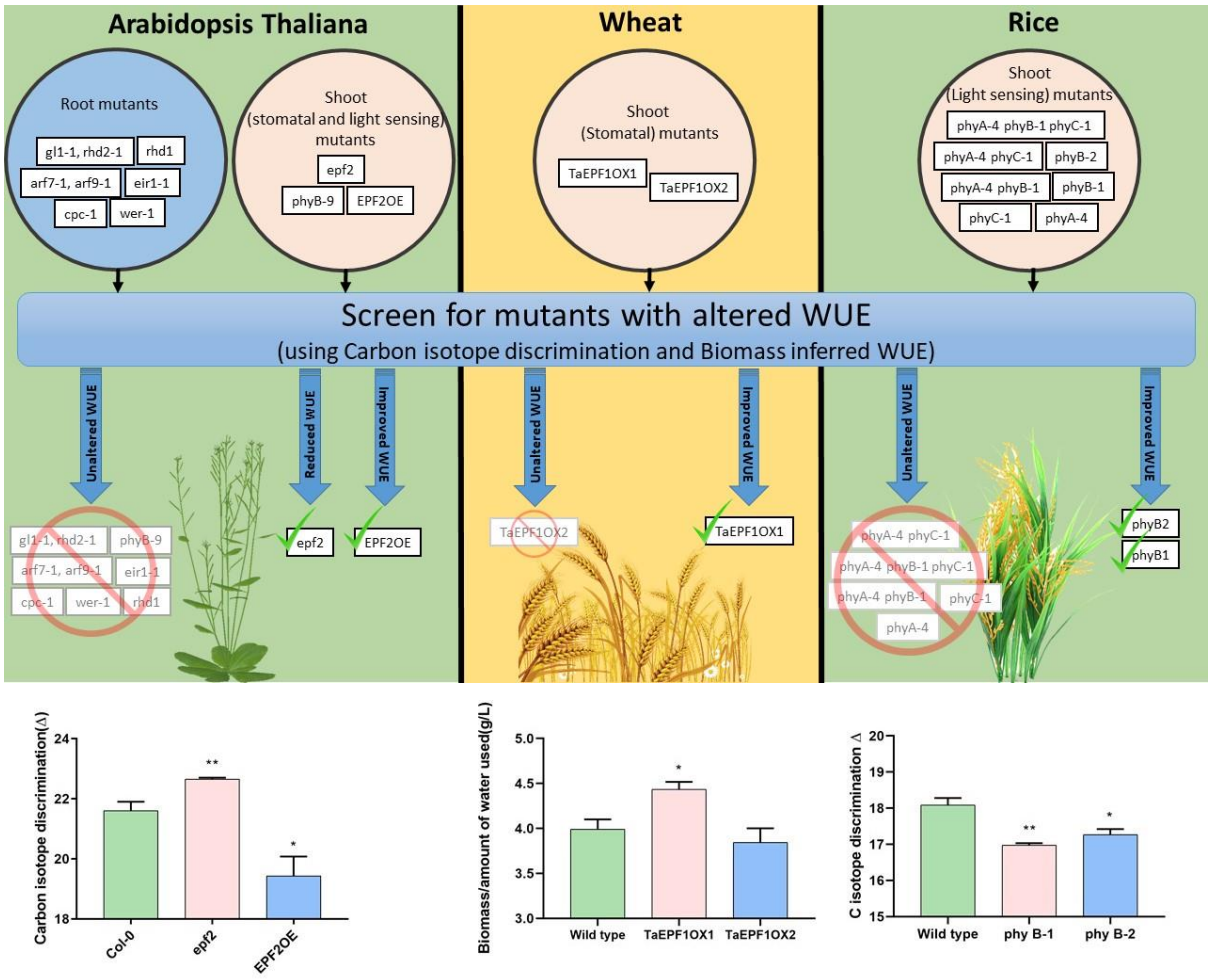

Figure 75 A schematic summary of the mutant plant screening for alteration of WUE in the different species used in this thesis. In the upper panel, the green ticks indicate varieties that displayed the required improved WUE (and for *Arabidopsis thaliana* epf2 a reduced WUE). In the lower plots evidence of these WUE alteration are replotted from Figures 23A, 43E and 65F respectively.

6.2 Physiological properties of WUE plants

The WUE plants identified in the initial screening experiments were then grown for characterisation of their physiological properties and yield potential. For Arabidopsis (Chapter 3) there was no significant difference in the root and shoot biomass production between the mutant and the wild type plants whilst stomatal density and consequently transpiration was significantly reduced for the WUE mutant plants resulting in an increase in WUE_B. In wheat WUE mutant

plants (Chapter 4), no significant differences were found in terms of total and grain biomass production between one of the WUE (TaEPF1OX1) mutant lines and the wild type whilst on the other hand total and grain biomass production was significantly reduced in the second mutant (TaEPF1OX2). Further analysis of some of the leaves of the TaEPF1OX2 mutant revealed an abnormality in the mutant which may have caused the reduction in biomass production. In terms of SD, both wheat mutants showed significantly reduced SD which was assumed to have led to a reduction in transpiration as compared to wild type plants.

In terms of rice plants (Chapter 5), the WUE mutant plants showed significantly reduced root biomass production as compared to wild type plants, however, both mutant plants were able to set seed whilst wild type plants showed severely delayed flowering. This delay in flowering of the WT plants may be linked to nitrogen or phosphorus availability since the growth regime did not include any fertiliser treatments; as such this may indicate that rice *phyB* mutants have enhanced nutrient use efficiency as well as WUE. The total biomass of one of the mutants *phyB-2* was significantly higher than that of wild type plants. In terms of transpiration, both *phyB* mutants exhibited reduced transpiration rates as compared to wild type plants.

6.3 Impact of WUE on RSA

Root system architecture comparison in Arabidopsis (Chapter 3) indicated that the wild type plants had larger RSA as compared to both the WUE and less WUE mutant under both WW and IW conditions. This seems to suggest that alteration in the EP2 gene may have a negative impact on root growth in arabidopsis plants contrary to what has been shown by others in literature (Hepworth *et al.* 2016). In wheat plants (Chapter 4), there was no significant difference in the RSA of the WUE mutant line as compared to the wild type plants at different time points during their growth. This seemed to suggest that alteration in the EPF1 gene did not seem to affect root growth for the mutant lines studied. For rice plants (Chapter 5) similarly, no significant differences were observed between the mutant plants and the wild type plants however there was evidence to suggest that the WUE rice mutants had reduced root growth from non-invasive root scans. This was especially true after an extended growth period (150 days) as wild type plants showed almost double the root biomass of the mutant plants. This could have been due to the late maturity of the wild type plants as vegetative growth could have continued for a longer time. In general, however, in the different species under investigation, there was at least a marginal reduction in RSA of WUE plants for all the three genotypes of mutants used in the different species. This could impact on the ability of the potential productivity of the WUE plants used in this study as larger RSA are

often more desirable for resources acquisition, especially in hostile environments (Lynch 1995, Smith and De Smet 2012). Furthermore, this shows that it is essential to examine RSA properties of WUE plants more closely before adoption to ensure that they are competitive enough to cope with different environments.

6.4 Impact of WUE on soil structure

In terms of soil structural evolution, in Arabidopsis plants (Chapter 3), there were no significant differences in the stability of aggregates of the different plant lines when both a bulk soil and specific soil aggregate were used. This suggested that the growth of arabidopsis did not have a significant effect on soil structural stability in sandy loam soils. Similarly, in wheat plant lines (Chapter 4) there were no significant differences in soil structural stability in the different mutant lines however aggregate stability was seen to have increased over time in all the plant lines probably due to an increase in the root biomass of the plants. In terms of rice (Chapter 5) plants there were also no significant differences between the mutant and the wild type plants in both dryland and wetland grown rice plants. There was however a general reduction in aggregate stability under the wetland treatment as compared to the dryland grown plants possibly indicating that continuous saturation in rice fields could have an impact on aggregate stability. In general, however, this research did not find any conclusive evidence suggesting that the use of WUE plants in a sandy loam soil compromises soil structural integrity as inferred to by aggregate stability testing.

6.5 Limitations of study

As scientific investigations are never perfect, my study had its own set of limitations arising from factors that were out of my control. Firstly, one of the initial limitations of this study stemmed from the fact that WUE is not a static trait that can be investigated in isolation from other factors. The mutants that were used although having been shown to have altered WUE may also have as yet unexplored features that affect root architecture and consequently soil structure that may be unrelated to WUE. For instance, one of the wheat mutants (TaEPF1OX2) had an unexpected leaf phenotype which reduced its biomass production and consequently affected its WUE. This was despite the mutant having reduced stomatal density which has been shown to result in improvements in WUE. WUE is also controlled by a variety of different factors that were not controlled for in this study and were assumed to be constant (e.g. variations in atmospheric CO_2 concentration and light intensity) which could have had an impact on WUE as it is not a static plant property.

The limited genetic resources at my disposal meant it was not possible to study mutant plants with alterations in the same gene (or gene homologues) for each of the different species (having used EPF2 in Arabidopsis, EPF1 in Wheat and PHYB in rice). As a result different mechanism for the improvement of WUE were applied, for instance, PHYB mutants in rice did not have reduced SD phenotype as the EPF mutants and thus improvements in WUE were achieved via other mechanisms that were not determined in this study. This limits the generalisation of conclusions that can be drawn from these experiments. Further research in the development of similar EPF mutant lines is thus needed to that provide a better comparison for the mutants used in this experiment. Similarly, it would also be interesting to investigate PHYB mutants of wheat such as those initially trialled (without success) in order to get a better understanding of the underlying processes affecting WUE in different plant species.

Another limitation of my study was that the pots used for my experiments were restricted to about 375cm^3 for wheat and rice and 120cm^3 for Arabidopsis. This limitation came about due to the limited growth space which restricted the number of and size of plant pots I could use for experimentation. This limitation had an effect on root growth as plants were often pot bond by the end of experiments lasting more than a month thus potentially limiting conclusions that can be made from these experiments (Haynes and Beare 1997). An alternative would have been to grow the plants in the field however this was not possible due to the strict UK regulations that restrict the growth of transgenic plants in the field (Royal Society 2016). These experiments could, however, be potentially repeated in greenhouse conditions using much larger pots that enable the different plants to fully grow their roots in an unconstritcted environment allowing for better correlation with field conditions.

In terms of soil structural assessment, one of the major challenges I faced initially was the lack of consistency that arose from wet sieving by hand. The results I obtained from experiments carried out using this method were highly variable and thus a new wet sieving machine was designed and built to improve the replicability of my findings. This machine did indeed reduce the variability in my measurements whilst allowing for the increase in throughput of my study. Soil structural assessments tests are often done after interventions lasting over many seasons usually assessing the effect of either different tillage practices or plant species on soil structure. In this study, however, as time was limited, plants were only grown for single growth cycles before the assessment of soil structural stability was done. This may have limited the detectability of changes that may result due to the growth of different mutant plants. Assessments of how mutants of a

similar species affect soil structure is also relatively new and thus the available test may not be sensitive enough to differentiate between them. This was even more pertinent to a crop such as Arabidopsis which has a small root system that may reduce its effect on soil structural development. For Arabidopsis specifically, detectable changes in soil aggregate stability appeared only when aggregates of a particular size (0.5-1mm) were used as opposed to the use of bulk soil. This approach is similar to those used by (Materechera *et al.* 1992, 1994) to investigate the impacts of different plants on aggregate stability. However, it may be a method that's too simplistic as plants in nature grow in a wide variety of aggregates.

Finally, even though non-invasive imaging could reveal great detail of my mutants in 3D, as the replicates I could do were limited due to budgetary constraints, deriving meaningful scientific conclusions from my different non-invasive measurements was difficult due to the few plants I scanned. They did, however, give an insight into possible causes of variation in root growth in situ confirming measurements derived from ex-situ methods. The relatively low number of replicates from non-invasive imaging techniques such as the ones used in this study (X-ray and NCT) is not unique to my study. Morris *et al.* (2017) in their review on RSA studies noted that at present non-invasive techniques are currently too expensive and low throughput thus limiting inferences that can be made into RSA by them. Painstaking segmentation also limits the speed at which RSA results can be obtained as the available automated segmentation techniques are not optimised for every soil-plant system. It is thus essential to either develop cheaper non-invasive soil imaging techniques or use non-invasive imaging techniques along with confirmatory invasive imaging (as was employed in this study) to get more quantitative information about RSA traits. Machine learning and artificial intelligence could also be used to speed up segmentation of non-invasive images.

6.6 Unexpected and novel findings from my research

Non-invasive imaging of Arabidopsis roots (Chapter 3) growing in soil is relatively rare and thus this study added to the body of knowledge regarding in-situ Arabidopsis imaging. Relatively good quality scans of Arabidopsis plants were obtained showing comparatively more detail on root branching as compared to other studies e.g. (Tracy *et al.* 2010, Lucas *et al.* 2011). My study also produced evidence that demonstrated for the first time that the RSA of Arabidopsis plants can successfully be visualised in situ using NCT. This has the potential for allowing increased RSA studies of the model plant enabling investigations of more realistic, real-world experiments in situ. This is important as RSA studies in Arabidopsis are often exclusively done in transparent/soilless

media that react differently to soil. To the best of my knowledge, this was also the first-time aggregate stability has ever been measured after the growth of Arabidopsis plants. This was interesting as Arabidopsis is a weed plant which naturally grows in rocky and sandy areas and thus it may contribute to pedogenesis in young terrains.

My investigation of wheat RSA (Chapter 4) using NCT were also to the best of my knowledge, the first of their kind as NCT has only been used to show the RSA of a few plants e.g. lupines. Wheat root images were of a relatively good quality and segmentation was relatively easier as compared to X-Ray wheat scans due to the clear contrast between soil and roots. As NCT also has the ability to estimate relative water content, I was also able to show unexpected variations in root water content along the length of my wheat plants. For example, there were prominent reductions in root water content in air spaces between large aggregates. The TaEPF1OX2 as previously discussed also showed an unexpected leaf abnormality that appeared about 50DAS which had not previously been described in previous research using EPF1 mutants in wheat (Dunn *et al.* 2019). Further investigations may be needed to find out the origin of this abnormality investigating how this affects these mutant plants.

The rice *phyb* mutant (Chapter 5) plants grown in this study did not show the reductions in stomatal density as observed by Liu *et al.* (2012) using the same mutants. This is despite the rice plants having improved WUE and reduced transpiration rates in comparison to wild type plants. This points to an as yet unexplored mechanism of improvement of WUE in rice plants. Further investigations may be required to understand how the improvement in WUE came to being. Wild type plants used in this study had an extended period of vegetative growth and did not flower for at least 150 DAS even under a short-day photoperiod. This may require further investigation to find out the genesis of this problem. Investigations into how the rice lines (wild type and phyB-1) respond to growth in wetland, dryland and under limited moisture showed that generally, the wetland Nipponbare variety plants had relatively reduced growth rates in soils, not under saturation. Finally, rice roots proved difficult to image using NR as they comparatively seemed to have reduced root moisture as compared to other plants such as wheat. I hypothesized that this may be due to the aerenchyma within the roots that reduces contrast between the soil and rice roots. NCT of rice plants was on the other hand more successful as compared to NI despite the rice root still not being as distinct as did wheat plants.

6.7 Conclusions

The following conclusions can be made from the research presented in this thesis:

- This research did not find conclusive evidence suggesting that altering WUE by overexpressing the EPF2 gene in Arabidopsis leads to significant alterations in their RSA as well as the soil structural stability of a sandy loam soils.
- Non-invasive X-ray CT can successfully be used to study the RSA of Arabidopsis plants in great detail when grown in an aggregated sandy loam soil.
- Enhancing WUE by manipulation of the TaEPF1 gene in rice did not significantly affect the plant RSA and the structure of a sandy loam soil.
- I demonstrated for the first time that NCT could be used successfully to measure the wheat RSA in an aggregated sandy loam soil with moderately high amounts of soil organic matter.
- There was also reasonable evidence suggesting that improving WUE by altering the *PHYB* gene in rice could have a negative impact on RSA of mutant plants when grown in a sandy loam soil.
- PHYB rice mutant plants with improved WUE also seemed to reduce the stability of 1-2mm soil aggregates when grown under saturated conditions.

6.8 Future research

As improving WUE is a key priority in the 21st century, future work should be dedicated to further the understanding of WUE plants as they will play a key role in reducing the water scarcity problems especially in water-limited environments. Looking at the plants I studied, as the mechanisms that resulted in the attainment of improved WUE were different, broad inferences and comparisons between plants as was hoped for at the beginning of these experiments was not possible. As such it is necessary for the further development of similar transgenic plant lines with alteration in the same gene (e.g. EPF2 in Arabidopsis) in all the plant species I looked at. This would help piece together a more complete picture of how specific gene alterations could affect root and soil properties. Interestingly towards the end of my research work, transgenic rice plants (OsEPF1 plant lines) that were similar to the TaEPF1 plant lines I used in wheat were developed as detailed by Caine *et al.* (2019). These plant lines are ideal candidates for use in future experiments as they were similar to the ones in this study and thus would enable better inferences into the role of the EPF1 overexpression on root and soil properties in general.

Time is an essential element in understanding the development of soil structure (Abiven *et al.* 2009). As hypothesised by Monnier (1965) changes in soil structure occur over different times scales ranging from weeks, months and even years and as such to have a true idea of the long-term impacts of improved WUE on soil structure it would require a more extended period of time as opposed to the limited time used in this experiment. Although my study provided useful information on the short-term consequences of altered WUE, this was just a snippet of what could be expected to be the case over the long term. As such it is necessary to have longer running (possibly over multiple years) field trials in the future that would assess how soil structure evolves in fields where WUE plants are grown. Such tests could also be done in soils of different textures thus also allowing for wider conclusions to be made regardless of the kinds of soil the plants are grown in.

Assessing changes in soil structure as induced by different plants using purely aggregate testing although relatively easy to do may miss some of the intricate dynamics that affect the plant-soil system. As a result of this, further research encompassing the use of high-resolution imaging such as XRSI could be useful to determine changes that may occur in the rhizosphere non-invasively. This has already been demonstrated by (Koebernick *et al.* 2017) and as such, these methodologies could be interesting to use in determining the soil structural changes as a result of altered WUE. In prospective studies collaboration with computer programmers could also be necessary in order to develop faster and more robust segmentation techniques. One of the methods I could suggest especially for rice roots with hollow aerenchyma would be to design algorithms that could identify 'eye looking' hollow tubes recognising them as root and thus enabling improved segmentation (Figure 76). This would allow for faster and less subjective root segmentation. Automated instead of intuitive image processing could also help speed up the process of getting useful information from different scans.

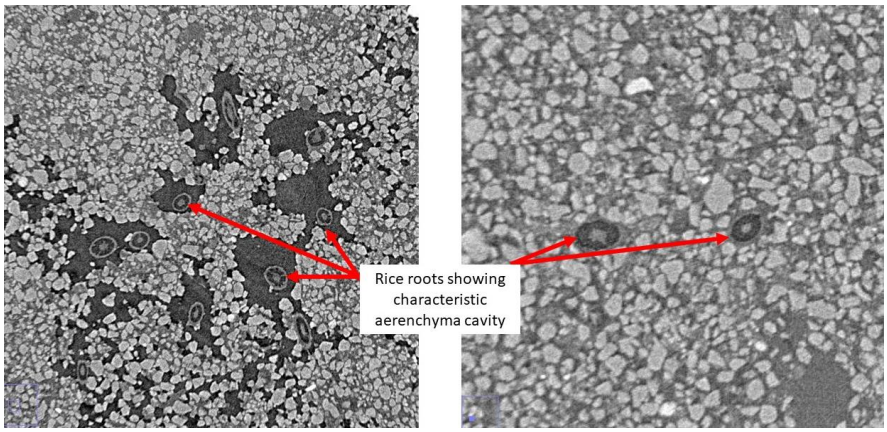

Figure 76: Rice XRSI images showing the characteristic aerenchyma that could be used for improved segmentation

References

Abiven, S., Menasseri, S., and Chenu, C., 2009. The effects of organic inputs over time on soil aggregate stability - A literature analysis. *Soil Biology and Biochemistry*, 41 (1), 1–12.

Abogadallah, G.M., Nada, R.M., Malinowski, R., and Quick, P., 2011. Overexpression of HARDY, an AP2/ERF gene from Arabidopsis, improves drought and salt tolerance by reducing transpiration and sodium uptake in transgenic Trifolium alexandrinum L. *Planta*, 233 (6), 1265–1276.

Agrawal, RP and Jhorar, B., 1987. Soil Aggregates and Growth of Wheat. *J. Agronomy & Crop Science*, 158, 160–163.

Agrawal, R.P., Mundra, M., and Jhorar, B.S., 1984. Seedbed tilth and nitrogen response of wheat. *Soil & Tillage Research*, 4, 25–34.

Ahmed, M.A., Kroener, E., Holz, M., Zarebanadkouki, M., and Carminati, A., 2014. Mucilage exudation facilitates root water uptake in dry soils. *Functional Plant Biology*, 41 (11), 1129–1137.

Ahmed, M.A., Zarebanadkouki, M., Ahmadi, K., Kroener, E., Kostka, S., Kaestner, A., and Carminati, A., 2017. Engineering Rhizosphere Hydraulics: Pathways to Improve Plant Adaptation to Drought. *Vadose Zone Journal*, 0 (0), 0.

Ahmed, M.A., Zarebanadkouki, M., Meunier, F., Javaux, M., Kaestner, A., and Carminati, A., 2018. Root type matters: Measurement of water uptake by seminal, crown, and lateral roots in maize. *Journal of Experimental Botany*, 69 (5), 1199–1206.

Ahmed, S., Klassen, T.N., Keyes, S., Daly, M., Jones, D.L., Mavrogordato, M., Sinclair, I., and Roose, T., 2016. Imaging the interaction of roots and phosphate fertiliser granules using 4D X-ray tomography. *Plant and Soil*, 401 (1–2), 125–134.

Aida, M., Vernoux, T., Furutani, M., Traas, J., and Tasaka, M., 2002. Roles of PIN-FORMED1 and MONOPTEROS in pattern formation of the apical region of the Arabidopsis embryo. *Development*, 129 (17), 3965–3974.

Alahmad, S., El Hassouni, K., Bassi, F.M., Dinglasan, E., Youssef, C., Quarry, G., Aksoy, A., Mazzucotelli, E., Juhász, A., Able, J.A., Christopher, J., Voss-Fels, K.P., and Hickey, L.T., 2019. A Major Root Architecture QTL Responding to Water Limitation in Durum Wheat. *Frontiers in Plant Science*, 10, 436.

Alberts, B., Johnson, A., Lewis, J., Raff, M., Roberts, K., and Walter, P., 2002. Studying Gene Expression and Function.

Alexander, K.G. and Miller, M.H., 1991. The effect of soil aggregate size on early growth and shoot-root ratio of maize (Zea mays L.). *Plant and Soil*, 138 (2), 189–194.

Alexandratos, N. and Bruinsma, J., 2003. World agriculture: towards 2015/2030: an FAO perspective. *Land Use Policy*, 20 (4), 375.

Amezketa, E., Singer, M.., and Le Bissonnais, Y., 1996. Testing a New procedure for measuring water-stable aggregation, 888–894.

Anderson, I.S., 2009. *Neutron Imaging and Applications*.

Anderson, W.B. and Kemper, W.D., 1964. Corn Growth as Affected by Aggregate Stability, Soil

Temperature, and Soil Moisture. *Agronomy Journal*, 56 (5), 1–4.

Angers, D.A. and Caron, J., 1998. Plant-induces changes in soil structure: Processes and feedbacks. *Biogeochemistry*.

AQUASTAT, 2014. FAO's Information System on Water and Agriculture [online]. Available from: http://www.fao.org/nr/water/aquastat/didyouknow/index3.stm [Accessed 22 Sep 2019].

Aravena, J.E., Berli, M., Menon, M., Ghezzehei, T.A., Mandava, A.K., Regentova, E.E., Pillai, N.S., Steude, J., Young, M.H., Nico, P.S., and Tyler, S.W., 2013. Synchrotron X-Ray Microtomography - New Means to Quantify Root Induced Changes of Rhizosphere Physical Properties. *Soil–Water–Root Processes: Advances in Tomography and Imaging. SSSA Special Publication 61*, sssaspecia (soilwaterrootpr), 39–68.

Ariani, A., Francini, A., Andreucci, A., and Sebastiani, L., 2016. Over-expression of AQUA1 in Populus alba Villafranca clone increases relative growth rate and water use efficiency, under Zn excess condition. *Plant cell reports*, 35 (2), 289–301.

Atkinson, J.A., Pound, M.P., Bennett, M.J., and Wells, D.M., 2019. Uncovering the hidden half of plants using new advances in root phenotyping. *Current Opinion in Biotechnology*, 55, 1–8.

Bačić, G. and Ratković, S., 1987. NMR studies of radial exchange and distribution of water in maize roots: The relevance of modelling of exchange kinetics. *Journal of Experimental Botany*, 38 (8), 1284–1297.

Bacon, M.A., 2004. *Water use efficiency in plant biology*. October.

Ball, B.C., Batey, T., and Munkholm, L.J., 2007. Field assessment of soil structural quality - a development of the Peerdklamp test. *Soil Use and Management*, 23 (4), 329–337.

Banavath, J.N., Chakradhar, T., Pandit, V., Konduru, S., Guduru, K.K., Akila, C.S., Podha, S., and Puli, C.O.R., 2018. Stress Inducible Overexpression of AtHDG11 Leads to Improved Drought and Salt Stress Tolerance in Peanut (Arachis hypogaea L.). *Frontiers in chemistry*, 6, 34.

Barker, R., Dawe, D., Tuong, T.P., Bhuiyan, S.I., and Guerra, L.C., 1999. The outlook for water resources in the year 2020 : challenges for research on water management in rice production. *Southeast Asia*, 1, 1–5.

Berardini, T.Z., Reiser, L., Li, D., Mezheritsky, Y., Muller, R., Strait, E., and Huala, E., 2015. The arabidopsis information resource: Making and mining the "gold standard" annotated reference plant genome. *genesis*, 53 (8), 474–485.

Berners-Lee, M., Kennelly, C., Watson, R., and Hewitt, C.N., 2018. Current global food production is sufficient to meet human nutritional needs in 2050 provided there is radical societal adaptation. *Elem Sci Anth*, 6 (1), 52.

Bertolino, L.T., Caine, R.S., and Gray, J.E., 2019. Impact of Stomatal Density and Morphology on Water-Use Efficiency in a Changing World. *Frontiers in Plant Science*, 10 (March), 225.

Bhagat, R., 2003. Management of soil physical properties of lowland puddled rice soil for sustainable food production. *Lecture given at the College on Soil Physics*, (March), 65–75.

Bhatnagar-Mathur, P., Devi, M.J., Vadez, V., and Sharma, K.K., 2009. Differential antioxidative responses in transgenic peanut bear no relationship to their superior transpiration efficiency

under drought stress. *Journal of plant physiology*, 166 (11), 1207–17.

Le Bissonnais, Y., 1996. Aggregate stability and assessment of soil crustability and erodibility: I. Theory and methodology. *European Journal of Soil Science*, 47 (4), 425–437.

Blankinship, J.C., Fonte, S.J., Six, J., and Schimel, J.P., 2016. Biotic versus abiotic controls on soil aggregate stability in a seasonally dry ecosystem. *Geoderma*, In review, 39–50.

Blilou, I., Xu, J., Wildwater, M., Willemsen, V., Paponov, I., Friml, J., Heidstra, R., Aida, M., Palme, K., and Scheres, B., 2005. The PIN auxin efflux facilitator network controls growth and patterning in Arabidopsis roots. *Nature*, 433 (7021), 39–44.

Blum, a., Munns, R., Passioura, J.B., Turner, N.C., Sharp, R.E., Boyer, J.S., Nguyen, H.T., Hsiao, T.C., Verma, D., and Hong, Z., 1996. Genetically Engineered Plants Resistant to Soil Drying and Salt Stress: How to Interpret Osmotic Relations? *Plant physiology*, 110 (4), 1051–1053.

Blum, A., 2005. Drought resistance, water-use efficiency, and yield potential—are they compatible, dissonant, or mutually exclusive? *Australian Journal of Agricultural Research*, 56 (11), 1159.

Blum, A., 2009. Effective use of water (EUW) and not water-use efficiency (WUE) is the target of crop yield improvement under drought stress. *Field Crops Research*, 112 (2–3), 119–123.

Blunk, S., Malik, A.H., de Heer, M.I., Ekblad, T., Bussell, J., Sparkes, D., Fredlund, K., Sturrock, C.J., and Mooney, S.J., 2017. Quantification of seed-soil contact of sugar beet (Beta vulgaris) using X-ray Computed Tomography. *Plant Methods*, 13 (1), 1–14.

Boccalandro, H.E., Rugnone, M.L., Moreno, J.E., Ploschuk, E.L., Serna, L., Yanovsky, M.J., and Casal, J.J., 2009. Phytochrome B enhances photosynthesis at the expense of water-use efficiency in Arabidopsis. *Plant physiology*, 150 (2), 1083–1092.

Bodner, G., Nakhforoosh, A., and Kaul, H.P., 2015. Management of crop water under drought: a review. *Agronomy for Sustainable Development*, 35 (2), 401–442.

Bois, J.F. and Couchat, P.H., 1983. Comparison of the Effects of Water Stress on the Root Systems of Two Cultivars of Upland Rice (Oryza satíva L .). *Annals of Botany*, 52, 479–487.

Bonsch, M., Popp, A., Biewald, A., Rolinski, S., Schmitz, C., Weindl, I., Stevanovic, M., H??gner, K., Heinke, J., Ostberg, S., Dietrich, J.P., Bodirsky, B., Lotze-Campen, H., and Humpen??der, F., 2015. Environmental flow provision: Implications for agricultural water and land-use at the global scale. *Global Environmental Change*, 30, 113–132.

Borland, A.M., Hartwell, J., Weston, D.J., Schlauch, K.A., Tschaplinski, T.J., Tuskan, G.A., Yang, X., and Cushman, J.C., 2014. Engineering crassulacean acid metabolism to improve water-use efficiency. *Trends in Plant Science*, 19 (5), 327–338.

Borlaug, N. and Dowswell, C., 2003. Feeding a world of ten billion people: a 21st century challenge. … *of the International Congress in the Wake* …, (May 2003), 3–23.

Bot, A.J., Nachtergaele, F.O., and Young, A., 2000. Land resource potential and constraints at regional and country levels. *World Soil Resources Reports*, 90, 1–114.

Boutraa, T., 2010. Improvement of Water Use Efficiency in Irrigated Agriculture: A Review. *Journal of Agronomy*, 9 (11), 1–8.

Brady, N.C. and Weil, R.R., 2017. *The nature and properties of soils*. 15th ed. Pearson.

Braunack, M.. and Dexter, A.., 1989. Soil Aggregation in the Seedbed: a Review. II. Effect of Aggregate Sizes on Plant Growth M.V. *Soil & Tillage Research,* 14, 281–298.

Briggs, L.J. and Shantz, H.L., 1913. The water requirements of plants I. *Bureau of Plant Industry Bulletin, USDA, Washington D.C*, 284.

Bronick, C.J. and Lal, R., 2005. Soil structure and management: A review. *Geoderma*, 124 (1–2), 3–22.

Brouwer, C. and Heibloem, M., 1986. Irrigation water needs. *Irrigation Water Management*, Vol. 102 (3), 1–40.

Brown, D.P., Pratum, T.K., Bledsoe, C., Ford, E.D., Cothern, J.S., and Perry, D., 1991. Noninvasive studies of conifer roots: nuclear magnetic resonance (NMR) imaging of Douglas-fir seedlings. *Canadian Journal of Forest Research*, 21, 1559–1566.

Brown, J.C., 2018. Photoreceptor regulation of plant responses to light and carbon dioxide. The University of Sheffield.

Brugière, N., Zhang, W., Xu, Q., Scolaro, E.J., Lu, C., Kahsay, R.Y., Kise, R., Trecker, L., Williams, R.W., Hakimi, S., Niu, X., Lafitte, R., and Habben, J.E., 2017. Overexpression of RING Domain E3 Ligase ZmXerico1 Confers Drought Tolerance through Regulation of ABA Homeostasis. *Plant physiology*, 175 (3), 1350–1369.

Burca, G., Kockelmann, W., James, J.A., and Fitzpatrick, M.E., 2013. Modelling of an imaging beamline at the ISIS pulsed neutron source. *Journal of Instrumentation*, 8 (10).

Burca, G., Nagella, S., Clark, T., Tasev, D., Rahman, I.A., Garwood, R.J., Spencer, A.R.T., Turner, M.J., and Kelleher, J.F., 2018. Exploring the potential of neutron imaging for life sciences on IMAT. *Journal of Microscopy*, 00 (0), 1–6.

Burr-Hersey, J.E., Mooney, S.J., Bengough, A.G., Mairhofer, S., and Ritz, K., 2017. Developmental morphology of cover crop species exhibit contrasting behaviour to changes in soil bulk density, revealed by X-ray computed tomography. *PLoS ONE*, 12 (7), 1–18.

Cailloux, M., 1972. Metabolism and the absorption of water by root hairs. *Canadian Journal of Botany*, 50 (3), 557–573.

Caine, R.S., Yin, X., Sloan, J., Harrison, E.L., Mohammed, U., Fulton, T., Biswal, A.K., Dionora, J., Chater, C.C., Coe, R.A., Bandyopadhyay, A., Murchie, E.H., Swarup, R., Quick, W.P., and Gray, J.E., 2019. Rice with reduced stomatal density conserves water and has improved drought tolerance under future climate conditions. *New Phytologist*, 221 (1), 371–384.

Cao, H.-X., Zhang, Z.-B., Xu, P., Chu, L.-Y., Shao, H.-B., Lu, Z.-H., and Liu, J.-H., 2007. Mutual physiological genetic mechanism of plant high water use efficiency and nutrition use efficiency. *Colloids and Surfaces B: Biointerfaces*, 57 (1), 1–7.

Carminati, A., Moradi, A.B., Vetterlein, D., Vontobel, P., Lehmann, E., Weller, U., Vogel, H.J., and Oswald, S.E., 2010. Dynamics of soil water content in the rhizosphere. *Plant and Soil*.

Carter, M.R. and Gregorich, E.G., 2006. *Soil Sampling and Methods of Analysis*. Measurement.

Cass, A., Gusli, S., and MacLeod, D.A., 1994. Sustainability of soil structure quality in rice paddy— soya-bean cropping systems in South Sulawesi, Indonesia. *Soil and Tillage Research*, 31 (4), 339–352.

Cassman, K.G., 1999. Ecological intensification of cereal production systems: yield potential, soil

quality, and precision agriculture. *Proceedings of the National Academy of Sciences of the United States of America*, 96 (11), 5952–9.

Casson, S.A., Franklin, K.A., Gray, J.E., Grierson, C.S., Whitelam, G.C., and Hetherington, A.M., 2009. phytochrome B and PIF4 Regulate Stomatal Development in Response to Light Quantity. *Current Biology*, 19 (3), 229–234.

Chaerle, L., Saibo, N., and Van Der Straeten, D., 2005. Tuning the pores: towards engineering plants for improved water use efficiency. *Trends in Biotechnology*, 23 (6), 308–315.

Chapman, H.D., 1965. Cation-exchange capacity 1. *Methods of soil analysis. Part 2. Chemical and microbiological properties*, (methodsofsoilanb), 891–901.

Chen, Y.-S., Lo, S.-F., Sun, P.-K., Lu, C.-A., Ho, T.-H.D., and Yu, S.-M., 2015. A late embryogenesis abundant protein HVA1 regulated by an inducible promoter enhances root growth and abiotic stress tolerance in rice without yield penalty. *Plant biotechnology journal*, 13 (1), 105–16.

Chen, Z., Ti, J. song, and Chen, F., 2017. Soil aggregates response to tillage and residue management in a double paddy rice soil of the Southern China. *Nutrient Cycling in Agroecosystems*, 109 (2), 103–114.

Clark, R.T., Famoso, A.N., Zhao, K., Shaff, J.E., Craft, E.J., Bustamante, C.D., Mccouch, S.R., Aneshansley, D.J., and Kochian, L. V., 2013. High-throughput two-dimensional root system phenotyping platform facilitates genetic analysis of root growth and development. *Plant, Cell and Environment*, 36 (2), 454–466.

Clough, S.J. and Bent, A.F., 1998. Floral dip: A simplified method for Agrobacterium-mediated transformation of Arabidopsis thaliana. *Plant Journal*, 16 (6), 735–743.

Colorado Wheat, 2013. Why is the Wheat Genome So Complicated? | Colorado Wheat [online]. Available from: https://coloradowheat.org/2013/11/why-is-the-wheat-genome-so-complicated/ [Accessed 12 Sep 2018].

Condon, a. G., Richards, R. a., and Farquhar, G.D., 1987. Carbon Isotope Discrimination is Positively Correlated with Grain Yield and Dry Matter Production in Field-Grown Wheat1. *Crop Science*, 27 (5), 996.

Condon, A.G., Richards, R.A., Rebetzke, G.J., and Farquhar, G.D., 2004. Breeding for high water-use efficiency. *Journal of Experimental Botany*, 55 (407), 2447–2460.

Cornforth, I.S., 1968. The effect of the size of soil aggregates on nutrient supply. *The Journal of Agricultural Science*, 70, 83–85.

Couchat, P., Moutonnet, P., Houelle, M., and Picard, D., 1980. In situ study of corn seedling root and shoot growth by neutron radiography. *Agronomy Journal*, 72, 321-324 ST-In situ study of corn seedling root.

Cregg, B. and Zhang, J., 2000. Carbon isotope discrimination as a tool to screen for improved drought tolerance. *11th Metropolitan Tree Improvement Alliance (METRIA) Conference*, 13–20.

Crestana, S., Cesareo, R., and Mascarenhas, S., 1986. Using a computed tomography miniscanner in soil science. *Soil Science*, 142 (1), 56–61.

Czarnes, S., Hallett, P.D., Bengough, a. G., and Young, I.M., 2000. Root- and microbial-derived mucilages affect soil structure and water transport. *European Journal Of Soil Science*, 51 (3),

435–443.

D'Ambrosio, E., De Girolamo, A.M., and Rulli, M.C., 2018. Assessing sustainability of agriculture through water footprint analysis and in-stream monitoring activities. *Journal of Cleaner Production*, 200, 454–470.

Darwin, C., 1880. *The power of movement in plants*. London: John Murray.

Davras, B.E., 1974. Loss-on-ignition as an estimate of soil organic matter. *Soil Science Society of America Journal*, 38 (1), 150–151.

Day, P.R., 1965. *Particle fractionation and particle-size analysis*. American Society of Agronomy, Soil Science Society of America.

Daynes, C.N., Field, D.J., Saleeba, J.A., Cole, M.A., and McGee, P.A., 2013. Development and stabilisation of soil structure via interactions between organic matter, arbuscular mycorrhizal fungi and plant roots. *Soil Biology and Biochemistry*, 57, 683–694.

Dayod, M., Aukett, L., Henderson, S., Tyerman, S.D., Shearer, M.K., Athman, A., Fuentes, S., Xu, B., Conn, S.J., Conn, V., Gilliham, M., and Hocking, B., 2013. Protocol: optimising hydroponic growth systems for nutritional and physiological analysis of Arabidopsis thaliana and other plants. *Plant Methods*, 9 (1), 4.

Derpsch, R., 1997. History of Crop Production , With & Without Tillage, 150–154.

Dexter, A.., 1978. A stochastic model for the growth of root s in tilled soil. *Journal of soil science*, (29), 102–116.

Dhakarey, R., Raorane, M.L., Treumann, A., Peethambaran, P.K., Schendel, R.R., Sahi, V.P., Hause, B., Bunzel, M., Henry, A., Kohli, A., and Riemann, M., 2017. Physiological and Proteomic Analysis of the Rice Mutant cpm2 Suggests a Negative Regulatory Role of Jasmonic Acid in Drought Tolerance. *Frontiers in Plant Science*, 8, 1903.

Dharmappa, P.M., Doddaraju, P., Malagondanahalli, M. V., Rangappa, R.B., Mallikarjuna, N.M., Rajendrareddy, S.H., Ramanjinappa, R., Mavinahalli, R.P., Prasad, T.G., Udayakumar, M., and Sheshshayee, S.M., 2019. Introgression of Root and Water Use Efficiency Traits Enhances Water Productivity: An Evidence for Physiological Breeding in Rice (Oryza sativa L.). *Rice*, 12 (1), 14.

Diamond Light Source, 2019. Bird's eye view of the synchrotron [online]. Available from: https://www.diamond.ac.uk/Science/Machine/Components.html [Accessed 19 Sep 2019].

Diaz-Vivancos, P., Faize, L., Nicolás, E., Clemente-Moreno, M.J., Bru-Martinez, R., Burgos, L., and Hernández, J.A., 2016. Transformation of plum plants with a cytosolic ascorbate peroxidase transgene leads to enhanced water stress tolerance. *Annals of botany*, 117 (7), 1121–31.

Díaz-Zorita, M., Perfect, E., and Grove, J.H., 2002. Disruptive methods for assessing soil structure. *Soil and Tillage Research*, 64 (1–2), 3–22.

Dierick, M., Masschaele, B., and Van Hoorebeke, L., 2004. Octopus, a fast and user-friendly tomographic reconstruction package developed in LabView. *Measurement Science and Technology*, 15 (7), 1366–1370.

Dillard, H.R., 2019. Global food and nutrition security: from challenges to solutions. *Food Security*, 11 (1), 249–252.

Doheny-Adams, T., Hunt, L., Franks, P.J., Beerling, D.J., and Gray, J.E., 2012. Genetic manipulation of stomatal density influences stomatal size, plant growth and tolerance to restricted water supply across a growth carbon dioxide gradient. *Phil. Trans. R. Soc. B*, 367, 547–555.

Donald, R., Kay, B., and Miller, M., 1987. The effect of soil aggregate size on early shoot and root growth of maize (Zea mays L.). *Plant and soil*, 103 (2), 251–259.

de Dorlodot, S., Forster, B., Pagès, L., Price, A., Tuberosa, R., and Draye, X., 2007a. Root system architecture: opportunities and constraints for genetic improvement of crops. *Trends in Plant Science*, 12 (10), 474–481.

de Dorlodot, S., Forster, B., Pagès, L., Price, A., Tuberosa, R., and Draye, X., 2007b. Root system architecture: opportunities and constraints for genetic improvement of crops. *Trends in Plant Science*.

Downie, H., Holden, N., Otten, W., Spiers, A.J., Valentine, T.A., and Dupuy, L.X., 2012. Transparent Soil for Imaging the Rhizosphere. *PLoS ONE*, 7 (9), 1–6.

Downie, H.F., Adu, M.O., Schmidt, S., Otten, W., Dupuy, L.X., White, P.J., and Valentine, T.A., 2015. Challenges and opportunities for quantifying roots and rhizosphere interactions through imaging and image analysis. *Plant, Cell and Environment*.

Drakopoulos, M., Connolley, T., Reinhard, C., Atwood, R., Magdysyuk, O., Vo, N., Hart, M., Connor, L., Humphreys, B., Howell, G., Davies, S., Hill, T., Wilkin, G., Pedersen, U., Foster, A., Maio, N. De, Basham, M., Yuan, F., and Wanelik, K., 2017. beamlines I12 : the Joint Engineering , Environment and Processing (JEEP) beamline at Diamond Light Source beamlines, (2015), 828–838.

Dunn, J., Hunt, L., Afsharinafar, M., Meselmani, M. Al, Mitchell, A., Howells, R., Wallington, E., Fleming, A.J., and Gray, J.E., 2019. Reduced stomatal density in bread wheat leads to increased water-use efficiency. *Journal of Experimental Botany*.

Eckardt, N.A., 2000. Sequencing the rice genome. *The Plant cell*, 12 (11), 2011–7.

Edwards, K., Johnstone, C., and Thompson, C., 1991. A simple and rapid method for the preparation of plant genomic DNA for PCR analysis. *Nucleic Acids Research*, 19 (6), 1349.

Ehrenfeld, J.G., Ravit, B., and Elgersma, K., 2005. Feedback in the Plant-Soil System. *Annual Review of Environment and Resources*, 30 (1), 75–115.

Erni, R., Rossell, M.D., Kisielowski, C., and Dahmen, U., 2009. Atomic Resolution Imaging with a sub-50 pm Electron Probe. *Physical Review Letters*, 102 (9), 1–10.

Eshel, A. and Beeckman, T., 2013. *Plant roots: the hidden half*.

ESRF, 2019. What is synchrotron light? [online]. Available from: https://www.esrf.eu/home/education/what-is-the-esrf/what-is-synchrotron-light.html [Accessed 19 Sep 2019].

Esser, H.G., Carminati, A., Vontobel, P., Lehmann, E.H., and Oswald, S.E., 2010. Neutron radiography and tomography of water distribution in the root zone. *Journal of Plant Nutrition and Soil Science*, 173 (5), 757–764.

Eyck, T. and Albert, M., 1899. *A Study of the Root Systems of Wheat, Oats, Flax, Corn, Potatoes and Sugar Beets, and of the Soil in which They Grew*. North Dakota Agricultural College,

Governmental Agricultural Experiment ….

Fairhurst, T. and Dobermann, A., 2002. Rice in the Global Food Supply. *Rice Production*, 16 (May), 47.

Falasca, G. and Altamura, M.M., 2003. Histological analysis of adventitious rooting in *Arabidopsis thaliana* (L.) Heynh seedlings. *Plant Biosystems - An International Journal Dealing with all Aspects of Plant Biology*, 137 (3), 265–273.

Fang, H., Rong, H., Hallett, P.D., Mooney, S.J., Zhang, W., Zhou, H., and Peng, X., 2019. Impact of soil puddling intensity on the root system architecture of rice (Oryza sativa L.)seedlings. *Soil and Tillage Research*, 193 (May), 1–7.

FAO, 2009. How to Feed the World in 2050. *Insights from an expert meeting at FAO*, 2050 (1), 1–35.

FAO, 2017. Water for Sustainable Food and Agriculture Water for Sustainable Food and Agriculture. *A report produced for the G20 Presidency of Germany*, 1–33.

FAOSTAT, 2019. FAOSTAT database [online]. *Food and Agriculture Organization of the United Nations, Rome, Italy*. Available from: http://www.fao.org/faostat/en/#home.

Farquhar, G D. Ehleringer, J.R. Hubic, K.T., Farquhar, G.D., Ehleringer, J.R., and Hubick, K.T., 1989. Carbon isotope discrimination and photosynthesis. *Plant physiology*, 40, 503–537.

Farquhar, G.D., Ehleringer, J.R., and Hubick, K.T., 1989. Carbon Isotope Discrimination and Photosynthesis. *Plant physiology*, 40, 503–537.

FEI, 2015. User's guide Avizo ® 9 [online].

Ferdous, J., Whitford, R., Nguyen, M., Brien, C., Langridge, P., and Tricker, P.J., 2017. Drought-inducible expression of Hv-miR827 enhances drought tolerance in transgenic barley. *Functional & integrative genomics*, 17 (2–3), 279–292.

Figueroa-Bustos, V., Palta, J., Chen, Y., and Siddique, K., 2018. Characterization of Root and Shoot Traits in Wheat Cultivars with Putative Differences in Root System Size. *Agronomy*.

Flavel, R.J., Guppy, C.N., Rabbi, S.M.R., and Young, I.M., 2017. An image processing and analysis tool for identifying and analysing complex plant root systems in 3D soil using non-destructive analysis : Root1, 1–18.

Flavel, R.J., Guppy, C.N., Tighe, M., Watt, M., McNeill, A., and Young, I.M., 2012. Non-destructive quantification of cereal roots in soil using high-resolution X-ray tomography. *Journal of Experimental Botany*, 63 (7), 2503–2511.

Flavel, R.J., Guppy, C.N., Tighe, M.K., Watt, M., and Young, I.M., 2014. Quantifying the response of wheat (Triticum aestivum L) root system architecture to phosphorus in an Oxisol. *Plant and Soil*, 385 (1–2), 303–310.

Francis, G.S., Haynes, R.J., and Koppi, A.J., 1994. Plant mediated improvement of soil structure after long-term arable cropping. *In*: *Proc New Zealand Soc Soil Sci Conf, Lincoln*.

Franks, P.J., W. Doheny-Adams, T., Britton-Harper, Z.J., and Gray, J.E., 2015. Increasing water-use efficiency directly through genetic manipulation of stomatal density. *New Phytologist*, 207 (1), 188–195.

French, A., Ubeda-Tomas, S., Holman, T.J., Bennett, M.J., and Pridmore, T., 2009. High-Throughput Quantification of Root Growth Using a Novel Image-Analysis Tool. *Plant*

Physiology, 150 (4), 1784–1795.

Fulgencio, A.-C., Carlos, C.-V., Enrique, I.-L., Lenin, Y.-V., Claudia-Anahi, P.-T., Araceli, O.-A., Alfonso, M.-B., Sandra-Isabel, G.-M., Dolores, G.-A., Alejandra, C.-L., Betsy-Anaid, P.-O., Luis, H.-E., Alatorre-Cobos, F., Calderón-Vázquez, C., Ibarra-Laclette, E., Yong-Villalobos, L., Pérez-Torres, C.-A., Oropeza-Aburto, A., Méndez-Bravo, A., González-Morales, S.-I., Gutiérrez-Alanís, D., Chacón-López, A., Peña-Ocaña, B.-A., and Herrera-Estrella, L., 2014. An improved , low-cost , hydroponic system for growing Arabidopsis and other plant species under aseptic conditions. *BMC plant biology*, 14, 69.

Furukawa, J., Nakanishi, T.M., and Matsubayashi, M., 1999. Neutron radiography of a root growing in soil with vanadium. *Nuclear Instruments and Methods in Physics Research, Section A: Accelerators, Spectrometers, Detectors and Associated Equipment*, 424 (1), 116–121.

Gao, W., Schlüter, S., R.G.A.Blaser, S., Shen, J., and Vetterlein, D., 2019. A shape-based method for automatic and rapid segmentation of roots in soil from X-ray computed tomography images : Rootine.

Gewin, V., 2010. An underground revolution. *Nature*, 466 (July), 522–533.

Gibbs, H.K.K. and Salmon, J.M.M., 2015. Mapping the world's degraded lands. *Applied Geography*, 57, 12–21.

Giehl, R.F.H., Gruber, B.D., and Von Wir??n, N., 2014. It's time to make changes: Modulation of root system architecture by nutrient signals. *Journal of Experimental Botany*, 65 (3), 769–778.

Glinski, J. and Lipiec, J., 1990. *Soil Physical Conditions and Plant Growth*. CRC Press. CRC Press.

Godfray, H.C.J., Beddington, J.R., Crute, I.R., Haddad, L., Lawrence, D., Muir, J.F., Pretty, J., Robinson, S., Thomas, S.M., and Toulmin, C., 2010. Food security: the challenge of feeding 9 billion people., 327 (5967), 812–8.

Goff, S.A., Ricke, D., Lan, T., Presting, G., Wang, R., Dunn, M., Glazebrook, J., Sessions, A., Oeller, P., Varma, H., Hadley, D., Hutchison, D., Martin, C., Katagiri, F., Lange, B.M., Moughamer, T., Xia, Y., Budworth, P., Zhong, J., Miguel, T., Paszkowski, U., Zhang, S., Colbert, M., Sun, W., Chen, L., Cooper, B., Park, S., Wood, T.C., Mao, L., Quail, P., Wing, R., Dean, R., Yu, Y., Zharkikh, A., Shen, R., Sahasrabudhe, S., Thomas, A., Cannings, R., Gutin, A., Pruss, D., Reid, J., Tavtigian, S., Mitchell, J., Eldredge, G., Scholl, T., Miller, R.M., Bhatnagar, S., Adey, N., Rubano, T., Tusneem, N., Robinson, R., Feldhaus, J., Macalma, T., Oliphant, A., and Briggs, S., 2005. A Draft Sequence of the Rice Genome (Oryza sativa L. ssp. japonica). *Science*, 296 (August), 92–101.

González, C.V., Ibarra, S.E., Piccoli, P.N., Botto, J.F., and Boccalandro, H.E., 2012. Phytochrome B increases drought tolerance by enhancing ABA sensitivity in Arabidopsis thaliana. *Plant, Cell and Environment*, 35 (11), 1958–1968.

Goss, M.J., 1976. Effects of Mechanical Impedance on Root Growth in Barley (Hordeum vulgare L .) AXES. *Journal of Experimental Botany*, 28 (102), 96–111.

Graf, F. and Frei, M., 2013. Soil aggregate stability related to soil density, root length, and mycorrhiza using site-specific Alnus incana and Melanogaster variegatus s.l. *Ecological Engineering*, 57, 314–323.

Greenland, D.., 1981. Recent Progress in Studies of Soil Structure, and its Relation to Properties and Management of Paddy Soils. *In*: *Proceedings of Symposium on Paddy Soils*. 42–58.

Gregory, P., 2006. *Plant roots, growth, activity and interaction with soils*. Blackwell Publishing Ltd,. Oxford.

Gregory, P., 2009. Measuring root system architecture: Opportunities and challenges. *Asrr.Boku.Ac.At*, (September), 2–4.

Gregory, P.J., McGowan, M., Biscoe, P. V., and Hunter, B., 1979. Water relations of winter wheat. *The Journal of Agricultural Science*, 93 (2), 494–494.

Grierson, C., Nielsen, E., Ketelaarc, T., and Schiefelbein, J., 2014. Root Hairs. *The Arabidopsis Book*, 12 (Figure 2), e0172.

Gruber, B.D., Giehl, R.F.H., Friedel, S., and von Wiren, N., 2013. Plasticity of the Arabidopsis Root System under Nutrient Deficiencies. *Plant Physiology*, 163 (1), 161–179.

Grzebisz, W., Floris, W., and van Noordwijk, M., 1989. Loss of dry matter and cell contents from fibrous roots of sugar beet due to sampling , storage and washing *, 57, 53–57.

Gu, D., Zhen, F., Hannaway, D.B., Zhu, Y., Liu, L., Cao, W., and Tang, L., 2017. Quantitative Classification of Rice (Oryza sativa L.) Root Length and Diameter Using Image Analysis. *PloS one*, 12 (1), e0169968.

Hallett, P.D., Feeney, D.S., Bengough, A.G., Rillig, M.C., Scrimgeour, C.M., and Young, I.M., 2009. Disentangling the impact of AM fungi versus roots on soil structure and water transport. *Plant and Soil*, 314 (1–2), 183–196.

Hammer, G.L., Dong, Z., McLean, G., Doherty, A., Messina, C., Schussler, J., Zinselmeier, C., Paszkiewicz, S., and Cooper, M., 2009. Can changes in canopy and/or root system architecture explain historical maize yield trends in the U.S. corn belt? *Crop Science*, 49 (1), 299–312.

Hara, K., Kajita, R., Torii, K.U., Bergmann, D.C., and Kakimoto, T., 2007. The secretory peptide gene EPF1 enforces the stomatal one-cell-spacing rule. *Genes and Development*, 21 (14), 1720–1725.

Hara, K., Yokoo, T., Kajita, R., Onishi, T., Yahata, S., Peterson, K.M., Torii, K.U., and Kakimoto, T., 2009. Epidermal cell density is autoregulated via a secretory peptide, EPIDERMAL PATTERNING FACTOR 2 in arabidopsis leaves. *Plant and Cell Physiology*, 50 (6), 1019–1031.

Hatfield, J.L. and Dold, C., 2019. Water-use efficiency: Advances and challenges in a changing climate. *Frontiers in Plant Science*, 10 (February), 1–14.

Haynes, R.. and Beare, M.H., 1997. Influence Stability of Six Crop Species on Aggregate and Some Labile Organic Matter Fractions. *Science*, 29 (1), 1647–1653.

He, F., Wang, H.-L., Li, H.-G., Su, Y., Li, S., Yang, Y., Feng, C.-H., Yin, W., and Xia, X., 2018. PeCHYR1, a ubiquitin E3 ligase from Populus euphratica, enhances drought tolerance via ABA-induced stomatal closure by ROS production in Populus. *Plant biotechnology journal*, 16 (8), 1514–1528.

Hejazi, M., Edmonds, J., Chaturvedi, V., Davies, E., and Eom, J., 2013. Scenarios of global municipal water-use demand projections over the 21st century. *Hydrological Sciences Journal*, 58 (3), 519–538.

Helliwell, J.R., Sturrock, C.J., Grayling, K.M., Tracy, S.R., Flavel, R.J., Young, I.M., Whalley,

W.R., and Mooney, S.J., 2013. Applications of X-ray computed tomography for examining biophysical interactions and structural development in soil systems: A review. *European Journal of Soil Science*, 64 (3), 279–297.

Hepworth, C., Doheny-adams, T., Hunt, L., Cameron, D.D., and Gray, J.E., 2015. Rapid report Manipulating stomatal density enhances drought tolerance without deleterious effect on nutrient uptake. *New Phytologist*, 208, 336–341.

Hepworth, C., Turner, C., Landim, M.G., Cameron, D., and Gray, J.E., 2016. Balancing Water Uptake and Loss through the Coordinated Regulation of Stomatal and Root Development. *Plos One*, 11 (6), e0156930.

Herold, A. and McNeil, P.H., 1979. Restoration of Photosynthesis in Pot-Bound Tobacco Plants. *Journal of Experimental Botany*, 30 (6), 1187–1194.

Hess, L. and De Kroon, H., 2007. Effects of rooting volume and nutrient availability as an alternative explanation for root self/non-self discrimination. *Journal of Ecology*, 95 (2), 241–251.

Hess, T., Andersson, U., Mena, C., and Williams, A., 2015. The impact of healthier dietary scenarios on the global blue water scarcity footprint of food consumption in the UK. *Food Policy*, 50, 1–10.

Hewitt, J.. and Dexter, A.., 1984. The behaviour of roots encountering cracks in soil: I1. Development of a predictive model. *Plant and Soil*, 28, 11–28.

Hillel, D., 2004. Environmental soil physics. *In*: *Environmental soil physics*. 73–89.

Himmelbauer, M.L., Scholl, P., Bodner, G., and Loiskandl, W., 2017. Root system architecture - Budget experimental system for monitoring and analyses. *Biologia (Poland)*, 72 (9), 988–994.

Hoekstra, A.Y. and Wiedmann, T.O., 2014. Humanity's unsustainable environmental footprint. *Science*, 344 (6188), 1114–1117.

Hoffmann, M.H., 2002. Biogeography of Arabidopsis thaliana (L .). *Journal of Biogeography*, 29, 125–134.

Hong, S., Piao, S., Chen, A., Liu, Y., Liu, L., Peng, S., Sardans, J., Sun, Y., Peñuelas, J., and Zeng, H., 2018. Afforestation neutralizes soil pH. *Nature communications*, 9 (1), 520.

Hoogeveen, J., Faurès, J.-M., Peiser, L., Burke, J., and van de Giesen, N., 2015. GlobWat – a global water balance model to assess water use in irrigated agriculture. *Hydrology and Earth System Sciences*, 19 (9), 3829–3844.

Hoogsteen, M.J.J., Lantinga, E.A., Bakker, E.J., Groot, J.C.J., and Tittonell, P.A., 2015. Estimating soil organic carbon through loss on ignition: Effects of ignition conditions and structural water loss. *European Journal of Soil Science*, 66 (2), 320–328.

Huang, X., Jiang, H., Li, Y., Ma, Y., Tang, H., Ran, W., and Shen, Q., 2016. The role of poorly crystalline iron oxides in the stability of soil aggregate-associated organic carbon in a rice-wheat cropping system. *Geoderma*, 279, 1–10.

Hughes, J., Hepworth, C., Dutton, C., Dunn, J.A., Hunt, L., Stephens, J., Cameron, D., Waugh, R., and Gray, J.E., 2017. Reducing stomatal density in barley improves drought tolerance without impacting on yield. *Plant Physiology*, pp.01844.2016.

Hughes, J., Hepworth, C., Dutton, C., Dunn, J.A., Hunt, L., Stephens, J., Waugh, R., Cameron,

D.D., and Gray, J.E., 2017. Reducing stomatal density in barley improves drought tolerance without impacting on yield. *Plant Physiology*, 174 (2), 776–787.

Hunt, L. and Gray, J.E., 2009. The Signaling Peptide EPF2 Controls Asymmetric Cell Divisions during Stomatal Development. *Current Biology*, 19 (10), 864–869.

Impre Media, 2019. Syringa Leaf Labeled [online]. Available from: http://impremedia.net/syringa-leaf-labeled/ [Accessed 18 Sep 2019].

International Energy Agency, 2012. *Technology Roadmap: Hydropower*. International Energy Agency.

International Wheat Genome Sequencing Consortium (IWGSC), 2018. Shifting the limits in wheat research and breeding using a fully annotated reference genome. *Science (New York, N.Y.)*, 361 (6403), eaar7191.

IPCC, 2007. Climate Change 2007: The Physical Science Basis. *In*: S.D. Solomon, M. Qin, M. Manning, Z. Chen, M. Marquis, K.B. Averyt, M. Tignor, and H.L. Miller, eds. *Contribution of Working Group I to the Fourth Assess- ment Report of the Intergovernmental Panel on Climate Change*. Cambridge,UK and New York, USA.

IPCC, 2013. Summary for Policymakers Drafting. *In*: F.B. France, U. Cubasch, P.F. Uk, P. Friedlingstein, P.C. France, M.C. Uk, and C. Josefino, eds.

IPCC, 2018. *Summary for Policymakers. In: Global warming of 1.5°C. An IPCC Special Report on the impacts of global warming of 1.5°C above pre-industrial levels and related global greenhouse gas emission pathways, in the context of strengthening the global response to*. Geneva, Switzerland.

Itoh, H., Nonoue, Y., Yano, M., and Izawa, T., 2010. A pair of floral regulators sets critical day length for Hd3a florigen expression in rice. *Nature Genetics*, 42 (7), 635–638.

Izawa, T. and Shimamoto, K., 1996. Becoming a model plant: The importance of rice to plant science. *Trends in Plant Science*, 1 (3), 95–99.

Jastrow, J.D. and Miller, R.M., 1991. Methods for assessing the effects of biota on soil structure. *Agriculture, Ecosystems and Environment*, 34 (1–4), 279–303.

Jenneson, P.M., Gilboy, W.B., Morton, E.J., Luggar, R.D., and Gregory, P.J., 1999. Optimisation of X-ray micro-tomography. *In*: *1999 IEEE Nuclear Science Symposium. Conference Record. 1999 Nuclear Science Symposium and Medical Imaging Conference (Cat. No.99CH37019)*.

Kar, S., Varade, S.B., and Ghildyal, B.P., 1979. Pore size distribution and root growth relations of rice in artificially synthesized soils. *Soil Science*.

Karaba, A., Dixit, S., Greco, R., Aharoni, A., Trijatmiko, K.R., Marsch-Martinez, N., Krishnan, A., Nataraja, K.N., Udayakumar, M., and Pereira, A., 2007. Improvement of water use efficiency in rice by expression of HARDY, an Arabidopsis drought and salt tolerance gene. *Proceedings of the National Academy of Sciences of the United States of America*, 104 (39), 15270–5.

Karch, J., Dudák, J., Žemlička, J., Vavřík, D., Kumpová, I., Kvaček, J., Heřmanová, Z., Šoltés, J., Viererbl, L., Morgano, M., Kaestner, A., and Trtík, P., 2017. X-ray micro-CT and neutron CT as complementary imaging tools for non-destructive 3D imaging of rare silicified fossil plants. *Journal of Instrumentation*, 12 (12).

Katerji, N., Mastrorilli, M., and Rana, G., 2008. Water use efficiency of crops cultivated in the Mediterranean region: Review and analysis. *European Journal of Agronomy*, 28 (4), 493–507.

Kato, Y., Kamoshita, A., and Yamagishi, J., 2006. Growth of Three Rice Cultivars (*Oryza sativa*

L.) under Upland Conditions with Different Levels of Water Supply. *Plant Production Science*, 9 (4), 435–445.

Kawata, S. and Soejima, M., 1974. On Superficial Root Formation in Rice Plants. *Japanese journal of crop science*, 43 (3), 354–374.

Kellermeier, F., Armengaud, P., Seditas, T.J., Danku, J., Salt, D.E., and Amtmann, A., 2014. Analysis of the root system architecture of Arabidopsis provides a quantitative readout of crosstalk between nutritional signals. *Plant Cell*, 26 (4), 1480–1496.

Kemper, W.D. and Rosenau, R.C., 1986. Aggregate Stability and Size Distributlon. *Methods of Soil Analysis, Part 1 - Physical and Mineralogical Methods*, 9 (9), 425–442.

Keyes, S., 2013. X-ray Computed Tomography and image-based modelling of plant, root and soil systems, for better understanding of phosphate uptake. University of Southampton.

Keyes, S.D., Daly, K.R., Gostling, N.J., Jones, D.L., Talboys, P., Pinzer, B.R., Boardman, R., Sinclair, I., Marchant, A., and Roose, T., 2013. High resolution synchrotron imaging of wheat root hairs growing in soil and image based modelling of phosphate uptake. *New Phytologist*, 198 (4), 1023–1029.

Keyes, S.D., Gillard, F., Soper, N., Mavrogordato, M.N., Sinclair, I., and Roose, T., 2016. Mapping soil deformation around plant roots using in vivo 4D X-ray computed tomography and digital volume correlation. *Journal of Biomechanics*, c (9), 1802–1811.

Khoury, C.K., Bjorkman, A.D., Dempewolf, H., Ramirez-Villegas, J., Guarino, L., Jarvis, A., Rieseberg, L.H., and Struik, P.C., 2014. Increasing homogeneity in global food supplies and the implications for food security. *Proceedings of the National Academy of Sciences of the United States of America*, 111 (11), 4001–6.

Khush, G.S., 2005. What it will take to Feed 5.0 Billion Rice consumers in 2030. *Plant Molecular Biology*, 59 (1), 1–6.

Kima, A.S., Chung, W.G., and Wang, Y.M., 2014. Improving irrigated lowland rice water use efficiency under saturated soil culture for adoption in tropical climate conditions. *Water (Switzerland)*, 6 (9), 2830–2846.

Kirby, E.J.., 2002. Botany of the wheat plant [online]. *Bread Wheat: Improvement and production*. Available from: http://www.fao.org/3/y4011e/y4011e05.htm [Accessed 4 Aug 2019].

Kirchhof, G. and So, H.B., 2005. Soil puddling for rice production under glasshouse conditions - Its quantification and effect on soil physical properties. *Australian Journal of Soil Research*, 43 (5), 617–622.

Knox, J., Hess, T., Daccache, A., and Wheeler, T., 2012. Climate change impacts on crop productivity in Africa and South Asia. *Environmental Research Letters*, 7 (3), 34032.

Koch, A., Mcbratney, A., Adams, M., Field, D., Hill, R., Crawford, J., Minasny, B., Lal, R., Abbott, L., O'Donnell, A., Angers, D., Baldock, J., Barbier, E., Binkley, D., Parton, W., Wall, D.H., Bird, M., Bouma, J., Chenu, C., Flora, C.B., Goulding, K., Grunwald, S., Hempel, J., Jastrow, J., Lehmann, J., Lorenz, K., Morgan, C.L., Rice, C.W., Whitehead, D., Young, I., and Zimmermann, M., 2013. Soil Security: Solving the Global Soil Crisis. *Global Policy*, 4 (4), 434–441.

Kochian, L. V., 2016. Root architecture. *Journal of Integrative Plant Biology*, 58 (3), 190–192.

Kockelmann, W., Zhang, S.Y., Kelleher, J.F., Nightingale, J.B., Burca, G., and James, J.A., 2013. IMAT - A new imaging and diffraction instrument at ISIS. *Physics Procedia*, 43 (0), 100–110.

Koebernick, N., Daly, K.R., Keyes, S.D., George, T.S., Brown, L.K., Raffan, A., Cooper, L.J., Naveed, M., Bengough, A.G., Sinclair, I., Hallett, P.D., and Roose, T., 2017. High-resolution synchrotron imaging shows that root hairs influence rhizosphere soil structure formation. *New Phytologist*.

Koech, R. and Langat, P., 2018. Improving irrigation water use efficiency: A review of advances, challenges and opportunities in the Australian context. *Water (Switzerland)*, 10 (12).

Koevoets, I.T., Venema, J.H., Elzenga, J.T.M., and Testerink, C., 2016. Roots Withstanding their Environment: Exploiting Root System Architecture Responses to Abiotic Stress to Improve Crop Tolerance. *Frontiers in Plant Science*, 07 (August), 1–19.

Kögel-Knabner, I., Amelung, W., Cao, Z., Fiedler, S., Frenzel, P., Jahn, R., Kalbitz, K., Kölbl, A., and Schloter, M., 2010. Biogeochemistry of paddy soils. *Geoderma*, 157 (1–2), 1–14.

Koornneef, M., Van Eden, J., Hanhart, C.J., Stam, P., Braaksma, F.J., and Feenstra, W.., 1983. Linkage map of Arabidopsis thaliana. *Journal of Heredity*, 74 (4), 265-272.

Korner, C., Pelaez, M.-R.S., and John, P., 1989. Why Are Bonsai Plants Small? A Consideration of Cell Size. *Functional Plant Biology*, 16 (5), 443.

Kreuzer, K., Adamczyk, J., Iijima, M., Wagner, M., Scheu, S., and Bonkowski, M., 2006. Grazing of a common species of soil protozoa (Acanthamoeba castellanii) affects rhizosphere bacterial community composition and root architecture of rice (Oryza sativa L.). *Soil Biology and Biochemistry*, 38 (7), 1665–1672.

Kumar, A., Nayak, A.K., Pani, D.R., and Das, B.S., 2017. Physiological and morphological responses of four different rice cultivars to soil water potential based deficit irrigation management strategies. *Field Crops Research*, 205, 78–94.

Kumar, P., Yadava, R., Gollen, B., … S.K.-L.S. and, and 2011, U., 2011. Nutritional Contents and Medicinal Properties of Wheat: A Review. *Life Sciences and Medicine Research*, 2011 (1), 22.

Kuo, S., 1996. Phosphorus. p. 869–919. DL Sparks (ed.) Methods of soil analysis. Part 3. SSSA Book Ser. 5. SSSA, Madison, WI. *Phosphorus. p. 869–919. In DL Sparks (ed.) Methods of soil analysis. Part 3. SSSA Book Ser. 5. SSSA, Madison, WI.*

Laibach, F., 1943. Arabidopsis thaliana (L.) Heynh. als Objekt für genetische und entwicklungsphysiologische Untersuchungen. *Bot. Archiv*, 44, 439–455.

Lal, R., 1997a. Degradation and resilience of soils. *Philosophical Transactions of the Royal Society B: Biological Sciences*, 352 (1356), 997–1010.

Lal, R., 1997b. Long-term tillage and maize monoculture effects on a tropical Alfisol in western Nigeria. I. Crop yield and soil physical properties. *Soil and Tillage Research*, 42 (3), 145–160.

Lal, R., 2015. Restoring Soil Quality to Mitigate Soil Degradation. *Sustainability*, 7 (5), 5875–5895.

Lal, R., 2016. Feeding 11 billion on 0.5 billion hectare of area under cereal crops.

Lal, R. and Shulka, M.., 2004. *Principles of soil physics*. Marcel Dekker.

Landl, M., Schnepf, A., Vanderborght, J., Bengough, A.G., Bauke, S.L., Lobet, G., Bol, R., and Vereecken, H., 2018. Measuring root system traits of wheat in 2D images to parameterize

3D root architecture models. *Plant and Soil*, 425 (1–2), 457–477.

Latif, M.A., Mehuys, G.R., MacKenzie, A.F., Alli, I., and Faris, M.A., 1992. Effect of Legumes on Soil Physical Quality in a Maize Crop. *Plant Soil*, 140 (1972), 15–23.

Lavkulich, L.M., 1981. Methods Manual, Pedology Laboratory. Department of Soil Science, University of British Columbia, Vancouver. *British Columbia, Canada*.

Leakey, A.D.B., Ferguson, J.N., Pignon, C.P., Wu, A., Jin, Z., Hammer, G.L., and Lobell, D.B., 2019. Water Use Efficiency as a Constraint and Target for Improving the Resilience and Productivity of C3 and C4 Crops. *Annual Review of Plant Biology*, 70 (1), 781–808.

Lee, J.S., Lee, M.H., Chun, Y.Y., and Lee, K.M., 2018. Uncertainty analysis of the water scarcity footprint based on the AWARE model considering temporal variations. *Water (Switzerland)*, 10 (3), 1–13.

Lee, M.M. and Schiefelbein, J., 1999. WEREWOLF, a MYB-Related Protein in Arabidopsis, Is a Position-Dependent Regulator of Epidermal Cell Patterning. *Cell*, 99 (5), 473–483.

Lehmann, E.H., 2017. Neutron imaging facilities in a global context. *Journal of Imaging*, 3 (4).

Leite, J.P., Barbosa, E.G.G., Marin, S.R.R., Marinho, J.P., Carvalho, J.F.C., Pagliarini, R.F., Cruz, A.S., Oliveira, M.C.N., Farias, J.R.B., Neumaier, N., Guimarães, F.C.M., Yoshida, T., Kanamori, N., Fujita, Y., Nakashima, K., Shinozaki, K.Y., Desidério, J.A., and Nepomuceno, A.L., 2014. Overexpression of the activated form of the AtAREB1 gene (AtAREB1ΔQT) improves soybean responses to water deficit. *Genetics and Molecular Research*, 13 (3), 6272–6286.

Lightsources.org, 2019. Light sources of the world [online]. Available from: https://lightsources.org/lightsources-of-the-world/ [Accessed 19 Sep 2019].

Liu, J., Zhang, F., Zhou, J., Chen, F., Wang, B., and Xie, X., 2012. Phytochrome B control of total leaf area and stomatal density affects drought tolerance in rice. *Plant Molecular Biology*, 78 (3), 289–300.

Liu, Y., Qin, L., Han, L., Xiang, Y., and Zhao, D., 2015. Overexpression of maize SDD1 (ZmSDD1) improves drought resistance in Zea mays L. by reducing stomatal density. *Plant Cell, Tissue and Organ Culture*, 122 (1), 147–159.

Liu, Z., Qian, J., Liu, B., Wang, Q., Ni, X., Dong, Y., Zhong, K., and Wu, Y., 2014. Effects of the Magnetic Resonance Imaging Contrast Agent Gd-DTPA on Plant Growth and Root Imaging in Rice. *PLoS ONE*, 9 (6), e100246.

Lo, S.-F., Ho, T.-H.D., Liu, Y.-L., Jiang, M.-J., Hsieh, K.-T., Chen, K.-T., Yu, L.-C., Lee, M.-H., Chen, C.-Y., Huang, T.-P., Kojima, M., Sakakibara, H., Chen, L.-J., and Yu, S.-M., 2017. Ectopic expression of specific GA2 oxidase mutants promotes yield and stress tolerance in rice. *Plant biotechnology journal*, 15 (7), 850–864.

Logsdon, S.D., Parker, J.C., and Reneau, R.B., 1987. Root growth as influenced by aggregate size. *Plant and Soil*, 99 (2–3), 267–275.

Low, A.J., 1972. The effect of cultivation on the structure and other physical characteristics of grassland and arable soils (1945-1970). *Journal of Soil Science*, 23 (4), 363–380.

Lucas, M., Swarup, R., Paponov, I.A., Swarup, K., Casimiro, I., Lake, D., Peret, B., Zappala, S., Mairhofer, S., Whitworth, M., Wang, J., Ljung, K., Marchant, A., Sandberg, G., Holdsworth,

M.J., Palme, K., Pridmore, T., Mooney, S., and Bennett, M.J., 2011. SHORT-ROOT Regulates Primary, Lateral, and Adventitious Root Development in Arabidopsis. *Plant Physiology*, 155 (January), 384–398.

Ludwig, F., van Slobbe, E., and Cofino, W., 2014. Climate change adaptation and Integrated Water Resource Management in the water sector. *Journal of Hydrology*, 518 (PB), 235–242.

Luschnig, C., Gaxiola, R.A., Grisafi, P., and Fink, G.R., 1998. EIR1, a root specific protein involved in auxin transport, is required for gravitropism in Arabidopsis thaliana. *Genes Dev.*, 12, 2175–2187.

Lynch, J., 1995. Root Architecture and Plant Productivity. *Plant physiology*, 109 (1), 7–13.

Lynch, J.P., 2007. Roots of the second green revolution. *Australian Journal of Botany*, 55 (5), 493–512.

Lynch, J.P., 2013. Steep, cheap and deep: An ideotype to optimize water and N acquisition by maize root systems. *Annals of Botany*, 112 (2), 347–357.

Maarastawi, S.A., Frindte, K., Bodelier, P.L.E., and Knief, C., 2019. Rice straw serves as additional carbon source for rhizosphere microorganisms and reduces root exudate consumption. *Soil Biology and Biochemistry*, 135, 235–238.

Mairhofer, S., Sturrock, C.J., Bennett, M.J., Mooney, S.J., and Pridmore, T.P., 2015. Extracting multiple interacting root systems using X-ray microcomputed tomography. *Plant Journal*, 84 (5), 1034–1043.

Mairhofer, S., Zappala, S., Tracy, S., Sturrock, C., Bennett, M.J., Mooney, S.J., and Pridmore, T.P., 2013. Recovering complete plant root system architectures from soil via X-ray μ-Computed Tomography. *Plant Methods*, 9, 1.

Mairhofer, S., Zappala, S., Tracy, S.R., Sturrock, C., Bennett, M., Mooney, S.J., and Pridmore, T., 2012a. RooTrak: Automated Recovery of Three-Dimensional Plant Root Architecture in Soil from X-Ray Microcomputed Tomography Images Using Visual Tracking. *Plant Physiology*, 158 (2), 561–569.

Mairhofer, S., Zappala, S., Tracy, S.R., Sturrock, C., Bennett, M., Mooney, S.J., and Pridmore, T., 2012b. RooTrak: Automated Recovery of Three-Dimensional Plant Root Architecture in Soil from X-Ray Microcomputed Tomography Images Using Visual Tracking. *Plant Physiology*, 158 (2), 561–569.

Malin, F. and Rockström, J., 2004. *Balancing Water for Humans and Nature: The New Approach in Ecohydrology (,)*. Routledge.

Malthus, T.R., 1798. An Essay on the Principle of Population, as it Affects the Future Improvement of Society with Remarks on the Speculations of Mr. Godwin, M. Condorcet, and Other Writers, 340.

Mancosu, N., Snyder, R.L., Kyriakakis, G., and Spano, D., 2015. Water scarcity and future challenges for food production. *Water (Switzerland)*, 7 (3), 975–992.

Mancuso, S., 2012. Measuring roots: An updated approach. *Measuring Roots: An Updated Approach*, 1–382.

Manschadi, A.M., Christopher, J., Devoil, P., and Hammer, G.L., 2006. The role of root architectural traits in adaptation of wheat to water-limited environments. *Functional Plant*

Biology, 33 (9), 823–837.

Manschadi, A.M., Hammer, G.L., Christopher, J.T., and DeVoil, P., 2008. Genotypic variation in seedling root architectural traits and implications for drought adaptation in wheat (Triticum aestivum L.). *Plant and Soil*, 303 (1–2), 115–129.

Mao, H., Wang, H., Liu, S., Li, Z., Yang, X., Yan, J., Li, J., Tran, L.S.P., and Qin, F., 2015. A transposable element in a NAC gene is associated with drought tolerance in maize seedlings. *Nature Communications*, 6.

Martin, S.L., Mooney, S.J., Dickinson, M.J., and West, H.M., 2012. Soil structural responses to alterations in soil microbiota induced by the dilution method and mycorrhizal fungal inoculation. *Pedobiologia*, 55 (5), 271–281.

Masle, J., Gilmore, S.R., and Farquhar, G.D., 2005. The ERECTA gene regulates plant transpiration efficiency in Arabidopsis. *Nature*, 436 (7052), 866–870.

Materechera, S.A., Dexter, A.R., and Alston, A.M., 1992. Formation of aggregates by plant roots in homogenised soils. *Plant and Soil*, 142 (1), 69–79.

Materechera, S.A., Kirby, J.M., Alston, A.M., and Dexter, A.R., 1994. Modification of Soil Aggregation By Watering Regime and Roots Growing Through Beds of Large Aggregates. *Plant and Soil*, 160 (1), 57–66.

Matsumoto, T., Wu, J., Itoh, T., Numa, H., Antonio, B., and Sasaki, T., 2016. The Nipponbare genome and the next-generation of rice genomics research in Japan. *Rice*, 9 (1), 33.

Matsuo, N. and Mochizuki, T., 2009. Growth and Yield of Six Rice Cultivars under Three Water-saving Cultivations. *Plant Production Science*, 12 (4), 514–525.

Mawodza, T., Brooks, H., Burca, G., and Menon, M., 2018. Understanding root architecture and water uptake of water use efficient wheat mutants using neutron and X-Ray CT imaging. *STFC ISIS Neutron and Muon Source Data Journal*.

Meinke, D.W., Cherry, J.M., Dean, C., Rounsley, S.D., and Koornneef, M., 1998. Arabidopsis thaliana: A model plant for genome analysis. *Science*, 282 (5389).

Menon, M., 2006. Influence of soil pollution by heavy metals on the water relations of young forest ecosystems.

Menon, M., Robinson, B., Oswald, S.E., Kaestner, A., Abbaspour, K.C., Lehmann, E., and Schulin, R., 2007. Visualization of root growth in heterogeneously contaminated soil using neutron radiography. *European Journal of Soil Science*, 58 (3), 802–810.

Metzner, R., Eggert, A., van Dusschoten, D., Pflugfelder, D., Gerth, S., Schurr, U., Uhlmann, N., and Jahnke, S., 2015. Direct comparison of MRI and X-ray CT technologies for 3D imaging of root systems in soil: potential and challenges for root trait quantification. *Plant Methods*.

Minasny, B., Mcbratney, A.B., Brough, D.M., and Jacquier, D., 2011. Models relating soil pH measurements in water and calcium chloride that incorporate electrolyte concentration. *European Journal of Soil Science*, 62 (5), 728–732.

Minniti, T., Watanabe, K., Burca, G., Pooley, D.E., and Kockelmann, W., 2018. Characterization of the new neutron imaging and materials science facility IMAT. *Nuclear Instruments and Methods in Physics Research, Section A: Accelerators, Spectrometers, Detectors and Associated Equipment*, 888 (January), 184–195.

Misra, R.K., Alston, A.M., and Dexter, A.R., 1988. Root Growth and Phosphorus Uptake in Relation to the Size and Strength of Soil Aggregates. I. Experimental Studies, 11, 103–116.

Misra, R.K., Dexter, A.R., and Alston, A.M., 1986. Penetration of soil aggregates of finite size. *Plant and Soil*, 94 (1), 59–85.

Mohammed, U., Caine, R.S., Atkinson, J.A., Harrison, E.L., Wells, D., Chater, C.C., Gray, J.E., Swarup, R., and Murchie, E.H., 2019. Rice plants overexpressing OsEPF1 show reduced stomatal density and increased root cortical aerenchyma formation. *Scientific reports*, 9 (1), 5584.

Moin, M., Bakshi, A., Madhav, M.S., and Kirti, P.B., 2017. Expression Profiling of Ribosomal Protein Gene Family in Dehydration Stress Responses and Characterization of Transgenic Rice Plants Overexpressing RPL23A for Water-Use Efficiency and Tolerance to Drought and Salt Stresses. *Frontiers in Chemistry*, 5, 97.

Monnier, G., 1965. Action des matieres organiques sur la stabilite structurale de sols: 1ere these. Le concept de sol et son evolution: 2eme these. *Action des matieres organiques sur la stabilite structurale de sols: 1ere these. Le concept de sol et son evolution: 2eme these, Université de Paris (1965).*

Monroe, C.D. and Kladivko, E.J., 1987. Aggregate stability of a silt loam soil as affected by roots of corn, soybeans and wheat. *Communications in Soil Science and Plant Analysis*, 18 (10), 1077–1087.

Mooney, S.J., Morris, C., and Berry, P.M., 2006. Visualization and quantification of the effects of cereal root lodging on three-dimensional soil macrostructure using x-ray computed tomography. *Soil Science*, 171 (9), 706–718.

Mooney, S.J., Pridmore, T.P., Helliwell, J., and Bennett, M.J., 2012. Developing X-ray computed tomography to non-invasively image 3-D root systems architecture in soil. *Plant and Soil*, 352 (1–2), 1–22.

Moradi, A.B., Carminati, A., Vetterlein, D., Vontobel, P., Lehmann, E., Weller, U., Hopmans, J.W., Vogel, H.-J., and Oswald, S.E., 2011. Three-dimensional visualization and quantification of water content in the rhizosphere. *New Phytol.*, 192 (3), 653–663.

Moradi, A.B., Conesa, H.M., Robinson, B., Lehmann, E., Kuehne, G., Kaestner, A., Oswald, S., and Schulin, R., 2009. Neutron radiography as a tool for revealing root development in soil: Capabilities and limitations. *Plant and Soil*, 318 (1–2), 243–255.

Moradi, A.B., Hopmans, J.W., Oswald, S.E., Menon, M., Carminati, A., Lehmann, E., Anderson, S.H., and Hopmans, J.W., 2013. Applications of Neutron Imaging in Soil–Water–Root Systems, 113–136.

Morison, J.I.., Baker, N.., Mullineaux, P.., and Davies, W.., 2008. Improving water use in crop production. *Philosophical Transactions of the Royal Society B: Biological Sciences*, 363 (1491), 639–658.

Morita, S. and Nemoto, K., 1995. Morphology and anatomy of rice roots with special reference to coordination in organo- and histogenesis. *Structure and Function of Roots*, 75–86.

Morris, E.C., Griffiths, M., Golebiowska, A., Mairhofer, S., Burr-Hersey, J., Goh, T., Wangenheim, D. Von, Atkinson, B., Sturrock, C.J., Lynch, J.P., Vissenberg, K., Ritz, K., Wells, D.M., Mooney, S.J., Bennett, M.J., von Wangenheim, D., Atkinson, B., Sturrock, C.J., Lynch, J.P., Vissenberg, K., Ritz, K., Wells, D.M., Mooney, S.J., and Bennett, M.J., 2017. Shaping 3D Root System Architecture. *Current Biology*, 27 (17), R919–R930.

Müller, B. and Bartelheimer, M., 2013. Interspecific competition in Arabidopsis thaliana: Root hairs are important for competitive effect, but not for competitive response. *Plant and Soil*, 371 (1–2), 167–177.

Munjonji, L., 2017. Drought tolerant traits of triticale and cowpea genotypes under semi-arid conditions. Ghent University.

Munkholm, L.J., Heck, R.J., and Deen, B., 2013. Long-term rotation and tillage effects on soil structure and crop yield. *Soil and Tillage Research*, 127, 85–91.

Murasnige, T. and Skoog, F., 1962. A Revised Medium for Rapid Growth and Bio Agsays with Tohaoco Tissue Cultures. *Physiol. Plant*, 15 (3), 473–497.

Murungu, F.S., Nyamugafata, P., Chiduza, C., Clark, L.J., and Whalley, W.R., 2003. Effects of seed priming, aggregate size and soil matric potential on emergence of cotton (Gossypium hirsutum L.) and maize (Zea mays L.). *Soil and Tillage Research*, 74 (2), 161–168.

Nakamoto, T. and Oyanagi, A., 1994. The Direction of Growth of Seminal Roots of Triticum aestivum L. and Experimental Modification Thereof. *Annals of Botany*.

Nakamoto, T. and Suzuki, K., 2001. Influence of soybean and maize roots on the seasonal change in soil aggregate size and stability. *Plant Prod. Sci.*, 4, 317–319.

Nakanishi, T.M., Matsumoto, S., and Kobayashi, H., 1992. Morphological Change of Plant Root Revealed Radiography by Neutron of Tokyo, 641, 638–641.

Nakanishi, T.M., Okuni, Y., Hayashi, Y., and Nishiyama, H., 2005. Water gradient profiles at bean plant roots determined by neutron beam analysis. *Journal of Radioanalytical and Nuclear Chemistry*, 264 (2), 313–317.

Naveed, M., Brown, L.K., Raffan, A.C., George, T.S., Bengough, A.G., Roose, T., Sinclair, I., Koebernick, N., Cooper, L., Hackett, C.A., and Hallett, P.D., 2017. Plant exudates may stabilize or weaken soil depending on species, origin and time. *European Journal of Soil Science*, 68 (6), 806–816.

Negi, M., Sanagala, R., Rai, V., and Jain, A., 2016. Deciphering Phosphate Deficiency-Mediated Temporal Effects on Different Root Traits in Rice Grown in a Modified Hydroponic System. *Frontiers in Plant Science*, 7, 550.

Ni Jiang, Floro, E., Bray, A.L., Laws, B., Duncan, K.E., and Topp, C.N., 2018. High-resolution 4D spatiotemporal analysis reveals the contributions of local growth dynamics to contrasting maize root architectures, (314).

Nimmo, J.R. and Perkins, K.., 2002. Aggregate stability and size distribution. *Methods of soil analysis, Part 4-Physical methods*.

Niu, Y., Jin, G., Li, X., Tang, C., Zhang, Y., Liang, Y., and Yu, J., 2015. Phosphorus and magnesium interactively modulate the elongation and directional growth of primary roots in Arabidopsis thaliana (L .) Heynh, 66 (13), 3841–3854.

van Noordwijk, M. and Floris, J., 1979. Loss of dry weight during washing and storage of root samples. *Plant and Soil*, 53, 239–240.

Nyamangara, J., Marondedze, A., Masvaya, E.N., Mawodza, T., Nyawasha, R., Nyengerai, K., Tirivavi, R., Nyamugafata, P., and Wuta, M., 2014. Influence of basin-based conservation agriculture on selected soil quality parameters under smallholder farming in Zimbabwe. *Soil*

Use and Management, 30 (4), 550–559.

Oades, J.M., 1993. The role of biology in the formation, stabilization and degradation of soil structure. *Geoderma*, 56 (1–4), 377–400.

Octopus, 2019. Octopus reconstrsuction [online]. Available from: https://octopusimaging.eu/octopus/octopus-reconstruction [Accessed 1 Mar 2019].

Odegard, I., Bijleveld, M., and Naber, N., 2015. *Food Commodity Footprints*.

Ogura, T., Goeschl, C., Filiault, D., Mirea, M., Slovak, R., Wolhrab, B., Satbhai, S.B., and Busch, W., 2019a. Root System Depth in Arabidopsis Is Shaped by EXOCYST70A3 via the Dynamic Modulation of Auxin Transport. *Cell*, 178 (2), 400-412.e16.

Ogura, T., Goeschl, C., Filiault, D., Mirea, M., Slovak, R., Wolhrab, B., Satbhai, S.B., and Busch, W., 2019b. Root System Depth in Arabidopsis Is Shaped by EXOCYST70A3 via the Dynamic Modulation of Auxin Transport. *Cell*, 178 (2), 400-412.e16.

Okushima, Y., Fukaki, H., Onoda, M., Theologis, A., and Tasaka, M., 2007. ARF7 and ARF19 Regulate Lateral Root Formation via Direct Activation of LBD/ASL Genes in Arabidopsis. *the Plant Cell Online*, 19 (1), 118–130.

Okushima, Y., Overvoorde, P.J., Arima, K., Alonso, J.M., Chan, A., Chang, C., Ecker, J.R., Hughes, B., Lui, A., Nguyen, D., Onodera, C., Quach, H., and Smith, A., 2005. Functional Genomic Analysis of the AUXIN RESPONSE FACTOR Gene Family Members in Arabidopsis thaliOkushima, Y., Overvoorde, P. J., Arima, K., Alonso, J. M., Chan, A., Chang, C., Ecker, J. R., et al. (2005). Functional Genomic Analysis of the AUXIN RESPONSE. *The Plant Cell …*, 17 (February), 444–463.

Oldeman, L.R., Hakkeling, R.T.A., and Sombroek, W.G., 1991. *World map of the status of human-induced soil degradation: an explanatory note*. International Soil Reference and Information Centre.

Olsen, S.R., Cole, C.W., Watanabe, F.S., and Dean, L.A., 1954. *Estimation of available phosphorus in soils by extraction with sodium bicarbonate*. Estimation of available phosphorus in soils by extraction with sodium bicarbonate. p. 1–19. Circular 939. USDA, Washington, DC.

Ortiz-Ribbing, L.M. and Eastburn, D.M., 2003. Evaluation of Digital Image Acquisition Methods for Determining Soybean Root Characteristics. *Crop Management*, 2 (1), 0–0.

Osugi, A., Itoh, H., Ikeda-Kawakatsu, K., Takano, M., and Izawa, T., 2011. Molecular dissection of the roles of phytochrome in photoperiodic flowering in rice. *Plant Physiology*, 157 (3), 1128–1137.

Oswald, S.E., Menon, M., Carminati, A., Vontobel, P., Lehmann, E., and Schulin, R., 2008. Quantitative Imaging of Infiltration, Root Growth, and Root Water Uptake via Neutron Radiography. *Vadose Zone Journal*, 7 (3), 1035.

Oswald, S.E., Tötzke, C., Haber-Pohlmeier, S., Pohlmeier, A., Kaestner, A.P., and Lehmann, E., 2015. ScienceDirect Combining Neutron and Magnetic Resonance Imaging to Study the Interaction of Plant Roots and Soil. *Physics Procedia*, 69 (69), 237–243.

Paez-Garcia, A., Motes, C., Scheible, W.-R., Chen, R., Blancaflor, E., and Monteros, M., 2015. Root Traits and Phenotyping Strategies for Plant Improvement. *Plants*, 4 (2), 334–355.

Page, D.R. and Grossniklaus, U., 2002. The art and design of genetic screens: Arabidopsis

thaliana. *Nature Reviews Genetics*, 3 (2), 124–136.

Page, J. and Willard, C.J., 1947. Cropping Systems and Soil Properties 1. *Soil Science Society of America Journal*, 11 (C), 81–88.

Palta, J.A., Chen, X., Milroy, S.P., Rebetzke, G.J., Dreccer, M.F., and Watt, M., 2011. Large root systems: Are they useful in adapting wheat to dry environments? *Functional Plant Biology*, 38 (5), 347–354.

Panigrahy, M., Nageswara Rao, D., Yugandhar, P., Sravan Raju, N., Krishnamurthy, P., Voleti, S.R., Reddy, G.A., Mohapatra, T., Robin, S., Singh, A.K., Singh, K., Sheshshayee, M., Sharma, R.P., and Sarla, N., 2014. Hydroponic experiment for identification of tolerance traits developed by rice Nagina 22 mutants to low-phosphorus in field condition. *Archives of Agronomy and Soil Science*, 60 (4), 565–576.

Pankhurst, C., Doube, B.M., and Gupta, V., 1997. Biological indicators of soil health.

Papademetriou, M.K., Dent, F.J., and Herath, E.M., 2000. *Bridging the rice yield gap in the Asia-Pacific Region*. FAO Regional Office for Asia and the Pacific Bangkok, Thailand.

Papadopoulos, A., 2011. Soil Aggregates, Structure, and Stability. Springer, Dordrecht, 736–740.

Pask, A.J.D. and Reynolds, M.P., 2013. Breeding for yield potential has increased deep soil water extraction capacity in irrigated wheat. *Crop Science*, 53 (5), 2090–2104.

Passioura, J., 2006. Increasing crop productivity when water is scarce—from breeding to field management. *Agricultural Water Management*, 80 (1–3), 176–196.

Passioura, J.B. and Stirzaker, R.J., 1993. Feedforward Responses of Plants to Physically Inhospitable Soil. *International Crop Science I*, 715–719.

Pearce, S., Kippes, N., Chen, A., Debernardi, J.M., and Dubcovsky, J., 2016. RNA-seq studies using wheat PHYTOCHROME B and PHYTOCHROME C mutants reveal shared and specific functions in the regulation of flowering and shade-avoidance pathways. *BMC Plant Biology*, 16 (1), 141.

Pennisi, E., 2008. The Blue Revolution, Drop by Drop, Gene by Gene. *Science*, 320 (5873), 171–173.

Péret, B., Desnos, T., Jost, R., Kanno, S., Berkowitz, O., and Nussaume, L., 2014. Root architecture responses: in search of phosphate. *Plant physiology*, 166 (4), 1713–23.

Pfeifer, J., Kirchgessner, N., Colombi, T., and Walter, A., 2015. Rapid phenotyping of crop root systems in undisturbed field soils using X-ray computed tomography. *Plant Methods*, 11 (1), 41.

Pflugfelder, D., Metzner, R., Dusschoten, D. Van, Reichel, R., Jahnke, S., and Koller, R., 2017. Non-invasive imaging of plant roots in different soils using magnetic resonance imaging (MRI). *Plant Methods*, 1–9.

Pierre, C. Saint, Crossa, J.L., Bonnett, D., Yamaguchi-Shinozaki, K., and Reynolds, M.P., 2012. Phenotyping transgenic wheat for drought resistance. *Journal of Experimental Botany*, 63 (5), 1799–1808.

Pierret, A., Moran, C.J., and Doussan, C., 2005. Conventional detection methodology is limiting our ability to understand the roles and functions of fine roots. *New Phytologist*, 166 (3), 967–980.

Pires, L.F., Oliveira, O., and Bacchi, S., 2010. Changes in soil structure evaluated using computed tomography :Soil structure changes Evaluated with computed. *Brazilian Agricultural Research*, 1–11.

Poorter, H., Bühler, J., Van Dusschoten, D., Climent, J., and Postma, J.A., 2012. Pot size matters: A meta-analysis of the effects of rooting volume on plant growth. *Functional Plant Biology*, 39 (11), 839–850.

Porter, J.R. and Gawith, M., 1999. Temperatures and the growth and development of wheat: a review. *European Journal of Agronomy*, 10 (1), 23–36.

Preece, C., Farré-Armengol, G., Llusià, J., and Peñuelas, J., 2018. Thirsty tree roots exude more carbon. *Tree Physiology*, (January).

Preece, C. and Peñuelas, J., 2016. Rhizodeposition under drought and consequences for soil communities and ecosystem resilience. *Plant and Soil*, 409 (1–2), 1–17.

Raj Ratta, 2018. *Soil Quality and Soil Erosion*.

Rajabi, A., 2006. Carbon isotope discrimination and selective breeding of sugar beet (Beta vulgaris L.) for drought tolerance. University of Cambridge.

Ramalingam, P., Kamoshita, A., Deshmukh, V., Yaginuma, S., and Uga, Y., 2017. Association between root growth angle and root length density of a nearisogenic line of IR64 rice with DEEPER ROOTING 1 under different levels of soil compaction. *Plant Production Science*.

Rao, A.., Johnson D, E., Sivaprasad, B., Ladha, J, K., and Mortimer, A, M., 2008. Weed management in direct seeded rice. *Journal of Animal and Plant Sciences*, 18 (2–3), 86–88.

Ray, J.D. and Sinclair, T.R., 1998. The effect of pot size on growth and transpiration of maize and soybean during water deficit stress. *Journal of Experimental Botany*, 49 (325), 1381–1386.

Rebouillat, J., Dievart, A., Verdeil, J.L., Escoute, J., Giese, G., Breitler, J.C., Gantet, P., Espeout, S., Guiderdoni, E., and Périn, C., 2009. Molecular Genetics of Rice Root Development. *Rice*, 2 (1), 15–34.

Reed, J.W., Elumalai, R.P., and Chory, J., 1998. Suppressors of an Arabidopsis thaliana phyB mutation identify genes that control light signaling and hypocotyl elongation. *Genetics*, 148 (3), 1295–1310.

Reed, J.W., Nagpal, P., Poole, D.S., Furuya, M., and Chory, J., 1993. Mutations in the gene for the red/far-red light receptor phytochrome B alter cell elongation and physiological responses throughout Arabidopsis development. *The Plant cell*, 5 (2), 147–157.

Reid, J.. B. and Goss, M.. J., 1981. Effect of living roots of different plant species on the aggregate stability of two arable soils. *Journal of Soil science*, 32 (4), 521–541.

Rich, S.M. and Watt, M., 2013. Soil conditions and cereal root system architecture: Review and considerations for linking Darwin and Weaver. *Journal of Experimental Botany*, 64 (5), 1193–1208.

Robinson, B.H., Moradi, A., and Lehmann, E., 2008. Neutron Radiography for the Analysis of Plant – Soil Interactions. *Encyclopedia of Analytical Chemistry: Applications, Theory and Instrumentation*, 1–8.

Rockström, J., Williams, J., Daily, G., Noble, A., Matthews, N., Gordon, L., Wetterstrand, H., DeClerck, F., Shah, M., Steduto, P., de Fraiture, C., Hatibu, N., Unver, O., Bird, J., Sibanda,

L., and Smith, J., 2017. Sustainable intensification of agriculture for human prosperity and global sustainability. *Ambio*, 46 (1), 4–17.

Roder, W.R., 2001. *Slash-and-burn rice system in the hills of Northern Lao PDR: description, challenges, and opportunity*. Weed Research.

Rogers, E.D. and Benfey, P.N., 2015. Regulation of plant root system architecture: Implications for crop advancement. *Current Opinion in Biotechnology*.

Rogers, E.D., Monaenkova, D., Mijar, M., Nori, A., Goldman, D.I., and Benfey, P.N., 2016. X-Ray Computed Tomography Reveals the Response of Root System Architecture to Soil Texture. *Plant Physiology*, 171 (3), 2028–2040.

Ronchi, C.P., DaMatta, F.M., Batista, K.D., Moraes, G.A.B.K., Loureiro, M.E., and Ducatti, C., 2006. Growth and photosynthetic down-regulation in Coffea arabica in response to restricted root volume. *Functional Plant Biology*, 33 (11), 1013.

Royal Society, 2016. How are GM crops regulated? [online]. Available from: https://royalsociety.org/topics-policy/projects/gm-plants/how-are-gm-crops-regulated/ [Accessed 20 Sep 2019].

Roychoudhury, P., Pillai, G.R., Pandey, S.L., Krishna Murti, G.S.R., and Venkataraman, G.S., 1983. Effect of blue-green algae on aggregate stability and rice yield under different irrigation and nitrogen levels. *Soil and Tillage Research*, 3 (1), 61–65.

Rudolph-Mohr, N., Vontobel, P., and Oswald, S.E., 2014. A multi-imaging approach to study the root-soil interface. *Annals of Botany*, 114 (8), 1779–1787.

Ruggiero, A., Punzo, P., Landi, S., Costa, A., Oosten, M.J. Van, Grillo, S., Alvino, A., Freire, M.I., and Ferreira, R., 2017. Improving Plant Water Use Efficiency through Molecular Genetics, 1–22.

Sachs, T., 2005. *Pattern formation in plant tissues*. Cambridge University Press.

Saito, K., Asai, H., Zhao, D., Laborte, A.G., and Grenier, C., 2018. Progress in varietal improvement for increasing upland rice productivity in the tropics. *Plant Production Science*, 21 (3), 145–158.

Sander, T., Gerke, H.H., and Rogasik, H., 2008. Assessment of Chinese paddy-soil structure using X-ray computed tomography. *Geoderma*, 145 (3–4), 303–314.

Sanguineti, M.C., Li, S., MacCaferri, M., Corneti, S., Rotondo, F., Chiari, T., and Tuberosa, R., 2007. Genetic dissection of seminal root architecture in elite durum wheat germplasm. *Annals of Applied Biology*, 151 (3), 291–305.

Sarkar, N. and Aikat, K., 2012. Kinetic Study of Acid Hydrolysis of Rice Straw. *ISRN Biotechnology*, 2013, 1–5.

Sarkar, S., 2006. Water use efficiency of rice (Oryza sativa L.) under intermittent ponding and different intensity of puddling. *Archives of Agronomy and Soil Science*, 52 (3), 339–346.

Satbhai, S.B., Ristova, D., and Busch, W., 2015. Underground tuning: Quantitative regulation of root growth. *Journal of Experimental Botany*.

Sato, E.M., Hijazi, H., Bennett, M.J., Vissenberg, K., and Swarup, R., 2015. New insights into root gravitropic signalling. *Journal of Experimental Botany*, 66 (8), 2155–2165.

Scharlemann, J.P., Tanner, E.V., Hiederer, R., and Kapos, V., 2014. Global soil carbon: understanding and managing the largest terrestrial carbon pool. *Carbon Management*, 5 (1), 81–91.

Schellmann, S., Schnittger, A., Kirik, V., Wada, T., Okada, K., Beermann, A., Thumfahrt, J., Jürgens, G., and Hülskamp, M., 2002. TRIPTYCHON and CAPRICE mediate lateral inhibition during trichome and root hair patterning in Arabidopsis. *The EMBO Journal*, 21 (19), 5036–5046.

Schiefelbein, J.W., 1990. Genetic Control of Root Hair Development in Arabidopsis thaliana. *the Plant Cell Online*, 2 (3), 235–243.

Schrader, S., Rogasik, H., Onasch, I., and Jégou, D., 2007. Assessment of soil structural differentiation around earthworm burrows by means of X-ray computed tomography and scanning electron microscopy. *Geoderma*, 137 (3–4), 378–387.

Schuler, M.L., Mantegazza, O., and Weber, A.P.M., 2016. Engineering C4 photosynthesis into C3 chassis in the synthetic biology age. *The Plant journal : for cell and molecular biology*.

Schwarzenbach, R., Egli, T., … T.H.-A.R. of, and 2010, U., 2010. Global water pollution and human health. *Annual Review of Environment and Resources*, 35, 109.

Senapati, N. and Semenov, M.A., 2019. Assessing yield gap in high productive countries by designing wheat ideotypes. *Scientific reports*, 9 (1), 5516.

Shaheen, R. and Hood-Nowotny, R.C., 2005. Effect of drought and salinity on carbon isotope discrimination in wheat cultivars. *Plant Science*, 168 (4), 901–909.

Shen, H., Zhong, X., Zhao, F., Wang, Y., Yan, B., Li, Q., Chen, G., Mao, B., Wang, J., Li, Y., Xiao, G., He, Y., Xiao, H., Li, J., and He, Z., 2015. Overexpression of receptor-like kinase ERECTA improves thermotolerance in rice and tomato. *Nature biotechnology*, 33 (9), 996–1003.

Shepherd, G.., 2000. *VISUAL SOIL ASSESSMENT Volume 1: Field guide for cropping & pastoral grazing on flat to rolling country*. Palmerston North.: horizons.mw & Landcare Research.

Shewry, P.R. and Hey, S.J., 2015. The contribution of wheat to human diet and health. *Food and Energy Security*, 4 (3), 178–202.

Shrawat, A.K. and Lörz, H., 2006. Agrobacterium-mediated transformation of cereals: a promising approach crossing barriers. *Plant Biotechnology Journal*, 4 (6), 575–603.

Six, J., Bossuyt, H., Degryze, S., and Denef, K., 2004. A history of research on the link between (micro)aggregates, soil biota, and soil organic matter dynamics. *Soil and Tillage Research*, 79 (1), 7–31.

Slack, S., York, L., Roghazai, Y., Lynch, J., BioRxiv, M.B.-, and 2018, U., 2018. Wheat shovelomics II: Revealing relationships between root crown traits and crop growth. *biorxiv.org*.

Smit, A., Bengough, A., Engels, C., and Noordwijk, M. van, 2000. *Root Methods A Handbook*. Springer.

Smith, P., 2015. Malthus is still wrong: We can feed a world of 9-10 billion, but only by reducing food demand. *Proceedings of the Nutrition Society*, 74 (3), 187–190.

Smith, S. and De Smet, I., 2012. Root system architecture: insights from Arabidopsis and cereal

crops. *Philosophical Transactions of the Royal Society B: Biological Sciences*, 367 (April), 1441–1452.

Sotta, N. and Fujiwara, T., 2017. Preparing thin cross sections of arabidopsis roots without embedding. *BioTechniques*, 63 (6), 281–283.

Southon, T.E., Mattsson, A., and Jones, R.A., 1992. NMR imaging of roots: effects after root freezing of containerised conifer seedlings. *Physiologia Plantarum*, 329–334.

Sposito, G., 2013. Green Water and Global Food Security. *Vadose Zone Journal*, 12 (4).

Squire, G.R., Hawes, C., Valentine, T.A., and Young, M.W., 2015. Degradation rate of soil function varies with trajectory of agricultural intensification. *Agriculture, Ecosystems & Environment*, 202, 160–167.

Stanhill, G., 1986. Water use efficiency. *Advances in Agronomy*, 39.

Stingaciu, L., Schulz, H., Pohlmeier, A., Behnke, S., Zilken, H., Javaux, M., and Vereecken, H., 2013. In Situ Root System Architecture Extraction from Magnetic Resonance Imaging for Water Uptake Modeling. *Vadose Zone Journal*, 0 (0), 0.

Strobl, M., Manke, I., Kardjilov, N., Hilger, A., Dawson, M., and Banhart, J., 2009. Advances in neutron radiography and tomography. *Journal of Physics D: Applied Physics*, 42 (24).

Su, X., Chu, Y., Li, H., Hou, Y., Zhang, B., Huang, Q., Hu, Z., Huang, R., and Tian, Y., 2011. Expression of multiple resistance genes enhances tolerance to environmental stressors in transgenic poplar (Populus × euramericana 'Guariento'). *PloS one*, 6 (9), e24614.

Subira, J., Ammar, K., Alvaro, F., Garcia del Moral, L.F., Dreisigacker, S., and Royo, C., 2016. Changes in durum wheat root and aerial biomass caused by the introduction of the Rht-B1b dwarfing allele and their effects on yield formation. *Plant and Soil*, 403 (1–2), 291–304.

Sylvester-Bradley, R., Berry, P., Blake, J., Kindred, D., Spink, J., Bingham, I., McVittie, J., and Foulkes, J., 2015. Wheat Growth Guide. *AHDB Cereals & Oilseeds (Agriculture and Horticulture Development Board)*, 1–28.

Sys, C. and van Ranst, E., 1993. Land Evaluation III, (13 April 2007).

Takano, M., Inagaki, N., Xie, X., Yuzurihara, N., Hihara, F., Ishizuka, T., Yano, M., Nishimura, M., Miyao, A., Hirochika, H., and Shinomura, T., 2005. Distinct and cooperative functions of phytochromes A, B, and C in the control of deetiolation and flowering in rice. *The Plant cell*, 17 (December), 3311–3325.

Takano, M., Kanegae, H., Shinomura, T., Miyao, A., Hirochika, H., and Furuya, M., 2001. Isolation and characterization of rice phytochrome A mutants. *The Plant Cell*, 13 (3), 521–534.

Takano, M., Xie, X., Inagaki, N., and Shinomura, T., 2005. Distinct functions of phytochromes on the photomorphogenesis in rice. *Light Sensing in Plants*, 111–117.

Tanaka, N., Kato, M., Tomioka, R., Kurata, R., Fukao, Y., Aoyama, T., and Maeshima, M., 2014. Characteristics of a root hair-less line of arabidopsis thaliana under physiological stresses. *Journal of Experimental Botany*, 65 (6), 1497–1512.

Tanaka, Y., Sugano, S.S., Shimada, T., and Hara-Nishimura, I., 2013. Enhancement of leaf photosynthetic capacity through increased stomatal density in Arabidopsis. *New Phytologist*, 198 (3), 757–764.

Tang, X., Luo, Y., Lv, J., and Wei, C., 2012. Mechanisms of soil aggregates stability in purple paddy soil under conservation tillage of sichuan basin, China. *IFIP Advances in Information and Communication Technology*, 368 AICT (PART 1), 355–370.

Thao, H.T.B., George, T., Takeo, Y., and Widowati, L.R., 2008. Effects of soil aggregate size on phosphorus extractability and uptake by rice (Oryza sativa L.) and corn (Zea mays L.) in two Ultisols from the Philippines. *Soil Science and Plant Nutrition*, 54 (1), 148–158.

The Arabidopsis Genome Initiative., 2000. Analysis of the genome sequence of the flowering plant Arabidopsis thaliana. *Nature*, 408 (6814), 796–815.

The Royal Society of London, 2009. Reaping the benefits: science and the sustainable intensification of global agriculture. *The Royal society*, 2 (October), 35cm17.

Tisdall, J. and Oades, J., 1979. Stabilization of soil aggregates by the root systems of ryegrass. *Soil Research*, 17 (3), 429.

Tötzke, C., Kardjilov, N., Manke, I., and Oswald, S.E., 2017. Capturing 3D Water Flow in Rooted Soil by Ultra-fast Neutron Tomography. *Scientific Reports*, 7 (1), 6192.

Tracy, S.R., 2013. The response of root system architecture to soil compaction . , . *University of Nottingham*. University of Nottingham.

Tracy, S.R., Black, C.R., Roberts, J.A., Dodd, I.C., and Mooney, S.J., 2015. Using X-ray Computed Tomography to explore the role of abscisic acid in moderating the impact of soil compaction on root system architecture. *Environmental and Experimental Botany*, 110, 11–18.

Tracy, S.R., Black, C.R., Roberts, J.A., McNeill, A., Davidson, R., Tester, M., Samec, M., Korošak, D., Sturrock, C., and Mooney, S.J., 2012. Quantifying the effect of soil compaction on three varieties of wheat (Triticum aestivum L.) using X-ray Micro Computed Tomography (CT). *Plant and Soil*, 353 (1–2), 195–208.

Tracy, S.R., Black, C.R., Roberts, J.A., and Mooney, S.J., 2013. Exploring the interacting effect of soil texture and bulk density on root system development in tomato (Solanum lycopersicum L.). *Environmental and Experimental Botany*, 91, 38–47.

Tracy, S.R., Black, C.R., Roberts, J.A., Sturrock, C., Mairhofer, S., Craigon, J., and Mooney, S.J., 2012. Quantifying the impact of soil compaction on root system architecture in tomato (Solanum lycopersicum) by X-ray micro-computed tomography. *Annals of botany*, 110 (2), 511–519.

Tracy, S.R., Roberts, J.A., Black, C.R., McNeill, A., Davidson, R., and Mooney, S.J., 2010. The X-factor: Visualizing undisturbed root architecture in soils using X-ray computed tomography. *Journal of Experimental Botany*, 61 (2), 311–313.

Tron, S., Bodner, G., Laio, F., Ridolfi, L., and Leitner, D., 2015. Can diversity in root architecture explain plant water use efficiency? A modeling study. *Ecological Modelling*, 312, 200–210.

Tumlinson, L.G., Liu, H., Silk, W.K., and Hopmans, J.W., 2008. Thermal Neutron Computed Tomography of Soil Water and Plant Roots. *Soil Science Society of America Journal*, 72 (5), 1234.

Tung, S.A., Smeeton, R., White, C.A., Black, C.R., Taylor, I.B., Hilton, H.W., and Thompson, A.J., 2008. Over-expression of LeNCED1 in tomato (Solanum lycopersicum L.) with the rbcS3C promoter allows recovery of lines that accumulate very high levels of abscisic acid and exhibit severe phenotypes. *Plant, cell & environment*, 31 (7), 968–81.

Tuong, T.P. and Bhuiyan, S.I., 1999. Increasing water-use efficiency in rice production : farm-level perspectives, 40, 117–122.

Uga, Y., Sugimoto, K., Ogawa, S., Rane, J., Ishitani, M., Hara, N., Kitomi, Y., Inukai, Y., Ono, K., Kanno, N., Inoue, H., Takehisa, H., Motoyama, R., Nagamura, Y., Wu, J., Matsumoto, T., Takai, T., Okuno, K., and Yano, M., 2013. Control of root system architecture by DEEPER ROOTING 1 increases rice yield under drought conditions. *Nature Genetics*, 45 (9), 1097–102.

UNESCO, 2019. *The United Nations World Water Development Report 2019: Leaving No One Behind*. Paris.

UNIS, 2000. Secretary General address to Developing Countries 'South Summit'. *UN Information Service Press Release*.

United Nations, 2019. *World Population Prospects 2019: Data Booklet*. Department of Economic and Social Affairs Population Division. Department of Economic and Social Affairs Population Division.

Vijayan, P., Willick, I.R., Lahlali, R., Karunakaran, C., and Tanino, K.K., 2015. Synchrotron radiation sheds fresh light on plant research: The use of powerful techniques to probe structure and composition of plants. *Plant and Cell Physiology*, 56 (7), 1252–1263.

Vlassenbroeck, J., Masschaele, B., Cnudde, V., Dierick, M., Pieters, K., Van Hoorebeke, L., and Jacobs, P., 2006. Octopus 8: A High Performance Tomographic Reconstruction Package for X-ray Tube and Synchrotron micro-CT. *In*: *Advances in X-ray Tomography for Geomaterials*. London, UK: ISTE, 167–173.

Voorhess, W., Amemiya, M., Allmaras, R.R., and Larson, W.E., 1971. Some Effects of Aggregate Structure Heterogeneity on Root Growth. *Soil Science Society of America Journal*, 35 (4), 638–643.

Vörösmarty, C.J., McIntyre, P.B., Gessner, M.O., Dudgeon, D., Prusevich, a, Green, P., Glidden, S., Bunn, S.E., Sullivan, C. a, Liermann, C.R., and Davies, P.M., 2010. Global threats to human water security and river biodiversity. *Nature*, 467 (7315), 555–561.

Wada, T., 1997. Epidermal Cell Differentiation in Arabidopsis Determined by a Myb Homolog, CPC. *Science*, 277 (5329), 1113–1116.

Wada, T., Kurata, T., Tominaga, R., Koshino-Kimura, Y., Tachibana, T., Goto, K., Marks, M.D., Shimura, Y., and Okada, K., 2002. Role of a positive regulator of root hair development, CAPRICE, in Arabidopsis root epidermal cell differentiation. *Development*, 129 (23), 5409–5419.

Wada, Y., de Graaf, I.E.M., and van Beek, L.P.H., 2016. High-resolution modeling of human and climate impacts on global water resources. *Journal of Advances in Modeling Earth Systems*, 8 (2), 735–763.

Wada, Y., Wisser, D., and Bierkens, M.F.P., 2014. Global modeling of withdrawal, allocation and consumptive use of surface water and groundwater resources. *Earth System Dynamics*, 5 (1), 15–40.

Wadeson, N. and Basham, M., 2016. Savu: A Python-based, MPI Framework for Simultaneous Processing of Multiple, N-dimensional, Large Tomography Datasets.

Waines, J.G. and Ehdaie, B., 2007. Domestication and crop physiology: roots of green-

revolution wheat. *Annals of botany*, 100 (5), 991–8.

Wallace, J.. S., 2000. Increasing agricultural water use efficiency to meet future food production. *Agriculture, Ecosystems & Environment*, 82 (1–3), 105–119.

Wang, C., Liu, S., Dong, Y., Zhao, Y., Geng, A., Xia, X., and Yin, W., 2016. PdEPF1 regulates water-use efficiency and drought tolerance by modulating stomatal density in poplar. *Plant biotechnology journal*, 14 (3), 849–60.

Wang, D., Li, C., Parikh, S.J., and Scow, K.M., 2019. Impact of biochar on water retention of two agricultural soils – A multi-scale analysis. *Geoderma*, 340 (August 2018), 185–191.

Wang, M.-B. and Zhang, Q., 2009a. Issues in using the WinRHIZO system to determine physical characteristics of plant fine roots. *Acta Ecologica Sinica*, 29 (2), 136–138.

Wang, M. Ben and Zhang, Q., 2009b. Issues in using the WinRHIZO system to determine physical characteristics of plant fine roots. *Shengtai Xuebao/ Acta Ecologica Sinica*, 29 (2), 136–138.

Wang, X.-J., Zhang, J.-Y., Shahid, S., Guan, E.-H., Wu, Y., Gao, J., and He, R.-M., 2016. Adaptation to climate change impacts on water demand. *Mitigation and Adaptation Strategies for Global Change*, 21 (1), 81–99.

Wang, X., Yost, R.S., and Linquist, B.A., 2001. Soil Aggregate Size Affects Phosphorus Desorption from Highly Weathered Soils and Plant Growth. *Soil Science Society of America Journal*, 65 (1), 139–146.

Wang, Z., Han, Q., Zi, Q., Lv, S., Qiu, D., and Zeng, H., 2017. Enhanced disease resistance and drought tolerance in transgenic rice plants overexpressing protein elicitors from Magnaporthe oryzae. *PLoS ONE*, 12 (4).

Warren, J.M., Bilheux, H., Kang, M., Voisin, S., Cheng, C.L., Horita, J., and Perfect, E., 2013. Neutron imaging reveals internal plant water dynamics. *Plant and Soil*, 366 (1–2), 683–693.

Way, D.A., Katul, G.G., Manzoni, S., and Vico, G., 2014. Increasing water use efficiency along the C3 to C4 evolutionary pathway: a stomatal optimization perspective. *Journal of Experimental Botany*, 65 (13), 3683–3693.

Weaver, J.E., 1919. *The ecological relations of roots*. Carnegie Institution of Washington.

Whiteley, G.M. and Dexter, A.R., 1984. Displacement of soil aggregates by elongating roots and emerging shoots of crop plants. *Plant and Soil*, 77 (2–3), 131–140.

Whiteley, G.M., Hewitt, J.S., and Dexter, A.R., 1982a. The buckling of plant roots. *Physiologia Plantarum*, 54 (3), 333–342.

Whiteley, G.M., Hewitt, J.S., and Dexter, A.R., 1982b. The buckling of plant roots. *Physiologia Plantarum*, 54 (3), 333–342.

Wildenschild, D., Vaz, C.M.P., Rivers, M.L., Rikard, D., and Christensen, B.S.B., 2002. Using X-ray computed tomography in hydrology: Systems, resolutions, and limitations. *Journal of Hydrology*, 267 (3–4), 285–297.

Willatt, S.T. and Struss, R.G., 1979. Germination and Early Growth of Plants using neutron radiography, (March), 415–422.

Willatt, S.T., Struss, R.G., and Taylor, H.M., 1978. In situ Root Studies Using Neutron

Radiography, 1–6.

Wilmoth, J.C., Wang, S., Tiwari, S.B., Joshi, A.D., Hagen, G., Guilfoyle, T.J., Alonso, J.M., Ecker, J.R., and Reed, J.W., 2005. NPH4/ARF7 and ARF19 promote leaf expansion and auxin-induced lateral root formation. *Plant Journal*, 43 (1), 118–130.

Woodward, J., 1699. Some thoughts and Experiments concerining vegetation. *Royal Society, London*, 21 (253), 193–227.

WWF, 2003. Thirsty crops: Our food and clothes, eating up nature and wearing out the environment? *Living Waters*, 19, 1–20.

Xue, B., Huang, L., Huang, Y., Yin, Z., Li, X., and Lu, J., 2019. Effects of organic carbon and iron oxides on soil aggregate stability under different tillage systems in a rice–rape cropping system. *Catena*, 177 (January), 1–12.

Yadvinder-Singh, Bijay-Singh, and Timsina, J., 2005. Crop Residue Management for Nutrient Cycling and Improving Soil Productivity in Rice-Based Cropping Systems in the Tropics. *Advances in Agronomy*, 85, 269–407.

Yoder, R.E.R., 1936. A direct method of aggregate anylysis of soils and a study of the physical nature of erosion losses. *Agronomy Journal*, 28 (5), 1936.

Yu, J., Hu, S., Wang, J., Wong, G.K.S., Li, S., Liu, B., Deng, Y., Dai, L., Zhou, Y., Zhang, X., Cao, M., Liu, J., Sun, J., Tang, J., Chen, Y., Huang, X., Lin, W., Ye, C., Tong, W., Cong, L., Geng, J., Han, Y., Li, L., Li, W., Hu, G., Li, J., Liu, Z., Qi, Q., Li, T., Wang, X., Lu, H., Wu, T., Zhu, M., Ni, P., Han, H., Dong, W., Ren, X., Feng, X., Cui, P., Li, X., Wang, H., Xu, X., Zhai, W., Xu, Z., Zhang, J., He, S., Xu, J., Zhang, K., Zheng, X., Dong, J., Zeng, W., Tao, L., Ye, J., Tan, J., Chen, X., He, J., Liu, D., Tian, W., Tian, C., Xia, H., Bao, Q., Li, G., Gao, H., Cao, T., Zhao, W., Li, P., Chen, W., Zhang, Y., Hu, J., Liu, S., Yang, J., Zhang, G., Xiong, Y., Li, Z., Mao, L., Zhou, C., Zhu, Z., Chen, R., Hao, B., Zheng, W., Chen, S., Guo, W., Tao, M., Zhu, L., Yuan, L., and Yang, H., 2002. A draft sequence of the rice genome (Oryza sativa L. ssp. indica). *Science*, 296 (5565), 79–92.

Yu, L., Chen, X., Wang, Z., Wang, S., Wang, Y., Zhu, Q., Li, S., and Xiang, C., 2013. Arabidopsis enhanced drought tolerance1/HOMEODOMAIN GLABROUS11 confers drought tolerance in transgenic rice without yield penalty. *Plant physiology*, 162 (3), 1378–91.

Zappala, S., Helliwell, J.R., Tracy, S.R., Mairhofer, S., Sturrock, C.J., Pridmore, T., Bennett, M., and Mooney, S.J., 2013. Effects of X-Ray Dose On Rhizosphere Studies Using X-Ray Computed Tomography. *PLoS ONE*, 8 (6).

Zappala, S., Mairhofer, S., Tracy, S., Sturrock, C.J., Bennett, M., Pridmore, T., and Mooney, S.J., 2013. Quantifying the effect of soil moisture content on segmenting root system architecture in X-ray computed tomography images. *Plant and Soil*, 370 (1–2), 35–45.

Zarebanadkouki, M., Carminati, A., Kaestner, A., Mannes, D., Morgano, M., Peetermans, S., Lehmann, E., and Trtik, P., 2015. On-the-fly Neutron Tomography of Water Transport into Lupine Roots. *In*: *Physics Procedia*.

Zarebanadkouki, M., Kim, Y.X., and Carminati, A., 2013. Where do roots take up water? Neutron radiography of water flow into the roots of transpiring plants growing in soil. *New Phytologist*, 199 (4), 1034–1044.

Zarebanadkouki, M., Kim, Y.X., Moradi, A.B., Vogel, H.-J., Kaestner, A., and Carminati, A., 2012. Quantification and Modeling of Local Root Water Uptake Using Neutron

Radiography and Deuterated Water. *Vadose Zone Journal*, 11 (3).

Zarebanadkouki, M., Kroener, E., Kaestner, A., and Carminati, A., 2014. Visualization of root water uptake: quantification of deuterated water transport in roots using neutron radiography and numerical modeling. *Plant Physiol*, 166 (2), 487–499.

Zhao, D. and Liu, J., 2015. A new approach to assessing the water footprint of hydroelectric power based on allocation of water footprints among reservoir ecosystem services. *Physics and Chemistry of the Earth*, 79–82, 40–46.

Zhou, P. and Pan, G., 2007. Effect of different long-term fertilization treatments on particulate organic carbon in water-stable aggregates of a paddy soil. *Chinese Journal of Soil Science*, 38 (2), 256–261.

Zimin, A. V., Puiu, D., Hall, R., Kingan, S., Clavijo, B.J., and Salzberg, S.L., 2017. The first near-complete assembly of the hexaploid bread wheat genome, Triticum aestivum. *GigaScience*, 6 (11), 1–7.

Zobel, R.W., 2016. Arabidopsis: An adequate model for dicot root systems? *Frontiers in Plant Science*, 7 (FEB2016).

Zoulias, N., Harrison, E.L., Casson, S.A., and Gray, J.E., 2018. Molecular control of stomatal development. *The Biochemical journal*, 475 (2), 441–454.

Zuo, Q., Zhang, R., Shi, J., Timlin, D., and Ahuja, L.R., 2013. Characterization of the Root Length Density Distribution of Wheat Using a Generalized Function, 4, 93–118.

Appendix

Appendix 1: Neutron images of rice and wild grass illustrating the feint rice roots

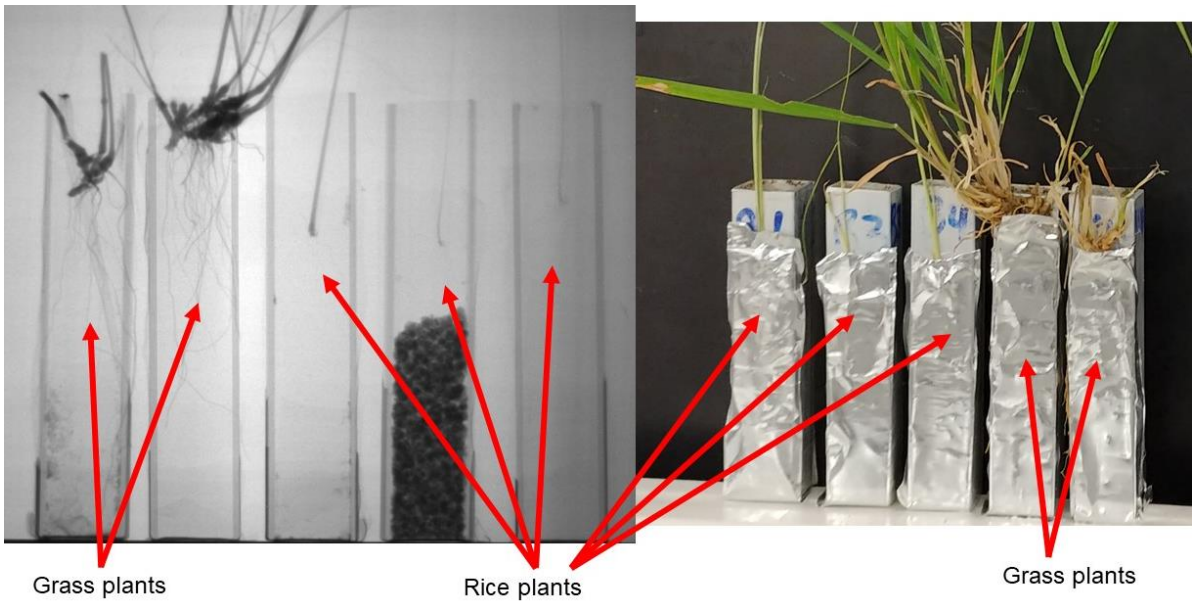

Appendix 2: Infrared camera images of Arabidopsis WUE mutants showing different leaf temperatures

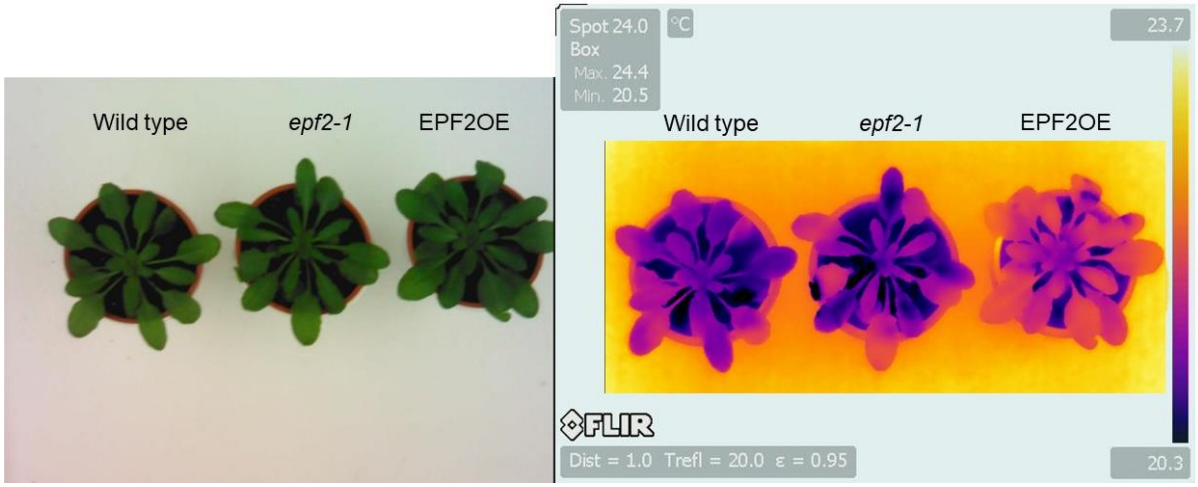

Wheat Root System Architecture and Soil Moisture Distribution in an Aggregated Soil using Neutron Computed Tomography.

Tinashe Mawodza[1*], Genoveva Burca[2], Stuart Casson[1], Manoj Menon[3]

[1]Department of Molecular Biology and Biotechnology, The University of Sheffield, Western Bank, Sheffield S10 2TN, United Kingdom

[2]STFC, Rutherford Appleton Laboratory, ISIS Facility, Harwell, OX11 0QX, UK

[3]Department of Geography, The University of Sheffield, 9 Northumberland Rd, Sheffield S10 2TN

* Corresponding author E-mail address: tmawodza1@sheffield.ac.uk

Non-invasive techniques are essential to deepen our understanding of root-soil interactions *in situ*. Neutron computed tomography (NCT) is an example of such techniques that have been successfully used to study these interactions in high resolution. Many of the studies using NCT however, have invariably focused on lupine plants and thus there is limited information available on other more commercially important staple crop plants such as wheat and rice. Also considering the high neutron sensitivity to hydrogen (e.g. water in roots or soil organic matter), nearly all previous in-situ NCT studies have used a relatively homogeneous porous media such as sand, low in soil organic matter and free from soil aggregates, to obtain high-quality images. However to expand the scope of the use of NCT to other more commercially important crops and in less homogenous soils, in this study we focused on wheat root growth in a soil that contained a considerable amount of soil organic matter (SOM) and different sized aggregates. As such, the main aims of this research were (1) to unravel wheat (*Triticum aestivum* cv. Fielder) root system architecture (RSA) when grown in an aggregated sandy loam soil (<4 mm) with 4% SOM content, (2) Map in 3D, soil water distribution after a brief drying period and

(3) to understand how the root system interacts with soil moisture distribution brought about by soil structural heterogeneity. To achieve these, wheat seedlings were grown for 13-days in aluminium tubes (100 mm height and 18 mm diameter) packed with soil and imaged for the first time at the IMAT neutron beamline (in the Rutherford Appleton Laboratory, UK). To the best of our knowledge, this is also the first study to use NCT to study wheat root architectural development. Our study proved that NCT can successfully be used to reveal wheat RSA in a heterogeneous aggregated soils with moderate amounts of SOM. Lateral root growth within the soil column was increased in regions with increased finer soil separates. NCT was also able to successfully map water distribution in a 3D and we show that large macro-aggregates preferentially retained relatively higher soil moisture in comparison to the smaller soil separates within our samples (Fig. 1). This highlights the importance large macro-aggregates in sustainable soil management as they may be able to provide plants water during periodic dry spells. More in situ investigations are required to further understand the impact of different aggregate sizes on RSA and water uptake.

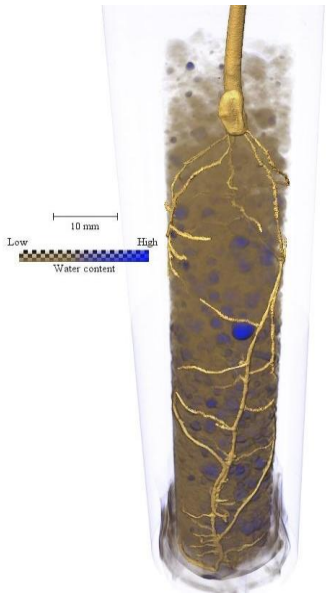

Figure 77: NCT image of a 13-day old wheat seedling root growing in an aggregated sandy loam soil. The colour map indicates water distribution within the soil column.

Key Words: Wheat, Root architecture, Neutron Computed tomography; Water dynamics

1. Introduction

The seemingly insurmountable task of feeding a growing global population with increasingly limited natural resources is one of the greatest challenges facing humanity in the 21st century (Borlaug and Dowswell 2003, Lal 2016). With the effects of climate change threatening to further disturb global production patterns across the world, it is imperative for the research community to devise possible strategies to increase global crop productivity in the forthcoming decades (IPCC 2007, Knox *et al.* 2012). This will require a deeper understanding of factors affecting crop production systems using contemporary technologies. One such area of research that has received increased attention of late is that of belowground root-soil interactions. These interactions are a vital part of the crop production system as plants acquire the majority of the resources they use for production via these associations and thus increasing our understanding of these interactions may hold the key for a 'second green revolution' required to feed a rapidly growing population (Lynch 2007, Gewin 2010, Rich and Watt 2013).

Understanding root-soil interactions especially amongst the worlds' major cereal crops (maize, wheat, rice) is of paramount importance for the attainment of sustainable global food security as these crops provide more than two thirds of all human dietary energy (Cassman 1999, Khoury *et al.* 2014, FAOSTAT 2019). This understanding is crucial for wheat in particular as it is arguably the worlds' most important staple food crop. It accounts for more than 15% (220 million ha) of global arable land use, (the highest for any cultivated plant) and often yields in excess of 700 million metric tonnes of grain per annum globally (FAOSTAT 2019). In spite of its great importance however, yield gaps in wheat production still exist, often as a result of poor adaptation of its root system to varying edaphic conditions (Waines and Ehdaie 2007, Senapati and Semenov 2019). As such increased research into root-soil interactions in wheat to tailor its

root system for different soil environments is pivotal for improving wheat yields especially in marginal areas (Waines and Ehdaie 2007, Figueroa-Bustos *et al.* 2018, Alahmad *et al.* 2019).

Traditionally these root-soil interactions have been investigated using either inference root health from the development of above ground parts (shoots) or by the more labour intensive invasive soil excavation methods (Pierret, *et al*. 2005). These observations however, although useful, lacked critical root developmental detail required to make conclusive inferences into how best to improve plant productivity (Mooney *et al.* 2012). Even when elements of the root-soil interactions were deduced, high throughput measurements were often very difficult to obtain which limited research into subterranean interactions.

The advent of non-invasive soil imaging in the late 70's marked a significant step forward in the study of plant-soil interactions with technologies such as X-Ray Computed Tomography (X-Ray CT) (Crestana, *et al*, 1986; Keyes *et al.*, 2013; Tracy *et al.*, 2013; Ahmed *et al.*, 2016; Blunk *et al.*, 2017; Burr-Hersey *et al.*, 2017; Koebernick *et al.*, 2017), Magnetic Resonance Imagery (MRI) (Stingaciu *et al.* 2013, Metzner *et al.* 2015, Pflugfelder *et al.* 2017), Nuclear Magnetic Resonance imaging (NMR)(Bačić and Ratković, 1987; Brown *et al.*, 1991; Southon, *et al*, 1992) and Neutron imaging (NI) (Willatt, et al, 1978; Furukawa, et al. 1999; Menon *et al.*, 2007; Tötzke *et al.*, 2017) being used to answer a multitude of questions about root-soil interactions in great detail. Of these technologies NI has been the most effective non-invasive soil imaging technique used when studying water dynamics and root growth within the soil due to its high sensitivity to hydrogen which is abundant in water (Robinson, et al. 2008). Willatt. et al, (1978), demonstrated the use of this method for the first time, successfully imaging roots of different plants (soya bean and maize) growing in soil. Subsequently this technology was used by in many studies including Willatt and Struss (1979), Couchat *et al.*, (1980), Bois and Couchat, (1983), (Nakanishi, et al 1992) as well as Furukawa, et al. (1999). Two papers by

Menon *et al* (2007) and Moradi *et al.*, (2009) also provided a comprehensive, accurate description of NI that subsequently led to even more insightful studies using NI.

Initial plant experiments with NI involved the use of 2 dimensional neutron radiography (NR) to study the root architectural properties in situ (Willatt and Struss 1979, Couchat *et al.* 1980, Bois and Couchat 1983) using thin slabs made of aluminium. The most extensively used plants in NI have been maize *(Zea mays L.)* pioneered in experiments by Willatt, et al. (1978) and lupine (*Lupinus albus L.)* first used by Nakanishi, et al. (1992) with the majority of papers being published on NI in plant-soil interaction mainly focusing on them. Research in soil NI has since moved on to the study of more complex root-soil processes such as dynamics of water flux and the extent of rhizosphere which had previously been difficult to study using other techniques (Oswald *et al.* 2008, Carminati *et al.* 2010). Visualisation of water movement coupled with the ability to use tracers such as heavy water (D_2O) in NI has led to a better understanding of water uptake and transport in specific roots with Zarebanadkouki, *et al.* (2013) showing that most of the water uptake in 3 week old lupine plants is carried out by the lateral roots with the tap root mainly acting as a conduit for upwards water movement.

Unlike NR, there have been fewer studies that have used neutron computed tomography (NCT) to study soil-root water dynamics despite the fact that computed tomography has the potential to provide even more detailed 3D visualisation of plant-soil systems as compared to NR. Its uptake may have been limited by the size of the specimen that can be successfully imaged in detail (usually no more than 20mm in diameter) as well as the time required for such images to be taken, which is much longer than that for individual neutron radiographs (Warren *et al.* 2013). The initial work done by Tumlinson *et al.*, (2008) and Esser *et al.*, (2010) with maize seedlings and lupine seedlings showed that visualisation of root and water distribution dynamics in soils can be visualised successfully in 3D using NCT with improved root-soil

contrast as compared to other non-invasive imaging techniques. Moradi *et al.*, (2011) went a step further in their study with lupine plants showing that water dynamics at the microscale can be accurately observed in 3D and thus can be used in complex and precise modelling operations explaining rhizosphere water flux. Recent advancement in NCT by Zarebanadkouki et al., (2015) who visualised 3D water dynamics of lupine plants in real time, provide great prospects of the use of NCT in further plant-soil interaction studies.

Regardless of the recent advancements in NCT in plant-soil interaction studies, there are some important limitations for this technique. For example, all of the previous studies utilising NCT have used soils containing no less than 90% sand, which are mostly devoid of organic matter or macro-aggregates. Therefore, for a wider application of this method it will require testing further using a variety of soil textures and structures. Also conspicuous in many NI studies to date is the absence wheat root architectural investigations using this technology despite the crop being major contributor to global food security. As such it is important to test the feasibility of the use of NI on wheat plants, with the aim of enhancing knowledge on wheat roots and their interactions with soil moisture.

In this paper, we thus aimed at determining the 3D root architecture of wheat seedlings grown in an aggregated sandy loam soil with 4% organic matter content using NCT. Our specific objectives were to use NCT to: a) Map 3D wheat root architectural distribution within an aggregated sandy loam soil b) Visualise in 3D, soil water distribution after a brief drying period and (c) to understand how the root system architecture interacts with soil moisture distribution as brought about by soil structural heterogeneity within an aggregated soil.

2. Materials and methods

2.1 Sample preparation and plant growth

The soil used in this experiment was a sandy loam soil (70% Sand, 17% Clay, and 13% Silt) obtained from Cove farm (53°30'03.7"N 0°53'57.2"W) and had an organic carbon content of 5.59%. This soil was air dried and mechanically sieved through a 4mm sieve to eliminate large clods and aggregates. The sieving produced a dry aggregate size distribution of 24% for particles <250µm, 36% for 250-500µm, 13% for 500-1000 µm, 13% for 1000-2000µm and 14% for 2000-4000µm with 4% SOM. This was then packed into specially designed, closed bottom, cylindrical aluminium tubes (18mm internal diameter × 100mm height) to ensure a bulk density of 1.2g cm^{-3} within the tubes. A single wheat (*Triticum Aestivum*. L cv. Fielder) seed was sown about 1cm underneath the surface of the soil and the tubes were watered to a volumetric moisture content (θ) of 16.0±3.0% which was experimentally determined (using gravimetric methods) to be the field capacity of our growth tubes. This water content was maintained during the course of this experiment by daily surface irrigation to the predetermined weight corresponding to the above mentioned θ for each tube. The wheat seedlings were grown for 13 days (starting from date of planting) in a growth chamber maintained at a temperature of 22°C (day)/18°C (night) and a relative humidity of 55% with light intensity averaging 400µmol m^2 s^{-1} with an 8-hour day length. Watering was stopped 4 days before neutron imaging was carried out to enhance the contrast between the root and soil.

2.2 Neutron computed tomography set up

Neutron CT imaging was carried out at the IMAT neutron imaging beamline of the ISIS Neutron and Muon Source at the Rutherford Appleton Laboratory, UK. A more detailed

description of the IMAT imaging station can be found in (Burca *et al.*, 2013); Kockelmann et al., 2013 and Burca *et al.*, 2018). For these experiments the neutron beam was shaped to the field of view of 112.7 mm × 112.7 mm accompanied by a multiaxial tomography stage allowing for 2 simultaneous scans. The neutron radiographies were acquired with an optical camera box equipped with Andor Zyla 4.2 PLUS sCMOS with 2048×2048 pixels, an 85mm lens and 100 µm 6LiF/ZnS: Ag scintillator. The images produced had a pixel and voxel size of 55µm with 30s being the exposure time for each projection and an L(10000mm) /D (40mm)= 250. The time taken for a single scan of the plants was almost 6 hours with 654 radiographs being recorded using a rotation step of 0.55°. This was the best set up achievable on IMAT, suitable for our experiment (Mawodza *et al.* 2018).

2.3 Image reconstruction, root segmentation and analysis

The images were reconstructed using the commercial available Octopus 8.9 software (Octopus 2019), and images were corrected for neutron beam variation and camera noise using the flat images and dark images taken before and after image acquisition (Dierick *et al.* 2004, Vlassenbroeck *et al.* 2006). We did not use an scattering correction when processing our images. The final reconstructed stack of images were imported into Avizo ® 9.0.1 for root segmentation and analysis (FEI 2015).

We attempted to use automated root segmentation algorithms RooTrack (Mairhofer *et al.* 2012a) and Root1 (Flavel *et al.* 2017) but due to the great heterogeneity in water content both the soil and within roots, these proved unreliable for our samples. To get the best results, roots were manually segmented using the limited range paintbrush editor in the segmentation module in Avizo software. The segmented roots obtained from this process were then used to calculate root lengths, thickness, surface area and volume for each root scan. Segmentation of the larger seminal roots was primarily done using automated thresholding techniques available in Avizo

as there was a clear attenuation contrast between the soil and these roots. This was however not done universally throughout the whole root system as most of the smaller lateral roots as well as some sections of the larger seminal roots had attenuation values that poorly contrasted or were even lower than that of moist soil and aggregates surrounding them as shown in Figure 78. Time consuming manual segmentation based on a combination of localised differences in attenuation and the connectivity of circularly shaped pixel groups (as roots are usually circular in shape) enabled the segmentation of the outstanding lateral roots and seminal root sections throughout the soil columns. Calibration for water content was done using the same soil used in our experiments with known volumetric water contents similar to what was done in Moradi *et al.*, (2011). We then used this calibration to relate the relative neutron attenuation to the moisture content for all the images we acquired.

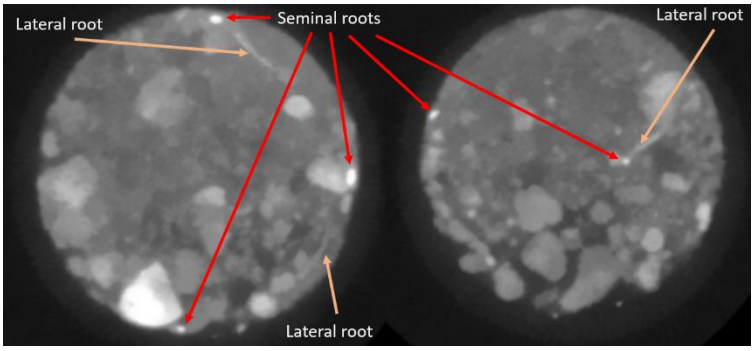

Figure 78: Grayscale images used to segment out roots showing how the different root types contrasted with the soil.

2.4 WinRhizo® root analysis

As segmentation was a subjective process, we compared the root properties obtained from our analysis with those obtained from flatbed scanning results analysed using WinRhizo ® (Regents Instruments, Inc.). Therefore, after CT scanning, the soils columns were destructively sampled and the soil was washed off from the roots over a 250µm sieve. The washed roots were then placed in a specially designed water tray and scanned using an Epson

Expression 10000XL Pro at 600dpi resolution. This scan obtained 2D images of the plant roots which were then analysed using WinRHIZO® 2016a software to determine the root properties (Wang and Zhang 2009b). These roots alongside their shoots were then dried at 65°C for 48 hours to obtain their dry biomass.

2.5 Statistical analysis

All graphs and statistical analysis for these experiments was performed using GraphPad Prism 8.0.1 (https://www.graphpad.com/) with a two tailed paired T tests used to separate means.

3. Results

3.1 3D wheat root architecture from NCT

Three-dimensional root architectural properties of the 13-day old wheat seedlings rendered from neutron scanning were successfully mapped with images in Fig 3. illustrating the different root systems of the six plants that were grown.

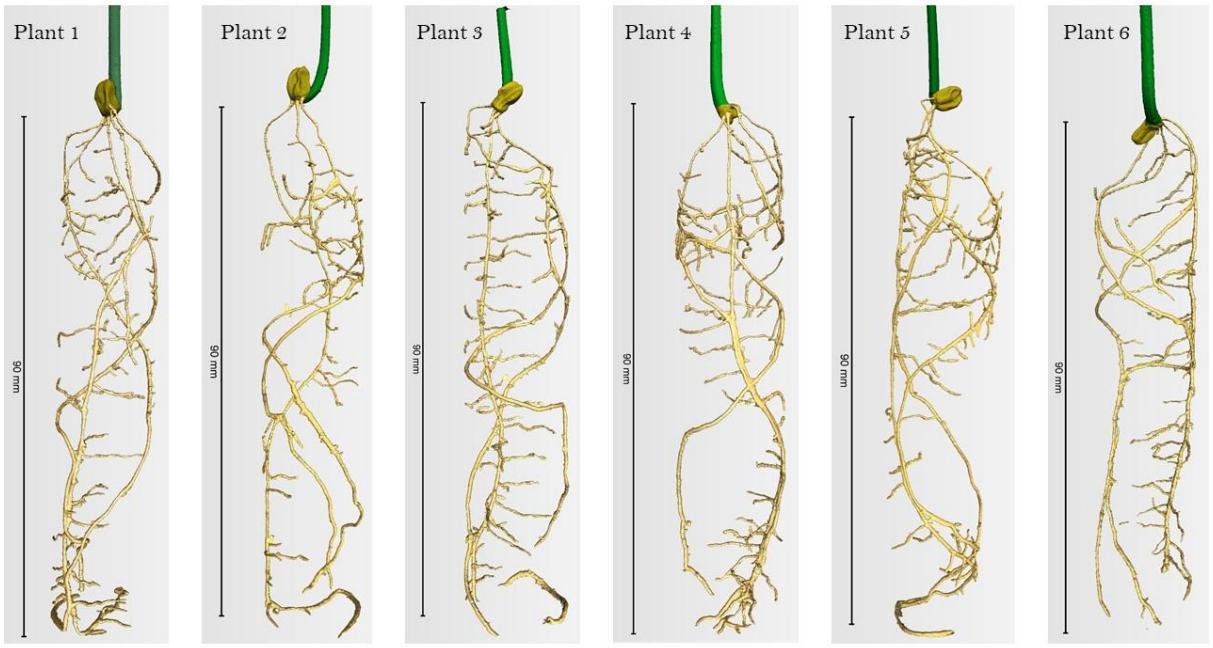

Figure 79: Images revealing the root architecture of the 6 different plants grown

The root architecture of the plants was broadly similar with an average total root length of 89.775 cm ±4.418 (SEM). The plants had 3-5 seminal roots at the time of imaging with least one of the roots (mainly the primary root) having grown to reach to the base of the growth tube they were growing in. Lateral roots of the different plants extended throughout the soil column with visible differences in lateral root growth especially in regions where the seminal roots were in close proximity to larger aggregates (1-4mm) that had large pores in-between them. Lateral roots growing in these regions tended to be fewer and longer whilst those growing in finer soil particles were more numerous but visibly shorter. This can be seen in Figure 80 where due to the random segregation of particles when packing, larger aggregates settled on one side of the column. Roots in some of the columns (plant 1, 4 and 6 in Figure 79) also coalesced together and grew side by side in their downwards trajectory, only disentangling lower down the soil column.

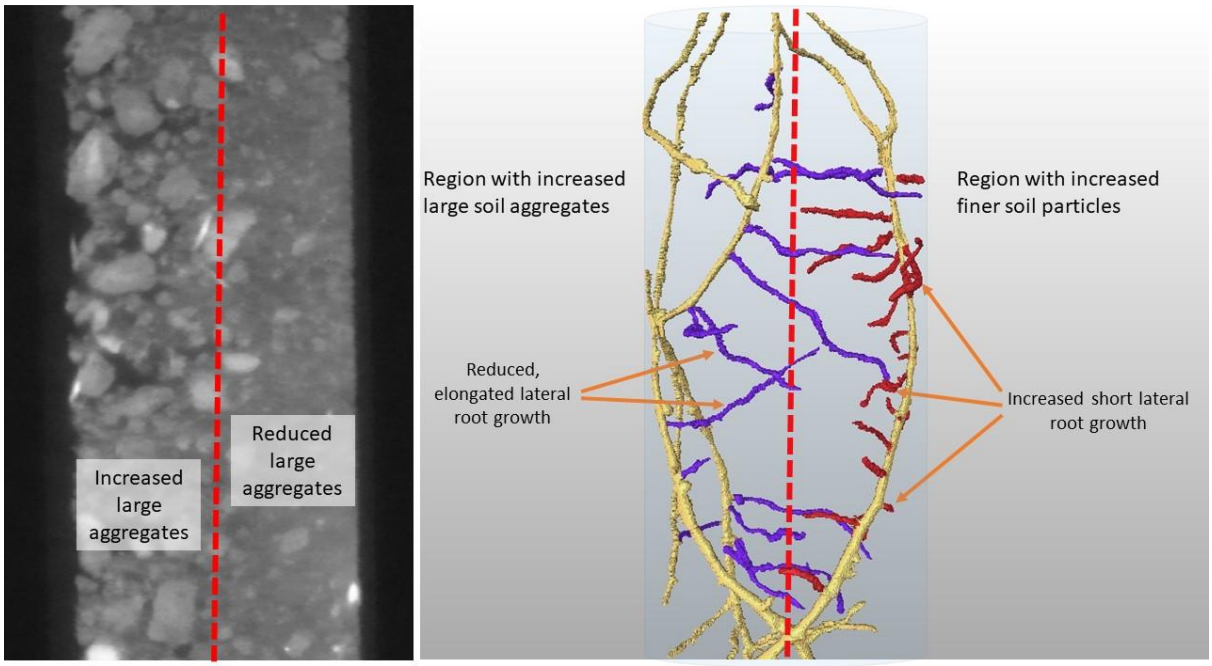

Figure 80 (Left)Greyscale image of a growth tube showing a segregation of large aggregates towards the left side of growth tube. (Right) increased shorter lateral root growth in regions with finer soil particles whilst lateral roots growing in regions with increased larger aggregates are reduced and longer. The red line demarcates an arbitrary boundary between regions dominated by large aggregates or finer particles. Longer lateral roots are shown in purple whilst short lateral roots are shown in red.

3.2 Comparison between 3D and 2D root properties

Root properties calculated using WinRhizo ® from the flatbed scanning and 3D NCT enabled the correlation of the two methods thus ensuring the validity of the method we used to segment out the roots. Visual comparison between images obtained using the two methods as shown in Figure 49 showed great similarities between them.

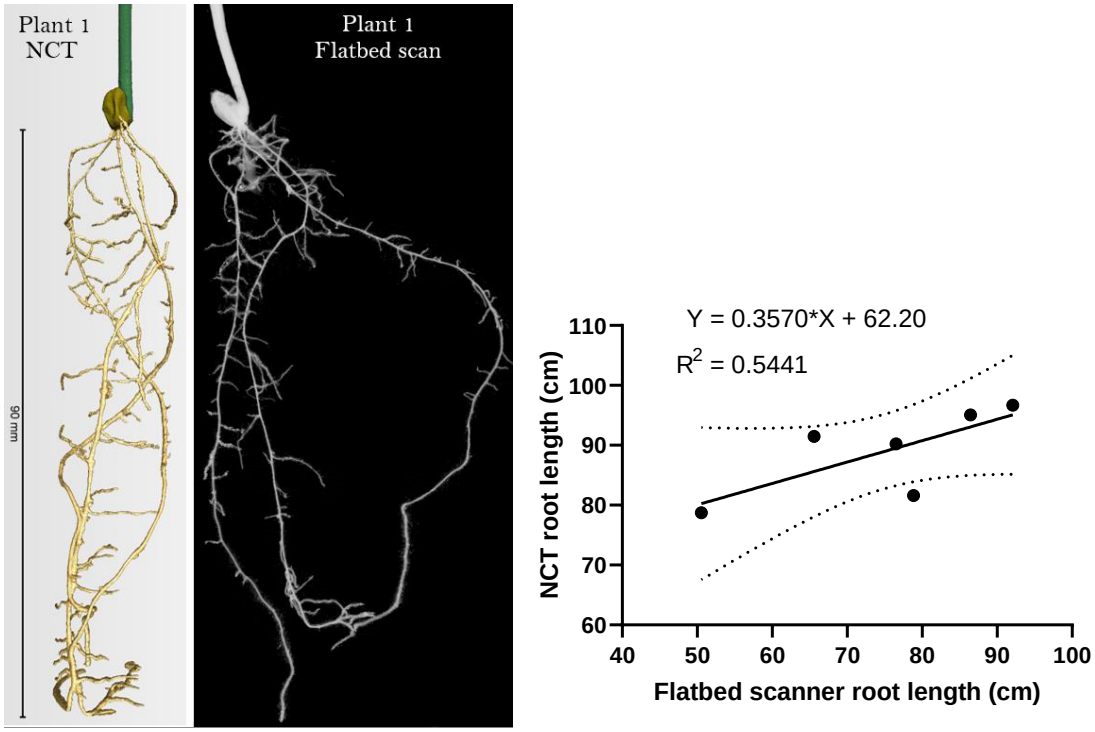

Figure 81: Side by side comparison of the same plant imaged using NCT and flatbed scanning

There was also a moderately strong linear relationship (R^2= 0.5441) between the root length estimated by the two methods as given in Figure 49. As shown in Figure 50, estimates of root length and surface area from neutron scans were significantly ($P<0.05$) higher than those from flatbed scanning whilst root volume and thickness did not vary between the two methods. The thinnest roots we could detect were around 110µm (2 voxels) in diameter which corresponds to double our image pixel size according to Nyquist–Shannon theorem.

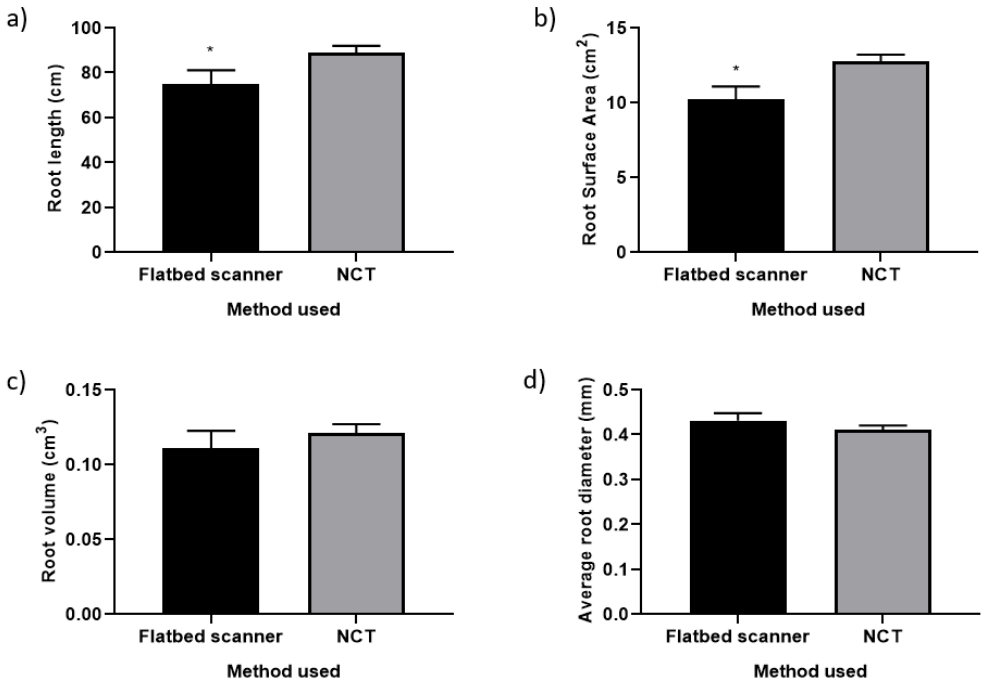

Figure 82: Comparison of root architectural properties as estimated by flatbed scanning and NCT. a) Root length (P= 0.0250), b) Root surface area, c) Root volume and d) Average root diameter. The error bars indicate Standard Error of the mean and * indicates significant differences (P< 0.05)

3.3 Soil moisture distribution

Similar to root architecture, the visualisation of soil moisture distribution was possible in 3D NCT as illustrated in Figure 83 with neutron attenuation being used as a proxy for θ using calibrated estimates of water content. These were calibrated by a series of scans of dry soil samples similar (but not identical) to those used for plant growth. It is worth noting however that our estimation of moisture content may encompass an add on effect with the high organic matter which increases neutron attenuation.

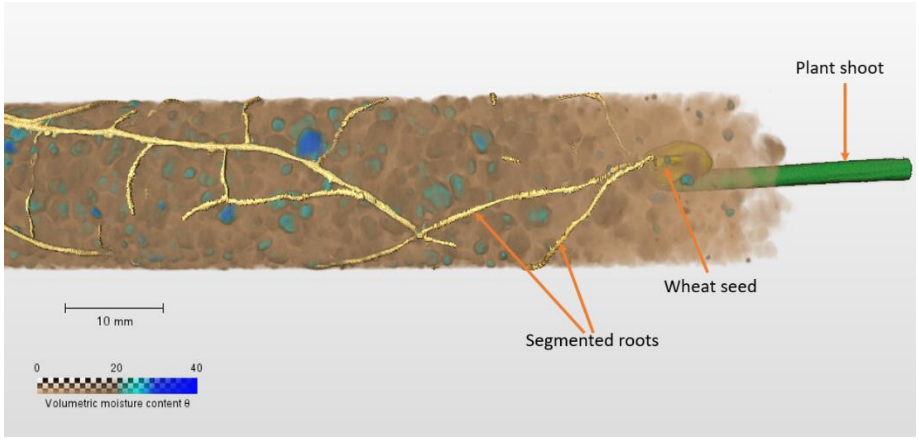

Figure 83: 3D NCT rendering of water distribution in aggregated soil where wheat seedling is growing

Water distribution within the columns was sporadic with regions of increased moisture localisation and depletion throughout the different tubes. Water depletion was greatest in the top 20mm of the soil with soil moisture gradually increasing between 20-60mm from the top of the column until it reached its greatest extent at the base of the tube. Water was largely localised in regions with nearly spherically shape regions within the soil as shown in Figure 84. Upon further analysis, it was discovered that this moisture accumulation was mainly associated with the heterogeneously distributed soil aggregates within the soil. As compared to finer particles, all or parts of aggregates have a $\theta > 20\%$.

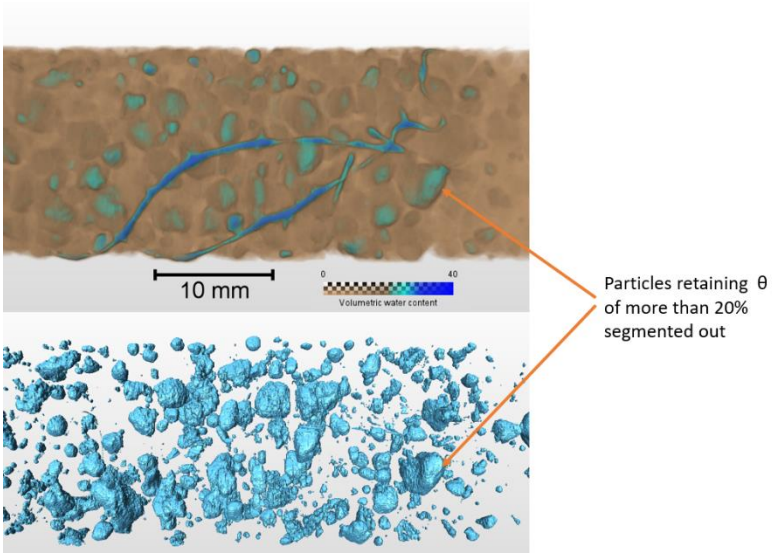

Figure 84: Showing segmenting out of particles retaining greater θ >20%

3.4 Root interactions with soil moisture

Wheat roots did not preferentially grow in regions of increased θ (blue regions with θ >20). Many of the roots that were observed did not penetrate into water rich aggregates but rather grew around them. Roots that were in direct contact with aggregates with a higher θ exhibited an increase in their internal θ. In large pores in-between soil aggregates, roots had reduced θ which was especially true in smaller lateral roots as opposed to the much larger seminal root network. Some seminal roots however also showed this unexpected internal θ decrease when growing through larger inter-aggregate pores. The rhizosphere around the roots as shown in Figure 52, did not show great differences in θ as compared to the rest of the soil with delineation of the extent of the rhizosphere being difficult decipher.

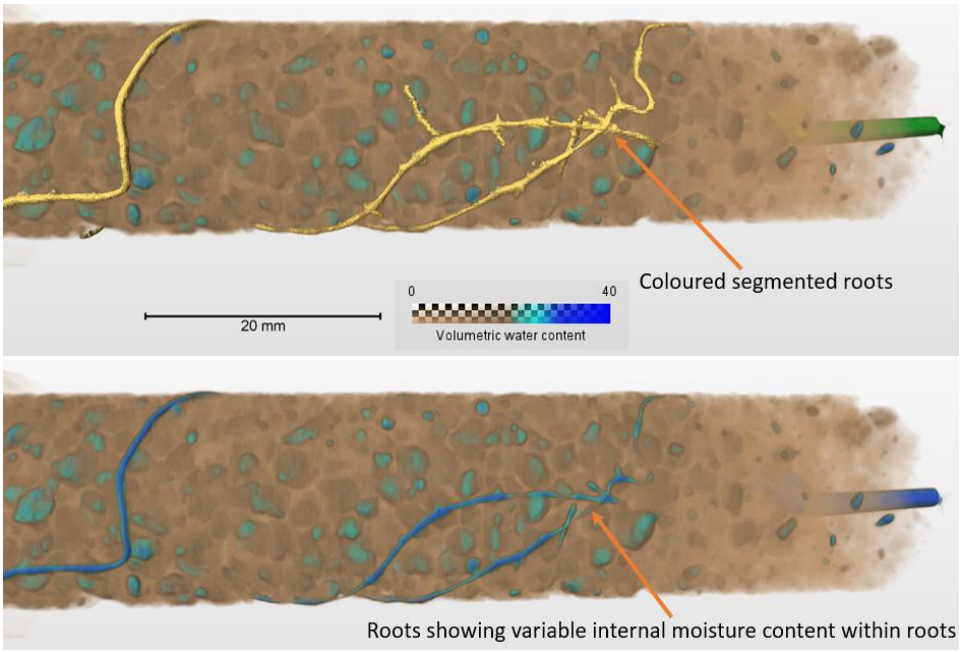

Figure 85: Variations in internal water content within roots growing through soil. The top image shows segmented root indicated in yellow whilst in the bottom image, only root moisture content can be visualised

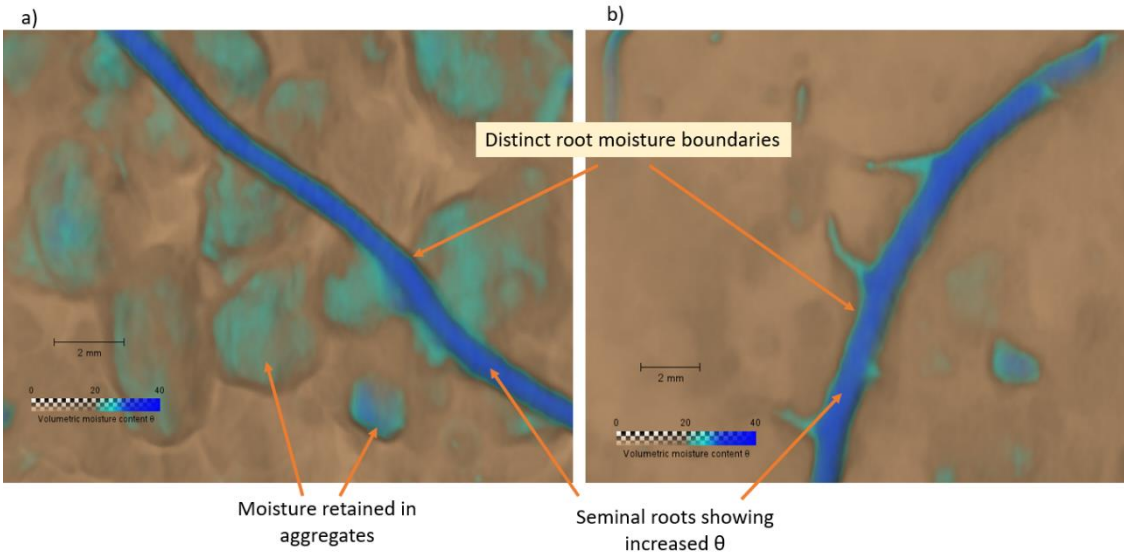

Figure 86: Close up view of the water-map in around seminal roots at a) 3cm and b) 5 cm below the soil surface showing distinct boundaries around the roots

4. Discussion

4.1 3D NCT wheat root architecture

The results presented show that detailed 3D root architectural properties of wheat growing in an aggregated soil with a moderately high organic matter content can successfully be visualised using NCT. To the best of our knowledge, this is the first study to use NCT to study root architectural development in wheat plants in detail. This research also represents a significant step away from many of the previous NCT root architectural studies such as those done by Nakanishi *et al.*, (2005), Moradi *et al.*, (2011), Warren *et al.*, (2013) and Tötzke *et al.*, (2017) that have used predominantly sand soils (with >90% sand). The sand soils used in the previously mentioned studies are more or less homogeneous and often lack aggregation. This study thereby seeks to break with convention by using a heterogeneous, aggregated soil with increased SOM. We recognise however, that the use of an aggregated soils as in this study presents a potential challenge when attempting to segment out wheat roots. This difficulty is brought about by the heterogeneity in soil properties with isolated regions retaining increased moisture and/or being high in organic matter (e.g. soil aggregates) that are highly neutron attenuating due to their increased hydrogen content (Robinson, *et al.* 2008). As a consequence of such features, there is a reduction in the clear attenuation difference between the soil and plant root matter that is characteristic in sand soils thus complicating segmentation as simple thresholding would yield inaccurate results. In this study we were able to overcome such difficulty by both localised thresholding using the increased attenuation and interconnectivity between roots as well as intuitive manual segmentation techniques.

This study represents a move away from the use of the leguminous dicotyledonous plant lupine (*Lupinus albus. L*) that has been popularly studied in many NCT and neutron radiography experiments ever since the pioneering work of (Nakanishi, et al. 1992) and then Menon *et al.*, (2007) who established this plant as a 'model' for non-invasive neutron imaging studies in plant-soil systems (Zarebanadkouki *et al.*, 2012; Rudolph-Mohr, *et al.* 2014; Ahmed *et al.*, 2017). Our use of the monocotyledonous graminae family plant, wheat represents one of the

first attempts at visualising the RSA of a staple food crop using NCT. Many of the non-invasive imagery done on wheat plants has been carried out exclusively using X-Ray CT (Jenneson *et al.* 1999, Mooney *et al.* 2006, Flavel *et al.* 2012, 2014, Tracy, Black, Roberts, McNeill, *et al.* 2012). This study thereby demonstrates the feasibility of using NCT to study the RSA of not only wheat plants but also other staple monocotyledonous crops such as rice and maize.

4.2 Comparison between 3D and 2D root properties

As the manual segmentation methods we used to reveal root architecture from NCT scans could be subjective, a comparison between the results obtained from NCT scanning and flatbed scanner scanning was done. This is the first time results from NCT have been compared to images flatbed scanning results. Similar correlations have previously been done in on X-Ray CT scan root measurements such as those by Tracy et al., (2015) and Flavel et al., (2012). In this study, here was moderately good correlation ($R^2 = 0.54$) between the two methods with respect to key essential root characteristics, root length and volume with estimates from flatbed scanning being significantly lower in root length. This could be explained by the fact that some roots are inevitably lost during washing with literature estimating a loss of about 20-40% of dry matter during storage and washing operations for wheat roots (van Noordwijk and Floris, 1979; Grzebisz. *et al*, 1989). These losses though, may be partially compensated for by the inability of our NCT to measure and quantify roots less than 110 µm (55µm pixel size ×2) which is 2 times each voxel size that is widely regarded as the effective spatial resolution limit of CT images (Moradi *et al.* 2011). Roots of this thickness can be picked up by flatbed scanning provided they are not lost during the washing process.

4.3 Soil moisture distribution

Similar to root system architecture, visualisation of soil moisture distribution was possible in 3D with the greyscale intensity acting as a proxy for θ. The high soil moisture heterogeneity

within the scanned tubes was as expected since soil heterogeneity often results in variable hydraulic conductivity throughout the soil which has a direct bearing on the θ in unsaturated conditions. As plants were surface irrigated, θ was lowest at the soil surface increasing steadily towards the base of the growth tube. This accumulation of water at the base of the tubes may have been brought about by the lack drainage as they were sealed at the base to allow for accurate determination of the gravimetric water content. Localisation of water as shown in Figure 84, which was presumed to be as a result to the preferential retention of water in aggregates. This preferential water retention was presumed to arise from the pore size distribution within soil aggregates which is often comprised of multiple micro-pores with the ability to store water at higher suctions as opposed to the inter-aggregate pores referred to in literature as structural pore spaces that are characteristically bigger and thus can freely transmit water. This preferential water retention however was not universal as some aggregates were also relatively dry at the time of imaging with some parts of the moist aggregates also being relatively drier as compared to the rest of the aggregate. This may suggest that that some aggregates may have pores large enough to drain freely at lower suction levels.

Inference of soil moisture status using NCT and neutron radiography is not new with several scholars having shown soil moisture distribution in sand soils. This study builds on their findings adding further complexity by looking at an aggregated soil that has an increased organic matter content. This introduces inaccuracies with the estimation of water content as in such a soil, water is not the only highly neutron attenuating substance as organic matter has increased hydrogen atom content as compared to soil (Robinson, et al. 2008; Tumlinson *et al.*, 2008). This thus means the total attenuation of each voxel is dependent on the water content as well as the organic matter content for the particular volume of soil under review. In this study we calibrated for water content using the same soil at varying levels of θ, however in doing this we assumed that the organic matter content throughout the soil was constant and variation in

attenuation was primarily due to increased soil moisture content. This estimation would be inaccurate especially in regions with localised elevated level of soil organic matter. As such our interpretation of soil moisture distribution should be taken with this in consideration.

4.4 Root interactions with soil moisture

As roots did not seem to grow preferentially in regions of relative high θ (are not highly hydrotropic), it is clear that many other factors such as gravity, pore size distribution and nutrient status of the soil may have also contributed to root growth patterns (Kar, et al. 1979; Niu *et al.*, 2015; Sato *et al.*, 2015). As roots grew around different aggregates probably as a consequence of trying to find the path of least resistance, many of the roots had good contact with the surface of the moist aggregates. Roots in contact with moist aggregate surfaces seemed to be able to extract water from these aggregates as more often than not, these roots exhibited an increased in θ. It was striking however that roots growing though large air spaces within the soil in some cases seemed to exhibit a reduction in θ as they passed through the pore space. This is thought to be as a result of increased evaporative water loss from the root surface within these large air spaces. Such large inter-aggregate pores may thus act as a hindrance to internal root hydraulic conductivity and thus limiting the functionality of roots growing through them. This finding could in part explain some of the observations seen by (Passioura and Stirzaker 1993) as well as Alexander and Miller (1991) who noticed a general reduction in plant growth when artificial holes are introduced or when plants are grown soils with large aggregate sizes.

Another unexpected result from our study was the absence of a distinct region of increased θ around the roots demarcating rhizosphere soil around the roots as shown in Figure 52. This is contrary to what has been observed in many neutron studies such as those done by (Moradi *et al.* 2011) who noticed this distinct feature in all the plants they studied. This variation could be as a result of our use of a different textured soil that may not produce such distinct features as

soil moisture was heterogeneously distributed within the soil. Differences in plant species difference i.e. wheat used in this study as compared to maize or lupins mainly used in previous studies could also be a contributory factor to our observed differences. Another plausible explanation for this could be in the difference of root segmentation protocols that were used in the different studies. In this case where semi-automatic and manual segmentation was employed based on the roots distinct increased attenuation properties, the edges of the roots could be mistaken to lie within the rhizosphere. This is however unlikely as the root thickness as estimated NCT compare well to that found by flatbed scanning. Questions may also be asked about the demarcation of root boundaries in the previous studies as many of these studies did not compare the thickness of the roots found in their scans to those obtained by manual measurement.

5. Conclusion

NCT was found to be able to reveal root architecture of wheat plants grown in an aggregated sandy loam soil with appreciable amounts of organic matter and inherent heterogeneity. This marks a step forward from the use of predominantly sand soils in NCT, albeit with new challenges of its own. Macro-aggregates increased water storage within the soil with their heterogeneous distribution determining the water distribution patterns across the soil after a period of drying which could help plants water acquisition in times of limited water supply. Lateral root growth was found to be reduced in regions with increased macro aggregates with roots growing through large inter-aggregate pores exhibiting loss of moisture that could potentially limit root function. Our work highlights how soil heterogeneity may affect water distribution and plant-soil interactions thus encouraging the further use of NCT technology to answer questions related soil water distribution in heterogeneous media for better modelling of soil water movement.

Funding and Acknowledgements

This research was funded as part of a PhD studentship by the Grantham Centre for Sustainable Futures at the University of Sheffield. Neutron imaging beamline grant (RB1820361) was provided by STFC ISIS Facility from Rutherford Appleton Laboratory, UK (Mawodza *et al.* 2018).

Conflicts of Interest

The authors declare no conflict of interest. The funders had no role in the design of the study; in the collection, analyses, or interpretation of data; in the writing of the manuscript, or in the decision to publish the results.

References

Abiven, S., Menasseri, S., and Chenu, C., 2009. The effects of organic inputs over time on soil aggregate stability - A literature analysis. *Soil Biology and Biochemistry*, 41 (1), 1–12.

Abogadallah, G.M., Nada, R.M., Malinowski, R., and Quick, P., 2011. Overexpression of HARDY, an AP2/ERF gene from Arabidopsis, improves drought and salt tolerance by reducing transpiration and sodium uptake in transgenic Trifolium alexandrinum L. *Planta*, 233 (6), 1265–1276.

Agrawal, RP and Jhorar, B., 1987. Soil Aggregates and Growth of Wheat. *J. Agronomy & Crop Science*, 158, 160–163.

Agrawal, R.P., Mundra, M., and Jhorar, B.S., 1984. Seedbed tilth and nitrogen response of wheat. *Soil & Tillage Research*, 4, 25–34.

Ahmed, M.A., Kroener, E., Holz, M., Zarebanadkouki, M., and Carminati, A., 2014.

Mucilage exudation facilitates root water uptake in dry soils. *Functional Plant Biology*, 41 (11), 1129–1137.

Ahmed, M.A., Zarebanadkouki, M., Ahmadi, K., Kroener, E., Kostka, S., Kaestner, A., and Carminati, A., 2017. Engineering Rhizosphere Hydraulics: Pathways to Improve Plant Adaptation to Drought. *Vadose Zone Journal*, 0 (0), 0.

Ahmed, M.A., Zarebanadkouki, M., Meunier, F., Javaux, M., Kaestner, A., and Carminati, A., 2018. Root type matters: Measurement of water uptake by seminal, crown, and lateral roots in maize. *Journal of Experimental Botany*, 69 (5), 1199–1206.

Ahmed, S., Klassen, T.N., Keyes, S., Daly, M., Jones, D.L., Mavrogordato, M., Sinclair, I., and Roose, T., 2016. Imaging the interaction of roots and phosphate fertiliser granules using 4D X-ray tomography. *Plant and Soil*, 401 (1–2), 125–134.

Aida, M., Vernoux, T., Furutani, M., Traas, J., and Tasaka, M., 2002. Roles of PIN-FORMED1 and MONOPTEROS in pattern formation of the apical region of the Arabidopsis embryo. *Development*, 129 (17), 3965–3974.

Alahmad, S., El Hassouni, K., Bassi, F.M., Dinglasan, E., Youssef, C., Quarry, G., Aksoy, A., Mazzucotelli, E., Juhász, A., Able, J.A., Christopher, J., Voss-Fels, K.P., and Hickey, L.T., 2019. A Major Root Architecture QTL Responding to Water Limitation in Durum Wheat. *Frontiers in Plant Science*, 10, 436.

Alberts, B., Johnson, A., Lewis, J., Raff, M., Roberts, K., and Walter, P., 2002. Studying Gene Expression and Function.

Alexander, K.G. and Miller, M.H., 1991. The effect of soil aggregate size on early growth and shoot-root ratio of maize (Zea mays L.). *Plant and Soil*, 138 (2), 189–194.

Alexandratos, N. and Bruinsma, J., 2003. World agriculture: towards 2015/2030: an FAO

perspective. *Land Use Policy*, 20 (4), 375.

Amezketa, E., Singer, M.., and Le Bissonnais, Y., 1996. Testing a New procedure for measuring water-stable aggregation, 888–894.

Anderson, I.S., 2009. *Neutron Imaging and Applications*.

Anderson, W.B. and Kemper, W.D., 1964. Corn Growth as Affected by Aggregate Stability, Soil Temperature, and Soil Moisture. *Agronomy Journal*, 56 (5), 1–4.

Angers, D.A. and Caron, J., 1998. Plant-induces changes in soil structure: Processes and feedbacks. *Biogeochemistry*.

AQUASTAT, 2014. FAO's Information System on Water and Agriculture [online]. Available from: http://www.fao.org/nr/water/aquastat/didyouknow/index3.stm [Accessed 22 Sep 2019].

Aravena, J.E., Berli, M., Menon, M., Ghezzehei, T.A., Mandava, A.K., Regentova, E.E., Pillai, N.S., Steude, J., Young, M.H., Nico, P.S., and Tyler, S.W., 2013. Synchrotron X-Ray Microtomography - New Means to Quantify Root Induced Changes of Rhizosphere Physical Properties. *Soil–Water–Root Processes: Advances in Tomography and Imaging. SSSA Special Publication 61*, sssaspecia (soilwaterrootpr), 39–68.

Ariani, A., Francini, A., Andreucci, A., and Sebastiani, L., 2016. Over-expression of AQUA1 in Populus alba Villafranca clone increases relative growth rate and water use efficiency, under Zn excess condition. *Plant cell reports*, 35 (2), 289–301.

Atkinson, J.A., Pound, M.P., Bennett, M.J., and Wells, D.M., 2019. Uncovering the hidden half of plants using new advances in root phenotyping. *Current Opinion in Biotechnology*, 55, 1–8.

Bačić, G. and Ratković, S., 1987. NMR studies of radial exchange and distribution of water in maize roots: The relevance of modelling of exchange kinetics. *Journal of Experimental Botany*, 38 (8), 1284–1297.

Bacon, M.A., 2004. *Water use efficiency in plant biology*. October.

Ball, B.C., Batey, T., and Munkholm, L.J., 2007. Field assessment of soil structural quality - a development of the Peerdklamp test. *Soil Use and Management*, 23 (4), 329–337.

Banavath, J.N., Chakradhar, T., Pandit, V., Konduru, S., Guduru, K.K., Akila, C.S., Podha, S., and Puli, C.O.R., 2018. Stress Inducible Overexpression of AtHDG11 Leads to Improved Drought and Salt Stress Tolerance in Peanut (Arachis hypogaea L.). *Frontiers in chemistry*, 6, 34.

Barker, R., Dawe, D., Tuong, T.P., Bhuiyan, S.I., and Guerra, L.C., 1999. The outlook for water resources in the year 2020 : challenges for research on water management in rice production. *Southeast Asia*, 1, 1–5.

Berardini, T.Z., Reiser, L., Li, D., Mezheritsky, Y., Muller, R., Strait, E., and Huala, E., 2015. The arabidopsis information resource: Making and mining the "gold standard" annotated reference plant genome. *genesis*, 53 (8), 474–485.

Berners-Lee, M., Kennelly, C., Watson, R., and Hewitt, C.N., 2018. Current global food production is sufficient to meet human nutritional needs in 2050 provided there is radical societal adaptation. *Elem Sci Anth*, 6 (1), 52.

Bertolino, L.T., Caine, R.S., and Gray, J.E., 2019. Impact of Stomatal Density and Morphology on Water-Use Efficiency in a Changing World. *Frontiers in Plant Science*, 10 (March), 225.

Bhagat, R., 2003. Management of soil physical properties of lowland puddled rice soil for

sustainable food production. *Lecture given at the College on Soil Physics*, (March), 65–75.

Bhatnagar-Mathur, P., Devi, M.J., Vadez, V., and Sharma, K.K., 2009. Differential antioxidative responses in transgenic peanut bear no relationship to their superior transpiration efficiency under drought stress. *Journal of plant physiology*, 166 (11), 1207–17.

Le Bissonnais, Y., 1996. Aggregate stability and assessment of soil crustability and erodibility: I. Theory and methodology. *European Journal of Soil Science*, 47 (4), 425–437.

Blankinship, J.C., Fonte, S.J., Six, J., and Schimel, J.P., 2016. Biotic versus abiotic controls on soil aggregate stability in a seasonally dry ecosystem. *Geoderma*, In review, 39–50.

Blilou, I., Xu, J., Wildwater, M., Willemsen, V., Paponov, I., Friml, J., Heidstra, R., Aida, M., Palme, K., and Scheres, B., 2005. The PIN auxin efflux facilitator network controls growth and patterning in Arabidopsis roots. *Nature*, 433 (7021), 39–44.

Blum, a., Munns, R., Passioura, J.B., Turner, N.C., Sharp, R.E., Boyer, J.S., Nguyen, H.T., Hsiao, T.C., Verma, D., and Hong, Z., 1996. Genetically Engineered Plants Resistant to Soil Drying and Salt Stress: How to Interpret Osmotic Relations? *Plant physiology*, 110 (4), 1051–1053.

Blum, A., 2005. Drought resistance, water-use efficiency, and yield potential—are they compatible, dissonant, or mutually exclusive? *Australian Journal of Agricultural Research*, 56 (11), 1159.

Blum, A., 2009. Effective use of water (EUW) and not water-use efficiency (WUE) is the target of crop yield improvement under drought stress. *Field Crops Research*, 112 (2–3),

119–123.

Blunk, S., Malik, A.H., de Heer, M.I., Ekblad, T., Bussell, J., Sparkes, D., Fredlund, K., Sturrock, C.J., and Mooney, S.J., 2017. Quantification of seed-soil contact of sugar beet (Beta vulgaris) using X-ray Computed Tomography. *Plant Methods*, 13 (1), 1–14.

Boccalandro, H.E., Rugnone, M.L., Moreno, J.E., Ploschuk, E.L., Serna, L., Yanovsky, M.J., and Casal, J.J., 2009. Phytochrome B enhances photosynthesis at the expense of water-use efficiency in Arabidopsis. *Plant physiology*, 150 (2), 1083–1092.

Bodner, G., Nakhforoosh, A., and Kaul, H.P., 2015. Management of crop water under drought: a review. *Agronomy for Sustainable Development*, 35 (2), 401–442.

Bois, J.F. and Couchat, P.H., 1983. Comparison of the Effects of Water Stress on the Root Systems of Two Cultivars of Upland Rice (Oryza satíva L .). *Annals of Botany*, 52, 479–487.

Bonsch, M., Popp, A., Biewald, A., Rolinski, S., Schmitz, C., Weindl, I., Stevanovic, M., H??gner, K., Heinke, J., Ostberg, S., Dietrich, J.P., Bodirsky, B., Lotze-Campen, H., and Humpen??der, F., 2015. Environmental flow provision: Implications for agricultural water and land-use at the global scale. *Global Environmental Change*, 30, 113–132.

Borland, A.M., Hartwell, J., Weston, D.J., Schlauch, K.A., Tschaplinski, T.J., Tuskan, G.A., Yang, X., and Cushman, J.C., 2014. Engineering crassulacean acid metabolism to improve water-use efficiency. *Trends in Plant Science*, 19 (5), 327–338.

Borlaug, N. and Dowswell, C., 2003. Feeding a world of ten billion people: a 21st century challenge. *… of the International Congress in the Wake …*, (May 2003), 3–23.

Bot, A.J., Nachtergaele, F.O., and Young, A., 2000. Land resource potential and constraints at regional and country levels. *World Soil Resources Reports*, 90, 1–114.

Boutraa, T., 2010. Improvement of Water Use Efficiency in Irrigated Agriculture: A Review. *Journal of Agronomy*, 9 (11), 1–8.

Brady, N.C. and Weil, R.R., 2017. *The nature and properties of soils*. 15th ed. Pearson.

Braunack, M.. and Dexter, A.., 1989. Soil Aggregation in the Seedbed: a Review. II. Effect of Aggregate Sizes on Plant Growth M.V. *Soil & Tillage Research*, 14, 281–298.

Briggs, L.J. and Shantz, H.L., 1913. The water requirements of plants I. *Bureau of Plant Industry Bulletin, USDA, Washington D.C*, 284.

Bronick, C.J. and Lal, R., 2005. Soil structure and management: A review. *Geoderma*, 124 (1–2), 3–22.

Brouwer, C. and Heibloem, M., 1986. Irrigation water needs. *Irrigation Water Management*, Vol. 102 (3), 1–40.

Brown, D.P., Pratum, T.K., Bledsoe, C., Ford, E.D., Cothern, J.S., and Perry, D., 1991. Noninvasive studies of conifer roots: nuclear magnetic resonance (NMR) imaging of Douglas-fir seedlings. *Canadian Journal of Forest Research*, 21, 1559–1566.

Brown, J.C., 2018. Photoreceptor regulation of plant responses to light and carbon dioxide. The University of Sheffield.

Brugière, N., Zhang, W., Xu, Q., Scolaro, E.J., Lu, C., Kahsay, R.Y., Kise, R., Trecker, L., Williams, R.W., Hakimi, S., Niu, X., Lafitte, R., and Habben, J.E., 2017. Overexpression of RING Domain E3 Ligase ZmXerico1 Confers Drought Tolerance through Regulation of ABA Homeostasis. *Plant physiology*, 175 (3), 1350–1369.

Burca, G., Kockelmann, W., James, J.A., and Fitzpatrick, M.E., 2013. Modelling of an imaging beamline at the ISIS pulsed neutron source. *Journal of Instrumentation*, 8 (10).

Burca, G., Nagella, S., Clark, T., Tasev, D., Rahman, I.A., Garwood, R.J., Spencer, A.R.T., Turner, M.J., and Kelleher, J.F., 2018. Exploring the potential of neutron imaging for life sciences on IMAT. *Journal of Microscopy*, 00 (0), 1–6.

Burr-Hersey, J.E., Mooney, S.J., Bengough, A.G., Mairhofer, S., and Ritz, K., 2017. Developmental morphology of cover crop species exhibit contrasting behaviour to changes in soil bulk density, revealed by X-ray computed tomography. *PLoS ONE*, 12 (7), 1–18.

Cailloux, M., 1972. Metabolism and the absorption of water by root hairs. *Canadian Journal of Botany*, 50 (3), 557–573.

Caine, R.S., Yin, X., Sloan, J., Harrison, E.L., Mohammed, U., Fulton, T., Biswal, A.K., Dionora, J., Chater, C.C., Coe, R.A., Bandyopadhyay, A., Murchie, E.H., Swarup, R., Quick, W.P., and Gray, J.E., 2019. Rice with reduced stomatal density conserves water and has improved drought tolerance under future climate conditions. *New Phytologist*, 221 (1), 371–384.

Cao, H.-X., Zhang, Z.-B., Xu, P., Chu, L.-Y., Shao, H.-B., Lu, Z.-H., and Liu, J.-H., 2007. Mutual physiological genetic mechanism of plant high water use efficiency and nutrition use efficiency. *Colloids and Surfaces B: Biointerfaces*, 57 (1), 1–7.

Carminati, A., Moradi, A.B., Vetterlein, D., Vontobel, P., Lehmann, E., Weller, U., Vogel, H.J., and Oswald, S.E., 2010. Dynamics of soil water content in the rhizosphere. *Plant and Soil*.

Carter, M.R. and Gregorich, E.G., 2006. *Soil Sampling and Methods of Analysis*. Measurement.

Cass, A., Gusli, S., and MacLeod, D.A., 1994. Sustainability of soil structure quality in rice

paddy— soya-bean cropping systems in South Sulawesi, Indonesia. *Soil and Tillage Research*, 31 (4), 339–352.

Cassman, K.G., 1999. Ecological intensification of cereal production systems: yield potential, soil quality, and precision agriculture. *Proceedings of the National Academy of Sciences of the United States of America*, 96 (11), 5952–9.

Casson, S.A., Franklin, K.A., Gray, J.E., Grierson, C.S., Whitelam, G.C., and Hetherington, A.M., 2009. phytochrome B and PIF4 Regulate Stomatal Development in Response to Light Quantity. *Current Biology*, 19 (3), 229–234.

Chaerle, L., Saibo, N., and Van Der Straeten, D., 2005. Tuning the pores: towards engineering plants for improved water use efficiency. *Trends in Biotechnology*, 23 (6), 308–315.

Chapman, H.D., 1965. Cation-exchange capacity 1. *Methods of soil analysis. Part 2. Chemical and microbiological properties*, (methodsofsoilanb), 891–901.

Chen, Y.-S., Lo, S.-F., Sun, P.-K., Lu, C.-A., Ho, T.-H.D., and Yu, S.-M., 2015. A late embryogenesis abundant protein HVA1 regulated by an inducible promoter enhances root growth and abiotic stress tolerance in rice without yield penalty. *Plant biotechnology journal*, 13 (1), 105–16.

Chen, Z., Ti, J. song, and Chen, F., 2017. Soil aggregates response to tillage and residue management in a double paddy rice soil of the Southern China. *Nutrient Cycling in Agroecosystems*, 109 (2), 103–114.

Clark, R.T., Famoso, A.N., Zhao, K., Shaff, J.E., Craft, E.J., Bustamante, C.D., Mccouch, S.R., Aneshansley, D.J., and Kochian, L. V., 2013. High-throughput two-dimensional root system phenotyping platform facilitates genetic analysis of root growth and

development. *Plant, Cell and Environment*, 36 (2), 454–466.

Clough, S.J. and Bent, A.F., 1998. Floral dip: A simplified method for Agrobacterium-mediated transformation of Arabidopsis thaliana. *Plant Journal*, 16 (6), 735–743.

Colorado Wheat, 2013. Why is the Wheat Genome So Complicated? | Colorado Wheat [online]. Available from: https://coloradowheat.org/2013/11/why-is-the-wheat-genome-so-complicated/ [Accessed 12 Sep 2018].

Condon, a. G., Richards, R. a., and Farquhar, G.D., 1987. Carbon Isotope Discrimination is Positively Correlated with Grain Yield and Dry Matter Production in Field-Grown Wheat1. *Crop Science*, 27 (5), 996.

Condon, A.G., Richards, R.A., Rebetzke, G.J., and Farquhar, G.D., 2004. Breeding for high water-use efficiency. *Journal of Experimental Botany*, 55 (407), 2447–2460.

Cornforth, I.S., 1968. The effect of the size of soil aggregates on nutrient supply. *The Journal of Agricultural Science*, 70, 83–85.

Couchat, P., Moutonnet, P., Houelle, M., and Picard, D., 1980. In situ study of corn seedling root and shoot growth by neutron radiography. *Agronomy Journal*, 72, 321-324 ST-In situ study of corn seedling root.

Cregg, B. and Zhang, J., 2000. Carbon isotope discrimination as a tool to screen for improved drought tolerance. *11th Metropolitan Tree Improvement Alliance (METRIA) Conference*, 13–20.

Crestana, S., Cesareo, R., and Mascarenhas, S., 1986. Using a computed tomography miniscanner in soil science. *Soil Science*, 142 (1), 56–61.

Czarnes, S., Hallett, P.D., Bengough, a. G., and Young, I.M., 2000. Root- and microbial-

derived mucilages affect soil structure and water transport. *European Journal Of Soil Science*, 51 (3), 435–443.

D'Ambrosio, E., De Girolamo, A.M., and Rulli, M.C., 2018. Assessing sustainability of agriculture through water footprint analysis and in-stream monitoring activities. *Journal of Cleaner Production*, 200, 454–470.

Darwin, C., 1880. *The power of movement in plants*. London: John Murray.

Davras, B.E., 1974. Loss-on-ignition as an estimate of soil organic matter. *Soil Science Society of America Journal*, 38 (1), 150–151.

Day, P.R., 1965. *Particle fractionation and particle-size analysis*. American Society of Agronomy, Soil Science Society of America.

Daynes, C.N., Field, D.J., Saleeba, J.A., Cole, M.A., and McGee, P.A., 2013. Development and stabilisation of soil structure via interactions between organic matter, arbuscular mycorrhizal fungi and plant roots. *Soil Biology and Biochemistry*, 57, 683–694.

Dayod, M., Aukett, L., Henderson, S., Tyerman, S.D., Shearer, M.K., Athman, A., Fuentes, S., Xu, B., Conn, S.J., Conn, V., Gilliham, M., and Hocking, B., 2013. Protocol: optimising hydroponic growth systems for nutritional and physiological analysis of Arabidopsis thaliana and other plants. *Plant Methods*, 9 (1), 4.

Derpsch, R., 1997. History of Crop Production , With & Without Tillage, 150–154.

Dexter, A.., 1978. A stochastic model for the growth of root s in tilled soil. *Journal of soil science*, (29), 102–116.

Dhakarey, R., Raorane, M.L., Treumann, A., Peethambaran, P.K., Schendel, R.R., Sahi, V.P., Hause, B., Bunzel, M., Henry, A., Kohli, A., and Riemann, M., 2017. Physiological and

Proteomic Analysis of the Rice Mutant cpm2 Suggests a Negative Regulatory Role of Jasmonic Acid in Drought Tolerance. *Frontiers in Plant Science*, 8, 1903.

Dharmappa, P.M., Doddaraju, P., Malagondanahalli, M. V., Rangappa, R.B., Mallikarjuna, N.M., Rajendrareddy, S.H., Ramanjinappa, R., Mavinahalli, R.P., Prasad, T.G., Udayakumar, M., and Sheshshayee, S.M., 2019. Introgression of Root and Water Use Efficiency Traits Enhances Water Productivity: An Evidence for Physiological Breeding in Rice (Oryza sativa L.). *Rice*, 12 (1), 14.

Diamond Light Source, 2019. Bird's eye view of the synchrotron [online]. Available from: https://www.diamond.ac.uk/Science/Machine/Components.html [Accessed 19 Sep 2019].

Diaz-Vivancos, P., Faize, L., Nicolás, E., Clemente-Moreno, M.J., Bru-Martinez, R., Burgos, L., and Hernández, J.A., 2016. Transformation of plum plants with a cytosolic ascorbate peroxidase transgene leads to enhanced water stress tolerance. *Annals of botany*, 117 (7), 1121–31.

Díaz-Zorita, M., Perfect, E., and Grove, J.H., 2002. Disruptive methods for assessing soil structure. *Soil and Tillage Research*, 64 (1–2), 3–22.

Dierick, M., Masschaele, B., and Van Hoorebeke, L., 2004. Octopus, a fast and user-friendly tomographic reconstruction package developed in LabView. *Measurement Science and Technology*, 15 (7), 1366–1370.

Dillard, H.R., 2019. Global food and nutrition security: from challenges to solutions. *Food Security*, 11 (1), 249–252.

Doheny-Adams, T., Hunt, L., Franks, P.J., Beerling, D.J., and Gray, J.E., 2012. Genetic manipulation of stomatal density influences stomatal size, plant growth and tolerance to

restricted water supply across a growth carbon dioxide gradient. *Phil. Trans. R. Soc. B*, 367, 547–555.

Donald, R., Kay, B., and Miller, M., 1987. The effect of soil aggregate size on early shoot and root growth of maize (Zea mays L.). *Plant and soil*, 103 (2), 251–259.

de Dorlodot, S., Forster, B., Pagès, L., Price, A., Tuberosa, R., and Draye, X., 2007a. Root system architecture: opportunities and constraints for genetic improvement of crops. *Trends in Plant Science*, 12 (10), 474–481.

de Dorlodot, S., Forster, B., Pagès, L., Price, A., Tuberosa, R., and Draye, X., 2007b. Root system architecture: opportunities and constraints for genetic improvement of crops. *Trends in Plant Science*.

Downie, H., Holden, N., Otten, W., Spiers, A.J., Valentine, T.A., and Dupuy, L.X., 2012. Transparent Soil for Imaging the Rhizosphere. *PLoS ONE*, 7 (9), 1–6.

Downie, H.F., Adu, M.O., Schmidt, S., Otten, W., Dupuy, L.X., White, P.J., and Valentine, T.A., 2015. Challenges and opportunities for quantifying roots and rhizosphere interactions through imaging and image analysis. *Plant, Cell and Environment*.

Drakopoulos, M., Connolley, T., Reinhard, C., Atwood, R., Magdysyuk, O., Vo, N., Hart, M., Connor, L., Humphreys, B., Howell, G., Davies, S., Hill, T., Wilkin, G., Pedersen, U., Foster, A., Maio, N. De, Basham, M., Yuan, F., and Wanelik, K., 2017. beamlines I12 : the Joint Engineering , Environment and Processing (JEEP) beamline at Diamond Light Source beamlines, (2015), 828–838.

Dunn, J., Hunt, L., Afsharinafar, M., Meselmani, M. Al, Mitchell, A., Howells, R., Wallington, E., Fleming, A.J., and Gray, J.E., 2019. Reduced stomatal density in bread wheat leads to increased water-use efficiency. *Journal of Experimental Botany*.

Eckardt, N.A., 2000. Sequencing the rice genome. *The Plant cell*, 12 (11), 2011–7.

Edwards, K., Johnstone, C., and Thompson, C., 1991. A simple and rapid method for the preparation of plant genomic DNA for PCR analysis. *Nucleic Acids Research*, 19 (6), 1349.

Ehrenfeld, J.G., Ravit, B., and Elgersma, K., 2005. Feedback in the Plant-Soil System. *Annual Review of Environment and Resources*, 30 (1), 75–115.

Erni, R., Rossell, M.D., Kisielowski, C., and Dahmen, U., 2009. Atomic Resolution Imaging with a sub-50 pm Electron Probe. *Physical Review Letters*, 102 (9), 1–10.

Eshel, A. and Beeckman, T., 2013. *Plant roots: the hidden half*.

ESRF, 2019. What is synchrotron light? [online]. Available from: https://www.esrf.eu/home/education/what-is-the-esrf/what-is-synchrotron-light.html [Accessed 19 Sep 2019].

Esser, H.G., Carminati, A., Vontobel, P., Lehmann, E.H., and Oswald, S.E., 2010. Neutron radiography and tomography of water distribution in the root zone. *Journal of Plant Nutrition and Soil Science*, 173 (5), 757–764.

Eyck, T. and Albert, M., 1899. *A Study of the Root Systems of Wheat, Oats, Flax, Corn, Potatoes and Sugar Beets, and of the Soil in which They Grew*. North Dakota Agricultural College, Governmental Agricultural Experiment ….

Fairhurst, T. and Dobermann, A., 2002. Rice in the Global Food Supply. *Rice Production*, 16 (May), 47.

Falasca, G. and Altamura, M.M., 2003. Histological analysis of adventitious rooting in *Arabidopsis thaliana* (L.) Heynh seedlings. *Plant Biosystems - An International Journal*

Dealing with all Aspects of Plant Biology, 137 (3), 265–273.

Fang, H., Rong, H., Hallett, P.D., Mooney, S.J., Zhang, W., Zhou, H., and Peng, X., 2019. Impact of soil puddling intensity on the root system architecture of rice (Oryza sativa L.)seedlings. *Soil and Tillage Research*, 193 (May), 1–7.

FAO, 2009. How to Feed the World in 2050. *Insights from an expert meeting at FAO*, 2050 (1), 1–35.

FAO, 2017. Water for Sustainable Food and Agriculture Water for Sustainable Food and Agriculture. *A report produced for the G20 Presidency of Germany*, 1–33.

FAOSTAT, 2019. FAOSTAT database [online]. *Food and Agriculture Organization of the United Nations, Rome, Italy*. Available from: http://www.fao.org/faostat/en/#home.

Farquhar, G D. Ehleringer, J.R. Hubic, K.T., Farquhar, G.D., Ehleringer, J.R., and Hubick, K.T., 1989. Carbon isotope discrimination and photosynthesis. *Plant physiology*, 40, 503–537.

Farquhar, G.D., Ehleringer, J.R., and Hubick, K.T., 1989. Carbon Isotope Discrimination and Photosynthesis. *Plant physiology*, 40, 503–537.

FEI, 2015. User's guide Avizo ® 9 [online].

Ferdous, J., Whitford, R., Nguyen, M., Brien, C., Langridge, P., and Tricker, P.J., 2017. Drought-inducible expression of Hv-miR827 enhances drought tolerance in transgenic barley. *Functional & integrative genomics*, 17 (2–3), 279–292.

Figueroa-Bustos, V., Palta, J., Chen, Y., and Siddique, K., 2018. Characterization of Root and Shoot Traits in Wheat Cultivars with Putative Differences in Root System Size. *Agronomy*.

Flavel, R.J., Guppy, C.N., Rabbi, S.M.R., and Young, I.M., 2017. An image processing and analysis tool for identifying and analysing complex plant root systems in 3D soil using non-destructive analysis : Root1, 1–18.

Flavel, R.J., Guppy, C.N., Tighe, M., Watt, M., McNeill, A., and Young, I.M., 2012. Non-destructive quantification of cereal roots in soil using high-resolution X-ray tomography. *Journal of Experimental Botany*, 63 (7), 2503–2511.

Flavel, R.J., Guppy, C.N., Tighe, M.K., Watt, M., and Young, I.M., 2014. Quantifying the response of wheat (Triticum aestivum L) root system architecture to phosphorus in an Oxisol. *Plant and Soil*, 385 (1–2), 303–310.

Francis, G.S., Haynes, R.J., and Koppi, A.J., 1994. Plant mediated improvement of soil structure after long-term arable cropping. *In*: *Proc New Zealand Soc Soil Sci Conf, Lincoln*.

Franks, P.J., W. Doheny-Adams, T., Britton-Harper, Z.J., and Gray, J.E., 2015. Increasing water-use efficiency directly through genetic manipulation of stomatal density. *New Phytologist*, 207 (1), 188–195.

French, A., Ubeda-Tomas, S., Holman, T.J., Bennett, M.J., and Pridmore, T., 2009. High-Throughput Quantification of Root Growth Using a Novel Image-Analysis Tool. *Plant Physiology*, 150 (4), 1784–1795.

Fulgencio, A.-C., Carlos, C.-V., Enrique, I.-L., Lenin, Y.-V., Claudia-Anahi, P.-T., Araceli, O.-A., Alfonso, M.-B., Sandra-Isabel, G.-M., Dolores, G.-A., Alejandra, C.-L., Betsy-Anaid, P.-O., Luis, H.-E., Alatorre-Cobos, F., Calderón-Vázquez, C., Ibarra-Laclette, E., Yong-Villalobos, L., Pérez-Torres, C.-A., Oropeza-Aburto, A., Méndez-Bravo, A., González-Morales, S.-I., Gutiérrez-Alanís, D., Chacón-López, A., Peña-Ocaña, B.-A.,

and Herrera-Estrella, L., 2014. An improved , low-cost , hydroponic system for growing Arabidopsis and other plant species under aseptic conditions. *BMC plant biology*, 14, 69.

Furukawa, J., Nakanishi, T.M., and Matsubayashi, M., 1999. Neutron radiography of a root growing in soil with vanadium. *Nuclear Instruments and Methods in Physics Research, Section A: Accelerators, Spectrometers, Detectors and Associated Equipment*, 424 (1), 116–121.

Gao, W., Schlüter, S., R.G.A.Blaser, S., Shen, J., and Vetterlein, D., 2019. A shape-based method for automatic and rapid segmentation of roots in soil from X-ray computed tomography images : Rootine.

Gewin, V., 2010. An underground revolution. *Nature*, 466 (July), 522–533.

Gibbs, H.K.K. and Salmon, J.M.M., 2015. Mapping the world's degraded lands. *Applied Geography*, 57, 12–21.

Giehl, R.F.H., Gruber, B.D., and Von Wir??n, N., 2014. It's time to make changes: Modulation of root system architecture by nutrient signals. *Journal of Experimental Botany*, 65 (3), 769–778.

Glinski, J. and Lipiec, J., 1990. *Soil Physical Conditions and Plant Growth*. CRC Press. CRC Press.

Godfray, H.C.J., Beddington, J.R., Crute, I.R., Haddad, L., Lawrence, D., Muir, J.F., Pretty, J., Robinson, S., Thomas, S.M., and Toulmin, C., 2010. Food security: the challenge of feeding 9 billion people., 327 (5967), 812–8.

Goff, S.A., Ricke, D., Lan, T., Presting, G., Wang, R., Dunn, M., Glazebrook, J., Sessions, A., Oeller, P., Varma, H., Hadley, D., Hutchison, D., Martin, C., Katagiri, F., Lange, B.M., Moughamer, T., Xia, Y., Budworth, P., Zhong, J., Miguel, T., Paszkowski, U.,

Zhang, S., Colbert, M., Sun, W., Chen, L., Cooper, B., Park, S., Wood, T.C., Mao, L., Quail, P., Wing, R., Dean, R., Yu, Y., Zharkikh, A., Shen, R., Sahasrabudhe, S., Thomas, A., Cannings, R., Gutin, A., Pruss, D., Reid, J., Tavtigian, S., Mitchell, J., Eldredge, G., Scholl, T., Miller, R.M., Bhatnagar, S., Adey, N., Rubano, T., Tusneem, N., Robinson, R., Feldhaus, J., Macalma, T., Oliphant, A., and Briggs, S., 2005. A Draft Sequence of the Rice Genome (Oryza sativa L. ssp. japonica). *Science*, 296 (August), 92–101.

González, C.V., Ibarra, S.E., Piccoli, P.N., Botto, J.F., and Boccalandro, H.E., 2012. Phytochrome B increases drought tolerance by enhancing ABA sensitivity in Arabidopsis thaliana. *Plant, Cell and Environment*, 35 (11), 1958–1968.

Goss, M.J., 1976. Effects of Mechanical Impedance on Root Growth in Barley (Hordeum vulgare L .) AXES. *Journal of Experimental Botany*, 28 (102), 96–111.

Graf, F. and Frei, M., 2013. Soil aggregate stability related to soil density, root length, and mycorrhiza using site-specific Alnus incana and Melanogaster variegatus s.l. *Ecological Engineering*, 57, 314–323.

Greenland, D.., 1981. Recent Progress in Studies of Soil Structure, and its Relation to Properties and Management of Paddy Soils. *In*: *Proceedings of Symposium on Paddy Soils*. 42–58.

Gregory, P., 2006. *Plant roots, growth, activity and interaction with soils*. Blackwell Publishing Ltd,. Oxford.

Gregory, P., 2009. Measuring root system architecture: Opportunities and challenges. *Asrr.Boku.Ac.At*, (September), 2–4.

Gregory, P.J., McGowan, M., Biscoe, P. V., and Hunter, B., 1979. Water relations of winter

wheat. *The Journal of Agricultural Science*, 93 (2), 494–494.

Grierson, C., Nielsen, E., Ketelaarc, T., and Schiefelbein, J., 2014. Root Hairs. *The Arabidopsis Book*, 12 (Figure 2), e0172.

Gruber, B.D., Giehl, R.F.H., Friedel, S., and von Wiren, N., 2013. Plasticity of the Arabidopsis Root System under Nutrient Deficiencies. *Plant Physiology*, 163 (1), 161–179.

Grzebisz, W., Floris, W., and van Noordwijk, M., 1989. Loss of dry matter and cell contents from fibrous roots of sugar beet due to sampling , storage and washing *, 57, 53–57.

Gu, D., Zhen, F., Hannaway, D.B., Zhu, Y., Liu, L., Cao, W., and Tang, L., 2017. Quantitative Classification of Rice (Oryza sativa L.) Root Length and Diameter Using Image Analysis. *PloS one*, 12 (1), e0169968.

Hallett, P.D., Feeney, D.S., Bengough, A.G., Rillig, M.C., Scrimgeour, C.M., and Young, I.M., 2009. Disentangling the impact of AM fungi versus roots on soil structure and water transport. *Plant and Soil*, 314 (1–2), 183–196.

Hammer, G.L., Dong, Z., McLean, G., Doherty, A., Messina, C., Schussler, J., Zinselmeier, C., Paszkiewicz, S., and Cooper, M., 2009. Can changes in canopy and/or root system architecture explain historical maize yield trends in the U.S. corn belt? *Crop Science*, 49 (1), 299–312.

Hara, K., Kajita, R., Torii, K.U., Bergmann, D.C., and Kakimoto, T., 2007. The secretory peptide gene EPF1 enforces the stomatal one-cell-spacing rule. *Genes and Development*, 21 (14), 1720–1725.

Hara, K., Yokoo, T., Kajita, R., Onishi, T., Yahata, S., Peterson, K.M., Torii, K.U., and Kakimoto, T., 2009. Epidermal cell density is autoregulated via a secretory peptide,

EPIDERMAL PATTERNING FACTOR 2 in arabidopsis leaves. *Plant and Cell Physiology*, 50 (6), 1019–1031.

Hatfield, J.L. and Dold, C., 2019. Water-use efficiency: Advances and challenges in a changing climate. *Frontiers in Plant Science*, 10 (February), 1–14.

Haynes, R.. and Beare, M.H., 1997. Influence Stability of Six Crop Species on Aggregate and Some Labile Organic Matter Fractions. *Science*, 29 (1), 1647–1653.

He, F., Wang, H.-L., Li, H.-G., Su, Y., Li, S., Yang, Y., Feng, C.-H., Yin, W., and Xia, X., 2018. PeCHYR1, a ubiquitin E3 ligase from Populus euphratica, enhances drought tolerance via ABA-induced stomatal closure by ROS production in Populus. *Plant biotechnology journal*, 16 (8), 1514–1528.

Hejazi, M., Edmonds, J., Chaturvedi, V., Davies, E., and Eom, J., 2013. Scenarios of global municipal water-use demand projections over the 21st century. *Hydrological Sciences Journal*, 58 (3), 519–538.

Helliwell, J.R., Sturrock, C.J., Grayling, K.M., Tracy, S.R., Flavel, R.J., Young, I.M., Whalley, W.R., and Mooney, S.J., 2013. Applications of X-ray computed tomography for examining biophysical interactions and structural development in soil systems: A review. *European Journal of Soil Science*, 64 (3), 279–297.

Hepworth, C., Doheny-adams, T., Hunt, L., Cameron, D.D., and Gray, J.E., 2015. Rapid report Manipulating stomatal density enhances drought tolerance without deleterious effect on nutrient uptake. *New Phytologist*, 208, 336–341.

Hepworth, C., Turner, C., Landim, M.G., Cameron, D., and Gray, J.E., 2016. Balancing Water Uptake and Loss through the Coordinated Regulation of Stomatal and Root Development. *Plos One*, 11 (6), e0156930.

Herold, A. and McNeil, P.H., 1979. Restoration of Photosynthesis in Pot-Bound Tobacco Plants. *Journal of Experimental Botany*, 30 (6), 1187–1194.

Hess, L. and De Kroon, H., 2007. Effects of rooting volume and nutrient availability as an alternative explanation for root self/non-self discrimination. *Journal of Ecology*, 95 (2), 241–251.

Hess, T., Andersson, U., Mena, C., and Williams, A., 2015. The impact of healthier dietary scenarios on the global blue water scarcity footprint of food consumption in the UK. *Food Policy*, 50, 1–10.

Hewitt, J.. and Dexter, A.., 1984. The behaviour of roots encountering cracks in soil: I1. Development of a predictive model. *Plant and Soil*, 28, 11–28.

Hillel, D., 2004. Environmental soil physics. *In*: *Environmental soil physics*. 73–89.

Himmelbauer, M.L., Scholl, P., Bodner, G., and Loiskandl, W., 2017. Root system architecture - Budget experimental system for monitoring and analyses. *Biologia (Poland)*, 72 (9), 988–994.

Hoekstra, A.Y. and Wiedmann, T.O., 2014. Humanity's unsustainable environmental footprint. *Science*, 344 (6188), 1114–1117.

Hoffmann, M.H., 2002. Biogeography of Arabidopsis thaliana (L .). *Journal of Biogeography*, 29, 125–134.

Hong, S., Piao, S., Chen, A., Liu, Y., Liu, L., Peng, S., Sardans, J., Sun, Y., Peñuelas, J., and Zeng, H., 2018. Afforestation neutralizes soil pH. *Nature communications*, 9 (1), 520.

Hoogeveen, J., Faurès, J.-M., Peiser, L., Burke, J., and van de Giesen, N., 2015. GlobWat – a global water balance model to assess water use in irrigated agriculture. *Hydrology and*

Earth System Sciences, 19 (9), 3829–3844.

Hoogsteen, M.J.J., Lantinga, E.A., Bakker, E.J., Groot, J.C.J., and Tittonell, P.A., 2015. Estimating soil organic carbon through loss on ignition: Effects of ignition conditions and structural water loss. *European Journal of Soil Science*, 66 (2), 320–328.

Huang, X., Jiang, H., Li, Y., Ma, Y., Tang, H., Ran, W., and Shen, Q., 2016. The role of poorly crystalline iron oxides in the stability of soil aggregate-associated organic carbon in a rice-wheat cropping system. *Geoderma*, 279, 1–10.

Hughes, J., Hepworth, C., Dutton, C., Dunn, J.A., Hunt, L., Stephens, J., Cameron, D., Waugh, R., and Gray, J.E., 2017. Reducing stomatal density in barley improves drought tolerance without impacting on yield. *Plant Physiology*, pp.01844.2016.

Hughes, J., Hepworth, C., Dutton, C., Dunn, J.A., Hunt, L., Stephens, J., Waugh, R., Cameron, D.D., and Gray, J.E., 2017. Reducing stomatal density in barley improves drought tolerance without impacting on yield. *Plant Physiology*, 174 (2), 776–787.

Hunt, L. and Gray, J.E., 2009. The Signaling Peptide EPF2 Controls Asymmetric Cell Divisions during Stomatal Development. *Current Biology*, 19 (10), 864–869.

Impre Media, 2019. Syringa Leaf Labeled [online]. Available from: http://impremedia.net/syringa-leaf-labeled/ [Accessed 18 Sep 2019].

International Energy Agency, 2012. *Technology Roadmap: Hydropower*. International Energy Agency.

International Wheat Genome Sequencing Consortium (IWGSC), 2018. Shifting the limits in wheat research and breeding using a fully annotated reference genome. *Science (New York, N.Y.)*, 361 (6403), eaar7191.

IPCC, 2007. Climate Change 2007: The Physical Science Basis. *In*: S.D. Solomon, M. Qin, M. Manning, Z. Chen, M. Marquis, K.B. Averyt, M. Tignor, and H.L. Miller, eds. *Contribution of Working Group I to the Fourth Assess- ment Report of the Intergovernmental Panel on Climate Change*. Cambridge,UK and New York, USA.

IPCC, 2013. Summary for Policymakers Drafting. *In*: F.B. France, U. Cubasch, P.F. Uk, P. Friedlingstein, P.C. France, M.C. Uk, and C. Josefino, eds.

IPCC, 2018. *Summary for Policymakers. In: Global warming of 1.5°C. An IPCC Special Report on the impacts of global warming of 1.5°C above pre-industrial levels and related global greenhouse gas emission pathways, in the context of strengthening the global response to*. Geneva, Switzerland.

Itoh, H., Nonoue, Y., Yano, M., and Izawa, T., 2010. A pair of floral regulators sets critical day length for Hd3a florigen expression in rice. *Nature Genetics*, 42 (7), 635–638.

Izawa, T. and Shimamoto, K., 1996. Becoming a model plant: The importance of rice to plant science. *Trends in Plant Science*, 1 (3), 95–99.

Jastrow, J.D. and Miller, R.M., 1991. Methods for assessing the effects of biota on soil structure. *Agriculture, Ecosystems and Environment*, 34 (1–4), 279–303.

Jenneson, P.M., Gilboy, W.B., Morton, E.J., Luggar, R.D., and Gregory, P.J., 1999. Optimisation of X-ray micro-tomography. *In*: *1999 IEEE Nuclear Science Symposium. Conference Record. 1999 Nuclear Science Symposium and Medical Imaging Conference (Cat. No.99CH37019)*.

Kar, S., Varade, S.B., and Ghildyal, B.P., 1979. Pore size distribution and root growth relations of rice in artificially synthesized soils. *Soil Science*.

Karaba, A., Dixit, S., Greco, R., Aharoni, A., Trijatmiko, K.R., Marsch-Martinez, N.,

Krishnan, A., Nataraja, K.N., Udayakumar, M., and Pereira, A., 2007. Improvement of water use efficiency in rice by expression of HARDY, an Arabidopsis drought and salt tolerance gene. *Proceedings of the National Academy of Sciences of the United States of America*, 104 (39), 15270–5.

Karch, J., Dudák, J., Žemlička, J., Vavřík, D., Kumpová, I., Kvaček, J., Heřmanová, Z., Šoltés, J., Viererbl, L., Morgano, M., Kaestner, A., and Trtík, P., 2017. X-ray micro-CT and neutron CT as complementary imaging tools for non-destructive 3D imaging of rare silicified fossil plants. *Journal of Instrumentation*, 12 (12).

Katerji, N., Mastrorilli, M., and Rana, G., 2008. Water use efficiency of crops cultivated in the Mediterranean region: Review and analysis. *European Journal of Agronomy*, 28 (4), 493–507.

Kato, Y., Kamoshita, A., and Yamagishi, J., 2006. Growth of Three Rice Cultivars (*Oryza sativa* L.) under Upland Conditions with Different Levels of Water Supply. *Plant Production Science*, 9 (4), 435–445.

Kawata, S. and Soejima, M., 1974. On Superficial Root Formation in Rice Plants. *Japanese journal of crop science*, 43 (3), 354–374.

Kellermeier, F., Armengaud, P., Seditas, T.J., Danku, J., Salt, D.E., and Amtmann, A., 2014. Analysis of the root system architecture of Arabidopsis provides a quantitative readout of crosstalk between nutritional signals. *Plant Cell*, 26 (4), 1480–1496.

Kemper, W.D. and Rosenau, R.C., 1986. Aggregate Stability and Size Distributlon. *Methods of Soil Analysis, Part 1 - Physical and Mineralogical Methods*, 9 (9), 425–442.

Keyes, S., 2013. X-ray Computed Tomography and image-based modelling of plant, root and soil systems, for better understanding of phosphate uptake. University of Southampton.

Keyes, S.D., Daly, K.R., Gostling, N.J., Jones, D.L., Talboys, P., Pinzer, B.R., Boardman, R., Sinclair, I., Marchant, A., and Roose, T., 2013. High resolution synchrotron imaging of wheat root hairs growing in soil and image based modelling of phosphate uptake. *New Phytologist*, 198 (4), 1023–1029.

Keyes, S.D., Gillard, F., Soper, N., Mavrogordato, M.N., Sinclair, I., and Roose, T., 2016. Mapping soil deformation around plant roots using in vivo 4D X-ray computed tomography and digital volume correlation. *Journal of Biomechanics*, c (9), 1802–1811.

Khoury, C.K., Bjorkman, A.D., Dempewolf, H., Ramirez-Villegas, J., Guarino, L., Jarvis, A., Rieseberg, L.H., and Struik, P.C., 2014. Increasing homogeneity in global food supplies and the implications for food security. *Proceedings of the National Academy of Sciences of the United States of America*, 111 (11), 4001–6.

Khush, G.S., 2005. What it will take to Feed 5.0 Billion Rice consumers in 2030. *Plant Molecular Biology*, 59 (1), 1–6.

Kima, A.S., Chung, W.G., and Wang, Y.M., 2014. Improving irrigated lowland rice water use efficiency under saturated soil culture for adoption in tropical climate conditions. *Water (Switzerland)*, 6 (9), 2830–2846.

Kirby, E.J.., 2002. Botany of the wheat plant [online]. *Bread Wheat: Improvement and production*. Available from: http://www.fao.org/3/y4011e/y4011e05.htm [Accessed 4 Aug 2019].

Kirchhof, G. and So, H.B., 2005. Soil puddling for rice production under glasshouse conditions - Its quantification and effect on soil physical properties. *Australian Journal of Soil Research*, 43 (5), 617–622.

Knox, J., Hess, T., Daccache, A., and Wheeler, T., 2012. Climate change impacts on crop

productivity in Africa and South Asia. *Environmental Research Letters*, 7 (3), 34032.

Koch, A., Mcbratney, A., Adams, M., Field, D., Hill, R., Crawford, J., Minasny, B., Lal, R., Abbott, L., O'Donnell, A., Angers, D., Baldock, J., Barbier, E., Binkley, D., Parton, W., Wall, D.H., Bird, M., Bouma, J., Chenu, C., Flora, C.B., Goulding, K., Grunwald, S., Hempel, J., Jastrow, J., Lehmann, J., Lorenz, K., Morgan, C.L., Rice, C.W., Whitehead, D., Young, I., and Zimmermann, M., 2013. Soil Security: Solving the Global Soil Crisis. *Global Policy*, 4 (4), 434–441.

Kochian, L. V., 2016. Root architecture. *Journal of Integrative Plant Biology*, 58 (3), 190–192.

Kockelmann, W., Zhang, S.Y., Kelleher, J.F., Nightingale, J.B., Burca, G., and James, J.A., 2013. IMAT - A new imaging and diffraction instrument at ISIS. *Physics Procedia*, 43 (0), 100–110.

Koebernick, N., Daly, K.R., Keyes, S.D., George, T.S., Brown, L.K., Raffan, A., Cooper, L.J., Naveed, M., Bengough, A.G., Sinclair, I., Hallett, P.D., and Roose, T., 2017. High-resolution synchrotron imaging shows that root hairs influence rhizosphere soil structure formation. *New Phytologist*.

Koech, R. and Langat, P., 2018. Improving irrigation water use efficiency: A review of advances, challenges and opportunities in the Australian context. *Water (Switzerland)*, 10 (12).

Koevoets, I.T., Venema, J.H., Elzenga, J.T.M., and Testerink, C., 2016. Roots Withstanding their Environment: Exploiting Root System Architecture Responses to Abiotic Stress to Improve Crop Tolerance. *Frontiers in Plant Science*, 07 (August), 1–19.

Kögel-Knabner, I., Amelung, W., Cao, Z., Fiedler, S., Frenzel, P., Jahn, R., Kalbitz, K.,

Kölbl, A., and Schloter, M., 2010. Biogeochemistry of paddy soils. *Geoderma*, 157 (1–2), 1–14.

Koornneef, M., Van Eden, J., Hanhart, C.J., Stam, P., Braaksma, F.J., and Feenstra, W.., 1983. Linkage map of Arabidopsis thaliana. *Journal of Heredity*, 74 (4), 265-272.

Korner, C., Pelaez, M.-R.S., and John, P., 1989. Why Are Bonsai Plants Small? A Consideration of Cell Size. *Functional Plant Biology*, 16 (5), 443.

Kreuzer, K., Adamczyk, J., Iijima, M., Wagner, M., Scheu, S., and Bonkowski, M., 2006. Grazing of a common species of soil protozoa (Acanthamoeba castellanii) affects rhizosphere bacterial community composition and root architecture of rice (Oryza sativa L.). *Soil Biology and Biochemistry*, 38 (7), 1665–1672.

Kumar, A., Nayak, A.K., Pani, D.R., and Das, B.S., 2017. Physiological and morphological responses of four different rice cultivars to soil water potential based deficit irrigation management strategies. *Field Crops Research*, 205, 78–94.

Kumar, P., Yadava, R., Gollen, B., … S.K.-L.S. and, and 2011, U., 2011. Nutritional Contents and Medicinal Properties of Wheat: A Review. *Life Sciences and Medicine Research*, 2011 (1), 22.

Kuo, S., 1996. Phosphorus. p. 869–919. DL Sparks (ed.) Methods of soil analysis. Part 3. SSSA Book Ser. 5. SSSA, Madison, WI. *Phosphorus. p. 869–919. In DL Sparks (ed.) Methods of soil analysis. Part 3. SSSA Book Ser. 5. SSSA, Madison, WI.*

Laibach, F., 1943. Arabidopsis thaliana (L.) Heynh. als Objekt für genetische und entwicklungsphysiologische Untersuchungen. *Bot. Archiv*, 44, 439–455.

Lal, R., 1997a. Degradation and resilience of soils. *Philosophical Transactions of the Royal Society B: Biological Sciences*, 352 (1356), 997–1010.

Lal, R., 1997b. Long-term tillage and maize monoculture effects on a tropical Alfisol in western Nigeria. I. Crop yield and soil physical properties. *Soil and Tillage Research*, 42 (3), 145–160.

Lal, R., 2015. Restoring Soil Quality to Mitigate Soil Degradation. *Sustainability*, 7 (5), 5875–5895.

Lal, R., 2016. Feeding 11 billion on 0.5 billion hectare of area under cereal crops.

Lal, R. and Shulka, M.., 2004. *Princicples of soil physics*. Marcel Dekker.

Landl, M., Schnepf, A., Vanderborght, J., Bengough, A.G., Bauke, S.L., Lobet, G., Bol, R., and Vereecken, H., 2018. Measuring root system traits of wheat in 2D images to parameterize 3D root architecture models. *Plant and Soil*, 425 (1–2), 457–477.

Latif, M.A., Mehuys, G.R., MacKenzie, A.F., Alli, I., and Faris, M.A., 1992. Effect of Legumes on Soil Physical Quality in a Maize Crop. *Plant Soil*, 140 (1972), 15–23.

Lavkulich, L.M., 1981. Methods Manual, Pedology Laboratory. Department of Soil Science, University of British Columbia, Vancouver. *British Columbia, Canada*.

Leakey, A.D.B., Ferguson, J.N., Pignon, C.P., Wu, A., Jin, Z., Hammer, G.L., and Lobell, D.B., 2019. Water Use Efficiency as a Constraint and Target for Improving the Resilience and Productivity of C3 and C4 Crops. *Annual Review of Plant Biology*, 70 (1), 781–808.

Lee, J.S., Lee, M.H., Chun, Y.Y., and Lee, K.M., 2018. Uncertainty analysis of the water scarcity footprint based on the AWARE model considering temporal variations. *Water (Switzerland)*, 10 (3), 1–13.

Lee, M.M. and Schiefelbein, J., 1999. WEREWOLF, a MYB-Related Protein in Arabidopsis,

Is a Position-Dependent Regulator of Epidermal Cell Patterning. *Cell*, 99 (5), 473–483.

Lehmann, E.H., 2017. Neutron imaging facilities in a global context. *Journal of Imaging*, 3 (4).

Leite, J.P., Barbosa, E.G.G., Marin, S.R.R., Marinho, J.P., Carvalho, J.F.C., Pagliarini, R.F., Cruz, A.S., Oliveira, M.C.N., Farias, J.R.B., Neumaier, N., Guimarães, F.C.M., Yoshida, T., Kanamori, N., Fujita, Y., Nakashima, K., Shinozaki, K.Y., Desidério, J.A., and Nepomuceno, A.L., 2014. Overexpression of the activated form of the AtAREB1 gene (AtAREB1ΔQT) improves soybean responses to water deficit. *Genetics and Molecular Research*, 13 (3), 6272–6286.

Lightsources.org, 2019. Light sources of the world [online]. Available from: https://lightsources.org/lightsources-of-the-world/ [Accessed 19 Sep 2019].

Liu, J., Zhang, F., Zhou, J., Chen, F., Wang, B., and Xie, X., 2012. Phytochrome B control of total leaf area and stomatal density affects drought tolerance in rice. *Plant Molecular Biology*, 78 (3), 289–300.

Liu, Y., Qin, L., Han, L., Xiang, Y., and Zhao, D., 2015. Overexpression of maize SDD1 (ZmSDD1) improves drought resistance in Zea mays L. by reducing stomatal density. *Plant Cell, Tissue and Organ Culture*, 122 (1), 147–159.

Liu, Z., Qian, J., Liu, B., Wang, Q., Ni, X., Dong, Y., Zhong, K., and Wu, Y., 2014. Effects of the Magnetic Resonance Imaging Contrast Agent Gd-DTPA on Plant Growth and Root Imaging in Rice. *PLoS ONE*, 9 (6), e100246.

Lo, S.-F., Ho, T.-H.D., Liu, Y.-L., Jiang, M.-J., Hsieh, K.-T., Chen, K.-T., Yu, L.-C., Lee, M.-H., Chen, C.-Y., Huang, T.-P., Kojima, M., Sakakibara, H., Chen, L.-J., and Yu, S.-M., 2017. Ectopic expression of specific GA2 oxidase mutants promotes yield and stress

tolerance in rice. *Plant biotechnology journal*, 15 (7), 850–864.

Logsdon, S.D., Parker, J.C., and Reneau, R.B., 1987. Root growth as influenced by aggregate size. *Plant and Soil*, 99 (2–3), 267–275.

Low, A.J., 1972. The effect of cultivation on the structure and other physical characteristics of grassland and arable soils (1945-1970). *Journal of Soil Science*, 23 (4), 363–380.

Lucas, M., Swarup, R., Paponov, I.A., Swarup, K., Casimiro, I., Lake, D., Peret, B., Zappala, S., Mairhofer, S., Whitworth, M., Wang, J., Ljung, K., Marchant, A., Sandberg, G., Holdsworth, M.J., Palme, K., Pridmore, T., Mooney, S., and Bennett, M.J., 2011. SHORT-ROOT Regulates Primary, Lateral, and Adventitious Root Development in Arabidopsis. *Plant Physiology*, 155 (January), 384–398.

Ludwig, F., van Slobbe, E., and Cofino, W., 2014. Climate change adaptation and Integrated Water Resource Management in the water sector. *Journal of Hydrology*, 518 (PB), 235–242.

Luschnig, C., Gaxiola, R.A., Grisafi, P., and Fink, G.R., 1998. EIR1, a root specific protein involved in auxin transport, is required for gravitropism in Arabidopsis thaliana. *Genes Dev.*, 12, 2175–2187.

Lynch, J., 1995. Root Architecture and Plant Productivity. *Plant physiology*, 109 (1), 7–13.

Lynch, J.P., 2007. Roots of the second green revolution. *Australian Journal of Botany*, 55 (5), 493–512.

Lynch, J.P., 2013. Steep, cheap and deep: An ideotype to optimize water and N acquisition by maize root systems. *Annals of Botany*, 112 (2), 347–357.

Maarastawi, S.A., Frindte, K., Bodelier, P.L.E., and Knief, C., 2019. Rice straw serves as

additional carbon source for rhizosphere microorganisms and reduces root exudate consumption. *Soil Biology and Biochemistry*, 135, 235–238.

Mairhofer, S., Sturrock, C.J., Bennett, M.J., Mooney, S.J., and Pridmore, T.P., 2015. Extracting multiple interacting root systems using X-ray microcomputed tomography. *Plant Journal*, 84 (5), 1034–1043.

Mairhofer, S., Zappala, S., Tracy, S., Sturrock, C., Bennett, M.J., Mooney, S.J., and Pridmore, T.P., 2013. Recovering complete plant root system architectures from soil via X-ray μ-Computed Tomography. *Plant Methods*, 9, 1.

Mairhofer, S., Zappala, S., Tracy, S.R., Sturrock, C., Bennett, M., Mooney, S.J., and Pridmore, T., 2012a. RooTrak: Automated Recovery of Three-Dimensional Plant Root Architecture in Soil from X-Ray Microcomputed Tomography Images Using Visual Tracking. *Plant Physiology*, 158 (2), 561–569.

Mairhofer, S., Zappala, S., Tracy, S.R., Sturrock, C., Bennett, M., Mooney, S.J., and Pridmore, T., 2012b. RooTrak: Automated Recovery of Three-Dimensional Plant Root Architecture in Soil from X-Ray Microcomputed Tomography Images Using Visual Tracking. *Plant Physiology*, 158 (2), 561–569.

Malin, F. and Rockström, J., 2004. *Balancing Water for Humans and Nature: The New Approach in Ecohydrology (,)*. Routledge.

Malthus, T.R., 1798. An Essay on the Principle of Population, as it Affects the Future Improvement of Society with Remarks on the Speculations of Mr. Godwin, M. Condorcet, and Other Writers, 340.

Mancosu, N., Snyder, R.L., Kyriakakis, G., and Spano, D., 2015. Water scarcity and future challenges for food production. *Water (Switzerland)*, 7 (3), 975–992.

Mancuso, S., 2012. Measuring roots: An updated approach. *Measuring Roots: An Updated Approach*, 1–382.

Manschadi, A.M., Christopher, J., Devoil, P., and Hammer, G.L., 2006. The role of root architectural traits in adaptation of wheat to water-limited environments. *Functional Plant Biology*, 33 (9), 823–837.

Manschadi, A.M., Hammer, G.L., Christopher, J.T., and DeVoil, P., 2008. Genotypic variation in seedling root architectural traits and implications for drought adaptation in wheat (Triticum aestivum L.). *Plant and Soil*, 303 (1–2), 115–129.

Mao, H., Wang, H., Liu, S., Li, Z., Yang, X., Yan, J., Li, J., Tran, L.S.P., and Qin, F., 2015. A transposable element in a NAC gene is associated with drought tolerance in maize seedlings. *Nature Communications*, 6.

Martin, S.L., Mooney, S.J., Dickinson, M.J., and West, H.M., 2012. Soil structural responses to alterations in soil microbiota induced by the dilution method and mycorrhizal fungal inoculation. *Pedobiologia*, 55 (5), 271–281.

Masle, J., Gilmore, S.R., and Farquhar, G.D., 2005. The ERECTA gene regulates plant transpiration efficiency in Arabidopsis. *Nature*, 436 (7052), 866–870.

Materechera, S.A., Dexter, A.R., and Alston, A.M., 1992. Formation of aggregates by plant roots in homogenised soils. *Plant and Soil*, 142 (1), 69–79.

Materechera, S.A., Kirby, J.M., Alston, A.M., and Dexter, A.R., 1994. Modification of Soil Aggregation By Watering Regime and Roots Growing Through Beds of Large Aggregates. *Plant and Soil*, 160 (1), 57–66.

Matsumoto, T., Wu, J., Itoh, T., Numa, H., Antonio, B., and Sasaki, T., 2016. The Nipponbare genome and the next-generation of rice genomics research in Japan. *Rice*, 9

(1), 33.

Matsuo, N. and Mochizuki, T., 2009. Growth and Yield of Six Rice Cultivars under Three Water-saving Cultivations. *Plant Production Science*, 12 (4), 514–525.

Mawodza, T., Brooks, H., Burca, G., and Menon, M., 2018. Understanding root architecture and water uptake of water use efficient wheat mutants using neutron and X-Ray CT imaging. *STFC ISIS Neutron and Muon Source Data Journal*.

Meinke, D.W., Cherry, J.M., Dean, C., Rounsley, S.D., and Koornneef, M., 1998. Arabidopsis thaliana: A model plant for genome analysis. *Science*, 282 (5389).

Menon, M., 2006. Influence of soil pollution by heavy metals on the water relations of young forest ecosystems.

Menon, M., Robinson, B., Oswald, S.E., Kaestner, A., Abbaspour, K.C., Lehmann, E., and Schulin, R., 2007. Visualization of root growth in heterogeneously contaminated soil using neutron radiography. *European Journal of Soil Science*, 58 (3), 802–810.

Metzner, R., Eggert, A., van Dusschoten, D., Pflugfelder, D., Gerth, S., Schurr, U., Uhlmann, N., and Jahnke, S., 2015. Direct comparison of MRI and X-ray CT technologies for 3D imaging of root systems in soil: potential and challenges for root trait quantification. *Plant Methods*.

Minasny, B., Mcbratney, A.B., Brough, D.M., and Jacquier, D., 2011. Models relating soil pH measurements in water and calcium chloride that incorporate electrolyte concentration. *European Journal of Soil Science*, 62 (5), 728–732.

Minniti, T., Watanabe, K., Burca, G., Pooley, D.E., and Kockelmann, W., 2018. Characterization of the new neutron imaging and materials science facility IMAT. *Nuclear Instruments and Methods in Physics Research, Section A: Accelerators,*

Spectrometers, Detectors and Associated Equipment, 888 (January), 184–195.

Misra, R.K., Alston, A.M., and Dexter, A.R., 1988. Root Growth and Phosphorus Uptake in Relation to the Size and Strength of Soil Aggregates. I. Experimental Studies, 11, 103–116.

Misra, R.K., Dexter, A.R., and Alston, A.M., 1986. Penetration of soil aggregates of finite size. *Plant and Soil*, 94 (1), 59–85.

Mohammed, U., Caine, R.S., Atkinson, J.A., Harrison, E.L., Wells, D., Chater, C.C., Gray, J.E., Swarup, R., and Murchie, E.H., 2019. Rice plants overexpressing OsEPF1 show reduced stomatal density and increased root cortical aerenchyma formation. *Scientific reports*, 9 (1), 5584.

Moin, M., Bakshi, A., Madhav, M.S., and Kirti, P.B., 2017. Expression Profiling of Ribosomal Protein Gene Family in Dehydration Stress Responses and Characterization of Transgenic Rice Plants Overexpressing RPL23A for Water-Use Efficiency and Tolerance to Drought and Salt Stresses. *Frontiers in Chemistry*, 5, 97.

Monnier, G., 1965. Action des matieres organiques sur la stabilite structurale de sols: 1ere these. Le concept de sol et son evolution: 2eme these. *Action des matieres organiques sur la stabilite structurale de sols: 1ere these. Le concept de sol et son evolution: 2eme these, Université de Paris (1965)*.

Monroe, C.D. and Kladivko, E.J., 1987. Aggregate stability of a silt loam soil as affected by roots of corn, soybeans and wheat. *Communications in Soil Science and Plant Analysis*, 18 (10), 1077–1087.

Mooney, S.J., Morris, C., and Berry, P.M., 2006. Visualization and quantification of the effects of cereal root lodging on three-dimensional soil macrostructure using x-ray

computed tomography. *Soil Science*, 171 (9), 706–718.

Mooney, S.J., Pridmore, T.P., Helliwell, J., and Bennett, M.J., 2012. Developing X-ray computed tomography to non-invasively image 3-D root systems architecture in soil. *Plant and Soil*, 352 (1–2), 1–22.

Moradi, A.B., Carminati, A., Vetterlein, D., Vontobel, P., Lehmann, E., Weller, U., Hopmans, J.W., Vogel, H.-J., and Oswald, S.E., 2011. Three-dimensional visualization and quantification of water content in the rhizosphere. *New Phytol.*, 192 (3), 653–663.

Moradi, A.B., Conesa, H.M., Robinson, B., Lehmann, E., Kuehne, G., Kaestner, A., Oswald, S., and Schulin, R., 2009. Neutron radiography as a tool for revealing root development in soil: Capabilities and limitations. *Plant and Soil*, 318 (1–2), 243–255.

Moradi, A.B., Hopmans, J.W., Oswald, S.E., Menon, M., Carminati, A., Lehmann, E., Anderson, S.H., and Hopmans, J.W., 2013. Applications of Neutron Imaging in Soil–Water–Root Systems, 113–136.

Morison, J.I.., Baker, N.., Mullineaux, P.., and Davies, W.., 2008. Improving water use in crop production. *Philosophical Transactions of the Royal Society B: Biological Sciences*, 363 (1491), 639–658.

Morita, S. and Nemoto, K., 1995. Morphology and anatomy of rice roots with special reference to coordination in organo- and histogenesis. *Structure and Function of Roots*, 75–86.

Morris, E.C., Griffiths, M., Golebiowska, A., Mairhofer, S., Burr-Hersey, J., Goh, T., Wangenheim, D. Von, Atkinson, B., Sturrock, C.J., Lynch, J.P., Vissenberg, K., Ritz, K., Wells, D.M., Mooney, S.J., Bennett, M.J., von Wangenheim, D., Atkinson, B., Sturrock, C.J., Lynch, J.P., Vissenberg, K., Ritz, K., Wells, D.M., Mooney, S.J., and

Bennett, M.J., 2017. Shaping 3D Root System Architecture. *Current Biology*, 27 (17), R919–R930.

Müller, B. and Bartelheimer, M., 2013. Interspecific competition in Arabidopsis thaliana: Root hairs are important for competitive effect, but not for competitive response. *Plant and Soil*, 371 (1–2), 167–177.

Munjonji, L., 2017. Drought tolerant traits of triticale and cowpea genotypes under semi-arid conditions. Ghent University.

Munkholm, L.J., Heck, R.J., and Deen, B., 2013. Long-term rotation and tillage effects on soil structure and crop yield. *Soil and Tillage Research*, 127, 85–91.

Murasnige, T. and Skoog, F., 1962. A Revised Medium for Rapid Growth and Bio Agsays with Tohaoco Tissue Cultures. *Physiol. Plant*, 15 (3), 473–497.

Murungu, F.S., Nyamugafata, P., Chiduza, C., Clark, L.J., and Whalley, W.R., 2003. Effects of seed priming, aggregate size and soil matric potential on emergence of cotton (Gossypium hirsutum L.) and maize (Zea mays L.). *Soil and Tillage Research*, 74 (2), 161–168.

Nakamoto, T. and Oyanagi, A., 1994. The Direction of Growth of Seminal Roots of Triticum aestivum L. and Experimental Modification Thereof. *Annals of Botany*.

Nakamoto, T. and Suzuki, K., 2001. Influence of soybean and maize roots on the seasonal change in soil aggregate size and stability. *Plant Prod. Sci.*, 4, 317–319.

Nakanishi, T.M., Matsumoto, S., and Kobayashi, H., 1992. Morphological Change of Plant Root Revealed Radiography by Neutron of Tokyo, 641, 638–641.

Nakanishi, T.M., Okuni, Y., Hayashi, Y., and Nishiyama, H., 2005. Water gradient profiles at

bean plant roots determined by neutron beam analysis. *Journal of Radioanalytical and Nuclear Chemistry*, 264 (2), 313–317.

Naveed, M., Brown, L.K., Raffan, A.C., George, T.S., Bengough, A.G., Roose, T., Sinclair, I., Koebernick, N., Cooper, L., Hackett, C.A., and Hallett, P.D., 2017. Plant exudates may stabilize or weaken soil depending on species, origin and time. *European Journal of Soil Science*, 68 (6), 806–816.

Negi, M., Sanagala, R., Rai, V., and Jain, A., 2016. Deciphering Phosphate Deficiency-Mediated Temporal Effects on Different Root Traits in Rice Grown in a Modified Hydroponic System. *Frontiers in Plant Science*, 7, 550.

Ni Jiang, Floro, E., Bray, A.L., Laws, B., Duncan, K.E., and Topp, C.N., 2018. High-resolution 4D spatiotemporal analysis reveals the contributions of local growth dynamics to contrasting maize root architectures, (314).

Nimmo, J.R. and Perkins, K.., 2002. Aggregate stability and size distribution. *Methods of soil analysis, Part 4-Physical methods*.

Niu, Y., Jin, G., Li, X., Tang, C., Zhang, Y., Liang, Y., and Yu, J., 2015. Phosphorus and magnesium interactively modulate the elongation and directional growth of primary roots in Arabidopsis thaliana (L .) Heynh, 66 (13), 3841–3854.

van Noordwijk, M. and Floris, J., 1979. Loss of dry weight during washing and storage of root samples. *Plant and Soil*, 53, 239–240.

Nyamangara, J., Marondedze, A., Masvaya, E.N., Mawodza, T., Nyawasha, R., Nyengerai, K., Tirivavi, R., Nyamugafata, P., and Wuta, M., 2014. Influence of basin-based conservation agriculture on selected soil quality parameters under smallholder farming in Zimbabwe. *Soil Use and Management*, 30 (4), 550–559.

Oades, J.M., 1993. The role of biology in the formation, stabilization and degradation of soil structure. *Geoderma*, 56 (1–4), 377–400.

Octopus, 2019. Octopus reconstrsuction [online]. Available from: https://octopusimaging.eu/octopus/octopus-reconstruction [Accessed 1 Mar 2019].

Odegard, I., Bijleveld, M., and Naber, N., 2015. *Food Commodity Footprints*.

Ogura, T., Goeschl, C., Filiault, D., Mirea, M., Slovak, R., Wolhrab, B., Satbhai, S.B., and Busch, W., 2019a. Root System Depth in Arabidopsis Is Shaped by EXOCYST70A3 via the Dynamic Modulation of Auxin Transport. *Cell*, 178 (2), 400-412.e16.

Ogura, T., Goeschl, C., Filiault, D., Mirea, M., Slovak, R., Wolhrab, B., Satbhai, S.B., and Busch, W., 2019b. Root System Depth in Arabidopsis Is Shaped by EXOCYST70A3 via the Dynamic Modulation of Auxin Transport. *Cell*, 178 (2), 400-412.e16.

Okushima, Y., Fukaki, H., Onoda, M., Theologis, A., and Tasaka, M., 2007. ARF7 and ARF19 Regulate Lateral Root Formation via Direct Activation of LBD/ASL Genes in Arabidopsis. *the Plant Cell Online*, 19 (1), 118–130.

Okushima, Y., Overvoorde, P.J., Arima, K., Alonso, J.M., Chan, A., Chang, C., Ecker, J.R., Hughes, B., Lui, A., Nguyen, D., Onodera, C., Quach, H., and Smith, A., 2005. Functional Genomic Analysis of the AUXIN RESPONSE FACTOR Gene Family Members in Arabidopsis thaliOkushima, Y., Overvoorde, P. J., Arima, K., Alonso, J. M., Chan, A., Chang, C., Ecker, J. R., et al. (2005). Functional Genomic Analysis of the AUXIN RESPONSE. *The Plant Cell …*, 17 (February), 444–463.

Oldeman, L.R., Hakkeling, R.T.A., and Sombroek, W.G., 1991. *World map of the status of human-induced soil degradation: an explanatory note*. International Soil Reference and Information Centre.

Olsen, S.R., Cole, C.W., Watanabe, F.S., and Dean, L.A., 1954. *Estimation of available phosphorus in soils by extraction with sodium bicarbonate*. Estimation of available phosphorus in soils by extraction with sodium bicarbonate. p. 1–19. Circular 939. USDA, Washington, DC.

Ortiz-Ribbing, L.M. and Eastburn, D.M., 2003. Evaluation of Digital Image Acquisition Methods for Determining Soybean Root Characteristics. *Crop Management*, 2 (1), 0–0.

Osugi, A., Itoh, H., Ikeda-Kawakatsu, K., Takano, M., and Izawa, T., 2011. Molecular dissection of the roles of phytochrome in photoperiodic flowering in rice. *Plant Physiology*, 157 (3), 1128–1137.

Oswald, S.E., Menon, M., Carminati, A., Vontobel, P., Lehmann, E., and Schulin, R., 2008. Quantitative Imaging of Infiltration, Root Growth, and Root Water Uptake via Neutron Radiography. *Vadose Zone Journal*, 7 (3), 1035.

Oswald, S.E., Tötzke, C., Haber-Pohlmeier, S., Pohlmeier, A., Kaestner, A.P., and Lehmann, E., 2015. ScienceDirect Combining Neutron and Magnetic Resonance Imaging to Study the Interaction of Plant Roots and Soil. *Physics Procedia*, 69 (69), 237–243.

Paez-Garcia, A., Motes, C., Scheible, W.-R., Chen, R., Blancaflor, E., and Monteros, M., 2015. Root Traits and Phenotyping Strategies for Plant Improvement. *Plants*, 4 (2), 334–355.

Page, D.R. and Grossniklaus, U., 2002. The art and design of genetic screens: Arabidopsis thaliana. *Nature Reviews Genetics*, 3 (2), 124–136.

Page, J. and Willard, C.J., 1947. Cropping Systems and Soil Properties 1. *Soil Science Society of America Journal*, 11 (C), 81–88.

Palta, J.A., Chen, X., Milroy, S.P., Rebetzke, G.J., Dreccer, M.F., and Watt, M., 2011. Large

root systems: Are they useful in adapting wheat to dry environments? *Functional Plant Biology*, 38 (5), 347–354.

Panigrahy, M., Nageswara Rao, D., Yugandhar, P., Sravan Raju, N., Krishnamurthy, P., Voleti, S.R., Reddy, G.A., Mohapatra, T., Robin, S., Singh, A.K., Singh, K., Sheshshayee, M., Sharma, R.P., and Sarla, N., 2014. Hydroponic experiment for identification of tolerance traits developed by rice Nagina 22 mutants to low-phosphorus in field condition. *Archives of Agronomy and Soil Science*, 60 (4), 565–576.

Pankhurst, C., Doube, B.M., and Gupta, V., 1997. Biological indicators of soil health.

Papademetriou, M.K., Dent, F.J., and Herath, E.M., 2000. *Bridging the rice yield gap in the Asia-Pacific Region*. FAO Regional Office for Asia and the Pacific Bangkok, Thailand.

Papadopoulos, A., 2011. Soil Aggregates, Structure, and Stability. Springer, Dordrecht, 736–740.

Pask, A.J.D. and Reynolds, M.P., 2013. Breeding for yield potential has increased deep soil water extraction capacity in irrigated wheat. *Crop Science*, 53 (5), 2090–2104.

Passioura, J., 2006. Increasing crop productivity when water is scarce—from breeding to field management. *Agricultural Water Management*, 80 (1–3), 176–196.

Passioura, J.B. and Stirzaker, R.J., 1993. Feedforward Responses of Plants to Physically Inhospitable Soil. *International Crop Science I*, 715–719.

Pearce, S., Kippes, N., Chen, A., Debernardi, J.M., and Dubcovsky, J., 2016. RNA-seq studies using wheat PHYTOCHROME B and PHYTOCHROME C mutants reveal shared and specific functions in the regulation of flowering and shade-avoidance pathways. *BMC Plant Biology*, 16 (1), 141.

Pennisi, E., 2008. The Blue Revolution, Drop by Drop, Gene by Gene. *Science*, 320 (5873), 171–173.

Péret, B., Desnos, T., Jost, R., Kanno, S., Berkowitz, O., and Nussaume, L., 2014. Root architecture responses: in search of phosphate. *Plant physiology*, 166 (4), 1713–23.

Pfeifer, J., Kirchgessner, N., Colombi, T., and Walter, A., 2015. Rapid phenotyping of crop root systems in undisturbed field soils using X-ray computed tomography. *Plant Methods*, 11 (1), 41.

Pflugfelder, D., Metzner, R., Dusschoten, D. Van, Reichel, R., Jahnke, S., and Koller, R., 2017. Non-invasive imaging of plant roots in different soils using magnetic resonance imaging (MRI). *Plant Methods*, 1–9.

Pierre, C. Saint, Crossa, J.L., Bonnett, D., Yamaguchi-Shinozaki, K., and Reynolds, M.P., 2012. Phenotyping transgenic wheat for drought resistance. *Journal of Experimental Botany*, 63 (5), 1799–1808.

Pierret, A., Moran, C.J., and Doussan, C., 2005. Conventional detection methodology is limiting our ability to understand the roles and functions of fine roots. *New Phytologist*, 166 (3), 967–980.

Pires, L.F., Oliveira, O., and Bacchi, S., 2010. Changes in soil structure evaluated using computed tomography :Soil structure changes Evaluated with computed. *Brazilian Agricultural Research*, 1–11.

Poorter, H., Bühler, J., Van Dusschoten, D., Climent, J., and Postma, J.A., 2012. Pot size matters: A meta-analysis of the effects of rooting volume on plant growth. *Functional Plant Biology*, 39 (11), 839–850.

Porter, J.R. and Gawith, M., 1999. Temperatures and the growth and development of wheat: a

review. *European Journal of Agronomy*, 10 (1), 23–36.

Preece, C., Farré-Armengol, G., Llusià, J., and Peñuelas, J., 2018. Thirsty tree roots exude more carbon. *Tree Physiology*, (January).

Preece, C. and Peñuelas, J., 2016. Rhizodeposition under drought and consequences for soil communities and ecosystem resilience. *Plant and Soil*, 409 (1–2), 1–17.

Raj Ratta, 2018. *Soil Quality and Soil Erosion*.

Rajabi, A., 2006. Carbon isotope discrimination and selective breeding of sugar beet (Beta vulgaris L.) for drought tolerance. University of Cambridge.

Ramalingam, P., Kamoshita, A., Deshmukh, V., Yaginuma, S., and Uga, Y., 2017. Association between root growth angle and root length density of a nearisogenic line of IR64 rice with DEEPER ROOTING 1 under different levels of soil compaction. *Plant Production Science*.

Rao, A.., Johnson D, E., Sivaprasad, B., Ladha, J, K., and Mortimer, A, M., 2008. Weed management in direct seeded rice. *Journal of Animal and Plant Sciences*, 18 (2–3), 86–88.

Ray, J.D. and Sinclair, T.R., 1998. The effect of pot size on growth and transpiration of maize and soybean during water deficit stress. *Journal of Experimental Botany*, 49 (325), 1381–1386.

Rebouillat, J., Dievart, A., Verdeil, J.L., Escoute, J., Giese, G., Breitler, J.C., Gantet, P., Espeout, S., Guiderdoni, E., and Périn, C., 2009. Molecular Genetics of Rice Root Development. *Rice*, 2 (1), 15–34.

Reed, J.W., Elumalai, R.P., and Chory, J., 1998. Suppressors of an Arabidopsis thaliana phyB

mutation identify genes that control light signaling and hypocotyl elongation. *Genetics*, 148 (3), 1295–1310.

Reed, J.W., Nagpal, P., Poole, D.S., Furuya, M., and Chory, J., 1993. Mutations in the gene for the red/far-red light receptor phytochrome B alter cell elongation and physiological responses throughout Arabidopsis development. *The Plant cell*, 5 (2), 147–157.

Reid, J.. B. and Goss, M.. J., 1981. Effect of living roots of different plant species on the aggregate stability of two arable soils. *Journal of Soil science*, 32 (4), 521–541.

Rich, S.M. and Watt, M., 2013. Soil conditions and cereal root system architecture: Review and considerations for linking Darwin and Weaver. *Journal of Experimental Botany*, 64 (5), 1193–1208.

Robinson, B.H., Moradi, A., and Lehmann, E., 2008. Neutron Radiography for the Analysis of Plant – Soil Interactions. *Encyclopedia of Analytical Chemistry: Applications, Theory and Instrumentation*, 1–8.

Rockström, J., Williams, J., Daily, G., Noble, A., Matthews, N., Gordon, L., Wetterstrand, H., DeClerck, F., Shah, M., Steduto, P., de Fraiture, C., Hatibu, N., Unver, O., Bird, J., Sibanda, L., and Smith, J., 2017. Sustainable intensification of agriculture for human prosperity and global sustainability. *Ambio*, 46 (1), 4–17.

Roder, W.R., 2001. *Slash-and-burn rice system in the hills of Northern Lao PDR: description, challenges, and opportunity*. Weed Research.

Rogers, E.D. and Benfey, P.N., 2015. Regulation of plant root system architecture: Implications for crop advancement. *Current Opinion in Biotechnology*.

Rogers, E.D., Monaenkova, D., Mijar, M., Nori, A., Goldman, D.I., and Benfey, P.N., 2016. X-Ray Computed Tomography Reveals the Response of Root System Architecture to

Soil Texture. *Plant Physiology*, 171 (3), 2028–2040.

Ronchi, C.P., DaMatta, F.M., Batista, K.D., Moraes, G.A.B.K., Loureiro, M.E., and Ducatti, C., 2006. Growth and photosynthetic down-regulation in Coffea arabica in response to restricted root volume. *Functional Plant Biology*, 33 (11), 1013.

Royal Society, 2016. How are GM crops regulated? [online]. Available from: https://royalsociety.org/topics-policy/projects/gm-plants/how-are-gm-crops-regulated/ [Accessed 20 Sep 2019].

Roychoudhury, P., Pillai, G.R., Pandey, S.L., Krishna Murti, G.S.R., and Venkataraman, G.S., 1983. Effect of blue-green algae on aggregate stability and rice yield under different irrigation and nitrogen levels. *Soil and Tillage Research*, 3 (1), 61–65.

Rudolph-Mohr, N., Vontobel, P., and Oswald, S.E., 2014. A multi-imaging approach to study the root-soil interface. *Annals of Botany*, 114 (8), 1779–1787.

Ruggiero, A., Punzo, P., Landi, S., Costa, A., Oosten, M.J. Van, Grillo, S., Alvino, A., Freire, M.I., and Ferreira, R., 2017. Improving Plant Water Use Efficiency through Molecular Genetics, 1–22.

Sachs, T., 2005. *Pattern formation in plant tissues*. Cambridge University Press.

Saito, K., Asai, H., Zhao, D., Laborte, A.G., and Grenier, C., 2018. Progress in varietal improvement for increasing upland rice productivity in the tropics. *Plant Production Science*, 21 (3), 145–158.

Sander, T., Gerke, H.H., and Rogasik, H., 2008. Assessment of Chinese paddy-soil structure using X-ray computed tomography. *Geoderma*, 145 (3–4), 303–314.

Sanguineti, M.C., Li, S., MacCaferri, M., Corneti, S., Rotondo, F., Chiari, T., and Tuberosa,

R., 2007. Genetic dissection of seminal root architecture in elite durum wheat germplasm. *Annals of Applied Biology*, 151 (3), 291–305.

Sarkar, N. and Aikat, K., 2012. Kinetic Study of Acid Hydrolysis of Rice Straw. *ISRN Biotechnology*, 2013, 1–5.

Sarkar, S., 2006. Water use efficiency of rice (Oryza sativa L.) under intermittent ponding and different intensity of puddling. *Archives of Agronomy and Soil Science*, 52 (3), 339–346.

Satbhai, S.B., Ristova, D., and Busch, W., 2015. Underground tuning: Quantitative regulation of root growth. *Journal of Experimental Botany*.

Sato, E.M., Hijazi, H., Bennett, M.J., Vissenberg, K., and Swarup, R., 2015. New insights into root gravitropic signalling. *Journal of Experimental Botany*, 66 (8), 2155–2165.

Scharlemann, J.P., Tanner, E.V., Hiederer, R., and Kapos, V., 2014. Global soil carbon: understanding and managing the largest terrestrial carbon pool. *Carbon Management*, 5 (1), 81–91.

Schellmann, S., Schnittger, A., Kirik, V., Wada, T., Okada, K., Beermann, A., Thumfahrt, J., Jürgens, G., and Hülskamp, M., 2002. TRIPTYCHON and CAPRICE mediate lateral inhibition during trichome and root hair patterning in Arabidopsis. *The EMBO Journal*, 21 (19), 5036–5046.

Schiefelbein, J.W., 1990. Genetic Control of Root Hair Development in Arabidopsis thaliana. *the Plant Cell Online*, 2 (3), 235–243.

Schrader, S., Rogasik, H., Onasch, I., and Jégou, D., 2007. Assessment of soil structural differentiation around earthworm burrows by means of X-ray computed tomography and scanning electron microscopy. *Geoderma*, 137 (3–4), 378–387.

Schuler, M.L., Mantegazza, O., and Weber, A.P.M., 2016. Engineering C4 photosynthesis into C3 chassis in the synthetic biology age. *The Plant journal : for cell and molecular biology*.

Schwarzenbach, R., Egli, T., … T.H.-A.R. of, and 2010, U., 2010. Global water pollution and human health. *Annual Review of Environment and Resources*, 35, 109.

Senapati, N. and Semenov, M.A., 2019. Assessing yield gap in high productive countries by designing wheat ideotypes. *Scientific reports*, 9 (1), 5516.

Shaheen, R. and Hood-Nowotny, R.C., 2005. Effect of drought and salinity on carbon isotope discrimination in wheat cultivars. *Plant Science*, 168 (4), 901–909.

Shen, H., Zhong, X., Zhao, F., Wang, Y., Yan, B., Li, Q., Chen, G., Mao, B., Wang, J., Li, Y., Xiao, G., He, Y., Xiao, H., Li, J., and He, Z., 2015. Overexpression of receptor-like kinase ERECTA improves thermotolerance in rice and tomato. *Nature biotechnology*, 33 (9), 996–1003.

Shepherd, G.., 2000. *VISUAL SOIL ASSESSMENT Volume 1: Field guide for cropping & pastoral grazing on flat to rolling country*. Palmerston North.: horizons.mw & Landcare Research.

Shewry, P.R. and Hey, S.J., 2015. The contribution of wheat to human diet and health. *Food and Energy Security*, 4 (3), 178–202.

Shrawat, A.K. and Lörz, H., 2006. Agrobacterium-mediated transformation of cereals: a promising approach crossing barriers. *Plant Biotechnology Journal*, 4 (6), 575–603.

Six, J., Bossuyt, H., Degryze, S., and Denef, K., 2004. A history of research on the link between (micro)aggregates, soil biota, and soil organic matter dynamics. *Soil and Tillage Research*, 79 (1), 7–31.

Slack, S., York, L., Roghazai, Y., Lynch, J., BioRxiv, M.B.-, and 2018, U., 2018. Wheat shovelomics II: Revealing relationships between root crown traits and crop growth. *biorxiv.org*.

Smit, A., Bengough, A., Engels, C., and Noordwijk, M. van, 2000. *Root Methods A Handbook*. Springer.

Smith, P., 2015. Malthus is still wrong: We can feed a world of 9-10 billion, but only by reducing food demand. *Proceedings of the Nutrition Society*, 74 (3), 187–190.

Smith, S. and De Smet, I., 2012. Root system architecture: insights from Arabidopsis and cereal crops. *Philosophical Transactions of the Royal Society B: Biological Sciences*, 367 (April), 1441–1452.

Sotta, N. and Fujiwara, T., 2017. Preparing thin cross sections of arabidopsis roots without embedding. *BioTechniques*, 63 (6), 281–283.

Southon, T.E., Mattsson, A., and Jones, R.A., 1992. NMR imaging of roots: effects after root freezing of containerised conifer seedlings. *Physiologia Plantarum*, 329–334.

Sposito, G., 2013. Green Water and Global Food Security. *Vadose Zone Journal*, 12 (4).

Squire, G.R., Hawes, C., Valentine, T.A., and Young, M.W., 2015. Degradation rate of soil function varies with trajectory of agricultural intensification. *Agriculture, Ecosystems & Environment*, 202, 160–167.

Stanhill, G., 1986. Water use efficiency. *Advances in Agronomy*, 39.

Stingaciu, L., Schulz, H., Pohlmeier, A., Behnke, S., Zilken, H., Javaux, M., and Vereecken, H., 2013. In Situ Root System Architecture Extraction from Magnetic Resonance Imaging for Water Uptake Modeling. *Vadose Zone Journal*, 0 (0), 0.

Strobl, M., Manke, I., Kardjilov, N., Hilger, A., Dawson, M., and Banhart, J., 2009. Advances in neutron radiography and tomography. *Journal of Physics D: Applied Physics*, 42 (24).

Su, X., Chu, Y., Li, H., Hou, Y., Zhang, B., Huang, Q., Hu, Z., Huang, R., and Tian, Y., 2011. Expression of multiple resistance genes enhances tolerance to environmental stressors in transgenic poplar (Populus × euramericana 'Guariento'). *PloS one*, 6 (9), e24614.

Subira, J., Ammar, K., Alvaro, F., Garcia del Moral, L.F., Dreisigacker, S., and Royo, C., 2016. Changes in durum wheat root and aerial biomass caused by the introduction of the Rht-B1b dwarfing allele and their effects on yield formation. *Plant and Soil*, 403 (1–2), 291–304.

Sylvester-Bradley, R., Berry, P., Blake, J., Kindred, D., Spink, J., Bingham, I., McVittie, J., and Foulkes, J., 2015. Wheat Growth Guide. *AHDB Cereals & Oilseeds (Agriculture and Horticulture Development Board)*, 1–28.

Sys, C. and van Ranst, E., 1993. Land Evaluation III, (13 April 2007).

Takano, M., Inagaki, N., Xie, X., Yuzurihara, N., Hihara, F., Ishizuka, T., Yano, M., Nishimura, M., Miyao, A., Hirochika, H., and Shinomura, T., 2005. Distinct and cooperative functions of phytochromes A, B, and C in the control of deetiolation and flowering in rice. *The Plant cell*, 17 (December), 3311–3325.

Takano, M., Kanegae, H., Shinomura, T., Miyao, A., Hirochika, H., and Furuya, M., 2001. Isolation and characterization of rice phytochrome A mutants. *The Plant Cell*, 13 (3), 521–534.

Takano, M., Xie, X., Inagaki, N., and Shinomura, T., 2005. Distinct functions of

phytochromes on the photomorphogenesis in rice. *Light Sensing in Plants*, 111–117.

Tanaka, N., Kato, M., Tomioka, R., Kurata, R., Fukao, Y., Aoyama, T., and Maeshima, M., 2014. Characteristics of a root hair-less line of arabidopsis thaliana under physiological stresses. *Journal of Experimental Botany*, 65 (6), 1497–1512.

Tanaka, Y., Sugano, S.S., Shimada, T., and Hara-Nishimura, I., 2013. Enhancement of leaf photosynthetic capacity through increased stomatal density in Arabidopsis. *New Phytologist*, 198 (3), 757–764.

Tang, X., Luo, Y., Lv, J., and Wei, C., 2012. Mechanisms of soil aggregates stability in purple paddy soil under conservation tillage of sichuan basin, China. *IFIP Advances in Information and Communication Technology*, 368 AICT (PART 1), 355–370.

Thao, H.T.B., George, T., Takeo, Y., and Widowati, L.R., 2008. Effects of soil aggregate size on phosphorus extractability and uptake by rice (Oryza sativa L.) and corn (Zea mays L.) in two Ultisols from the Philippines. *Soil Science and Plant Nutrition*, 54 (1), 148–158.

The Arabidopsis Genome Initiative., 2000. Analysis of the genome sequence of the flowering plant Arabidopsis thaliana. *Nature*, 408 (6814), 796–815.

The Royal Society of London, 2009. Reaping the benefits: science and the sustainable intensification of global agriculture. *The Royal society*, 2 (October), 35cm17.

Tisdall, J. and Oades, J., 1979. Stabilization of soil aggregates by the root systems of ryegrass. *Soil Research*, 17 (3), 429.

Tötzke, C., Kardjilov, N., Manke, I., and Oswald, S.E., 2017. Capturing 3D Water Flow in Rooted Soil by Ultra-fast Neutron Tomography. *Scientific Reports*, 7 (1), 6192.

Tracy, S.R., 2013. The response of root system architecture to soil compaction . , . *University of Nottingham*. University of Nottingham.

Tracy, S.R., Black, C.R., Roberts, J.A., Dodd, I.C., and Mooney, S.J., 2015. Using X-ray Computed Tomography to explore the role of abscisic acid in moderating the impact of soil compaction on root system architecture. *Environmental and Experimental Botany*, 110, 11–18.

Tracy, S.R., Black, C.R., Roberts, J.A., McNeill, A., Davidson, R., Tester, M., Samec, M., Korošak, D., Sturrock, C., and Mooney, S.J., 2012. Quantifying the effect of soil compaction on three varieties of wheat (Triticum aestivum L.) using X-ray Micro Computed Tomography (CT). *Plant and Soil*, 353 (1–2), 195–208.

Tracy, S.R., Black, C.R., Roberts, J.A., and Mooney, S.J., 2013. Exploring the interacting effect of soil texture and bulk density on root system development in tomato (Solanum lycopersicum L.). *Environmental and Experimental Botany*, 91, 38–47.

Tracy, S.R., Black, C.R., Roberts, J.A., Sturrock, C., Mairhofer, S., Craigon, J., and Mooney, S.J., 2012. Quantifying the impact of soil compaction on root system architecture in tomato (Solanum lycopersicum) by X-ray micro-computed tomography. *Annals of botany*, 110 (2), 511–519.

Tracy, S.R., Roberts, J.A., Black, C.R., McNeill, A., Davidson, R., and Mooney, S.J., 2010. The X-factor: Visualizing undisturbed root architecture in soils using X-ray computed tomography. *Journal of Experimental Botany*, 61 (2), 311–313.

Tron, S., Bodner, G., Laio, F., Ridolfi, L., and Leitner, D., 2015. Can diversity in root architecture explain plant water use efficiency? A modeling study. *Ecological Modelling*, 312, 200–210.

Tumlinson, L.G., Liu, H., Silk, W.K., and Hopmans, J.W., 2008. Thermal Neutron Computed Tomography of Soil Water and Plant Roots. *Soil Science Society of America Journal*, 72 (5), 1234.

Tung, S.A., Smeeton, R., White, C.A., Black, C.R., Taylor, I.B., Hilton, H.W., and Thompson, A.J., 2008. Over-expression of LeNCED1 in tomato (Solanum lycopersicum L.) with the rbcS3C promoter allows recovery of lines that accumulate very high levels of abscisic acid and exhibit severe phenotypes. *Plant, cell & environment*, 31 (7), 968–81.

Tuong, T.P. and Bhuiyan, S.I., 1999. Increasing water-use efficiency in rice production : farm-level perspectives, 40, 117–122.

Uga, Y., Sugimoto, K., Ogawa, S., Rane, J., Ishitani, M., Hara, N., Kitomi, Y., Inukai, Y., Ono, K., Kanno, N., Inoue, H., Takehisa, H., Motoyama, R., Nagamura, Y., Wu, J., Matsumoto, T., Takai, T., Okuno, K., and Yano, M., 2013. Control of root system architecture by DEEPER ROOTING 1 increases rice yield under drought conditions. *Nature Genetics*, 45 (9), 1097–102.

UNESCO, 2019. *The United Nations World Water Development Report 2019: Leaving No One Behind*. Paris.

UNIS, 2000. Secretary General address to Developing Countries 'South Summit'. *UN Information Service Press Release*.

United Nations, 2019. *World Population Prospects 2019: Data Booklet*. Department of Economic and Social Affairs Population Division. Department of Economic and Social Affairs Population Division.

Vijayan, P., Willick, I.R., Lahlali, R., Karunakaran, C., and Tanino, K.K., 2015. Synchrotron

radiation sheds fresh light on plant research: The use of powerful techniques to probe structure and composition of plants. *Plant and Cell Physiology*, 56 (7), 1252–1263.

Vlassenbroeck, J., Masschaele, B., Cnudde, V., Dierick, M., Pieters, K., Van Hoorebeke, L., and Jacobs, P., 2006. Octopus 8: A High Performance Tomographic Reconstruction Package for X-ray Tube and Synchrotron micro-CT. *In*: *Advances in X-ray Tomography for Geomaterials*. London, UK: ISTE, 167–173.

Voorhess, W., Amemiya, M., Allmaras, R.R., and Larson, W.E., 1971. Some Effects of Aggregate Structure Heterogeneity on Root Growth. *Soil Science Society of America Journal*, 35 (4), 638–643.

Vörösmarty, C.J., McIntyre, P.B., Gessner, M.O., Dudgeon, D., Prusevich, a, Green, P., Glidden, S., Bunn, S.E., Sullivan, C. a, Liermann, C.R., and Davies, P.M., 2010. Global threats to human water security and river biodiversity. *Nature*, 467 (7315), 555–561.

Wada, T., 1997. Epidermal Cell Differentiation in Arabidopsis Determined by a Myb Homolog, CPC. *Science*, 277 (5329), 1113–1116.

Wada, T., Kurata, T., Tominaga, R., Koshino-Kimura, Y., Tachibana, T., Goto, K., Marks, M.D., Shimura, Y., and Okada, K., 2002. Role of a positive regulator of root hair development, CAPRICE, in Arabidopsis root epidermal cell differentiation. *Development*, 129 (23), 5409–5419.

Wada, Y., de Graaf, I.E.M., and van Beek, L.P.H., 2016. High-resolution modeling of human and climate impacts on global water resources. *Journal of Advances in Modeling Earth Systems*, 8 (2), 735–763.

Wada, Y., Wisser, D., and Bierkens, M.F.P., 2014. Global modeling of withdrawal, allocation and consumptive use of surface water and groundwater resources. *Earth System*

Dynamics, 5 (1), 15–40.

Wadeson, N. and Basham, M., 2016. Savu: A Python-based, MPI Framework for Simultaneous Processing of Multiple, N-dimensional, Large Tomography Datasets.

Waines, J.G. and Ehdaie, B., 2007. Domestication and crop physiology: roots of green-revolution wheat. *Annals of botany*, 100 (5), 991–8.

Wallace, J.. S., 2000. Increasing agricultural water use efficiency to meet future food production. *Agriculture, Ecosystems & Environment*, 82 (1–3), 105–119.

Wang, C., Liu, S., Dong, Y., Zhao, Y., Geng, A., Xia, X., and Yin, W., 2016. PdEPF1 regulates water-use efficiency and drought tolerance by modulating stomatal density in poplar. *Plant biotechnology journal*, 14 (3), 849–60.

Wang, D., Li, C., Parikh, S.J., and Scow, K.M., 2019. Impact of biochar on water retention of two agricultural soils – A multi-scale analysis. *Geoderma*, 340 (August 2018), 185–191.

Wang, M.-B. and Zhang, Q., 2009a. Issues in using the WinRHIZO system to determine physical characteristics of plant fine roots. *Acta Ecologica Sinica*, 29 (2), 136–138.

Wang, M. Ben and Zhang, Q., 2009b. Issues in using the WinRHIZO system to determine physical characteristics of plant fine roots. *Shengtai Xuebao/ Acta Ecologica Sinica*, 29 (2), 136–138.

Wang, X.-J., Zhang, J.-Y., Shahid, S., Guan, E.-H., Wu, Y., Gao, J., and He, R.-M., 2016. Adaptation to climate change impacts on water demand. *Mitigation and Adaptation Strategies for Global Change*, 21 (1), 81–99.

Wang, X., Yost, R.S., and Linquist, B.A., 2001. Soil Aggregate Size Affects Phosphorus Desorption from Highly Weathered Soils and Plant Growth. *Soil Science Society of*

America Journal, 65 (1), 139–146.

Wang, Z., Han, Q., Zi, Q., Lv, S., Qiu, D., and Zeng, H., 2017. Enhanced disease resistance and drought tolerance in transgenic rice plants overexpressing protein elicitors from Magnaporthe oryzae. *PLoS ONE*, 12 (4).

Warren, J.M., Bilheux, H., Kang, M., Voisin, S., Cheng, C.L., Horita, J., and Perfect, E., 2013. Neutron imaging reveals internal plant water dynamics. *Plant and Soil*, 366 (1–2), 683–693.

Way, D.A., Katul, G.G., Manzoni, S., and Vico, G., 2014. Increasing water use efficiency along the C3 to C4 evolutionary pathway: a stomatal optimization perspective. *Journal of Experimental Botany*, 65 (13), 3683–3693.

Weaver, J.E., 1919. *The ecological relations of roots*. Carnegie Institution of Washington.

Whiteley, G.M. and Dexter, A.R., 1984. Displacement of soil aggregates by elongating roots and emerging shoots of crop plants. *Plant and Soil*, 77 (2–3), 131–140.

Whiteley, G.M., Hewitt, J.S., and Dexter, A.R., 1982a. The buckling of plant roots. *Physiologia Plantarum*, 54 (3), 333–342.

Whiteley, G.M., Hewitt, J.S., and Dexter, A.R., 1982b. The buckling of plant roots. *Physiologia Plantarum*, 54 (3), 333–342.

Wildenschild, D., Vaz, C.M.P., Rivers, M.L., Rikard, D., and Christensen, B.S.B., 2002. Using X-ray computed tomography in hydrology: Systems, resolutions, and limitations. *Journal of Hydrology*, 267 (3–4), 285–297.

Willatt, S.T. and Struss, R.G., 1979. Germination and Early Growth of Plants using neutron radiography, (March), 415–422.

Willatt, S.T., Struss, R.G., and Taylor, H.M., 1978. In situ Root Studies Using Neutron Radiography, 1–6.

Wilmoth, J.C., Wang, S., Tiwari, S.B., Joshi, A.D., Hagen, G., Guilfoyle, T.J., Alonso, J.M., Ecker, J.R., and Reed, J.W., 2005. NPH4/ARF7 and ARF19 promote leaf expansion and auxin-induced lateral root formation. *Plant Journal*, 43 (1), 118–130.

Woodward, J., 1699. Some thoughts and Experiments concerining vegetation. *Royal Society, London*, 21 (253), 193–227.

WWF, 2003. Thirsty crops: Our food and clothes, eating up nature and wearing out the environment? *Living Waters*, 19, 1–20.

Xue, B., Huang, L., Huang, Y., Yin, Z., Li, X., and Lu, J., 2019. Effects of organic carbon and iron oxides on soil aggregate stability under different tillage systems in a rice–rape cropping system. *Catena*, 177 (January), 1–12.

Yadvinder-Singh, Bijay-Singh, and Timsina, J., 2005. Crop Residue Management for Nutrient Cycling and Improving Soil Productivity in Rice-Based Cropping Systems in the Tropics. *Advances in Agronomy*, 85, 269–407.

Yoder, R.E.R., 1936. A direct method of aggregate anylysis of soils and a study of the physical nature of erosion losses. *Agronomy Journal*, 28 (5), 1936.

Yu, J., Hu, S., Wang, J., Wong, G.K.S., Li, S., Liu, B., Deng, Y., Dai, L., Zhou, Y., Zhang, X., Cao, M., Liu, J., Sun, J., Tang, J., Chen, Y., Huang, X., Lin, W., Ye, C., Tong, W., Cong, L., Geng, J., Han, Y., Li, L., Li, W., Hu, G., Li, J., Liu, Z., Qi, Q., Li, T., Wang, X., Lu, H., Wu, T., Zhu, M., Ni, P., Han, H., Dong, W., Ren, X., Feng, X., Cui, P., Li, X., Wang, H., Xu, X., Zhai, W., Xu, Z., Zhang, J., He, S., Xu, J., Zhang, K., Zheng, X., Dong, J., Zeng, W., Tao, L., Ye, J., Tan, J., Chen, X., He, J., Liu, D., Tian, W., Tian, C.,

Xia, H., Bao, Q., Li, G., Gao, H., Cao, T., Zhao, W., Li, P., Chen, W., Zhang, Y., Hu, J., Liu, S., Yang, J., Zhang, G., Xiong, Y., Li, Z., Mao, L., Zhou, C., Zhu, Z., Chen, R., Hao, B., Zheng, W., Chen, S., Guo, W., Tao, M., Zhu, L., Yuan, L., and Yang, H., 2002. A draft sequence of the rice genome (Oryza sativa L. ssp. indica). *Science*, 296 (5565), 79–92.

Yu, L., Chen, X., Wang, Z., Wang, S., Wang, Y., Zhu, Q., Li, S., and Xiang, C., 2013. Arabidopsis enhanced drought tolerance1/HOMEODOMAIN GLABROUS11 confers drought tolerance in transgenic rice without yield penalty. *Plant physiology*, 162 (3), 1378–91.

Zappala, S., Helliwell, J.R., Tracy, S.R., Mairhofer, S., Sturrock, C.J., Pridmore, T., Bennett, M., and Mooney, S.J., 2013. Effects of X-Ray Dose On Rhizosphere Studies Using X-Ray Computed Tomography. *PLoS ONE*, 8 (6).

Zappala, S., Mairhofer, S., Tracy, S., Sturrock, C.J., Bennett, M., Pridmore, T., and Mooney, S.J., 2013. Quantifying the effect of soil moisture content on segmenting root system architecture in X-ray computed tomography images. *Plant and Soil*, 370 (1–2), 35–45.

Zarebanadkouki, M., Carminati, A., Kaestner, A., Mannes, D., Morgano, M., Peetermans, S., Lehmann, E., and Trtik, P., 2015. On-the-fly Neutron Tomography of Water Transport into Lupine Roots. *In*: *Physics Procedia*.

Zarebanadkouki, M., Kim, Y.X., and Carminati, A., 2013. Where do roots take up water? Neutron radiography of water flow into the roots of transpiring plants growing in soil. *New Phytologist*, 199 (4), 1034–1044.

Zarebanadkouki, M., Kim, Y.X., Moradi, A.B., Vogel, H.-J., Kaestner, A., and Carminati, A., 2012. Quantification and Modeling of Local Root Water Uptake Using Neutron

Radiography and Deuterated Water. *Vadose Zone Journal*, 11 (3).

Zarebanadkouki, M., Kroener, E., Kaestner, A., and Carminati, A., 2014. Visualization of root water uptake: quantification of deuterated water transport in roots using neutron radiography and numerical modeling. *Plant Physiol*, 166 (2), 487–499.

Zhao, D. and Liu, J., 2015. A new approach to assessing the water footprint of hydroelectric power based on allocation of water footprints among reservoir ecosystem services. *Physics and Chemistry of the Earth*, 79–82, 40–46.

Zhou, P. and Pan, G., 2007. Effect of different long-term fertilization treatments on particulate organic carbon in water-stable aggregates of a paddy soil. *Chinese Journal of Soil Science*, 38 (2), 256–261.

Zimin, A. V., Puiu, D., Hall, R., Kingan, S., Clavijo, B.J., and Salzberg, S.L., 2017. The first near-complete assembly of the hexaploid bread wheat genome, Triticum aestivum. *GigaScience*, 6 (11), 1–7.

Zobel, R.W., 2016. Arabidopsis: An adequate model for dicot root systems? *Frontiers in Plant Science*, 7 (FEB2016).

Zoulias, N., Harrison, E.L., Casson, S.A., and Gray, J.E., 2018. Molecular control of stomatal development. *The Biochemical journal*, 475 (2), 441–454.

Zuo, Q., Zhang, R., Shi, J., Timlin, D., and Ahuja, L.R., 2013. Characterization of the Root Length Density Distribution of Wheat Using a Generalized Function, 4, 93–118.